A thesis submitted in partial fulfilment of the requirements for the Degree of

DOCTOR OF PHILOSOPHY

by

YONG-ZHUANG LI

ON THE LAGRANGIAN PERTURBATION THEORY OF STRUCTURE FORMATION IN GENERAL RELATIVITY

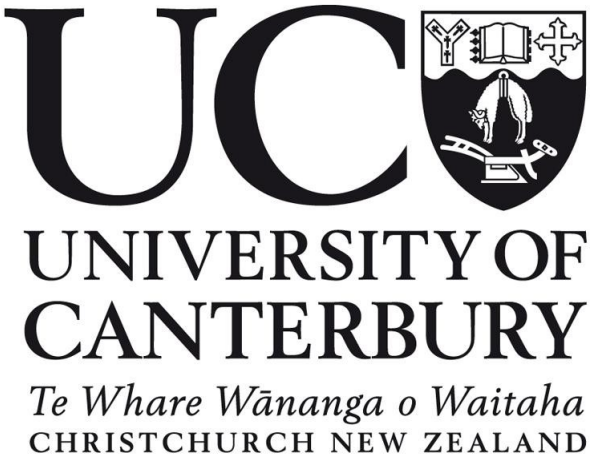

Supervisor: Prof. David L. Wiltshire

UNIVERSITY OF CANTERBURY

Department of Physics & Astronomy

August 2018

To my parents.

UNIVERSITY OF CANTERBURY
Te Whare Wānanga o Waitaha
CHRISTCHURCH NEW ZEALAND

Deputy Vice-Chancellor's Office
Postgraduate Office

Co-Authorship Form

This form is to accompany the submission of any thesis that contains research reported in co-authored work that has been published, accepted for publication, or submitted for publication. A copy of this form should be included for each co-authored work that is included in the thesis. Completed forms should be included at the front (after the thesis abstract) of each copy of the thesis submitted for examination and library deposit.

Please indicate the chapter/section/pages of this thesis that are extracted from co-authored work and provide details of the publication or submission from the extract comes:

Chapter 3 is extracted from the co-authored publication: Yong-zhuang Li, Pierre Mourier, Thomas Buchert, David L. Wiltshire, "*Lagrangian theory of structure formation in relativistic cosmology. V. Irrotational fluids*", *PHYSICAL REVIEW D* ***98,*** *043507 (2018).*

Please detail the nature and extent (%) of contribution by the candidate:

The candidate contributed the original draft of the paper, and many of the calculations, including the trace and traceless parts of the perturbation equations. He also performed numerical calculations leading to the plotted figures with the support of Pierre Mourier.

Pierre Mourier contributed calculations including the electric/magnetic split of the traceless part and a method for constructing explicit solutions, and finished the final draft with Thomas Buchert. Thomas Buchert determined the overall structure of the final draft, as well as suggesting calculations attempted in consultation with David Wiltshire. All 4 authors each checked some individual calculations, while David Wiltshire also checked English style.

The candidate's overall contribution as lead author was at least 40%.

Certification by Co-authors:

If there is more than one co-author then a single co-author can sign on behalf of all
The undersigned certify that:

- The above statement correctly reflects the nature and extent of the PhD candidate's contribution to this co-authored work
- In cases where the candidate was the lead author of the co-authored work he wrote the text

Name:	Signature:	Date:
David L Wiltshire	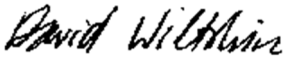	*13/08/2018*
Pierre Mourier		*13/08/2018*
Thomas Buchert		*13/08/2018*

ABSTRACT

In this thesis we focus on two different problems in the study of the formation and evolution of large scale structure using the Lagrangian perturbation approach.

First, we study the effects of velocity dispersion in Newtonian cosmology in an Einstein-de Sitter universe which contains two different dust continua. We implement the basic feature of the adhesion approach, considering the velocity dispersion as an effective dynamical pressure to avoid the problem of the formation of caustics in the dust model. This strengthens our ability to study the evolution of large scale structure beyond the linear regime. Furthermore, it has been suggested in a dark matter dominated universe the baryonic matter does not simply track the dark matter, *i.e.*, the local baryon densities are not proportional to those of the dark matter and their velocities are not identical.

As a first step towards the relativistic Lagrangian perturbation description for such a two-component case, we have considered the corrections of the velocity dispersion up to second order, where the velocity dispersion with respect to each dust component is isotropic. The results show that the dynamics of mixture of two dust continuum can be described by a single dust continuum with an anisotropic effective pressure term as corrections. Such an effective term up to second-order will lead to a new decaying mode which is slower than the standard decaying mode in Eulerian linear perturbation theory. The evolution of each component can be derived by the dynamics of the eddfluid mixture. The second-order corrections will be affected by the spatial distribution of the density fields. For higher orders, the cosmic substructures can be subsequently added.

Second, as the major part of this thesis, we extend relativistic Lagrangian perturbation theory for a dust matter model to the case of perfect fluids, and also to cases that are relevant for the modelling of multistream regimes when the dust approximation breaks down. This will provide a framework not only to deal with a relativistic generalization of Newtonian Lagrangian perturbation theory with pressure at late epochs, but also to the fully relativistic situation of the early Universe.

By choosing a suitable set of coframes for the fluid matter model, we obtain the master partial differential equations for the evolution of the trace and traceless parts of the first–order deformation field that reduce to the corresponding

equations in the dust case. The trace part also matches the Newtonian limit of the corresponding Lagrangian perturbation problem. We generalize the procedure proposed in previous papers for finding solution for perturbations that propagate in the perturbed space. We apply this procedure to specific toy models, illustrating the mildly nonlinear evolution of the density contrast. We also discuss the limits of a first–order Lagrangian scheme, and propose ideas for a nonperturbative generalization, which is needed especially in application to cases where the pressure term is taken to model multistreaming beyond the mildly nonlinear regime. This part can be seen as a preparation for future work that accounts for two components in a relativistic universe.

ACKNOWLEDGMENTS

Four years ago, on 31st August, 2014, I arrived in this, the most beautiful country I have ever visited. At the moment when I set foot on this land, a special sense hit me. That was the smell of fresh earth, grass and even a little of livestock droppings. The mountains, embracing the area, were covered by snow. The sky was so pure, with cotton-like clouds drifting through. I told myself that this was the place in which I would live in the next four years.

I was so excited when I knew I had been chosen to be supported by the China Scholarship Council to study abroad. No one knew what this news meant to my parents, Yu-Ming Li and Fa-Qin Shen, who are typical Chinese farmers. They have spent almost fifty years on tillage, husbandry and harvesting. Only in winter can they have some leisure time. Farming was viewed as one of lifestyles with no future in China in the 1990s. So their hope was simple: none of their three boys should spend his life as a farmer. At the time when I got the news, my older brother, Yong-Qiang Li, was a doctor and my younger twin brother, Yong-Bang Li, was an engineer. When I told my parents I had the chance to continue my study as a PhD student, they knew their wish had become true. Now they are spending most of their time with their third grandson, enjoying the family fun. They are two of greatest parents in the world.

I also have to thank my brothers. In the last four years, it was them who took care of our parents. On the holiday of the Chinese Spring Festival, it was them staying with our parents and warming our parents' hearts to make them happy in the cold of winter. The eve of the Chinese New Year is the most important day for all of Chinese people. It is the day of family reunion. No matter where you are, after sunset, you should sit next to your family and enjoy a sumptuous dinner. I have not attended such family reunion for four years. Thanks to my brothers, our parents never felty lonely.

As an international student, it is reassuring when you know someone will pick you up after you arrive. When I first met my supervisor, David Wiltshire, he was holding a paper signboard with my name on it, waiting at the arrival gate.

This is one of moments I will never forget.

David is a true physicist, and will fight for his research and ambition. In the last four years I have received much help from him. He also taught me how to solve physical problems using my "physics brain". Without his support and help, this thesis would never exist.

The four years in New Zealand have given me a chance to meet many new friends. Thanks to them, my life has been full of fun and happiness. I have been invited many times by Hui Ye (Hector) and Ze-Zhou Man (Jennifer) to join them for dinners, hiking and many other activities. Of course I will never forget you guys: Shan-Jiu Cao (Ross), Jing Hu (Jane), Hao Yang (Sappho), Feng Zhu (Otto) and Xiao-Shi Xie, Yu-Jue Chen (Jason) and Fang-Yan Lin, Jun-Sheng Su, Bo-Wen Lu, Ting Wu, Wen-Hao Li. We have so many times had wonderful dinner parties and holiday parties. We are really a big family.

Also I have to thank Qing-Jun Yu, Jing-Ya Huang (Helen), Xuan-Yi Fu (Nina), Feng Cao and Hui-Lin Ni. Actually things were quite contradictory during the year we met. I experienced the most marvelous moment of my life, and also I experienced one of the most ludicrous moments.

Special thanks to Asta Heinesen and Pierre Mourier. They are two of most brilliant and smart PhD students I have ever known. I have learned a lot from them. Concentration, hard-working and exuberant curiosities are what they showed to me. In three months in Lyon, we have several times visited the museums and city together. Thanks to Pierre for inviting us to visit his home. Mâcon is a very peaceful and beautiful village.

Thanks to Prof. Thomas Buchert on the joint work of Chapter 3.

Thanks to my other friends, Hadis Bagherpour, Amirreza Raissi, Sarang Shah, Nan Yang and his wife Celine Yang, Fei Guo, Jun-Hao Qian. It is really very nice to meet you guys.

My old friends, Chun-Hu Li, Song-Jun Hou and Qing-Qing Wu, of course deserve my thanks. Although I have not seen them for a very long time, they have never forgotten our friendships. I was so happy when I met Song-Jun and Qing-Qing again at the rail station of Lancaster, UK. We had an unforgettable two days at Lancaster University. I cannot wait to see you again.

Four years is quite long time. I am very glad I have had the chance to study and live in this beautiful country.

CONTENTS

LIST OF FIGURES

CHAPTER 1

Introduction: from homogeneity to inhomogeneity

The first and most important fact is that our observable Universe is inhomogeneous, and maybe anisotropic, on small enough scales, up to the scales of at least $100h^{-1}$ Mpc, where h is the dimensionless parameter related to the Hubble constant by $H_0 = 100h$ km s^{-1} Mpc^{-1}. It has been observed that the present Universe is dominated by voids in volume. Some of the present total volume of the Universe is in voids with a characteristic diameter $30h^{-1}$Mpc [Hoyle and Vogeley, 2002, 2004] and there are many smaller minivoids [Tikhonov and Karachentsev, 2006; Pan et al., 2012], and also rare large voids [Pan et al., 2012]. Once the statistics of voids of all sizes is included then the present Universe is void dominated. The exact fraction of the volume occupied by voids depends on how voids are defined, but could easily be of order $60\% - 80\%$. Our present Universe displays a complex hierarchical structure of inhomogeneity. Clusters of galaxies, the largest bound structures, are strung in this filaments that thread the voids, and in sheets that surround them, giving rise to a gigantic cosmic web [Springel et al., 2006]. This raises a very important question: is our successful phenomenological description of the Universe based on the spatially homogeneous and isotropic Friedmann-Lemaître-Robertson-Walker (FLRW) geometry still a powerful tool to study our Universe?

Another important fact about our present Universe is its apparently accelerating expansion. Accounting for this by introduction of a cosmological constant, Λ, leads to a fine-tuning problem since the acceleration only begins at late epochs. This is known as *the cosmic coincidence problem*. Some researchers also note that this epoch coincides with the one in which the large nonlinear structures begin to dominate [Gott III et al., 2005]. This second cosmic coincidence shows that the inhomogeneities of universe maybe play a significant role in the appar-

ent acceleration of expansion. While our current extremely successful standard model of cosmology relies on the contributions from dark energy and dark matter, there are no direct laboratory evidences to show that they actually exist. If the inhomogeneities really relate to the present acceleration then our current FLRW model of universe needs to be reconsidered.

In this chapter we will briefly introduce the history of the research of cosmology from the introduction of the homogeneous universe model to the discovery of inhomogeneities of our observable Universe. We will not discuss all the details but will focus on the chronological order in which ideas were proposed.

1.1 An overview of modern cosmology: the homogeneous approximation

1.1.1 Early studies of homogeneous and isotropic cosmological models

In 1917 Einstein first applied his theory of General Relativity (GR) to cosmology. At that time astronomers did not know that those nebulae which we now call galaxies are actually at vast distances from us. Following the best knowledge of the day, Einstein assumed that the typical objects in the Universe were stars – which he assumed to be particles of dust – a pressureless fluid constituting the energy-momentum tensor in his field equations. To satisfy *the Copernican Principle* – that we do not live in a privileged position in space – Einstein assumed a stronger *Cosmological Principle*, namely that the cosmological fluid is spatially homogeneous and isotropic. Then no spatial position is privileged, as far as its average dynamics is concerned.

In 1917 it was also that prevailing world view that the Universe should not have a beginning in time. This posed a problem since gravity with pressureless dust is attractive. To obtain a static universe Einstein introduced the cosmological constant with an energy density half of the mean energy density of the dust and a finely tuned positive scalar curvature [Einstein, 1917; O'Raifeartaigh et al., 2017]. In the same year, W. H. de Sitter introduced another static model with a pure cosmological constant, trying to explain the recession velocities of

spiral nebulae as a simple consequence of the gravitational field [de Sitter, 1917]. This model was criticized by Einstein on the grounds that de Sitter's universe is actually not an empty universe, but has matter concentrated in the "horizon" surface [Einstein, 1918]. To solve this problem, in 1922, Lanczos found a more physically satisfying interpretation of the de Sitter universe, by discarding the concept of a static three-dimensional space, and by assuming that space is expanding [Lanczos, 1922].

A few months before Lanczos' paper was published, Friedmann first described the possibility of a universe with a time-dependent but spatially homogeneous positive spatial curvature, and then generalized to the case with time-dependent negative spatial curvature [Friedmann, 1922, 1924]. Although Friedmann did not consider his model relevant to the real universe, his work still made significant contributions to General Relativity. After introducing new non-static coordinate for the de Sitter universe [Lemaître, 1925], in 1927, a young PhD student, Lemaître, independently introduced the new non-stationary solution, with a positive spatial curvature and a scale factor depending on the time [Lemaître, 1927]. In this paper Lemaître derived the first statement that the outward speed of distant objects in our universe is proportional to their distance from us, which later became known as Hubble's law. He also provided the first observational estimation of the Hubble constant. Furthermore, it was also in this paper that he considered the conservation of energy, and emphasized the importance of radiation pressure in the first stages of the cosmic expansion. Unfortunately, this work was virtually unknown at first since it was published in the little known journal, "Annales de la Société Scientifique de Bruxelles".

Two years later, Hubble [1929] examined the relation between the distance and redshift of galaxies, and discovered a roughly linear relation between the distances of the galaxies and their redshifts [1]. This effectively confirmed Lemaître's prediction of an expanding universe and established the terminology "Hubble's law". However, at the time Hubble and other astronomers did not know about the work of Lemaître. In 1930 after reading a report by Arthur Eddington and de Sitter calling for new astronomical surveys to verify the cosmic expansion, Lemaître wrote to Eddington pointing out his prior work. After this Eddington

[1] We have to mention that before this, other astronomers have published their radial velocity-distance relations. For example, see Lundmark [1924]; Stromberg [1925].

arranged for Lemaître's theory to be translated and reprinted in the "Monthly Notices of the Royal Astronomical Society" in 1931, thus publicized this work [Lemaître and Eddington, 1931].

In the same year, Eddington and de Sitter separately published several influential papers. Eddington [1930] reexamined the Einstein static model and found it was unstable, while de Sitter [1930a] discussed the expansion of the Universe, quantitatively analyzed the redshift-distance relation [de Sitter, 1930b]. He also discussed the consequences of Lemaître's solution [de Sitter, 1930c,d]. In the latter part of 1931, Lemaître [1931] first presented his proposal that the Universe might have an explosive beginning from an initial point, which he called the "primeval atom", and which we now call the "Big Bang".

Meanwhile, astronomers still paid a lot of attention to the static solution, trying to find an alternative explanation of recession velocities. Back in 1928 Robertson [1928] had discussed another coordinate transformation for the de Sitter universe, which is similar to the one Lemaître published in 1925 [Lemaître, 1925]. Without knowing about Lemaître's articles, somewhat later Robertson [1929] published one of his most important papers, in which he discussed in detail all possible mathematical models satisfying spatial homogeneity and isotropy. He found that the only possible stationary cosmologies are those of Einstein and de Sitter, being particular cases of a class of non-stationary cosmologies.

Still working in the framework of a static solution, Tolman [1929] also sought an explanation of recession velocities. However, in 1930 he suggested a non-static line element must be required to account for the redshift of the light from distant objects. Using a non-static spherically symmetric line element Tolman estimated the relation between distance, luminosity, redshift and angular extension [Tolman, 1930].

The 1930s were a very important decade for the understanding of our Universe, not only for models with homogeneous and isotropic expansion, but also for the beginning of the study of inhomogeneous universes. In the opening years of this decade, the expanding universe had been firmly established. Einstein finally accepted this theory and published a discussion on the expanding universe and the cosmological constant [Nussbaumer, 2014]. In 1932 Einstein and de Sitter [1932] published their well-known cosmological model with zero cosmological constant, which is called the Einstein-de Sitter model, showing that it is pos-

sible to accounting for the observed facts (the Universe is non-static) without assuming a curvature of three dimensional space. Thus one could abandon the cosmological constant. A good review paper was published in 1933 by Robertson [1933a], who summarized the results obtained to that date in the field of relativistic cosmology.

A few months later, Milne [1932] suggested a new purely kinematic solution to the problem of the expansion of the Universe, which is effectively a non-static slicing of empty space. This theory soon attracted extensive attention from the physics community[Kermack and McCrea, 1933; Robertson, 1933b; Dingle, 1933; Walker, 1934; Walker and Milne, 1935]. It then motivated H. R. Robertson and W. C. Walker to publish their very important articles, [Robertson, 1935, 1936a,b; Walker, 1937].

To summarize, by the 1930s the homogeneous and isotropic expanding universe was well understood, and is now generically known as the Friedmann-Lemaître-Robertson-Walker universe. For such a universe, the metric is given by

$$ds^2 = -c^2dt^2 + a^2(t)\left[\frac{1}{1-kr^2}dr^2 + r^2\left(d\theta^2 + \sin^2\theta d\psi^2\right)\right], \tag{1.1}$$

with the Friedmann equations

$$H^2 = \left(\frac{1}{a}\frac{da}{dt}\right)^2 = -\frac{c^2k}{a^2} + \frac{8\pi G\varrho_H}{3} + \frac{\Lambda c^2}{3}, \tag{1.2}$$

$$\frac{1}{a}\frac{d^2a}{dt^2} = -\frac{4\pi G}{3}\left(\varrho_H + \frac{3p_H}{c^2}\right) + \frac{\Lambda c^2}{3}, \tag{1.3}$$

where c, $k = -1,\ 0\ +1$, Λ, a, ϱ_H, p_H are the light speed, the spatial curvature, the cosmological constant, the scale factor, the homogeneous and isotropic energy density and pressure density, respectively. $H(t)$ is the Hubble parameter. The deceleration parameter, q, describing the rate at which the expansion of the Universe is "slowing" due to self-gravitation, is historically defined as

$$q = -\frac{d^2a}{dt^2}\frac{1}{H^2}\frac{1}{a^2}. \tag{1.4}$$

The homogeneous and isotropic model with above the cosmological parameters was widely adopted to fit observations and has achieved great success.

Although we have been recalling the history of the homogeneous and isotropic universe model, it should be mentioned that even at this early stage many astronomers and cosmologists were already aware of the inhomogeneities of our Universe.[2] The uniformity of matter (and pressure) distributed over the Universe was seen as a basic simplifying assumption that might not apply to the actual Universe.

In 1933 Lemaître [1933] considered the formation of 'nebulae', trying to apply exact solutions of Einstein's equation to particular cases of spherically symmetric inhomogeneities. One year later, Tolman [1934b] discussed the effect of inhomogeneities on the static Einstein and non-static Friedmann cosmological models, and predicted the development of condensations and rarefactions, while Sen [1934] also considered similar inhomogeneous effects by using different initial conditions to Tolman.

Bondi [1947] later discussed various properties of spherically symmetric pressure-free models, including geodesic equations, extending the work of McCrea, McVittie and Lemaître on the problem of condensation [McCrea and McVittie, 1931; McVittie, 1932, 1933; Lemaître and Eddington, 1931]. This spherically symmetric solution is most often known as the Lemaître-Tolman or the Lemaître-Tolman-Bondi universe models (LTB model hereafter).

Another inhomogeneous model known as the Swiss cheese universe, was first constructed by Einstein and Straus in 1945 by cutting and pasting spherically symmetric Schwarzschild vacuoles into a global FLRW geometry [Einstein and Straus, 1945]. It is widely used in studying lensing effects.

Other exact inhomogeneous solutions of Einstein's equations are also important for improving our knowledge of the actual universe. These include the

[2] Here we will not discuss the problem of anisotropic universe models in detail but give a very briefly outline. The cosmological models which are spatially homogeneous but not necessarily isotropic are known as the Bianchi universes, named after Bianchi's classification of Lie groups [Bianchi, 1898], with which they may be put in one-to-one correspondence. There are eight independent types, I, II, IV, V, VI_0, VII_0, VIII and IX. These types of universes have been extensively applied to studies of nonlinear dynamics, the early and late universe, general geometric and dynamics studies, and so on. For good research papers and reviews, see [Kantowski and Sachs, 1966; Kantowski, 1998; Misner, 1968; Ellis and Elst, 1999a; Ellis, 2006; Russell et al., 2014; Pradhan and Saha, 2015] and references therein. Though the Bianchi universe models have been widely studied, some observations have suggested that anisotropic expansion of the Universe is disfavoured even at a low level [Saadeh et al., 2016; Ade et al., 2014, 2016b].

Szekeres-Szafron family [Szekeres, 1975; Szafron, 1977] and the Stephani-Barnes family [Barnes, 1973; Stephani, 1987]. For very extensive and detailed reviews of inhomogeneous cosmological models, the reader is strongly recommended to check [Ellis, 2006; Krasiński, 1997; Ellis et al., 2012] and references therein.

The above history shows that as early as the 1930s-1940s most of the important cosmological models that astronomers and physicists still employ to describe the Universe had already been proposed and developed. Of course in this period some other significant developments also took place: for example, the prediction of the cosmic microwave background (CMB) [Gamow, 1948a,b; Alpher and Herman, 1948b] and the steady state cosmology (which was discovered to be inappropriate for describing the actual universe and so is not further discussed). Since then cosmology has became an active physical science.

1.1.2 Two significant observations: Cosmic Microwave Background (CMB) and cosmic acceleration

Just like the two sides of a coin, neither a pure theory unsubstantiated by observation nor an observable fact without theoretical support can be completely successful. While theoretical research was in full swing, new observations both validated the theoretical framework and stimulated new theoretical research. With the rapid development of computer systems and the advanced technologies of space and radio telescopes [3], it became possible for cosmologists to reach previously unexplored territory with images produced by the telescopes in many different wavelengths, and to simulate the evolution of the Universe, the large-scale structure and galaxy formations using supercomputers. Here we will just discuss two major milestones.

The first significant achievement was the discovery of the CMB. In 1965, working with the 20-foot horn-reflector antenna, Penzias and Wilson [1965] measured a background temperature about 3.5 ± 1.0 K higher than the expected effective

[3] It is very interesting to note that the world's first working electromechanical programmable, fully automatic digital computer was built in 1941, at a time that modern cosmology began to be active. The invention of the integrated circuit in the end of 1950s has led to an explosion in the wide use of computers in a period during which some of the most important observations were leading to great developments in modern cosmology. Including modern cosmology, physics has always been deeply influenced by the development of new technologies.

zenith noise temperature of the antenna at a 7.35 cm wavelength. Within the limits of their observations they found the excess temperature was isotropic, unpolarized and free from seasonal variations. This excess temperature was then identified as the CMB radiation left over from the Big Bang by Dicke et al. [1965]. Such a relic radiation had been predicted by physicists who had studied physical processes in a high density expanding plasma and the origin of elements.

As early as in 1922, Tolman [1922] studied the thermodynamic treatment of the possible formation of helium from hydrogen, with the conclusion that it was not possible to understand the observed H/He abundance ratio at temperatures less than 10^6 K and pressures above 10^{-100} atmospheres. Suzuki [1928] considered the thermal equilibrium of dissociation of atomic nuclei in stellar interiors in 1928, concluding that the H/He abundance ratio might be understood only at temperatures of about 10^9 K. Urey and Bradley [1931] later showed that the observed relative isotopic abundances would not result from thermodynamic equilibrium at any single temperatures.

In 1934, Tolman [1934a] introduced the idea of the thermodynamic history of an expanding universe, showing that the expansion of universe cools blackbody radiation while keeping the spectrum thermal, and the temperature varies inversely with the scale factor of the expanding homogeneous and isotropic universe. However, we note that most of these early papers assumed a scenario in which the origin and relative abundances of the elements could result from a frozen-in nuclear equilibrium. But this equilibrium theory had a number of difficulties as is discussed in detail by Alpher and Herman [1950]. Those difficulties led the astronomical and cosmological communities to the examination of non-equilibrium processes.

In 1942, Chandrasekhar and Henrich [1942] attempted to interpret the relative abundances of the elements and their isotopes by detailed equilibrium computations, concluding that the lighter elements would agree fairly and satisfactorily with the known cosmic abundances if the elements were produced in the physical conditions specified by a temperature $\sim 10^9$ K and matter density $\sim 10^7$ gm/cm^3. They also noted that their theoretical computations were unable to account for the existence of the heavy nuclei, and all the observed abundances could not be accommodated by a single set of temperature and densities. Thus they suggested that one may need to consider non-equilibrium processes, and the

cooling expanding the early Universe would be a possible site for such processes.

Gamow [1942] also discussed the problem of the origin of chemical elements in the same year. He suggested one should not consider some kind of thermodynamic-equilibrium hypothesis, but a non-equilibrium breaking-up of the original bulk of nuclear matter caused by a rapid expansion in the early evolutionary stages should be a better process to consider.

Later, within the framework of an expanding universe, Gamow [1946] pointed out that the necessary conditions for rapid nuclear reactions only existed for a very short time. This consideration was then developed in more detail in 1948 by himself, together with R. A. Alpher, R. Herman and H. Bethe [Alpher et al., 1948] and now is known as Big Bang nucleosynthesis. With the hypothesis of the "unfinished building-up process" developed in previous papers, Gamow [1948a] discussed the temperature and radiation density at early stages of evolution, showing that at the epoch of matter-radiation equality the temperature would be $\sim 10^3$ K. The good agreements between the calculated density and the radii for the galaxies with the observed ones strongly supported the rudimentary galactic formation theory of that time.

Alpher [1948] developed the non-equilibrium theory of the formation of the elements in which the elements were built up by a process of successive neutron captures. He estimated the radiation temperature at nucleosynthesis and concluded that the energy budget of the Universe must have then been dominated by radiation. In a later paper Alpher and Herman [1948a] corrected some errors in Gamow's *Nature* paper [Gamow, 1948b] (where he summarized previous work and discussed the formation of stars and galaxies). They predicted a relic radiation at the present epoch and estimated its present temperature to be 5 K. See also [Alpher and Herman, 1949] for detailed calculations and discussions. This value was seen as the first numerical estimate of the present CMB temperature. The first published discussions of possible observations of the CMB in the present Universe were given by Zel'dovich [1963], and Dicke et al. [1965] in the early 1960s.

Although the observations showed that the CMB was almost isotropic, physicists soon began to study the anisotropy of the CMB. The largest anisotropy of the CMB spectrum is the dipole anisotropy with an averaged amplitude $\Delta T \sim 3.35$ mK from different observations. It is conventionally interpreted

as the consequence of the Doppler shift caused by the Earth's motion relative to the CMB rest frame. It was discovered and confirmed in 1960s and early 1970s, by Partridge and Wilkinson [1967], Stewart and Sciama [1967], Conklin [1969], Henry [1971], Corey and Wilkinson [1976], and Smoot et al. [1977]. Detailed whole sky measurements of the dipole anisotropy were first made by the Cosmic Background Explorer satellite (COBE) in the early 1990s, fixing its amplitude to be $\Delta T = 3.372 \pm 0.014$ mK with 95% confidence level (CL), in a direction $(l, b) = (264.14^\circ \pm 0.03, 48.26^\circ \pm 0.30)$ (95% CL) in galactic coordinates [Fixsen et al., 1996].

Once the dipole anisotropy is eliminated by performing a local Lorentz boost from the heliocentric rest frame to one in which the dipole amplitude is zero, then smaller anisotropies at the level $\Delta T/T \sim 10^{-5}$ remain. These include primordial fluctuations. The most important of these is the *Sachs-Wolfe* effect considered by Sachs and Wolfe [1967], where anisotropies arise due to the gravitational redshift of photons in the gravitational potential wells of inhomogeneities at the surface of last scattering. Such fluctuations on the surface of last scattering are classified as primary fluctuations. When the photons traverse many time-dependent gravitational wells generated by growing concentrations of matter between the last scattering surface and our telescopes, their wavelengths will be further redshifted or blueshifted[4]. This effect is known as *the integrated Sachs-Wolfe effect* and is an example of secondary fluctuations. A similar effect, called *the Rees-Sciama effect* was considered by Rees and Sciama [1968]. In contrast to the integrated Sachs-Wolfe effect which is calculated to the linear regime of perturbation theory on a FLRW background, the Rees-Sciama effect refers to the general case, potentially beyond the regime of perturbation theory.

Other secondary CMB anisotropies arise from *the Sunyaev-Zel'dovich effect* theoretically predicted by R. A. Sunyaev and Zel'dovich in 1969, in which the low energy CMB photons receive an average energy boost during collisions with the high energy electrons in dense regions (the inverse Compton scattering), and could be used to detect the density perturbations of the Universe [Sunyaev and Zeldovich, 1970; Sunyaev and Zel'dovich, 1980]. This effect was first detected by Birkinshaw et al. [1984] from clusters of galaxies. All above effects are generated

[4] By "wells" we also refer to the potential "humps" of underdense voids as well as the over-densities of gravitationally bound structures.

by structures on small angular scales and consequently affect higher multipole anisotropies in the CMB.

The small angle anisotropies of the CMB temperature were first detected by the COBE satellite in 1992 [Smoot et al., 1992], showing statistically significant ($> 7\sigma$) structure was consistent with a thermal spectrum at 31, 53 and 90 GHz as expected for the CMB anisotropy. The four year results were published later by Bennett et al. [1996], where the authors found a power-law spectral index of $n = 1.2 \pm 0.3$ and a quadrupole normalization $Q_{rms-PS} = 15.3^{+3.8}_{-2.8}\mu K$. Based on the full 4-year of COBE Differential Microwave Radiometer (DMR) observations, they presented a detailed overall visual impression of the anisotropy with the signal-to-noise ratio $\sim$2 per 10° sky map patch. Early results reported in 1990 showed that the intensity of the background sky radiation was consistent with a black-body at 2.735 ± 0.06K, with deviations from this black-body at the spectral resolution of the instrument less than 1% of the peak brightness [Mather et al., 1990; Fixsen et al., 1994].

Later measurements can be summarized as follows. The first images of resolved structure in the microwave background anisotropies over a significant part of the sky were reported by de Bernardis et al. [2000], and confirmed a peak at $l \approx 200$. This peak represents the first excess of power due to more fluctuations at a length scale caused by one compression or rarefaction in the primordial plasma by the epoch of last scattering. Acoustic waves on smaller angular scales which undergo multiple compressions or rarefactions give rise to additional peaks. This angular scale of the first peak implied a spatially flat universe in the context of the FLRW model. Polarization of CMB was discovered by the Degree Angular Scale Interferometer (DASI) in 2002 [Kovac et al., 2002], which provided a model-independent test of the theoretical framework that could also be used to constrain cosmological parameters.

The Wilkinson Microwave Anisotropy Probe (WMAP) released their first high precision data in 2003 and could fit microwave observation on finer angular scale measurements [Spergel et al., 2003]. In subsequent years they continued to release improved measurements [Hinshaw et al., 2007; Larson et al., 2011] (culminating in new full-sky temperature maps in five frequency bands from 23-94 GHz in [Hinshaw et al., 2007]). Even greater precision was achieved by

the Planck satellite [5], who have fitted six acoustic peaks in the CMB down to angular scales of less than 0.1° ($l \approx 1800$) [Aghanim et al., 2016]. This has greatly constrained cosmological parameters fit to the FLRW model. For example, the 2015 Planck resultes have been summarized in [Adam et al., 2016; Ade et al., 2016a]. Fig. 1.1 shows the anisotropies of the cosmic microwave background (CMB) as observed by Planck Satellite.

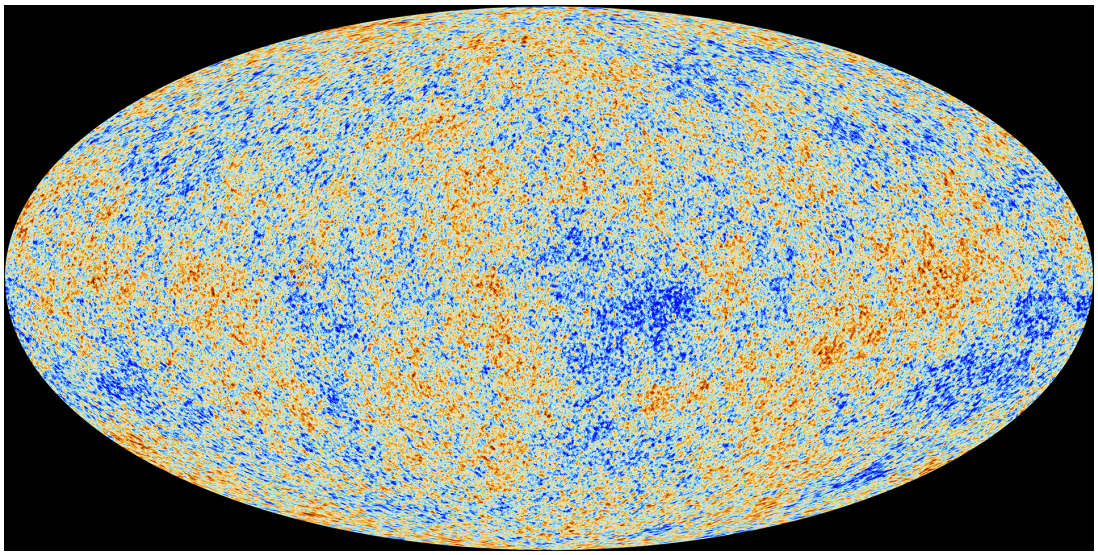

Figure 1.1: The anisotropies of the cosmic microwave background as observed by Planck, showing tiny temperature fluctuations that correspond to regions of slightly different densities which represent the seeds of all future structure: the stars and galaxies of today. The figure is taken from the ESA and Planck Collaboration, Credit: ESA

The discovery of the CMB is one of the most important milestones in our understanding of the Universe and has become one powerful tool for constraining the cosmological models. The abundant information contained in the CMB not only confirms the homogeneity and isotropy of the Universe on large scales, but also constraints cosmological parameters, and the properties of large-scale structures. It also constrains fundamental theories, such as cosmic inflation which makes predictions about the initial fluctuations of energy density. Together with

[5] For more information, see https://www.esa.int/Our_Activities/Space_Science/Planck.

the cosmological redshift-distance relation and light element abundances, the CMB was one of the most important pieces of evidence in establishing the hot Big Bang theory.

The most surprising observation in recent cosmological history is the fact that the expansion of our present Universe is accelerating – if modelled by a FLRW cosmology. Since gravity with ordinary matter that obeys the strong energy condition is universally attractive [6], it will always act to slow down any initial expansion. Consequently, it had been conventionally assumed that the present deceleration parameter $q_0 = q(t_0)$ would be positive.

For a universe containing matter in the form of pressureless dust with a density which scales as $\varrho_m = \varrho_{m0}\,(a_0/a)^3$ and radiation species with an energy density that scales as $\varrho_R = \varrho_{R0}\,(a_0/a)^4$ and pressure $p_R = \frac{1}{3}\,\varrho_R\,c^2$, the Friedmann equations (1.2), (1.3) may be rewritten as

$$\begin{aligned} 1 &= \Omega_m + \Omega_R + \Omega_k + \Omega_\Lambda, \\ q &= \frac{1}{2}\,\Omega_m + \Omega_R - \Omega_\Lambda. \end{aligned} \tag{1.5}$$

Here

$$\Omega_m \equiv \frac{\varrho_m}{\varrho_c},\ \Omega_R \equiv \frac{\varrho_R}{\varrho_c},\ \Omega_k \equiv -\frac{k\,c^2}{a^2\,H^2},\ \Omega_\Lambda \equiv \frac{\Lambda\,c^2}{3\,H^2},\ \varrho_c(t) = \frac{8\,\pi\,G}{3\,H^2}, \tag{1.6}$$

where ϱ_c is the critical density, namely the matter density given by the Friedmann equation (1.2) if $k = 0$ and $\Lambda = 0$. If $\Lambda = 0$ the spatially flat model demarcates between universes which undergo a Big Crunch ($k > 0$) and those that expand forever ($k \leq 0$).

Since $\Omega_R < 10^{-4}$ at the present day then a universe with $\Lambda = 0$ has $q_0 \approx \Omega_m/2$. With the assumption that the Universe only contained pressureless dust and radiation, for many decades observational cosmology was viewed as the "quest for two numbers": H_0 and q_0 [Sandage, 1970].

Determining these two numbers by accurate distance measurements was an extremely difficult problem that challenged more than one generation of as-

[6] The strong energy condition is the condition that $\mathcal{R}_{\mu\nu}\,V^\mu\,V^\nu \geq 0$ for any timelike vector field V^μ, and from the Einstein equations can be seen as a condition that matter focuses light rays. When applied to an perfect fluid with density ϱ and pressure p the strong energy condition gives $p \geq -\frac{1}{3}\varrho\,c^2$.

tronomers. It was only the advent of new large mosaic cameras incorporating charge coupled devices (CCDs) that made it possible to systematically survey wide areas of the sky and gather vast quantities of data for theoretical analysis. One of the most interesting and useful targets are the so-called Type Ia supernovae (hereafter, SNe Ia), which are considered to be "standard candles" for cosmological distance probes [Kowal, 1968; Phillips, 1993; Goobar and Leibundgut, 2011]. Taking advantage of these standardizable candles, Riess et al. [1998] of the High-z Supernovae Search Team presented the spectral and photometric observations of 16 Type Ia Supernovae in the redshift range $0.16 \leq z \leq 0.62$, showing that the observed high-z SNe Ia are dimmer than expected in a low mass density FLRW universe without a cosmological constant. Perlmutter et al. [1999] from the Supernovae Cosmology Project reported similar conclusions, suggesting a positive cosmological constant with a confidence $P(\Lambda > 0) = 99\%$. Both teams provided strong evidence that our Universe had entered a phase of accelerated expansion. A cosmological constant can be viewed as a form of energy with equation of state $p_\Lambda = -\varrho_\Lambda\, c^2$, *i.e.*, $p_\Lambda = w\, \varrho_\Lambda\, c^2$ with $w = -1$. However, any form of energy with $w < -1/3$ that violates the strong energy condition may also give rise to a accelerating expansion. In absence of understanding what such a field is, it has come to be called "dark energy".

Over the last two decades many other observations have strengthened and confirmed the apparently accelerated expansion, providing constraints on the parameter w. This has benefited from new large surveys. Major examples include the Hubble Space Telescope supernovae searches including $z > 1$ samples [Riess et al., 2001, 2004, 2007; Suzuki et al., 2012]; the Equation of State Supernova Cosmic Expansion Survey (ESSENCE supernovae survey) [Wood-Vasey et al., 2007]; the Supernova Legacy Survey (SNLS) [Conley et al., 2011; Sullivan et al., 2011; Li et al., 2011b]; the Sloan Digital Sky Survey (SDSS, including the Baryon Oscillations Spectroscopic Survey and the extend Baryon Oscillations Spectroscopic Survey, *i.e.*, BOSS and eBOSS) [Campbell et al., 2013; Sánchez et al., 2017; Grieb et al., 2017]; the Pan-STARRS1 Medium Deep Survey [Rest et al., 2014]; the Planck project [Ade et al., 2016a] (see also the references therein and citations.); the Combined Pantheon Sample [Scolnic et al., 2018]; and so on.

In addition to SNe Ia distances and redshifts, the large galaxy surveys on the list above are able to detect the echo of the first acoustic peak in the pri-

mordial plasma. Such an echo is characterized by a slight excess of galaxies separated by the corresponding comoving distance scale, close to $100 - 110h^{-1}$ Mpc. Huge numbers of galaxies are required to detect this Baryon Acoustic Oscillation (BAO) scale in the galaxy-galaxy correlation function. This provides an alternative standard ruler for cosmological tests, which is becoming increasingly useful as observational techniques reach greater precision.

Numerous papers have also been published trying to explain the physical characteristics of dark energy during last few decades. Several reviews have summarized the recent development of dark energy theories. Li et al. [2011a] reviewed the problem of dark energy in great detail, with a survey of theoretical models and some aspects of numerical studies. Copeland et al. [2006] discussed the observation evidence for the accelerating expansion, and presented some models explaining dark energy, with particular attention to the scalar field models. An older but still worthwhile review was published by Peebles and Ratra [2003], who presented the basic concepts and the status of the observational evidence for cosmic acceleration at that time. Weinberg and coauthors have written a more recent review on observational probes of cosmic acceleration [Weinberg et al., 2013]. See also [Frieman et al., 2008; Silvestri and Trodden, 2009; Caldwell and Kamionkowski, 2009] for other viewpoints.

Generally speaking, the ways people attack the problem are diverse: from the mathematically simplest cosmological constant to the backreaction of inhomogeneities. Here we just briefly introduce some of the competing candidates for dark energy and other alternative explanations for the apparent acceleration.

1. The cosmological constant:

This is the simplest way to explain the accelerating expansion, and mathematically corresponds to a perfect fluid with equation of state parameter $w = -1$. In his first cosmological paper [Einstein, 1917] Einstein introduced this cosmological constant in order to allow for a static universe[7]. In this original introduction the constant Λ was freely added to the left hand of Einstein's equation, not as a matter source. Soon after the discovery of cosmic expansion this constant was abandoned by Einstein himself as the static solution is unstable. The cosmo-

[7] This is obtained by setting $k = +1$, $p_H = 0$, $\Lambda = 4\pi G\varrho_H/c^2$, and $\varrho_H = c^2/(12\pi G\, a_0^2)$ in (1.2), (1.3) so that $\dot{a} = 0$ and $\ddot{a} = 0$, where a dot means a time derivative.

logical constant was largely ignored by most cosmologists once the Big Bang theory was successfully established until the late 1980s, when more and more observational datasets began to support models with $\Omega_{m0} \simeq 0.1 - 0.3$ [Turner et al., 1984; Efstathiou et al., 1990; Krauss and Turner, 1995]. While consistent with an open ($k = -1$) Friedmann universe, spatially flat models were preferred by many theorists as a natural outcome of cosmic inflation. This possibility is admitted if $\Omega_{\Lambda 0} \simeq 1 - \Omega_{m0}$.

If the cosmological constant is not just a "freely added term" then the vacuum energy density expected in theories of particle physics would be a likely potential explanation for it. However, the value expected from crude particle physics estimates is almost 120 orders of magnitude larger than what astronomical observation suggests. This is well-known as "the cosmological constant problem" and has been discussed by many authors. See [Weinberg, 1989; Rugh and Zinkernagel, 2002] and references therein.

Among many reviews we note a few. Several aspects of the cosmological term as a universal constant both from the cosmological and field theoretical viewpoints with an emphasis on conceptual and fundamental issues have been reviewed by Padmanabhan [2003]. A brief review on cosmology in the presence of a cosmological constant is discussed pedagogically by Carroll [2001]. An older review, focusing on the inevitability of the cosmological constant and the problems relating it to vacuum energy was published by Carroll et al. [1992] before the discovery of accelerating expansion.

2. Quintessence:

Another candidate for dark energy is a fundamental scalar field ϕ named *quintessence*, which is minimally coupled to gravity. Unlike vacuum energy or the cosmological constant, such a scalar field is dynamical, time-dependent and spatially homogeneous [Wetterich, 1988; Peebles and Ratra, 1988; Caldwell et al., 1998; Zlatev et al., 1999] [8]. The evolution of the equation of state parameter w will depend on the time derivative (kinetic term) and potential term $V(\phi)$ of the scalar field. For different evolutionary behaviours of w, the quintessence models can be broadly classified into two kinds: the thawing model and the freezing

[8] Models with an inhomogeneous scalar field are also considered. However, only the homogeneous background evolution of $\phi(t)$ is relevant here.

model [Caldwell and Linder, 2005]. Simply speaking, the former at early times has $w = -1$ when the kinetic term is negligible and then grows to less negative values of w as the kinetic term evolves. The later has $w \approx 0$ initially and then decreases with time until $w \approx -1$ [Pantazis et al., 2016].

A particular subclass of the freezing models, the so-called tracker solutions have the potential to produce the current quintessence energy density without facing the coincidence problem. If cosmological measurements show a dynamical dark energy density, then quintessence could be a good candidate. We mention two notable good reviews, Shinji [2013] paid particular attention to the evolution of w, and discussed the particle physics models of quintessence. Linder [2008] focused on the dynamics of the quintessence, with a discussions about classification of the different physical behaviours.

3. Modified Gravity:

The biggest current cosmological mysteries – dark energy and dark matter – both arise in the context of gravitational physics. Consequently, we should ask whether General Relativity is the correct alternative. GR has been tested to very high precision in isolated systems, such as the solar system, binary star systems and even for merging binary black holes [Abbott et al., 2016]. GR seems to be valid for all small scales, but an open question still exists: no one knows whether GR is still adequate for large scales within the Universe. Furthermore, there is as yet no quantum theory of gravity. Considered as a field theory Quantum General Relativity is not renormalizable. Rather than putting exotic sources of matter on the right hand side of Einstein's equations, a number of physicists have sought explanations for the present acceleration expansion by modifying the left hand side of the equations. A huge number of different approaches have been investigated [Clifton et al., 2012; Joyce et al., 2015]. One well-known class of modified theories replaces the Einstein-Hilbert action by a function of the Ricci scalar and is referred to as $f(R)$ theories. Such models have been applied to explain the cosmic accelerating without the appearance of dark energy by many authors. For example, see [Hu and Sawicki, 2007; Deruelle et al., 2008; Linder, 2009; Amendola and Tsujikawa, 2008]. However, all modified GR theories, including $f(R)$ theory, when being applied to cosmology have to obey two simple rules. First, they have to reduce to GR on the small scales on which it

is tested and, second, the matter-dominated era must be always followed by the cosmic accelerating era. A large wide of $f(R)$ dark energy models of the type $f(R) = \alpha R^{-n}$ or $f(R) = R + \alpha R^{-n}$ have been disfavoured if $n > 0$ or $n < -1$ [Amendola et al., 2007a,b]. Nonetheless modified GR is still an interesting and much studied competitor.

4. Backreaction/ Inhomogeneities:

A completely different alternative to either adding exotic fields on the right hand side if Einstein's equations or modifying the tensor on the left hand side is to realize cosmic acceleration as an apparent effect due to inhomogeneities of cosmological clumpy structures. In this relatively conservative approach the FLRW approximation (or the cosmological principle) in some sense is not assumed.

By assuming our position in the Universe to be special, the cosmological constant or dark energy can be avoided in an inhomogeneous model with an almost isotropic CMB. For example, the LTB model developed in the 1930s has been invoked to interpret the deviations of the observed magnitude-redshift relation of SNe Ia from the one in homogeneous model [Célérier, 2000; Kenji, 2000; Tomita, 2001; Iguchi et al., 2002; Enqvist, 2008]. Very often one considers a large void, with our position close to the centre, although the model closest to the standard cosmology actually has a density hump [Célérier et al., 2010]. However, such models violate the Copernican principle. Furthermore, it has been claimed that the observational data including CMB constraints is inconsistent with such void models, suggesting these models (not all) can be ruled out [Zibin et al., 2008; Zibin, 2011; Moss et al., 2011] [9]. Other more complex models, such as the Szekeres inhomogeneous cosmological models, have also been used to fit the luminosity distance and redshift relations by several authors [Nwankwo et al., 2011; Bolejko and Célérier, 2010].

Another important idea relating to the inhomogeneities of the Universe and having the potential to explain cosmic acceleration is the so-called backreaction effect. Rather than assuming that Einstein's equations hold exactly on cosmological scales, the relevant equations are averages of Einstein's equations. In such

[9] Advocates of this approach generally state that when trying to use the Lemaître-Tolman models in cosmology they must be considered as the first step before developing more sophisticated models, since they are only uncomplicated mathematical simplifications [Célérier, 2012].

schemes, no new physics appears at the level of the gravitational action, and the acceleration or dark energy is only a mirage from the backreaction effect of inhomogeneities. Over the last two decades, this idea has attracted more and more interest from the community of cosmologists, as it connects local structures to the averaged "global" properties of the Universe with General Relativity as the only local theory of gravity on small scales. More detailed discussions will be given in following sections.

1.2 The present Universe is inhomogeneous: averaging and backreation

For the last one hundred years, the standard cosmology based on the Cosmological Principle has made remarkable achievements, and greatly deepens our understanding of the nature of the Universe in which we live, with just a handful of parameters to account for all observations. However, the homogeneous distribution of matter is only an approximation and may be illusionary, as pointed out by Einstein himself [Einstein, 1917; O'Raifeartaigh and McCann, 2014]. Indeed, as mentioned in section 1.1 the observational data has shown that our present Universe is dominated by voids with most matter contained in galaxies in elongated filaments, sheet-like walls and knots of dense clusters [Pan et al., 2012]. All these large-scale structures, including the galaxies and groups contained in these structures are woven into the well-known "cosmic web" [Bond et al., 1996]. Fig. 1.2 shows the galaxy distribution obtained from spectroscopic redshift surveys and from mock catalogues constructed from cosmological simulations.

The rich hierarchies of large-scale structures in the Universe indicate that a detailed description of physical reality is likely to be extremely complicated. Consequently, a "smoothed-out" approximation is unavoidable for the theoretical understanding of the evolution of the Universe. In another sense, taking account of the locality of Einstein's field equations, such approximation corresponds to the question: on which scale the General Relativity is valid? There is no doubt that Einstein's field equations are valid for isolated systems, from small scale structures like the solar system to larger scale structures like a single void (For voids, one has to make a smooth approximation).

If we want to apply General Relativity on the scale of cosmic web, we have to ignore the details presented on small scales and, for example, use a background geometry to calculate the large-scale observables. This is what people do in standard FLRW cosmology, which is an exact solution of Einstein's field equations.

Simply admitting such an easy and uncomplicated framework raises several issues, however. The most well-known one is called the *fitting problem*, first discussed by Ellis [1984] and by Ellis and Stoeger [1987], namely what is the physical correct way to fit an idealised exactly homogeneous and isotropic cosmological model to a real lumpy universe. Another issue relates to structure formation itself. It has been suggested that structures may grow more rapidly than those in the standard approach using the FLRW model, perturbation theory and Newtonian N-body simulation, and a better theoretical approach may be needed [Peebles and Nusser, 2010]. Furthermore, we also need to specify which observers will make measurements closest to those of an ideal homogeneous and isotropic universe. Indeed, perhaps the most mysterious unsolved puzzle, "dark energy", could be explained by the consideration of effects of local large scale structures. Consequently, it is only in an averaged sense that we can apply spatial homogeneity to our present Universe, and the standard FLRW model may be not the best one to fit all observations [Buchert et al., 2016].

1.2.1 Averaging

When Einstein applied his equations to cosmology, the matter in the Universe was assumed to be a uniform continuous distribution. In this sense, one is actually averaging the right hand side of Einstein's field equation, while leaving the left hand side to be in unaveraged form:

$$G_{ab} = \frac{8\pi G}{c^4}\bar{T}_{ab}\,, \tag{1.7}$$

where G_{ab} is Einstein tensor describing the geometry of spacetime, $\bar{T}_{ab}$ is energy-momentum tensor after an averaging process, and g_{ab} is the metric of spacetime. Here G_{ab} is a function of g_{ab}. With the averaged energy-momentum tensor on the right hand side, one can easily derive a homogeneous and isotropic cosmological

model as the solution of Eq. (1.7). However, in principle, "half-averaged" equations may not be valid, whether from the microscopic or from the macroscopic viewpoint. We also need to average the left hand side to reach a fully averaged form of Einstein's field equations. But a fundamental property of inhomogeneous averaging is that usually the product of the mean of two quantities is not equal to their mean product, and similar for derivative operations. Thus in general one will have $\bar{G}_{ab}(\mathbf{g}) \neq G_{ab}(\bar{\mathbf{g}})$ where $\mathbf{g}$ denotes the general metric. Extra terms will appear in the averaged Einstein field equations, making them different to the local Einstein field equations. This problem was first (to my knowledge) discussed by Shirokov and Fisher [1963] where they investigated isotropic spaces with discrete masses sources. They stated that the fully averaged Einstein field equations should have a structure

$$G_{ab}(\bar{\mathbf{g}}) + C_{ab}(\bar{\mathbf{g}}) = \frac{8\pi G}{c^4}\bar{T}_{ab}\,, \tag{1.8}$$

where $C_{ab}(\bar{\mathbf{g}})$ are terms depending on the fluctuations of the microfield, *i.e.*, the local inhomogeneities. Rather than being seen as additional "correction" terms to Eq. (1.7), they pointed out that the appearance of these terms was a consequence of the averaging process. This already demonstrates the basic and significant issue of the averaging process: it does not commute with the implementing field equations. Thus the extra terms resulting from the averaging process may have significant effects on the evolution of large scale structure and the dynamics of the Universe. These extra terms are known as "backreaction terms" which I will discuss later.

Concerning the importance of averaging, different approaches have been presented and discussed. We will very briefly list some of them here.

1. Buchert's approach:

By adapting a fluid-flow comoving observer, Buchert and Ehlers [1997], Buchert [1996b] proposed a spatial averaging formalism on an arbitrary domain for the (nonlinear) equations of Newtonian cosmology in 1995. Buchert [2000a, 2001] later generalized this formalism to general relativistic cosmologies. In this procedure, the Einstein equations with a vorticity-free perfect fluid are averaged to give evolution equations for the averaged cosmological scalars like the expansion

and shear scalars[10]. A detailed discussion will be deferred to section 1.3.

One potential drawback of Buchert's approach is that the averaging procedure can only be applied to scalar quantities, whereas the full Einstein equations are of course tensorial. Nonetheless, it might be argued that for cosmology the most significant quantities to be averaged on the right hand side of the Einstein equations are scalars: the density and pressure of perfect fluids. Therefore a scalar averaging process is physically justified.

2. Zalaletdinov's approach:

Zalaletdinov [1992, 1993] initiated and developed a comprehensive approach to covariantly averaging tensors which he called Macroscopic Gravity. In this approach Zalaletdinov defined the so-called bi-tensor operator to compare tensors at different locations in spacetime. For a tensor $T_{ab}(x)$ and the bi-operator $\mathcal{A}^{a'}{}_{a}(x,x')$ the covariant spacetime average is defined

$$\bar{T}_{ab}(x) = \frac{\int_\Sigma \mathcal{A}^{a'}{}_{a}(x,x')\mathcal{A}^{b'}{}_{b}(x,x')T_{a'b'}(x')\sqrt{-g(x')}d^4x'}{\int_\Sigma \sqrt{-g(x')}d^4x'}, \tag{1.9}$$

where

$$\mathcal{A}^{a'}{}_{a}(x,x')\mathcal{A}^{b'}{}_{b}(x,x')T_{a'b'}(x') = T_{ab}(x,x') \tag{1.10}$$

is defined as the bi-tensor extension of T_{ab} at spacetime locations x and x'. Essentially Zalaletdinov added extra mathematical structure in order to deal with the mathematical complications of defining consistent tensorial averages. Such structure must be subject to physical interpretation. Zalaletdinov chose the structure to make the averaged theory have a structure similar to general covariance, when averaged on any scale. It was thus designed to apply to any situation in General Relativity, not only cosmology. However, it is not clear that general covariance – which is desired to consistently incorporate gravity into matter field equations – is the correct symmetry for a generic average of the gravitational degrees of freedom in the Einstein tensor.

3. Other approaches:

Besides the above two approaches, there are also other procedures focusing on the averaging problem of local inhomogeneous structures. Most of these

[10] A generalization to include vorticity is to be published shortly [Buchert et al., 2018].

approaches have been compared and discussed in many reviews. For example, see [Clarkson et al., 2011]. Each approach has its own advantages and drawbacks. The diversity of procedures for studying the averaging problem is indicative of a research field in which many open questions and challenges remain.

1.2.2 Backreaction

Although the averaging problem was identified as early as the 1960's [Shirokov and Fisher, 1963], it did not attract much attention from the community of cosmologists judging by its citation history. For many decades observational details about the matter distribution were imprecise, and researchers did not explore theoretical models beyond the simplest homogeneous ones. It is usually agreed that the importance of the averaging and backreaction problems were most visibly raised by Ellis [1984]; Ellis and Stoeger [1987]; Ellis [2011], and then developed by many other authors.

As an example, Futamase [1988, 1989] studied the effects of averaging and backreaction in a cosmological setting by developing an approximation scheme to construct a model of a fully inhomogeneous universe, where a perturbative expansion of the metric and a simple spatial averaging procedure were employed[11].

Zotov and Stoeger [1992] averaged the Einstein equation first for a space-like distribution of stars, then for an expanding system of galaxies and discussed the effect of inhomogeneities on cosmic expansion. However, in this case they had chosen some exact spherically symmetric background metric for averaging before discussing the effects of inhomogeneities.

Kasai [1993] discussed a scheme to construct inhomogeneous universes that are homogeneous and isotropic on average. By working in the framework of general relativistic inhomogeneous models containing dust and a cosmological constant, Kasai derived a propagation equation for the peculiar part of the deformation tensor. He then obtained an evolution equation for the exact density

[11] In [Futamase, 1988] the spatial average is simply defined as:

$$\langle Q \rangle = V^{-1} \int_V Q dV$$

where dV is the invariant volume element in the background space. This means the spatial averaging was taken with respect to the fixed background metric.

contrast defined by the ratio of the averaged density and the real local density. In contrast to the averaging procedure used by Futamase, Kasai defined his averaging procedure with respect to the physical metric of the inhomogeneous space. This formalism then was improved and developed by Buchert and his collaborators [Buchert and Ehlers, 1997; Buchert, 2000a, 2001; Buchert et al., 2018].

With the advances in observational techniques and the collection of larger data sets, the backreaction effects of local inhomogeneities have become a serious and important research arena for observational cosmology. How significant the effects of backreaction on the dynamics of the Universe are, is a subject of vigorous ongoing debate among the cosmologists and there is still no consensus on the issue. Three main different viewpoints have been summarized by Clarkson et al. [2011]. We will summarize as follows:

- Ishibashi and Wald [2006] and Green and Wald [2011, 2013, 2015] claim that the Universe can be accurately described by the standard FLRW cosmological model plus small perturbations, and backreaction is a small trace-free term that cannot mimic dark energy. However, this claim is based on a different definition of backreaction than that assumed by other members of community. In particular, Green and Wald prove a related theorem by assuming that the average evolution is an exact solution of Einstein's equations with a prescribed energy-momentum tensor at any scale of averaging. They then derive their result based on an approximation scheme in this setting. It was subsequently pointed out that even with this framework, particular assumptions of Green and Wald are not mathematically general[Buchert et al., 2015; Ostrowski and Roukema, 2017]. Furthermore, the assumption that the average evolution is an exact solution of Einstein's equations on arbitrary large scales of averaging is not made in any approach to backreaction which claims phenomenological success in dealing with dark energy.

- Another school of thought is that while backreaction effects are those of the more general class of models not considered by Green and Wald, they are not large enough to be responsible for the apparent acceleration of the Universe. However, they might lead to corrections of the order of at most

a few percent relative to an average Friedmann model. Such ideas are often based on perturbative calculations based on series expansions near a standard FLRW cosmology. The arguments between those who claim that the effects are too small to account for cosmic acceleration (*i.e.*, Flanagan [2005]; Vanderveld et al. [2007]; Adamek et al. [2016, 2017]) and those argue to the contrary (*i.e.* Kolb et al. [2006]; Kolb [2011]) then amount to different assumptions about which terms can be neglected, choices of gauge, or the order of the perturbation expansion. Some others argue that we can only resolve this issue with a deeper and better understanding of higher-order perturbation theory [Clarkson and Umeh, 2011].

- Those who argue for backreaction as a solution to the problem of dark energy do so in terms of a fully nonlinear approach to average cosmic evolution, in which the Friedmann equation is significantly violated at late cosmic epochs [Buchert, 2008; Wiltshire, 2007a,b, 2008]. An important question is then how to relate statistical averages of small scale solutions of Einstein's equations to light propagation on cosmological scales. A variety of phenomenological approaches have been employed [Wiltshire, 2007a, 2009; Larena, 2009; Lavinto et al., 2013]. Of these approaches, the timescape model has the most developed phenomenology [Wiltshire, 2007a,b, 2008; Duley et al., 2013; Nazer and Wiltshire, 2015]. In this approach, the backreaction term is at most of order 4% of the energy density as a volume average quantity. However, the volume averages must be recalibrated in terms of measurements made by observers in bound structures. The volume-averaged quantities – which include an always positive deceleration – are those inferred by an observer in a typical location by volume, namely one whose local spatial curvature is the same as the spatial curvature smoothed over the largest scales. Since the Universe is dominated by voids at late times this refers to an observer in a void, with local negative spatial curvature. By contrast, all actual observers and sources necessarily occupy regions which were greater than critical density. We have a mass-biased view of the Universe. Wiltshire's model is called the timescape on account of the recalibration of clocks between observers in bound structures and statistical volume average quantities. The Universe is effectively

described by more than a single age. This model has been successfully fit to supernova data [Leith et al., 2008; Smale and Wiltshire, 2011; Dam et al., 2017], and gamma-ray burst distances[Smale, 2011]. Investigations on the detailed features of the CMB by Nazer and Wiltshire [2015] show that there are systematic uncertainties in parameters such as the baryon-to-photon ratio, and the spectral index. These uncertainties arise from the fact that effects of backreaction in the primordial plasma – which are possibly of order 10^{-5} of average energy density at that epoch – have not been included.

To incorporate backreaction in the primordial plasma first requires a better approach to perturbation theory which is more tied to fluid particles. This is one of motivations for the studies made in this thesis.

For more complete discussion of the backreaction effects on the dynamics of the Universe, it is useful to check the following reviews: [Räsänen, 2004; Buchert, 2008; Ellis, 2011; Clarkson et al., 2011; Buchert, 2011; Kolb, 2011; Räsänen, 2011; Wiltshire, 2011, 2014].

1.3 A brief prescription of the spatial average of Einstein's equations

With the notions of averaging and backreaction introduced above, we present the spatial average of Einstein's equations in this subsection. Here we only consider the scalar averaging approach.

Before continuing, we will briefly introduce the $3+1$ decomposition of Einstein's equations, which has been widely accepted and used in General Relativity [12]. A comprehensive and detailed discussion is given in many standard textbooks. For example, see Gourgoulhon [2007]; Dengiz [2011].

[12] An alternative procedure of splitting spacetime is called the $1+3$ formalism, being built from a congruence of time-like integral curves, and providing a global time-like relation between points. For an introduction to this kind of procedure and its difference from the $3+1$ formalism, see Roy [2014].

1.3.1 The choice of foliations

Consider a time orientable spacetime $(\mathcal{M}, \mathbf{g})$, where $\mathcal{M}$ is a real smooth spacetime manifold of dimension 4 and $\mathbf{g}$ is the metric of this manifold with signature $(-,+,+,+)$. In the framework of General Relativity there is no absolute space and absolute time, but one can still consider a $3+1$ splitting of spacetime for understanding the dynamics of matter and geometry. Simply speaking, a $3+1$ splitting means the spacetime can be covered by a continuous set of hypersurfaces $(\Sigma_t)_{t\in\mathbb{R}}$, where a "hypersurface" Σ of $\mathcal{M}$ stands for the image of a 3-dimensional manifold $\hat{\Sigma}$ by an embedding $\Phi : \hat{\Sigma} \to \mathcal{M}$. The embedding usually means a homomorphism (*i.e.* one-to-one) mapping so that $\Sigma = \Phi(\hat{\Sigma})$ will not intersect itself. The subscript t comes from the alternative definition that a hypersurface can be locally defined as a set of points on $\mathcal{M}$ for which a scalar field t is constant, that is

$$\forall p \in \mathcal{M}, \quad p \in \Sigma \iff t(p) = const. \tag{1.11}$$

For a spacelike hypersurface Σ of $\mathcal{M}$, if each causal curve without endpoints on $\mathcal{M}$ intersects this hypersurface once and only once, then this spacelike hypersurface is called a Cauchy surface. A spacetime $(\mathcal{M}, \mathbf{g})$ is said to be globally hyperbolic if it admits a Cauchy surface. The topology of a globally hyperbolic spacetime is necessarily $\Sigma \times \mathbb{R}$, which is indeed "$3+1$". In common when we use the $3+1$ formalism to model the spacetime or cosmology, we consider the cosmic spacetime to be a globally hyperbolic one.

Furthermore, if a globally hyperbolic spacetime is continuously covered by a family of spacelike hypersurfaces $(\Sigma_t)_{t\in\mathbb{R}}$ then we say such a spacetime is foliated by this family of hypersurfaces. In general any globally hyperbolic spacetime can be foliated by $(\Sigma_t)_{t\in\mathbb{R}}$. In mathematical language, (similar to Eq. (1.11)) a foliation means there exists a smooth scalar field $\hat{t}$ with non-vanishing gradient on $\mathcal{M}$ so that each Σ_t will be a level surface of this field:

$$\forall p \in \mathcal{M}, \quad \Sigma_t \equiv \{p \in \mathcal{M}, \hat{t}(p) = t\}. \tag{1.12}$$

Notice for a $\hat{t}$ with non-vanishing gradient the hypersurfaces are non-intersecting: $\Sigma_t \cap \Sigma_{t'} = \emptyset$ for $t \neq t'$.

A coordinate system (usually a local system) is necessary for mathemati-

cally solving the Einstein equations. For a hypersurface Σ_t with scalar field $t = constant$, one can introduce a spatial coordinate system $(x^i) = (x^1, x^2, x^3)$ on this hypersurface. If this system varies smoothly between neighbouring hypersurfaces, then the coordinate system $(x^\alpha) = (t, x^1, x^2, x^3)$ constitutes a well-defined coordinate system on the spacetime manifold $\mathcal{M}$. Then the normal unit vector of Σ_t can be defined as

$$n^\alpha = -\frac{\nabla^\alpha t}{\sqrt{-\nabla^\beta t\, \nabla_\beta t}} = -N\, \nabla^\alpha t, \tag{1.13}$$

where

$$N = \left(\sqrt{-\nabla^\beta t\, \nabla_\beta t}\right)^{-1/2}, \tag{1.14}$$

is called the *lapse function*. Any future-directing vector t^a can be decomposed as the superposition of a part normal to Σ_t and a part tangent to Σ_t:

$$t^a = N n^a + N^a, \tag{1.15}$$

where N^a is tangent to the hypersurface and is called the shift vector.

Mathematically, Σ_t can be arbitrarily chosen with the scalar field, t, arbitrary up to suitable smoothness criteria. However, the various choices will have physical implications in any attempt to apply the $3+1$ formalism to realistic cosmological spacetimes. For structure formation, the choice of foliation is closely related to the issue of gauge fixing in perturbation theory [Bardeen, 1980; Ellis and Bruni, 1989]. Different choices of foliation determine the specific form of the $3 + 1$ Einstein system, and some preferred choices will lead to remarkable advantages for dealing with the Einstein system.

- *Geodesic slicing:* this is the simplest case where the lapse function is set to be unity: $N = 1$. This implies that the worldlines of the observers are geodesics and the proper time along these worldlines coincides with the coordinate time t. The disadvantage of this choice is that the geodesics will tend to focus to a caustic. Thus this type of foliation will become pathological within a finite range of t. In this case the 4-velocity of observer is the normal unit vector n^a of the hypersurface Σ_t and the observer is called the *Eulerian observer*.

- *Comoving with fluid flow:* in this case the observer is comoving with the fluid flow so the hypersurface is chosen to be normal to the observer's worldline. The relation between the 4-velocity u^a of the observer and the normal unit vector of Σ_t is $u^a = n^a$, while the shift vector will be zero. The observer comoving with the fluid flow is known as the *Lagrangian observer* and this type of foliation is the basis of the Lagrangian perturbation of structure formation. A problem of this choice is the fluid flow must be irrotational. For the case of an irrotational dust fluid one may choose $N = 1$, so that the comoving slicing is also geodesic.

- *Constant mean curvature foliations:* consider a spacelike hypersurface (Cauchy surfaces) in a spacetime $(\mathcal{M}, \mathbf{g})$. The extrinsic curvature of this hypersurface is denoted by $\mathcal{K}_{ab}$. If $\mathcal{K} = Tr\,(\mathcal{K}_{ab})$ is a constant, then this hypersurface is said to have constant mean curvature. In the particular case that $\mathcal{K} = 0$ this hypersurface is called the *maximal hypersurface*. It has been pointed out that the constant mean curvature foliation will provide a global time coordinate that is invariantly defined by the manifold [Rendall, 1996]. But not all spacetimes admit this type of surface, and even if a spacetime admits a constant mean curvature Cauchy hypersurface the entire spacetime is not necessarily be covered by a constant mean curvature foliation [Bartnik, 1988; Isenberg and Rendall, 1998].

Of course there are other useful choices of foliations. For a detailed discussion we refer the reader to Gourgoulhon [2007].

1.3.2 Basic equations in 3+1 form for different observers

In this section we will first clarify the relation of different quantities as determined by the Eulerian observer with 4-velocity n^a and a flow-comoving observer with 4-velocity u^a in the framework of $3 + 1$ procedure. Then we will simplify the result to the irrational perfect fluid case.

1.3.2.1 Metric

Without setting special foliations, a natural foliation is given by the hypersurfaces orthogonal to the worldline of Eulerian observers. The components of the unit

normal vector n_a and its contravariant components can be expressed in terms of N and N^a as

$$n_a = (-N, 0, 0, 0), \tag{1.16}$$

$$n^a = \frac{1}{N}(1, -N^1, -N^2, -N^3). \tag{1.17}$$

With respect to the spatial coordinates system $\{x^i\}$, one can introduce the 3-metric on the hypersurfaces Σ_t

$$f_{ab} \equiv g_{ab} + n_a\, n_b, \tag{1.18}$$

where g_{ab} is the spacetime metric in terms of 3+1 quantities:

$$g_{\alpha\beta} = \begin{pmatrix} g_{00} & g_{0j} \\ g_{i0} & g_{ij} \end{pmatrix} = \begin{pmatrix} -N^2 + N_i N^i & N_j \\ N_i & h_{ij} \end{pmatrix}. \tag{1.19}$$

Thus, the 4-dimensional line element can be decomposed as:

$$ds^2 = g_{\alpha\beta} dx^\alpha dx^\beta = -(N^2 - N_i\, N^i)dt^2 + 2N_i\, dt\, dx^i + f_{ij}\, dx^i dx^j. \tag{1.20}$$

Notice that

$$f_{ij} = g_{ab} h^a{}_i\, h^b{}_j \tag{1.21}$$

are the components of the 3-metric.

In the description of the dynamics of the fluid, different time parameters can be considered. Suppose τ is the time associated to the flow-comoving observers (namely the Lagrangian observers), along their flow lines whereas t is a general time coordinate depending on our choice of foliation of space-time, and τ_0 is the time associated with the Eulerian observers, attached to the foliation. Then it is possible to show that for any tensor field $\mathcal{F}$ [13]:

$$u^a \nabla_a \mathcal{F} \equiv \frac{d\mathcal{F}}{d\tau} = \frac{\gamma}{N} \frac{d\mathcal{F}}{dt} = \dot{\mathcal{F}}, \tag{1.22}$$

[13] Recall that the observers are comoving with the fluid so that the 3-velocity in their own frames is zero.

where

$$N = \frac{d\tau_0}{dt},\ \gamma = \frac{d\tau_0}{d\tau}.$$

This equation defines the overdot used in subsequent expressions. Furthermore, $\mathcal{F}$ is a function of t and x^i, so that

$$\begin{aligned} \frac{d\mathcal{F}}{dt} &= \frac{\partial \mathcal{F}}{\partial t} + \frac{dx^i}{dt}\frac{\partial \mathcal{F}}{\partial x^i} \\ &= \frac{\partial \mathcal{F}}{\partial t} + V_i \frac{\partial \mathcal{F}}{\partial x^i}, \end{aligned} \tag{1.23}$$

where $V_i \equiv dx^i/dt$ is the spatial coordinate velocity.

1.3.2.2 Energy-momentum tensor for a general model and the 3+1 decomposition of Einstein's equation

The energy-momentum tensor for a general matter model can be decomposed relative to the 4-velocity u^a in rest frame of the fluid as [Ehlers, 1971, 1993]:

$$T_{ab} = (\epsilon + p)u_a u_b + p g_{ab} + 2q_{(a}u_{b)} + \pi_{ab}, \tag{1.24}$$

where ϵ, p are the relativistic energy and pressure density respectively, $q_c \equiv -T_{ab}h^a{}_c\, u^b$ is the energy flux and $q_a u^a = 0$. $\pi_{ab} \equiv T_{cd}\, h^c{}_a\, h^d{}_b - \frac{1}{3}\, T_{cd}\, h^{cd}\, h_{ab}$ is anisotropic stress and $\pi_{ab}u^b = 0, \pi^a{}_a = 0$. Here we have defined $h_{ab} = g_{ab} + u_a\, u_b$ to be the projector orthogonal to the fluid flow lines – in contrast to f_{ab} which is the projector orthogonal to n^a.

It has been pointed out that the anisotropic dynamic quantities q_a and π_{ab} can in general encode either relative velocity effects or dissipative effects, or both [Barrow and Maartens, 1998]. However, one is free to choose the 4-velocity u^a to set $q^a = 0$, so that in the comoving frame no energy flux will be observed [Ehlers, 1971]. We will keep q^a explicitly in the following calculations.

Without loss of generality, one can assume that the normal vector and the 4-velocity are same, *i.e.*, $n^a = u^a$, if the matter model is irrotational. We will try to keep the formulas as general as possible until specifically choosing the foliation.

Any tensor P_{ab} which satisfies the orthogonality condition $n^a P_{ab} = 0$ is said to be the *spatial tensor*. Correspondingly, the *spatial derivative* of a spatial tensor

is defined as

$$D_a P^{b_1\cdots b_m}{}_{c_1\cdots c_n} = f^{b_1}{}_{d_1}\cdots f^{b_m}{}_{d_m} f^{e_1}{}_{c_1}\cdots f^{e_n}{}_{c_n} f^{f}{}_{a}\,\nabla_f P^{d_1\cdots d_m}{}_{e_1\cdots e_n}\,. \tag{1.25}$$

For a scalar p, the spatial derivative is its partial derivative $D_a p = \partial_a p$.

From the energy-momentum conservation equations $\nabla_b T^{ab} = 0$, the energy and momentum conservation laws are:

$$\dot{\epsilon} + (\epsilon + p)\Theta = \mathcal{A}, \tag{1.26}$$

$$(\epsilon + p)A_a + D_a p = \mathcal{B}_a, \tag{1.27}$$

where

$$\mathcal{A} = -D_a q^a - 2A_a\, q^a - \bar{\sigma}_{ab}\,\pi^{ab}, \tag{1.28}$$

$$\mathcal{B}_a = -D^b \pi_{ab} - \dot{q}_a - \frac{4}{3}\theta\, q_a - \bar{\sigma}_{ab}\, q^b - \bar{\omega}_{ab}\, q^b - A^b\,\pi_{ab} + u_a\, q^b\, A_b, \tag{1.29}$$

$$A_a = u^b\,\nabla_b u_a = \dot{u}_a, \tag{1.30}$$

$$\Theta = \nabla_a u^a, \tag{1.31}$$

$$\bar{\sigma}_{ab} = \nabla_a u_b - \frac{1}{3}\Theta\, h_{ab} + \dot{u}_b\, u_a - \bar{\omega}_{ab}. \tag{1.32}$$

A_a is the acceleration contained in the hypersurfaces with normal vector u^a, Θ is the rate of volume expansion. $\bar{\sigma}_{ab}$ is the shear tensor which is the trace-free part of Θ_{ab} and the shear scalar is defined by $\bar{\sigma}^2 \equiv \frac{1}{2}\bar{\sigma}_{ab}\,\bar{\sigma}^{ab}$, which $\bar{\omega}_{ab} \equiv \nabla_{[b}u_{a]} + A_{[a}u_{b]}$ is the twist or vorticity tensor. Define $\bar{B}_{ab} \equiv h^c{}_a\, h^d{}_b \nabla_c u_d$, then $\bar{B}_{ab} = \Theta_{ab} + \bar{\omega}_{ab}$ and $\Theta_{ab} = \bar{B}_{(ab)}$, $\bar{\omega}_{ab} = \bar{B}_{[ab]}$, with $h_{ab} = g_{ab} + u_a u_b$.

Generally speaking, the 4-velocity u^a can be decomposed as

$$u^a = \gamma\,(n^a + v^a)\,, \quad \gamma = (1 - v_a\, v^a)^{-1/2}\,, \tag{1.33}$$

where v^a is called the *tilt* denoting the spatial velocity of the fluid flow relative to the Eulerian frames and γ is the Lorentz factor. An equivalent form to (1.24) for the energy-momentum tensor T_{ab} observed by the Eulerian observers (if $n^a \neq u^a$) is given by:

$$T_{ab} = E\, n_a\, n_b + 2\, n_{(a} J_{b)} + S_{ab} + 2\, n_{(a} I_{b)} + W_{ab}, \tag{1.34}$$

where

$$E = \epsilon\,\gamma^2 + (\gamma^2 - 1)\,p, \quad J_a = \gamma^2\,(\epsilon + p)v_a, \tag{1.35}$$

$$S_{ab} = \gamma^2(\epsilon + p)v_a\,v_b + p\,h_{ab}, \quad I_a = \gamma\,q_a, \tag{1.36}$$

$$W_{ab} = 2\,\gamma\,v_{(a}q_{b)} + \pi_{ab}, \quad U_{ab} = W_{ab} + 2\,n_{(a}I_{b)}. \tag{1.37}$$

Here q_a and π_{ab} are still the quantities defined in (1.24) with respect to u^a. The orthogonality is described by

$$n_a J^a = 0, \quad S_{ab}\,n^a = 0. \tag{1.38}$$

Furthermore,

$$S = g^{ab}\,S_{ab} = (\gamma^2 - 1)\,\epsilon + (\gamma^2 + 2)\,p, \quad U = g^{ab}\,U_{ab} = 0, \tag{1.39}$$

$$T_{ab}\,n^a\,n^b = E + U_{ab}\,n^a\,n^b = E + \mathcal{U}. \tag{1.40}$$

With the kinematical and geometrical quantities introduced above, we can decompose Einstein's equations as follows [14]. Defining the *extrinsic curvature* of the hypersurfaces $\mathcal{K}_{ab} = -f^c{}_a\,f^d{}_b\,\nabla_c n_d$, the Einstein equations with the energy-momentum tensor Eq. (1.24) may be cast into a set of constraint equations, *viz.* the *Hamiltonian and momentum constraints*:

$$\mathcal{R} + \mathcal{K}^2 - \mathcal{K}^a{}_b\,\mathcal{K}^b{}_a = 16\pi G\,T_{ab}\,n^a\,n^b + 2\Lambda, \tag{1.41}$$

$$D_a\mathcal{K}^a{}_c - D_c\mathcal{K} = -8\pi G\,J_c, \tag{1.42}$$

where $J_a = T_{bc}\,n^c f^b{}_a$, $\mathcal{R}$ is the Ricci scalar of the hypersurfaces.

We define the Lie derivative $\mathscr{L}$ of a tensor $T^{a_1\cdots a_k}{}_{b_1\cdots b_l}$ with respect to an arbitrary vector field v_a by

$$\mathscr{L}_{\vec{v}}\,T^{a_1\cdots a_k}{}_{b_1\cdots b_l} = v^c\,\nabla_c T^{a_1\cdots a_k}{}_{b_1\cdots b_l} - \sum_{i=1}^{k} T^{a_1\cdots c\cdots a_k}{}_{b_1\cdots b_l}\,\nabla_c v^{a_i} + \sum_{j=1}^{l} T^{a_1\cdots a_k}{}_{b_1\cdots c\cdots b_l}\,\nabla_{b_j} v^c. \tag{1.43}$$

Then the derivative of an arbitrary spatial tensor $U^{a_1\cdots a_k}{}_{b_1\cdots b_l}$ on hypersurfaces

[14] A very detailed calculation is given by Gourgoulhon [2007]

Σ_t with respect to t can be given by its Lie derivative:

$$\begin{aligned}\frac{\partial}{\partial t}U^{a_1\cdots a_k}{}_{b_1\cdots b_l} &= f^{a_1}{}_{c_1}\cdots f^{a_k}{}_{c_k} f^{d_1}{}_{b_1}\cdots f^{d_l}{}_{b_l}\mathscr{L}_{\vec{t}}\,U^{c_1\cdots c_k}{}_{d_1\cdots d_l}\\ &= \tilde{\mathscr{L}}_{\vec{t}}\,U^{c_1\cdots c_k}{}_{d_1\cdots d_l},\end{aligned} \tag{1.44}$$

where $\tilde{\mathscr{L}}$ denotes the spatial projection of $\mathscr{L}$.

With the definition of the Lie derivative, the evolution equations of the metric and the extrinsic curvature are

$$\begin{aligned}\frac{\partial}{\partial t}f_{ab} &= -2N\mathcal{K}_{ab} + 2D_{(a}N_{b)},\\ \frac{\partial}{\partial t}\mathcal{K}_{ab} &= -N\,f^c{}_a\,f^d{}_b\,R_{cd} + N\mathcal{R}_{ab} - 2N\mathcal{K}_{ac}\,\mathcal{K}^c{}_b + N\mathcal{K}\mathcal{K}_{ab} - D_aD_bN + \tilde{\mathscr{L}}_{\vec{N}}\,\mathcal{K}_{ab}\\ &= N\{\mathcal{R}_{ab} + \mathcal{K}\,\mathcal{K}_{ab} - 2\,\mathcal{K}_{ac}\,\mathcal{K}^c{}_b + 4\pi G[(S-E)\,f_{ab} - 2S_{ab} - 2W_{ab}] - f_{ab}\,\Lambda\}\\ &\quad - D_aD_bN + \tilde{\mathscr{L}}_{\vec{N}}\,\mathcal{K}_{ab}.\end{aligned} \tag{1.45}$$

One can prove that

$$\mathcal{K}_{ab}\frac{\partial}{\partial t}f^{ab} = -\mathcal{K}^{ab}\frac{\partial}{\partial t}f_{ab}, \tag{1.46}$$

so the evolution equation of the trace of extrinsic curvature is

$$\frac{\partial}{\partial t}\mathcal{K} = N[\mathcal{R} + \mathcal{K}^2 + 4\pi G(S - 3E - 2\mathcal{W}) - 3\Lambda] - D^aD_aN + N^aD_a\mathcal{K}, \tag{1.47}$$

where $\mathcal{W} = f^{ab}W_{ab} = \gamma\,v_a\,q^a + \pi_{ab}\,n^a\,n^b$.

One can define [15]

$$\bar{\mathcal{F}} \equiv n^a\nabla_a\mathcal{F} = \frac{1}{N}\frac{\partial}{\partial t}\mathcal{F} - \frac{1}{N}N^a\tilde{\nabla}_a\mathcal{F}, \tag{1.48}$$

so that

$$\bar{\mathcal{K}} = [\mathcal{R} + \mathcal{K}^2 + 4\pi G(S - 3E - 2\mathcal{W}) - 3\Lambda] - N^{-1}D^aD_aN, \tag{1.49}$$

which is same as the perfect fluid case Eq. (A2f) in Buchert [2001] if $\mathcal{W} = 0$.

[15] We use ∇ to denote the covariant derivative with respect to the metric g_{ab}, while $\tilde{\nabla}$ denotes the covariant derivative with respect to the spatial coordinates. Note that it can be proved that $\tilde{\nabla}_a = D_a$ at least in this case.

According to Eqs. (1.22, 1.23), one has

$$u^a\nabla_a\mathcal{F} = \dot{\mathcal{F}} = \frac{\gamma}{N}\Big(\frac{\partial\mathcal{F}}{\partial t} + V^i\tilde{\nabla}_i\mathcal{F}\Big) = \gamma\,\bar{\mathcal{F}} + \frac{\gamma}{N}\,V^i\,\tilde{\nabla}_i\mathcal{F} + \frac{\gamma}{N}\,N^a\tilde{\nabla}_a\mathcal{F}, \quad (1.50)$$

so in the frame of u^a,

$$\dot{\mathcal{K}} = \gamma\,\bar{\mathcal{K}} + \frac{\gamma}{N}\,V^i\,\tilde{\nabla}_i\mathcal{K} + \frac{\gamma}{N}\,N^a\tilde{\nabla}_a\mathcal{K} = \gamma\,\bar{\mathcal{K}} + \gamma\,v^a\nabla_a\mathcal{K}. \quad (1.51)$$

The covariant derivative of the observer velocity u^a can be decomposed into

$$\nabla_b u_a = \frac{1}{3}h_{ab}\,\Theta + \bar{\sigma}_{ab} + \bar{\omega}_{ab} - A_a\,u_b, \quad (1.52)$$

where we recall that $\Theta \equiv \nabla_a u^a$ is the volume expansion rate, the trace of expansion tensor Θ_{ab}. Similarly, the covariant derivative of the n^a can be decomposed into

$$\nabla_b n_a = \frac{1}{3}\,f_{ab}\hat{\theta} + \hat{\sigma}_{ab} + \hat{\omega}_{ab} - n^c\nabla_c n_a\,n_b, \quad (1.53)$$

and

$$\begin{aligned} &\hat{B}_{ab} \equiv f^c{}_a\,f^d{}_b\,\nabla_c n_d = \hat{\theta}_{ab} + \hat{\omega}_{ab}, \quad \hat{\theta} \equiv \nabla_a n^a, \\ &\hat{\omega}_{ab} \equiv \nabla_{[b}n_{a]} + n^c\nabla_c n_{[a}n_{b]}. \end{aligned} \quad (1.54)$$

According to Frobenius' theorem, both ω_{ab} and $\hat{\omega}_{ab}$ are zero in their own frames [Wald, 1984]. This fact leads to $f^c{}_a\,f^d{}_b\,\nabla_c n_d = \hat{\theta}_{ab} = -\mathcal{K}_{ab}$. Meanwhile, the relationship between Θ and $\hat{\theta}$ is

$$\Theta \;\; = \gamma\hat{\theta} + \gamma\nabla_a v^a + n^a\nabla_a\gamma + v^a\nabla_a\gamma. \quad (1.55)$$

Thus it is easy to show that

$$\begin{aligned} &n^a\nabla_a\hat{\theta} = -\bar{\mathcal{K}}, \\ &u^a\nabla_a\Theta = \hat{\theta}\,\dot{\gamma} + \gamma\,\dot{\hat{\theta}} + \dot{\gamma}\,\kappa + \gamma\,\dot{\kappa} + \dot{n}^b\,\hat{\gamma}_b + \dot{\hat{\gamma}}_b\,n^b + \dot{v}^b\,\hat{\gamma}_b + \dot{\hat{\gamma}}_b\,v^b, \end{aligned} \quad (1.56)$$

where $\hat{\gamma}_b \equiv \nabla_b\gamma$, $\kappa \equiv \nabla_a v^a$.

Finally, the evolution of the expansion rate in terms of $\mathcal{K}$ is

$$\dot{\Theta} = -\dot{\gamma}\,\mathcal{K} - \gamma\,\dot{\mathcal{K}} + \dot{\gamma}\,\kappa + \gamma\,\dot{\kappa} + (\dot{n}^b + \dot{v}^b)\,\hat{\gamma}_b + \dot{\hat{\gamma}}_b\,\left(n^b + v^b\right), \quad (1.57)$$

which will reduce to a much more simpler form $\dot{\theta} = -\dot{\mathcal{K}}$ if $n^a = u^a$. Eq. (1.57) is the generalized *Raychaudhuri's equation*.

The extrinsic curvature $\mathcal{K}_{ab}$ can be expressed in terms of the spatial metric according to Eq. (1.45):

$$\begin{aligned}\mathcal{K}_{ab} &= -\frac{1}{2N}\frac{\partial}{\partial t} f_{ab} + N^{-1} D_{(a} N_{b)}, \\ &= \frac{1}{2}[N^{-1} D_a N_b + N^{-1} D_b N_a + \gamma^{-1}\, v^c \nabla_c (n_a n_b) - \gamma^{-1}\, \dot{f}_{ab}].\end{aligned} \tag{1.58}$$

1.3.2.3 The expansion rate of the matter fluid measured by the observers with 4-velocity n^a

We have defined two expansion rates: Θ with respect to u^a and $\hat{\theta}$ with respect to n^a. In the other words, Θ is the expansion rate of the matter fluid as measured by the observers comoving with the matter fluid, while $\hat{\theta}$ is the expansion rate of a congruence of observers orthogonal to the hypersurfaces. The measurable quantity we are interested in is the matter expansion rate, θ, measured by the observers with 4-velocity n^a.

To define the expansion rate θ, note that the expansion rate Θ is defined by $\Theta \equiv g^{ab}\Theta_{ab}$ and $\Theta_{ab} = \bar{B}_{(ab)} \equiv h^c{}_{(a} h^d{}_{b)} \nabla_c u_d$, and f_{ab} is the projection tensor projecting other tensors onto hyperplane elements orthogonal to n^a. So we may define

$$\begin{aligned}\tilde{B}_{ab} &= f^c{}_a\, f^d{}_b\, \bar{B}_{cd}, \\ &= f^c{}_a\, f^d{}_b\, \nabla_c u_d + \gamma\, v_a\, v_b\, \dot{\gamma} + \gamma^2\, v_a (\dot{n}_b + \dot{v}_b).\end{aligned} \tag{1.59}$$

Thus we can firstly define $\theta^{(1)}_{ab} \equiv \tilde{B}_{(ab)}$, so that

$$\theta^{(1)} = \nabla_a u^a - n^a \nabla_a \gamma + \gamma\, \dot{\gamma} = \Theta + \gamma\, \dot{\gamma} - n^a \nabla_a \gamma. \tag{1.60}$$

However, there exists another definition of the expansion rate θ [Larena, 2009], namely $\theta^{(2)} = f^c{}_a\, f^{da} \nabla_c u_d$. The difference between $\theta^{(1)}$ and $\theta^{(2)}$ is clear: the former arises from projecting $\nabla_a u^a$ onto the rest space orthogonal to u^a first and then projecting the result onto the hypersurfaces orthogonal to n^a. The latter is the result of directly projecting $\nabla_a u^a$ onto the hypersurfaces orthogonal to n^a. One should use $\theta^{(2)}$ as the definition of the matter expansion rate measured

by the observers with 4-velocity n^a, so

$$\theta = \theta^{(2)} = f^c{}_a f^{da} \nabla_c u_d. \tag{1.61}$$

Then the relationships between θ and Θ, $\hat{\theta}$ are:

$$\theta = \gamma\hat{\theta} + \gamma\nabla_a v^a + v^a\nabla_a\gamma + \gamma\, n_a n^c \nabla_c v^a; \tag{1.62}$$

$$= \Theta - n^a\nabla_a\gamma + \gamma\, n_a n^c \nabla_c v^a. \tag{1.63}$$

Correspondingly, the vorticity is defined by $\omega_{ab} \equiv f^c{}_{[a} f^d{}_{b]} \nabla_c u_d$.

1.3.2.4 Summary

Thus far we have calculated the dynamical quantities of the general matter fluid with respect to different observers: the observers comoving with the fluid with the 4-velocity u^a and the observers with 4-velocity n^a. However, one can choose an arbitrary coordinate system to define the dynamical quantities of the matter fluid. Thus we consider large structure formation using the quantities for the cosmic fluid as seen by the observers with the 4-velocity n^a.

According to the results of the last subsection, the quantities associated with the cosmic fluid as measured by the observers with 4-velocity n^a are:

$$B_{ab} \equiv f^c{}_a f^d{}_b \nabla_c u_d, \quad \theta_{ab} \equiv B_{(ab)}, \quad \omega_{ab} \equiv B_{[ab]}; \tag{1.64}$$

$$\sigma_{ab} = B_{ab} - \frac{1}{3}\theta\, f_{ab} - \omega_{ab}, \quad \sigma^2 = \frac{1}{2}\sigma_{ab}\,\sigma^{ab}, \quad \omega^2 = \frac{1}{2}\omega_{ab}\,\omega^{ab}, \tag{1.65}$$

$$\dot{\theta} = \dot{\gamma}\nabla_a n^a + \gamma^2\, v^a\nabla_a\nabla_b n^b + \dot{\mathcal{C}}_1 + \gamma^2\, n^a\nabla_a\nabla_b n^b, \tag{1.66}$$

where $\mathcal{C}_1 \equiv \gamma\nabla_a v^a + v^a\nabla_a\gamma + \gamma\, n_a n^c\nabla_c v^a$. The evolution equation of the expansion θ is given by

$$\frac{\partial}{\partial t}\theta = \frac{1}{\gamma}(\partial_t\gamma - N^a\tilde{\nabla}_a\gamma)(\theta - \mathcal{C}_1) + N^a\tilde{\nabla}_a\theta + \dot{\mathcal{C}}_1 - (\theta - \mathcal{C}_1)v^a\nabla_a\gamma + \gamma v^a\nabla_a(\theta - \mathcal{C}_1) \tag{1.67}$$

$$- \gamma^2\,[\mathcal{R} + \mathcal{K}^2 + 4\pi G(S - 3E - 2\mathcal{W}) - 3\Lambda - N^{-1}D^a D_a N + N^{-1}N^a D_a\mathcal{K}]. \tag{1.68}$$

Finally, for matter flow with a uniquely determined 4-velocity u^a the positive proper rest-mass density ϱ remains conserved [Ehlers, 1993]:

$$\nabla_a(\varrho\, u^a) = 0, \tag{1.69}$$

so it is easy to show that

$$\nabla_a(\hat{\varrho}\, n^a) + \nabla_a(\hat{\varrho}\, v^a) = 0, \tag{1.70}$$

where $\hat{\varrho} = \gamma\varrho$ is the rest-mass density measured by the observers associated to n^a. For the observer associated with n^a the rest-mass of the matter flow is no longer conserved. We define the mass current [Poisson and Will, 2014]

$$j^a = \varrho\, u^a = \hat{\varrho}\, n^a + \hat{\varrho}\, v^a, \tag{1.71}$$

which then satisfies $\nabla_a j^a = 0$. The evolution equation of $\hat{\varrho}$ is

$$\frac{\partial}{\partial t}\hat{\varrho} = N^a\tilde{\nabla}_a\hat{\varrho} - N\,\hat{\varrho}\,(\hat{\theta} + \kappa) - N\,v^a\nabla_a\hat{\varrho}. \tag{1.72}$$

1.3.3 Perfect fluids without a heat flux or anisotropic stress

We will now specialise our results to the perfect fluids without a heat flux or anisotropic stress. This matter model is not only a complement of the simplest dust matter model. Indeed, at the earliest stages of structure formation the dominant energy density in the early Universe can be assumed to be a perfect fluid. Furthermore, fundamental scalar fields may also have a perfect fluid equation of state. Even for a collisionless dust matter model, a dynamical pressure can arise from the formation of multi-stream flows with the development of shell-crossing. In general, the energy momentum of the simple perfect fluid is given by

$$T_{ab} = (\epsilon + p)u_a u_b + p\, g_{ab} = E\, n_a\, n_b + S_{ab}, \tag{1.73}$$

with an equation of state $p = \alpha\,(\epsilon)$. Explicit expressions for $\alpha\,(\epsilon)$ will be left to the specific examples.

In the previous section we did not choose a special time slicing, but supposed that a slicing could be obtained once we chose the initial data. With regard to the lapse function N, an elliptic equation can be obtained by solving Eq. (1.47) if $\mathcal{W} = 0$:

$$D^a D_a N - N\left[\mathcal{K}_{ab}\mathcal{K}^{ab} + 4\pi G(S+E) - 3\Lambda\right] = -\mathscr{L}_{\vec{t}}\mathcal{K}. \tag{1.74}$$

In this equation, only N and N^a are unknown in any slice. Thus far we have not specified the evolution equations for those two variables.

We have introduced two kinds of observers: the Eulerian observers whose unit 4-velocity n^a is orthogonal to the hypsersurfaces Σ_t, and the fluid-comoving (Lagrangian) observers with the 4-velocity u^a. For simplicity, we will consider the case $n^a = u^a$. (Hereafter this choice will be assumed unless it is explicitly stated otherwise.) This corresponds to choosing a comoving gauge with an irrotational perfect fluid model. The kinematic and dynamical equations are then given by:
Constraint equations

$$\mathcal{R} + \mathcal{K}^2 - \mathcal{K}^a{}_b\,\mathcal{K}^b{}_a = 16\pi G\, T_{ab}\, n^a\, n^b + 2\Lambda\,, \tag{1.75}$$

$$D_a\mathcal{K}^a{}_c - D_c\mathcal{K} = -8\pi G J_c\,, \tag{1.76}$$

Evolution equations of the geometric quantities

$$\frac{\partial}{\partial t}h_{ab} = -2\,N\,\mathcal{K}_{ab}, \tag{1.77}$$

$$\frac{\partial}{\partial t}\mathcal{K}_{ab} = N\left\{\mathcal{R}_{ab} + \mathcal{K}\,\mathcal{K}_{ab} - 2\,\mathcal{K}_{ac}\,\mathcal{K}^c{}_b + 4\pi G\left[(S-E)h_{ab} - 2S_{ab}\right] - h_{ab}\Lambda\right\} - D_a D_b N, \tag{1.78}$$

$$\frac{\partial}{\partial t}\mathcal{K} = N\left[\mathcal{R} + \mathcal{K}^2 + 4\pi G(S-3E) - 3\Lambda\right] - D^a D_a N, \tag{1.79}$$

Evolution equations of the physical quantities

$$\frac{\partial}{\partial t}\epsilon = N\,(\epsilon + p)\mathcal{K}\,, \tag{1.80}$$

$$(\epsilon + p)A_a + D_a p = 0\,, \tag{1.81}$$

$$\frac{\partial}{\partial t}\varrho = N\,\varrho\,\mathcal{K}\,. \tag{1.82}$$

We see that none of the above equations contain time derivatives of the lapse function. The same is true for the shift vector in a more general gauge. We recall that they are associated with the choice of coordinates, so the coordinate freedom of General Relativity implies that one may freely choose the lapse (and shift). To reconstruct the full spacetime metric we need to specify h_{ab}, $\mathcal{K}_{ab}$, N and N^a. This is generally related to the problem of choices of the lapse function and shift vector, *i.e.*, to the choices of time slicing.

1.3.4 Thermodynamics of the irrotational perfect fluid

Now we consider the thermodynamics of irrotational perfect fluids. In general the first law of thermodynamics of general fluids is represented by

$$dU = T\,dS - p\,dV + \mu\,dN, \tag{1.83}$$

where U, T, S, p, μ, N are internal energy, temperature, entropy, pressure, chemical potential and number of particles contained in the volume V, respectively. If the fluid is composed of one type of particle only and the total particle number in the volume V is conserved, then Eq. (1.83) reduces to

$$du = T\,ds - p\,dv, \tag{1.84}$$

where $u = \epsilon/\varrho$, $v = 1/\varrho$ and s are called the specific internal energy, the specific volume and the specific entropy, respectively. One can further introduce the relativistic specific enthalpy by

$$h \equiv \frac{\epsilon + p}{\varrho}, \tag{1.85}$$

so that Eq. (1.84) can be written in the alternative convenient form

$$dp = \varrho\,dh - \varrho\,T\,ds; \qquad d\epsilon = h\,d\varrho + \varrho\,T\,ds. \tag{1.86}$$

We will see this quantity can be related to the lapse function N when special conditions apply.

For an observer comoving with the perfect fluid flow, the equations of energy

conservation and rest-mass conservation determined by that observer will lead to

$$u^a \nabla_a \epsilon - h\, u^a \nabla_a \varrho = 0\,. \tag{1.87}$$

Combining this equation with Eq. (1.86) one will immediately obtain the important result:

$$u^a \nabla_a s = 0, \tag{1.88}$$

which indicates the specific entropy s is conserved along the fluid worldlines. In other words, the perfect fluid is adiabatic according to the observer comoving with the fluid flow. If we add another assumption that the perfect fluid is also irrotational, then we obtain a generalization of Eq. (1.88)

$$\nabla_a s = 0, \tag{1.89}$$

which implies that irrotational perfect fluids are isentropic. However, it is not necessarily true to say isentropic perfect fluids are irrotational [Rezzolla and Zanotti, 2013]. This remark leads us to the result that

$$\frac{d\varrho}{\varrho} = \frac{d\epsilon}{\epsilon + p}, \qquad \frac{dh}{h} = \frac{dp}{\epsilon + p}. \tag{1.90}$$

The momentum conservation Eq. (1.81) yields

$$\frac{u^a \nabla_a N}{N} = -\frac{u^a \nabla_a p}{\epsilon + p}, \tag{1.91}$$

where we have assumed that the 4-velocity u^a of the Lagrangian observer is given by Eq.(1.16) and orthogonal to the hypersurface. Then Eq. (1.87) also implies that

$$\frac{u^a \nabla_a h}{h} = \frac{u^a \nabla_a p}{\epsilon + p} = -\frac{u^a \nabla_a \left(h^{-1}\right)}{h^{-1}}, \tag{1.92}$$

and so we have the relation

$$\frac{u^a \nabla_a N}{N} = \frac{u^a \nabla_a \left(h^{-1}\right)}{h^{-1}}. \tag{1.93}$$

Thus with the special conditions under consideration, the lapse function and the specific enthalpy differ mathematically by only a multiplier factor plus a

constant. Without loss of generality, we can set $N^{-1} = h$. With such a relation, we can relate the hypersurface to the dynamics of the matter model.

1.3.5 Buchert's averaging formalism

We have introduced the $3+1$ formalism of Einstein's equations in the above subsections, without introducing the Lagrangian coordinate system. However, Buchert's scalar averaging procedure applies to the Lagrangian observer who is comoving with the fluid flow. We will refer to these Lagrangian coordinates as the *fluid-comoving coordinate system*.

In his first fully general relativistic paper on averaging, Buchert derived a generalized form of Friedmann's equations for an 'effective' expansion factor $a_{\mathcal{D}}(t)$ of inhomogeneous cosmologies for general relativistic spacetimes filled with irrotational 'dust' [Buchert, 2000a]. In a subsequent paper Buchert [2001] generalized this procedure to the case of general relativistic spacetimes filled with an irrotational perfect fluid. Since dust is a special case of the perfect fluid, we will only present the later case.

1.3.5.1 The averaged equations for irrotational perfect fluids

In Buchert's averaging formalism, the averaged volume is a compact and simply-connected domain $\mathcal{D}$ contained within spatial hypersurfaces, which follows the flow lines of the fluid elements. The hypersurfaces are chosen to be orthogonal to the 4-velocity field of the fluid flow so that the total rest-mass of the fluid within the domain is required to be conserved, which means

$$M^{\mu} \equiv \varrho\, u^{\mu}, \qquad \nabla_{\mu} M^{\mu} = 0, \qquad \varrho > 0. \tag{1.94}$$

The 4-velocity of comoving observer can be defined using a scalar function S on hypersurfaces $S = constant$:

$$u^{\mu} = \frac{-\partial^{\mu} S}{h}, \qquad h = \sqrt{-\partial^{\alpha} S\, \partial_{\alpha} S} = u^{\mu} \partial_{\mu} S = \dot{S} > 0. \tag{1.95}$$

The irrotationality of the fluid requires the vorticity tensor ω_{ab} to be zero, and if the coordinates are denoted by X^i, then the line element of the metric

becomes

$$ds^2 = -N^2\,dt^2 + g_{ij}\,dX^i dX^j. \tag{1.96}$$

The inhomogeneities then will be encoded in the lapse function and the 3-metric. With this choice the unit normal coincides with the 4-velocity and the momentum flux density in the hypersurface Σ vanishes. Furthermore, g_{ij} is also the induced metric of the hypersurfaces.

Consider a scalar function $\Upsilon(X^i, t)$ on the hypersurface. Its average over the domain $\mathcal{D}$ is defined by

$$\langle\Upsilon\rangle_{\mathcal{D}} \equiv \frac{1}{V_{\mathcal{D}}}\int_{\mathcal{D}} \Upsilon\, J\, d^3X, \qquad J \equiv \sqrt{det(g_{ij})}, \tag{1.97}$$

where $V_{\mathcal{D}} = \int_{\mathcal{D}} J d^3X$ is the volume of the domain. With these definitions an effective dimensionless scale factor then will be introduced as

$$a_{\mathcal{D}}(t) \equiv \left(\frac{V_{\mathcal{D}}}{V_{\mathcal{D}_0}}\right)^{1/3}, \tag{1.98}$$

so that $a_{\mathcal{D}}$ is a function of coordinate time but depends on the domain's volume and relative position. Correspondingly, the time derivative of the volume $V_{\mathcal{D}}$ will be related to the averaged expansion of the domain $\mathcal{D}$ by

$$\frac{\partial_t V_{\mathcal{D}}(t)}{V_{\mathcal{D}}(t)} = \langle N\,\theta\rangle_{\mathcal{D}} = \langle\tilde{\theta}\rangle_{\mathcal{D}} = 3\,\frac{\partial_t a_{\mathcal{D}}}{a_{\mathcal{D}}} = 3\,\tilde{H}_{\mathcal{D}}, \tag{1.99}$$

with the relation $\dot{J} = \theta J$, $\tilde{\theta} \equiv N\,\theta$. With all these definitions, a very important result of Buchert's scalar averaging formalism is the commutation rule: for an arbitrary scalar field $\Upsilon(X^i, t)$:

$$\partial_t\langle\Upsilon\rangle_{\mathcal{D}} - \langle\partial_t\Upsilon\rangle_{\mathcal{D}} = -\langle\Upsilon\rangle_{\mathcal{D}}\langle\tilde{\theta}\rangle_{\mathcal{D}} + \langle\Upsilon\tilde{\theta}\rangle_{\mathcal{D}}, \tag{1.100}$$

or alternatively,

$$\partial_t\langle\Upsilon\rangle_{\mathcal{D}} + 3\tilde{H}_{\mathcal{D}}\langle\Upsilon\rangle_{\mathcal{D}} = \langle\partial_t\Upsilon + \Upsilon\tilde{\theta}\rangle_{\mathcal{D}}. \tag{1.101}$$

The commutation rule expresses the fact that the spatial average and time evolution do not commute. This characteristic is a significant difference between

Buchert's scalar averaging formalism and the standard approach. For the latter, the standard homogeneous and isotropic FLRW cosmological model is not derived but is assumed as empirically justified. The fluctuations are averaged out and then the "averaged" universe is evolved in time. The evolution of these fluctuations is described by the standard perturbation theory with this "averaged" universe taken as the background spacetime. In this sense, the initially "averaged" universe is assumed to evolve to the same result at the present day as if the initial universe were evolved to present epoch and then "averaged". However, Eq. (1.101) suggests the result will generally be affected by extra terms arising from spatial averaging.

Finally, the dynamics of the averaged domain $\mathcal{D}$ is described by two averaged equations which are similar to the Friedmann equations in the standard approach. Firstly, the *averaged Raychaudhuri equation* is:

$$3\frac{\partial_t^2 a_{\mathcal{D}}}{a_{\mathcal{D}}} + 4\pi G\langle\tilde{\epsilon} + 3\tilde{p}\rangle_{\mathcal{D}} = \tilde{\mathcal{Q}}_{\mathcal{D}} + \tilde{\mathcal{P}}_{\mathcal{D}}; \tag{1.102}$$

where $\tilde{\epsilon} = N^2\,\epsilon$ is the scaled energy density and $\tilde{p} = N^2\,p$ is scaled pressure density. Furthermore, the *averaged Hamiltonian constraint* is

$$6\,\tilde{H}_{\mathcal{D}}^2 - 16\,\pi\,G\,\langle\tilde{\epsilon}\rangle_{\mathcal{D}} = -(\tilde{\mathcal{Q}} + \langle\tilde{\mathcal{R}}\rangle_{\mathcal{D}}). \tag{1.103}$$

where $\tilde{\mathcal{Q}}_{\mathcal{D}}$ is the *kinematical backreaction* describing the impact of inhomogeneities on the scale factor due to the average shear and expansion fluctuations,

$$\tilde{\mathcal{Q}}_{\mathcal{D}} \equiv [2\,\langle N^2\,\mathbf{II}\rangle_{\mathcal{D}} - \frac{2}{3}\langle N\,\mathbf{I}\rangle_{\mathcal{D}}^2] = \frac{2}{3}\langle(\tilde{\theta} - \langle\tilde{\theta}\rangle_{\mathcal{D}})^2\rangle_{\mathcal{D}} - 2\langle\tilde{\sigma}^2\rangle_{\mathcal{D}}, \tag{1.104}$$

and $\tilde{\mathcal{P}}_{\mathcal{D}}$ is the *dynamical backreaction* related to the evolution of the lapse function

$$\tilde{\mathcal{P}}_{\mathcal{D}} \equiv \langle\tilde{\mathcal{A}}\rangle_{\mathcal{D}} + \langle\dot{N}\,\tilde{\theta}\rangle_{\mathcal{D}}. \tag{1.105}$$

Other parameters are defined as $\tilde{\mathcal{R}} \equiv N^2\,\mathcal{R}, \tilde{\sigma} \equiv N\,\sigma, \tilde{\mathcal{A}} \equiv N^2\,\mathcal{A}$, and

$$\mathbf{I} \equiv -K = \theta; \qquad 2\mathbf{II} \equiv K^2 - K^i{}_j\,K^j{}_i = \theta^2 - \theta^\mu{}_\nu\theta^\nu{}_\mu = \frac{2}{3}\,\theta^2 - 2\,\sigma^2, \tag{1.106}$$

are two scalar invariants [Ehlers, 1993; Ehlers and Buchert, 1996].

Furthermore, Eq. (1.102) and the time-derivative of Eq. (1.103) is equal to each other if and only if the following integrability condition is satisfied:

$$\begin{aligned}\partial_t\tilde{\mathcal{Q}}_{\mathcal{D}} + \tilde{H}_{\mathcal{D}}\,\tilde{\mathcal{Q}}_{\mathcal{D}} + \partial_t\langle\tilde{\mathcal{R}}\rangle_{\mathcal{D}} + 2\,\tilde{H}_{\mathcal{D}}\,\langle\tilde{\mathcal{R}}\rangle_{\mathcal{D}} \\ + 4\,\tilde{H}_{\mathcal{D}}\,\tilde{\mathcal{P}}_{\mathcal{D}} - 16\pi G\,[\partial_t\langle\tilde{\epsilon}\rangle_{\mathcal{D}} + 3\tilde{H}_{\mathcal{D}}\,\langle\tilde{\epsilon}+\tilde{p}\rangle_{\mathcal{D}}] = 0\,.\end{aligned} \tag{1.107}$$

The averaged energy conservation laws will obey the following equations:

$$\partial_t\langle\epsilon\rangle_{\mathcal{D}} + 3\tilde{H}_{\mathcal{D}}\langle\epsilon+p\rangle_{\mathcal{D}} = \langle\partial_t p\rangle_{\mathcal{D}} - \partial_t\langle p\rangle_{\mathcal{D}}. \tag{1.108}$$

and

$$\partial_t\langle\tilde{\epsilon}\rangle_{\mathcal{D}} + 3\tilde{H}_{\mathcal{D}}\langle\tilde{\epsilon}+p\rangle_{\mathcal{D}} = \langle\partial_t\tilde{p}\rangle_{\mathcal{D}} - \partial_t\langle\tilde{p}\rangle_{\mathcal{D}} + \langle 2\dot{N}\tilde{\epsilon}\rangle_{\mathcal{D}}. \tag{1.109}$$

The averaged energy conservation law includes non-commuting terms that are nonzero for inhomogeneous fluids.

As been mentioned in the previous section, the backreaction arising from the inhomogeneity has been suggested as a possible explanation for the current apparently accelerated expansion. Eq. (1.102) indicates that if $\tilde{\mathcal{Q}}_{\mathcal{D}} + \tilde{\mathcal{P}}_{\mathcal{D}} > 4\pi G\,\langle\tilde{\epsilon}+\tilde{p}\rangle_{\mathcal{D}}$ then the backreaction will accelerate the expansion of the averaged domain, behaving like a dark energy source. Conversely, if $\tilde{\mathcal{Q}}_{\mathcal{D}} + \tilde{\mathcal{P}}_{\mathcal{D}} < 4\pi G\,\langle\tilde{\epsilon}+\tilde{p}\rangle_{\mathcal{D}}$ then the backreaction behaves like dark matter, which will slow down the expansion of the domain [Wiegand and Buchert, 2010].

Both interpretations rely on assuming that the time parameter t relating to the averaged flow coincides with the proper time of actual observers in bound structures. But in the timescape model this is not the case. In the timescape model while the effects of the right hand side of Eq. (1.102) are not large enough to dominate over the averaged energy density $4\pi G\,\langle\tilde{\epsilon}\rangle_{\mathcal{D}}$. The conclusion is changed once a systematic recalibration of clocks is included. This effect is understood to arise from a regional locally isotropic volume deceleration of observers within gravitationally bound structures relative to an average position by volume, which is in a negatively curved region.

In last two decades Buchert's averaging formalism has been widely studied and generalized to other cases. For example, Larena [2009] discussed the spatially

averaged cosmology in an arbitrary coordinate system, and the generalisation on two non-interacting fluids, general matter content and averaging hypersurfaces can be found in [Jiménez et al., 2014; Räsänen, 2010]. Bose and Majumdar [2013] even studied the effect of inhomogeneities in the future evolution, by considering a two-scale model within the Buchert framework. Recently, Buchert et al. [2018] presented an general averaging formalism that only functionally depends on a metric. This formalism is then applicable to general $3+1$ foliations of spacetime and an arbitrary fluid with tilted flow.

1.4 Brief introduction of the perturbation theory for large-scale structure formation

Observation is our best and most powerful way to acquire knowledge about nature. Although there are many debates on whether the effect of inhomogeneities on average expansion is significant or not, there is no doubt that extensive observations by multiple methods investigating large-scale structure will give us important information about the local inhomogeneities. However, understanding this information depends heavily on the reliability of our mathematical descriptions of the inhomogeneities and the propagation of the light in such an inhomogeneous universe.

Consequently, the problems of what the primordial seeds of these large-scale structures are and how they grow to what we observe today become two fundamental questions for cosmology. Regarding the first question, it is now widely accepted that the large-scale inhomogeneous structures of the Universe we observe today, such as galaxies and clusters of galaxies, were formed from density fluctuations that arose from quantum fluctuations in the inflationary universe [Weinberg, 2008; Hawking, 1982; Guth and Pi, 1982].

Regarding the second question, a commonly used approach is the cosmological perturbation theory (CPT, hereafter), which was first applied by Lifshitz [1946] to study the gravitational stability of nonstationary models of the Universe. Since then the CPT has been proved to be a successful theory for describing the formation and evolution of large-scale structures and usually it is called the standard perturbation theory (SPT) [Kodama and Sasaki, 1984; Bernardeau

et al., 2002; Tsagas et al., 2008]. Its success has been supported by observational tests for the linear approximation [Percival et al., 2007; Aghanim et al., 2016] and N-body numerical simulations for regimes beyond the linear approximation based on the ΛCDM model and Newtonian gravity [Springel et al., 2005; Bouillot et al., 2015; Kuhlen et al., 2012].

Fig. 1.3 shows the good agreement between the redshift-space matter power spectrum recovered from the observational data and the best-fit model power spectrum computed from linear theory. It is clear that for the large-scale power spectrum they show good agreement but deviations will appear for small scales, because of nonlinear effects of the growth of perturbations. Fig. 1.4 shows some typical N-body numerical simulations of dark matter density field on different scales.

Although it has been stated that the hierarchical formation of structures is a highly nonlinear process and thus can only be accessible directly through numerical simulation [Davis et al., 1985; Springel et al., 2005], different approaches have been investigated in attempts to analytically describe particular aspects of the nonlinear regime of evolution of large-scale structures. Roughly speaking all of these approaches can be classified into two categories.

The first kind of scheme are the generalizations of the SPT, including the multi-point propagator method [Bernardeau et al., 2008], regularized multi-point propagator method (RegPT) [Bernardeau et al., 2012; Taruya et al., 2012], renormalized perturbation theory [Crocce and Scoccimarro, 2006a,b] and other techniques [Suto and Sasaki, 1991; Blas et al., 2013].

The second kind is the Lagrangian perturbation theory (LPT), which is motivated by the Zel'dovich approximation [Zel'dovich, 1970a] using Lagrange variables to study the nonlinear evolution of large-scale structures, and developed by many other authors [Shandarin and Zeldovich, 1989; Buchert, 1989; Moutarde et al., 1991; Bouchet et al., 1995; Buchert, 1996a; Ehlers and Buchert, 1996; Bouchet, 1996]. We will not discuss the details of LPT here but leave this to the next chapter.

Evidently, the most basic difference between SPT and LPT comes from the different perturbed dynamic variables. For SPT, the matter dynamics are described by a coordinate system not comoving with the matter, and the fundamental variables are the matter density and velocity fields on globally defined

spatial hypersurfaces. By contrast in LPT the dynamics are described by a comoving system of coordinates attached to the matter fluid flow. All the information about the evolution of the fluctuations is contained in the evolution of the so-called displacement fields, represented by the following equation

$$\mathbf{x} = \mathbf{X} + \mathbf{P}(\mathbf{X}, t), \tag{1.110}$$

where $\mathbf{x}$ are the Eulerian coordinates and $\mathbf{X}$ are the Lagrangian coordinates, $\mathbf{P}(\mathbf{X}, t)$ are the displacement fields, and $\mathbf{x}(t_0) = \mathbf{X}$ at initial time t_0. The energy density thus will be represented as

$$\varrho(\mathbf{X}, t) J(\mathbf{X}, t) = \varrho(\mathbf{X}, t_0), \tag{1.111}$$

where $J(\mathbf{X}, t)$ is the Jacobian of the transformation between the Lagrangian and Eulerian coordinates. See section 2.2 for details. Thus the LPT includes inherently nonlinear terms, and will give more nonlinear information about large-scale structure formation as compared to the EPT .

Both SPT and LPT have been successfully applied to the nonlinear regime of the evolution of local cosmic web structures, though both approaches are still limited by some weaknesses of their own. In this work I will mainly focus on the LPT of structure formation in relativistic cosmologies.

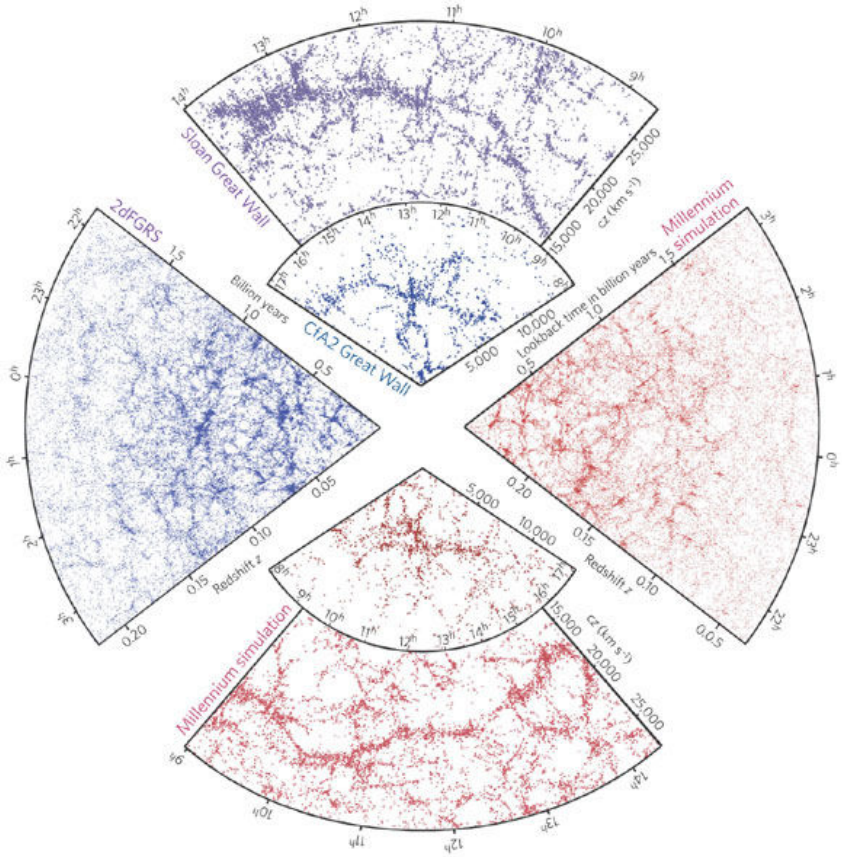

Figure 1.2: The galaxy distribution obtained from large-scale structure surveys and from the N-body cosmological simulations. The survey includes the 2dFGRS [Colless et al., 2001] and SDSS projects [Gott III et al., 2005]. The numerical simulations, the bottom and on the right panel figures are within the evolving dark matter distribution of the 'Millennium' simulation [Springel et al., 2005]. The figure is taken from Springel et al. [2006].

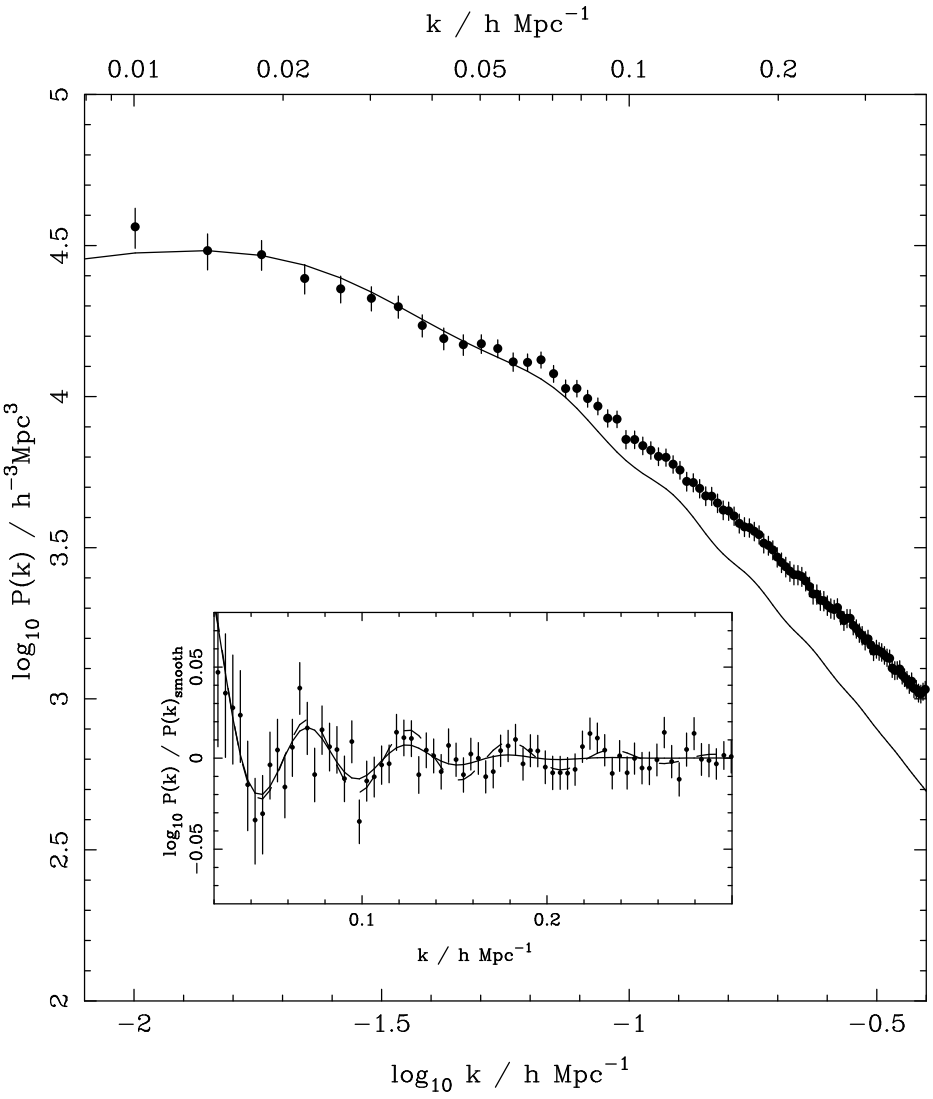

Figure 1.3: Redshift-space power spectrum recovered from the combined SDSS main galaxy and LRG sample. The cosmological parameters are assumed to be a spatial flat Λ cosmological model with $\Omega_M = 0.24$ and $\Omega_\Lambda = 0.76$. 1σ uncertainties are shown. The solid line is calculated from the linear power spectrum with cosmological parameters $h = 0.73$, $\Omega_M = 0.24$, $\Omega_\Lambda = 0.76$, $\Omega_B/\Omega_M = 0.174$ and $n_s = 0.96$ being taken from the WMAP 3 years temperature and polarization data [Spergel et al., 2007]. The normalization of the model power spectrum has been matched to that of the large-scale ($0.01h$ Mpc$^{-1} < k < 0.06h$ Mpc^{-1}). A deviation becomes visible for larger k resulting from the nonlinear effects of the growth of perturbation. The inset shows the power spectrum ratio to a smooth model compared to the baryon oscillations in the (WMAP 3 yr parameter) model (solid line). The figure is taken from Percival et al. [2007].

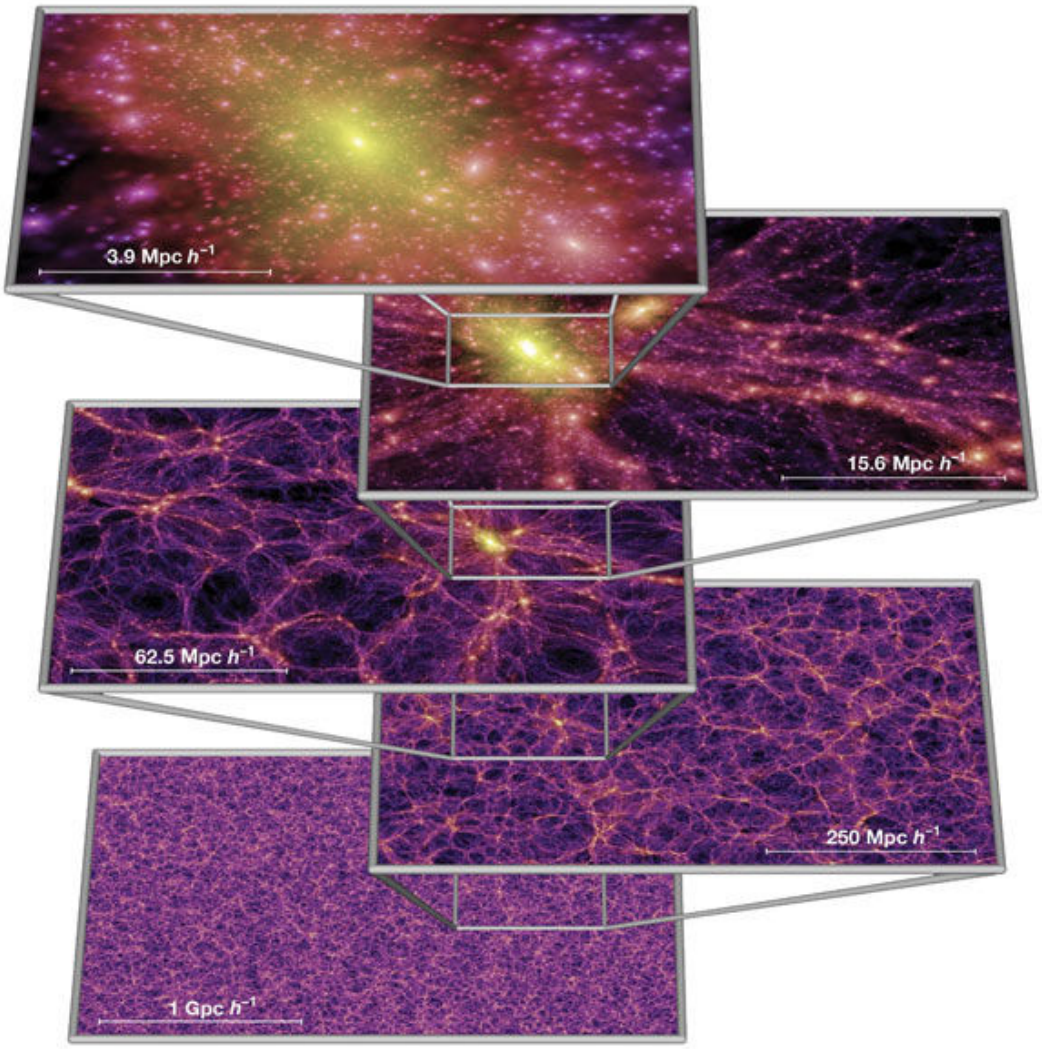

Figure 1.4: In this figure each individual image shows the projected dark matter density field in a slab of thickness $15h^{-1}$ Mpc, with colour indicating the density and local dark matter velocty dispersion. The figure is taken from Springel et al. [2005].

CHAPTER 2

Newtonian Lagrangian perturbation theory for two fluids in relative motion

It is widely accepted that the large scale structures of the present Universe are the result of gravitational amplification of small primordial fluctuations. Over many decades of research in cosmology, large scale structure formation has been modelled on the basis of a perturbative approach. This type of approaches makes use of the instability of the standard cosmologies of Friedmann–Lemaître type against perturbations of the density and velocity fields. The perturbations are evaluated as a function of Eulerian coordinates in this approach. However, this approach relies on physical densities being small. For the modelling of the high density excesses observed in the Universe, Zel'dovich proposed an approximate extrapolation of the linear perturbation solution into the nonlinear regime.

In contrast to this approach, the Lagrangian perturbation theory does not rely on the smallness of the density of the inhomogeneities. Only the deviations of the particle trajectories from the homogeneous Hubble flow are treated perturbatively, as the field of trajectories is the only dynamical variable in the Lagrangian picture. The density fields and velocity fields are treated as functions of this variable. Also the Zel'dovich approximation was found to be contained in a subclass of first-order irrotational perturbations solutions in this theory.

On the other hand, the content of the Universe at late time has been conventionally treated as a single dust or perfect fluid in the context of hydrodynamic approximation. This simplification benefits from the fact that the Universe is apparently dominated by dark matter and dark energy. Although the luminous universe we observe exists in the form of baryonic matter, the density and velocity distributions of baryonic matter are the same as those of the dark matter on large scale in the linear evolution of gravitational clustering perturbations. However, the evidence of observations show that this may be not the case, *i.e.*,

the baryon fraction is not uniform [Ettori and Fabian, 1999; Ettori, 2003; Sand et al., 2004]. This nonuniformity of the baryon fraction has been suggested to be a result of the statistical discrepancy of baryonic matter from the underlying dark matter during nonlinear evolution [Ping et al., 2005]. Obviously, complicated substructures will subsequently form if we consider the evolution of large scale structures in the realistic Universe.

As a first step towards investigating the effects of such baryon-dark matter discrepancy on the formation and evolution of large scale structures, we apply the LPT to two fluids in an Einstein-de Sitter universe in this chapter.

This chapter is organized as follows. In section 2.1 we will briefly review the coarse-grained dynamical equations in the context of the adhesion approach with a single species in a Newtonian cosmology. In section 2.2 we generalize such an approach to a Newtonian cosmology with two fluid components. Then we derive the evolution equations of the fluid mixture up to second order within the Lagrangian perturbation theory. We also present the evolution equations of each species. We claim that if we consider the velocity dispersions as small quantities then the effects of the relative motion on the large scale structure formation will be significant at third and higher orders. In last section, we introduce the relativistic Lagrangian perturbation approach.

2.1 The dynamical equations and the Eulerian perturbation scheme

2.1.1 The coarse-grained dynamical equations

Let us consider a self-gravitating particle system composed of a single species with a total number N. Usually the states of the system are prescribed by the positions and velocities of these N identical particles. But if N is very large then it is impossible to solve the equations of motion for all particles. Instead, one can switch to a statistical approach to describe the evolution of the system. In the cosmological context the hydrodynamic approximation has been successfully employed in the description of large-scale structure formation [Bernardeau et al., 2002]. Such an approximation ensures the possibility of the analytical pre-

scription of the formation of nonlinear structures. However, one can construct a different procedure for fluid-like descriptions of a particle system. Here we will briefly review the basic coarse-grained dynamical equations for this procedure. One can find more details in [Buchert and Domínguez, 1998; Domínguez, 2000; Buchert and Domínguez, 2005].

For simplicity, we consider Newtonian kinetic theory. In the Newtonian approximation, one can define the so-called Klimontovich density $f_K(\mathbf{x}, \mathbf{v}, t)$ in the one-element phase space as [Buchert and Domínguez, 2005]

$$f_K(\mathbf{x}, \mathbf{v}, t) = \sum_{i=1}^{N} \delta\left(\mathbf{x} - \boldsymbol{x}^{(i)}\right) \delta\left(\mathbf{v} - \boldsymbol{v}^{(i)}\right), \tag{2.1}$$

which describes the single element phase space density. Clearly each element has six degrees of freedom and the phase space has six dimensions (excluding the time dimension). Here $\boldsymbol{x}^{(i)}$ and $\boldsymbol{v}^{(}(i)$ refer to the physical particles' coordinates and coordinate velocities. Additionally, for each particle the equations of motion should be given by the Newtonian equations

$$\frac{d\boldsymbol{x}^{(i)}}{dt} = \dot{\boldsymbol{x}}^{(i)} = \boldsymbol{v}^{(i)}, \quad \dot{\boldsymbol{v}}^{(i)} = \boldsymbol{g}^{(i)}, \tag{2.2}$$

where the gravitational strength field $\boldsymbol{g}^{(i)}$ is determined by

$$\nabla^{(i)} \cdot \boldsymbol{g}^{(i)} = \Lambda - 4\pi G m \sum_{i \neq j}^{N} \delta\left(\boldsymbol{x}^{(i)} - \boldsymbol{x}^{(j)}\right), \tag{2.3}$$

$$\nabla^{(i)} \times \boldsymbol{g}^{(i)} = 0, \tag{2.4}$$

where Λ, m are the cosmological constant and the particle mass, respectively. Furthermore, if the particles are collisionless then along each path in the phase space the density $f_K(\mathbf{x}, \mathbf{v}, t)$ should be conserved, *i.e.*, the total time derivative should be equal to zero[1],

$$\frac{df_K}{dt} = \frac{\partial f_K}{\partial t} + \mathbf{v} \cdot \frac{\partial f_K}{\partial \mathbf{x}} + \boldsymbol{g} \cdot \frac{\partial f_K}{\partial \mathbf{v}} = 0, \tag{2.5}$$

[1] To prove this, note that for the Dirac delta function, $f(a)\delta(a-b) = f(b)\delta(a-b)$.

with $\mathbf{v}$, $\boldsymbol{g}$ given by Eqs. (2.3, 2.4). However, to reach a fluid-like description for studying the large-scale flow one needs to apply a smoothing procedure to the Klimontovich density. With such a procedure the newly defined quantities can be related to the observables of the Universe. The smoothed phase-space density can be defined as[2]

$$f(\mathbf{x},\mathbf{v},t) = \int \frac{d\mathbf{x}'}{\mathcal{L}^3}\frac{d\mathbf{v}'}{\mathcal{V}^3} W\left(\frac{\mathbf{x}-\mathbf{x}'}{\mathcal{L}}\right) W\left(\frac{\mathbf{v}-\mathbf{v}'}{\mathcal{V}}\right) f_K(\mathbf{x}',\mathbf{v}',t), \tag{2.6}$$

where $\mathcal{L}$, $\mathcal{V}$ are the spatial and velocity smoothing scales respectively, and W is a rotationally symmetric coarse-graining window function, whose integral is normalized to be unity. Roughly speaking, such a window function defines the boundary and smooths out the details in that bounded region [Domínguez, 2000]. Applying the phase-space conservation equation (2.5) for the collisionless matter component, one can obtain the evolution equation for this new smoothed density:

$$\frac{\partial f}{\partial t} + \mathbf{v}\cdot\frac{\partial f}{\partial \mathbf{x}} + \bar{\boldsymbol{g}}\cdot\frac{\partial f}{\partial \mathbf{v}} = -\mathcal{S}_{\mathcal{L}}(\mathbf{x},\mathbf{v},t) - \mathcal{S}_{\mathcal{V}}(\mathbf{x},\mathbf{v},t), \tag{2.7}$$

$$\nabla\cdot\bar{\boldsymbol{g}} = \Lambda - 4\pi G m\int d\mathbf{v}\, f(\mathbf{x},\mathbf{v},t), \quad \nabla\times\bar{\boldsymbol{g}} = 0. \tag{2.8}$$

where $\mathcal{S}_{\mathcal{L}(\mathcal{V})}(\mathbf{x},\mathbf{v},t)$ arise from the smoothing procedure:

$$\mathcal{S}_{\mathcal{L}}(\mathbf{x},\mathbf{v},t) = \frac{\partial}{\partial \mathbf{x}}\left[\int \frac{d\mathbf{x}'}{\mathcal{L}^3}\frac{d\mathbf{v}'}{\mathcal{V}^3} W\left(\frac{\mathbf{x}-\mathbf{x}'}{\mathcal{L}}\right) W\left(\frac{\mathbf{v}-\mathbf{v}'}{\mathcal{V}}\right)(\mathbf{v}'-\mathbf{v})\, f_K(\mathbf{x}',\mathbf{v}',t)\right], \tag{2.9}$$

$$\mathcal{S}_{\mathcal{V}}(\mathbf{x},\mathbf{v},t) = \frac{\partial}{\partial \mathbf{v}}\left[\int \frac{d\mathbf{x}'}{\mathcal{L}^3}\frac{d\mathbf{v}'}{\mathcal{V}^3} W\left(\frac{\mathbf{x}-\mathbf{x}'}{\mathcal{L}}\right) W\left(\frac{\mathbf{v}-\mathbf{v}'}{\mathcal{V}}\right)(\boldsymbol{g}-\bar{\boldsymbol{g}})\, f_K(\mathbf{x}',\mathbf{v}',t)\right]. \tag{2.10}$$

Note that here $\boldsymbol{g} \equiv \boldsymbol{g}(\mathbf{x}',t)$ and $\bar{\boldsymbol{g}} \equiv \bar{\boldsymbol{g}}(\mathbf{x},t)$. Clearly, if the two terms $\mathcal{S}_{\mathcal{L}(\mathcal{V})}$ are zero, then Eq. (2.7) reduces to the well-known collisionless Boltzmann equation, or Vlasov equation [Rezzolla and Zanotti, 2013].

It has been stated that the two terms $S_{\mathcal{L}(\mathcal{V})}$ represent the dynamical coupling to the degree of freedom removed by the smoothing operation [Buchert and

[2] Here the prime denotes the second set of phase space coordinates without potential confusion. In section 2.2.2.5 and in other chapters it is used as a derivative with respect to special coordinates.

Domínguez, 2005]. For a coarse-grained cell with smoothed scales $\mathcal{L}$ and $\mathcal{V}$, the term $\mathcal{S}_{\mathcal{L}}$ thus accounts for the velocity dispersion, *i.e.*, the fact that each particle in the smoothed cell usually has a different velocity from the center of mass. Likewise the term $\mathcal{S}_{\mathcal{V}}$ presents the departure from the mean field gravity in this cell.

Eq. (2.7) depends on seven variables which are of course too many to be practical. One can simplify the equation by taking the kinetic moments, *i.e.*, by integrating out the velocity fields at different orders. (See Bernardeau et al. [2002] for a standard procedure.) In general the cosmological observables of interest are the large-scale density and the velocity fields. To relate these observables with $f(\mathbf{x}, \mathbf{v}, t)$ one can define the mean mass density ϱ and mean fluid velocity $\bar{\mathbf{v}}$ as

$$\varrho\left(\mathbf{x}, t\right) = m \int d\mathbf{v} f\left(\mathbf{x}, \mathbf{v}, t\right) = \frac{m}{\mathcal{L}^3} \sum_i^N W\left(\frac{\mathbf{x} - \boldsymbol{x}^{(i)}}{\mathcal{L}}\right), \tag{2.11}$$

$$\varrho\, \bar{\mathbf{v}}\left(\mathbf{x}, t\right) = m \int d\mathbf{v}\, \mathbf{v} f\left(\mathbf{x}, \mathbf{v}, t\right) = \frac{m}{\mathcal{L}^3} \sum_i^N W\left(\frac{\mathbf{x} - \boldsymbol{x}^{(i)}}{\mathcal{L}}\right) \boldsymbol{v}^{(i)}. \tag{2.12}$$

Immediately, the evolution equations of these two mean fields are given by

$$\frac{\partial \varrho}{\partial t} + \nabla \cdot (\varrho \bar{\mathbf{v}}) = 0, \tag{2.13}$$

$$\frac{\partial \bar{\mathbf{v}}}{\partial t} + (\bar{\mathbf{v}} \cdot \nabla)\, \bar{\mathbf{v}} = \bar{\boldsymbol{g}} + \frac{1}{\varrho} \left(\boldsymbol{\mathcal{F}} - \nabla \cdot \boldsymbol{\mathcal{P}}\right), \tag{2.14}$$

$$\nabla \cdot \bar{\boldsymbol{g}} = \Lambda - 4\pi G \varrho, \quad \nabla \times \bar{\boldsymbol{g}} = 0, \tag{2.15}$$

with

$$\boldsymbol{\mathcal{F}}\left(\mathbf{x}, t\right) = \frac{m}{\mathcal{L}^3} \sum_i^N W\left(\frac{\mathbf{x} - \boldsymbol{x}^{(i)}}{\mathcal{L}}\right) \left(\boldsymbol{g}^{(i)} - \bar{\boldsymbol{g}}\left(\mathbf{x}, t\right)\right), \tag{2.16}$$

$$\boldsymbol{\mathcal{P}}\left(\mathbf{x}, t\right) = \frac{m}{\mathcal{L}^3} \sum_{i,j}^N W\left(\frac{\mathbf{x} - \boldsymbol{x}^{(i)}}{\mathcal{L}}\right) \left(\boldsymbol{v}^{(i)} \cdot \boldsymbol{v}^{(j)} - \bar{\mathbf{v}}^{(i)} \cdot \bar{\mathbf{v}}^{(j)}\right). \tag{2.17}$$

The definitions of the vector field $\boldsymbol{\mathcal{F}}$ and the symmetric second rank tensor $\boldsymbol{\mathcal{P}}$ suggest the former contains the departure from the mean field gravity, while the

latter will account for the velocity dispersion around the mean velocity. The system of equations Eqs. (2.13, 2.14, 2.15, 2.16, 2.17) constitute a hydrodynamic-like prescription for the dynamics of particle system, and will reduce to hydrodynamic approximation for large-scale structure formation if the two new terms $\boldsymbol{\mathcal{F}}$ and $\boldsymbol{\mathcal{P}}$ are zero.

One may note that the first equation (2.13) describes the conservation of mass and couples the mass density and mean velocity. The second equation (2.14) states momentum conservation and couples the mean velocity with the new fields. So it is expected that the dynamics of the new fields $\boldsymbol{\mathcal{F}}$ and $\boldsymbol{\mathcal{P}}$ will produce further new fields. To truncate such an infinite hierarchy, one needs to restrict to some approximations motivated by physical requirements. With special approximations $\boldsymbol{\mathcal{F}}$ and $\boldsymbol{\mathcal{P}}$ will become functions of ϱ and $\bar{\mathbf{v}}$. Further examples of different choices of the approximations are given in Refs. [Buchert et al., 1999; Domínguez, 2002; Buchert and Domínguez, 2005]

2.1.2 The Newtonian-Eulerian perturbation scheme

The dust model is the simplest matter model used to describe large-scale structure formation and can be found in many standard textbooks. With the hydrodynamic approximation, in a non-rotating Eulerian frame with coordinates $\mathbf{x}$ and time t, the equations for self–gravitating irrotational dust are

$$\frac{\partial \varrho}{\partial t} + \nabla \cdot (\varrho \mathbf{v}) = 0, \tag{2.18}$$

$$\frac{\partial \mathbf{v}}{\partial t} + (\mathbf{v} \cdot \nabla)\, \mathbf{v} = \boldsymbol{g}, \tag{2.19}$$

$$\nabla \cdot \boldsymbol{g} = \Lambda - 4\pi G \varrho, \quad \nabla \times \boldsymbol{g} = 0, \tag{2.20}$$

$$\nabla \times \mathbf{v} = 0. \tag{2.21}$$

The last equation states the irrotationality of the matter model. Compared with Eq. (2.14), here in hydrodynamic approximation, the vanishing of $\boldsymbol{\mathcal{F}}$ and $\boldsymbol{\mathcal{P}}$ indicates that the large-scale structure formation is driven only by collisionless matter with negligible velocity dispersion and pressure. At least in the early stages of the gravitational instabilities this is a good assumption. However, at later times this assumption will break down when structures evolve to the

nonlinear regime with higher densities. Then one has to deal with the generation of velocity dispersion and the issue of "shell crossing".

The above system of equations can be represented using the comoving coordinates: $\mathbf{x} = a(t)\mathbf{q}$ with cosmic scale factor $a(t)$:

$$\frac{\partial \varrho}{\partial t} + 3H\varrho + \frac{1}{a}\nabla_{\mathbf{q}} \cdot (\varrho \mathbf{u}) = 0, \tag{2.22}$$

$$\frac{\partial \mathbf{u}}{\partial t} + \frac{1}{a}(\mathbf{u} \cdot \nabla_{\mathbf{q}})\,\mathbf{u} + H\mathbf{u} = \mathbf{w}, \tag{2.23}$$

$$\nabla_{\mathbf{q}} \cdot \mathbf{w} = \Lambda - 4\pi G a (\varrho - \varrho_H), \quad \nabla_{\mathbf{q}} \times \mathbf{w} = 0, \tag{2.24}$$

$$\nabla_{\mathbf{q}} \times \mathbf{u} = 0, \tag{2.25}$$

where the peculiar velocity $\mathbf{u}$ and peculiar acceleration field $\mathbf{w}$ are defined as

$$\mathbf{u} = \mathbf{v} - H\mathbf{x}, \quad \mathbf{w} = \boldsymbol{g} + \frac{4\pi G\varrho_H - \Lambda}{3}\mathbf{x}. \tag{2.26}$$

The perturbation ansatz suggests that if the distributions of density and velocity fields are small compared to their "background" fields, which are homogeneous and isotropic, then it is possible to expand the density and velocity fields about these background values. The density perturbations can be represented as

$$\varrho(\mathbf{q}, t) = \varrho_H (1 + \delta\varrho(\mathbf{q}, t)) = \varrho_H \left(1 + \sum \delta\varrho^{(n)}(\mathbf{q}, t)\right). \tag{2.27}$$

Inserting this equation into the dynamical system Eqs. (2.22, 2.23) one has

$$\frac{\partial^2 \delta\varrho}{\partial t^2} + 2H\frac{\partial \delta\varrho}{\partial t} = \frac{1}{a^2}\nabla_{\mathbf{q}} \cdot [(1 + \delta\varrho)\,\mathbf{w}] + \frac{1}{a^2}\frac{\partial^2}{\partial q^i \partial q^j}\left[(1 + \delta\varrho)\,u^i u^j\right], \tag{2.28}$$

where the Einstein summation over the spatial (Eulerian) components is implied[3]. For the early stages of structure formation, where the gravitational instabilities

[3] The last term (not including a^{-2}) on the right hand side is equal to

$$\nabla_{\mathbf{q}}\{\nabla_{\mathbf{q}} \cdot [(1 + \delta\varrho)\,\mathbf{u}]\} \cdot \mathbf{u} + \nabla_{\mathbf{q}} \cdot \{(1 + \delta\varrho)\,[(\mathbf{u} \cdot \nabla_{\mathbf{q}})\,\mathbf{u}]\} + (\nabla_{\mathbf{q}}\delta\varrho \cdot \mathbf{u})(\nabla_{\mathbf{q}} \cdot \mathbf{u}) + (1 + \delta\varrho)(\nabla_{\mathbf{q}} \cdot \mathbf{u})(\nabla_{\mathbf{q}} \cdot \mathbf{u})$$

are in the linear regime, the above equation becomes at first order:

$$\frac{\partial^2 \delta\varrho^{(1)}}{\partial t^2} + 2H\frac{\partial \delta\varrho^{(1)}}{\partial t} - 4\pi G\varrho_H \delta\varrho^{(1)} = 0. \tag{2.29}$$

Furthermore, in the presence of a dynamical pressure Eq. (2.28) becomes

$$\frac{\partial^2 \delta\varrho}{\partial t^2} + 2H\frac{\partial \delta\varrho}{\partial t} = \frac{1}{a^2}\nabla_{\mathbf{q}}\cdot\left[(1+\delta\varrho)\,\mathbf{w}\right] + \frac{\nabla^2_{\mathbf{q}} p}{\varrho_H a^2} + \frac{1}{a^2}\frac{\partial^2}{\partial q^i \partial q^j}\left[(1+\delta\varrho)\,u^i u^j\right], \tag{2.30}$$

with the first order equation being

$$\frac{\partial^2 \delta\varrho^{(1)}}{\partial t^2} + 2H\frac{\partial \delta\varrho^{(1)}}{\partial t} - 4\pi G\varrho_H \delta\varrho^{(1)} = \frac{\nabla^2_{\mathbf{q}} p}{\varrho_H a^2}. \tag{2.31}$$

To close Eq. (2.30) one has to know the equation of state of the matter model.

As we have mentioned in section 1.4, although a lot can be accomplished by using the SPT for gravitational instabilities, LPT intrinsically includes more nonlinear information than SPT and remains valid longer. In next few sections, we will first briefly review the LPT in Newtonian cosmologies, and then discuss some first insights towards applying the LPT in Newtonian cosmologies with two different matter components. Finally, we will concisely introduce the LPT of large scale structure formation in relativistic cosmologies.

2.2 The Newtonian Lagrangian perturbation approach

In the 1970s, Zel'dovich [1970a] proposed a new approximate description of the weakly nonlinear regime, in which the perturbation is given in terms of the departure from the Lagrangian positions of the fluid elements, *i.e.*, $\mathbf{r} = a(t)\mathbf{q} + b(t)\mathbf{p}\,(\mathbf{q})$. Here $\mathbf{r}$ is the Eulerian position of a particle and $\mathbf{q}$ are its Lagrangian coordinates (its initial position). The first term $a(t)\mathbf{q}$ describes the cosmic expansion and the second term describes the perturbation. This approximation then was investigated as the so-called "pancake theory" [Zel'dovich, 1970b; Zeldovich, 1978; Arnold et al., 1982; Shandarin et al., 1983; Shandarin and Zeldovich, 1989; Yoshisato and Morikawa, 2006; Sergei et al., 2012].

Evidently, the Zel'dovich ansatz defined a map between the Lagrangian and Eulerian observer. In spirit of this approximation, Lagrangian perturbation theory was proposed and developed in the 1980s–1990s. Shandarin [1980] discussed the evolution of perturbations in a Friedmann universe with a pressureless medium, deriving approximate 3D solutions in the framework of the Zel'dovich approach. Buchert and Götz [1987] obtained a class of solutions of the three-dimensional hydrodynamical equations governing the motion of self-gravitating pressureless matter using the Lagrange method in Newtonian gravity. In a subsequent paper Buchert [1989] extended the results and formalism developed in the pancake theory and elaborated in detail the inhomogeneous 3D solutions in Newtonian theory without a cosmological constant. Moutarde et al. [1991] then discussed the nonlinear regime before shell crossing for 3D perturbations by studying the collapse around a simple isolated overdensity in an expanding cosmology consisting only of collisionless matter. This investigation initiated the perturbative approach in Lagrangian theory. At this stage it was already proved that the Zel'dovich approximation was a special first-order solution in a subclass of the Lagrangian framework.

Later Bildhauer et al. [1992] generalized these solutions to Newtonian cosmologies with a cosmological constant. Buchert and his collaborators discussed the solutions of first-order, second-order and third-order perturbations in the framework of the Lagrangian theory of gravitational instability of Friedmann-Lemaître cosmologies filled with dust matter in [Buchert, 1992; Buchert and Ehlers, 1993; Buchert, 1994]. Bouchet et al. [1992] derived analytic expressions for the second-order solutions with arbitrary density parameter Ω in a Friedmann-Lemaître model with vanishing Λ and a nonrelativistic pressureless fluid. A detailed investigation and generalization of these second-order solutions in a spatially flat Universe was discussed in a subsequent paper [Bouchet et al., 1995]. The formalism that allows the derivation of the general Lagrangian dynamical equations of motion for gravitating particles in a non-flat Friedmann universe with arbitrary density parameter and zero cosmological constant was presented by Catelan [1995], treating the set of particles as a Newtonian collisionless fluid. A very basic review was given by Ehlers and Buchert [1996], where they reconsidered the "Newtonian" theory of spatially unbounded, self-gravitating, pressureless continua in Lagrangian form in great detail. See [Buchert, 1993, 1996a;

Bouchet, 1996] for more information on LPT in Newtonian cosmologies with a dust matter model.

Since the Zel'dovich approximation and the LPT break down when multi-stream systems develop, the adhesion approximation had been proposed to repair this shortcoming [Gurbatov et al., 1989]. In such an approximation, if one assumes an isotropically distributed velocity dispersion, then an effective pressure can arise from the velocity dispersion, see Eq. (2.14). Buchert and Domínguez [1998] presented a method to construct models of large-scale structure within the multi-stream regime and derived an evolution equation for the mean peculiar velocity that relates to background solutions of Friedmann-Lemaître type in the Lagrangian framework. In particular, with an assumption of an isotropic velocity dispersion they obtained an "equation of state" (EOS) with $p(\mathbf{X},t) = \kappa(\mathbf{X})\ \varrho(\mathbf{X},t)^{5/3}$, where $p, \kappa, \varrho, \mathbf{X}$ are the effective pressure, a positive integration constant, the dust mass density and Lagrangian coordinates, respectively. Later, Buchert and Adler [1999] discussed Lagrangian perturbation theory in detail for modelling pressure-supported fluids with an EOS $p = \alpha(\varrho)$. The first-order equations were compared to the Eulerian theory of gravitational instability and to the case of plane-symmetric collapse. This framework extended the Zel'dovich approximation into the multi-streamed regime.

The Lagrangian perturbation equations for a polytropic fluid up to the second order have been introduced in [Morita and Tatekawa, 2001; Tatekawa et al., 2002]. Morita and Tatekawa [2001] considered first-order and second-order solutions limited to special cases, while Tatekawa et al. [2002] generalized the solutions to a large range. The third-order perturbative solutions were investigated in [Tatekawa, 2005a,b]. The fourth-order perturbative equations for a cosmological dust fluid in LPT were derived in [Tatekawa, 2013].

All the papers cited above discussed the LPT in Newtonian cosmologies with pressureless matter models. For their generalization to general matter models and general relativistic cosmologies, see section 2.3.

2.2.1 Mapping from Eulerian coordinates to Lagrangian coordinates

As we have already mentioned, the interesting variables in the Lagrangian picture are the trajectories of fluid elements, also known as the deformation fields of the medium. Motivated by the Zel'dovich approximation, the mapping from Eulerian coordinates to Lagrangian coordinates can be given as a diffeomorphism mapping:

$$\begin{aligned} \mathbf{f}: \mathbb{R}^3 &\longmapsto \mathbb{R}^3, \\ \mathbf{X} &\longmapsto \mathbf{x} = \mathbf{f}(\mathbf{X}, t), \end{aligned} \tag{2.32}$$

where $\mathbf{X} = \mathbf{f}(\mathbf{X}, t_{\mathbf{i}})$ are the Lagrangian coordinates and $\mathbf{x}$ the Eulerian coordinates. One has to keep in mind that when caustics form, one can still follow the trajectories $\mathbf{f}$ of the fluid elements across the caustics. Non-uniqueness of the flow is only realized in Eulerian space [Buchert, 1994]. The deformation fields thus can be defined as $\mathbf{P}(\mathbf{X}, t)$:

$$\mathbf{x} = \mathbf{f}(\mathbf{X}, t) = \mathbf{X} + \mathbf{P}(\mathbf{X}, t). \tag{2.33}$$

To simplify the calculations, for arbitrary functions $A(\mathbf{X}, t), B(\mathbf{X}, t), C(\mathbf{X}, t)$ one can form the Jacobian, $\mathcal{J}(A, B, C)$ by:

$$\begin{aligned} \mathcal{J}(A, B, C) = \frac{\partial(A, B, C)}{\partial(X_1, X_2, X_3)} &\equiv \begin{vmatrix} \frac{\partial A}{\partial X_1} & \frac{\partial B}{\partial X_1} & \frac{\partial C}{\partial X_1} \\ \frac{\partial A}{\partial X_2} & \frac{\partial B}{\partial X_2} & \frac{\partial C}{\partial X_2} \\ \frac{\partial A}{\partial X_3} & \frac{\partial B}{\partial X_3} & \frac{\partial C}{\partial X_3} \end{vmatrix} \\ &= \varepsilon_{klm}\, \partial_k A\, \partial_l B\, \partial_m C = \varepsilon_{klm} A_{|k} B_{|l} C_{|m}, \end{aligned} \tag{2.34}$$

where as usual we will use "|" and "," to distinguish partial derivative with respect to Lagrangian coordinates, $\mathbf{X}$, and Eulerian coordinates, $\mathbf{x}$, respectively. ε_{klm} is the Levi-Civita tensor. The functional determinants satisfy the following relations:

$$\begin{aligned} \mathcal{J}(A + D, B, C) &= \mathcal{J}(A, B, C) + \mathcal{J}(D, B, C), \\ \mathcal{J}(A, B, C) &= -\mathcal{J}(A, C, B), \\ \mathcal{J}(A, A, C) &= 0, \end{aligned} \tag{2.35}$$

$$\mathcal{J}\left(A\cdot D,B,C\right)=D\cdot\mathcal{J}\left(A,B,C\right)+A\cdot\mathcal{J}\left(D,B,C\right).$$

Using this notation, the Jacobian of the transformation between Eulerian and Lagrangian coordinates is given by

$$J\left(\mathbf{X},t\right)=\left|\frac{\partial\mathbf{x}}{\partial\mathbf{X}}\right|=\mathcal{J}\left(f^{i},f^{j},f^{k}\right)=\frac{1}{6}\varepsilon_{ijk}\varepsilon^{lmn}f^{i}{}_{|l}\,f^{j}{}_{|m}\,f^{k}{}_{|n} \tag{2.36}$$

Clearly for such a definition $J\left(\mathbf{X},t_{\mathbf{i}}\right)=1$. This definition also shows the singularity of J. At the first crossing of trajectories, different fluid elements from different initial positions $\mathbf{X}$ will meet at the same Eulerian positions $\mathbf{x}$. J will be zero in this case according to Eqs. (2.35). The correct description then should involve a summation over all possible streams in this multi-stream region. One way to solve this problem is to consider the mean velocity in the multi-stream region in the adhesion approximation [Buchert and Domínguez, 2005]. Another useful relation is the transformation of the derivative with respect to $\mathbf{X}$ and $\mathbf{x}$ for an arbitrary function $s\left(\mathbf{x},t\right)$ [Buchert and Adler, 1999]

$$s^{i}{}_{,j}=\frac{1}{2J}\,\varepsilon_{jpq}\,\mathcal{J}\left(s^{i},f^{p},f^{q}\right). \tag{2.37}$$

The continuity equation for the mass density represents the conservation of mass along the trajectories of the fluid elements. Thus the mass density at any time can be expressed as

$$\varrho\left(\mathbf{X},t\right)\,J\left(\mathbf{X},t\right)=\varrho\left(\mathbf{X},t_{\mathbf{i}}\right), \tag{2.38}$$

which is a non-perturbative expression of the evolution of mass density.

Consider the N-particles system, Eqs. (2.13, 2.14, 2.15) in Newtonian cosmologies. If we assume an isotropic velocity dispersion, (*i.e.*, $\boldsymbol{\mathcal{F}}=0$, $\mathcal{P}_{ij}=p\left(\varrho\right)\delta_{ij}$), then the Euler equations yield (for more details see [Buchert and Adler, 1999])

$$\mathbf{g}-\frac{\nabla_{\mathbf{x}}p}{\varrho}=\frac{d^{2}\mathbf{f}}{dt^{2}}. \tag{2.39}$$

Thus the h-th component of $\nabla_{\mathbf{x}} \times \mathbf{g}$ for the fluid element is given by

$$\begin{aligned} 0 = (\nabla_{\mathbf{x}} \times \mathbf{g})^h &= \left(\nabla_{\mathbf{x}} \times \ddot{\mathbf{f}}\right)^h + \left(\frac{\nabla_{\mathbf{x}} p \times \nabla_{\mathbf{x}} \varrho}{\varrho^2}\right)^h \\ &= \varepsilon^{hji}\, \ddot{f}_{i,j} + \frac{\varepsilon^{hji}}{\varrho^2}\, \varrho_{,i}\, p_{,j} \\ &= \frac{1}{J}\, \mathcal{J}\left(\ddot{f}_i, f_i, f_h\right) + \frac{1}{2\, J^2\, \varrho^2}\, \varepsilon^{jpq} \mathcal{J}\left(\varrho, f_h, f_j\right)\, \mathcal{J}\left(p, f_p, f_q\right). \end{aligned} \tag{2.40}$$

Another equation for $\mathbf{g}$ is given by

$$\begin{aligned} \Lambda - 4\pi G \varrho = \nabla_{\mathbf{x}} \cdot \mathbf{g} &= \nabla_{\mathbf{x}} \cdot \ddot{\mathbf{f}} + \nabla_{\mathbf{x}} \cdot \frac{\nabla_{\mathbf{x}} p}{\varrho} \\ &= \frac{1}{2J}\, \varepsilon^{jpq}\, \mathcal{J}\left(\ddot{f}_j, f_p, f_q\right) - \frac{1}{2\, J^3\, \varrho}\, \mathcal{J}\left(p, f_p, f_q\right) \mathcal{J}\left(J, f_p, f_q\right) \\ &- \frac{1}{2\, J^2\, \varrho^2}\, \mathcal{J}\left(p, f_p, f_q\right)\, \mathcal{J}\left(\varrho, f_p, f_q\right) \\ &+ \frac{1}{2\, J^2\, \varrho}\, \mathcal{J}\left(\mathcal{J}\left(p, f_p, f_q\right), f_p, f_q\right). \end{aligned} \tag{2.41}$$

Thus once the EOS is chosen, Eqs. (2.38, 2.40, 2.41) specify the evolution equations for large-scale structure formation in Newtonian cosmologies filled with dust matter, which is also supported by a kinetic pressure. This system is called the Lagrange-Newton system.

Evidently, this system is nonlinear and should be solved perturbatively, *i.e.*,

$$\mathbf{P}\left(\mathbf{X}, t\right) = \varepsilon\, \mathbf{P}^{(1)} + \varepsilon^2\, \mathbf{P}^{(2)} + \varepsilon^3\, \mathbf{P}^{(3)} \cdots, \tag{2.42}$$

with $\varepsilon \ll 1$. Solutions at various different orders have been investigated in many papers, as noted in the historical introduction above.

2.2.2 Lagrangian perturbation theory in Newtonian cosmologies with two fluid components: a first insight

2.2.2.1 The coarse-grained dynamical equations of fluid mixture with two components

Following the logic of section 2.1.1 one can generalize the approach to the case of a fluid mixture. Such cases have been discussed for many years in the study of plasma physics. For example, see Bittencourt [2004].

We will assume a N-particle system, which consists of two components A and B coupled solely by gravity. The total number of particles in such a system should be the sum of each component, thus $N = N_A + N_B$ where $N_{A(B)}$ is the particle number of component A (B). Since we have neglected all other interactions, each component should follow the Boltzmann equation (2.5) with the Klimontovich density f_{KA} and f_{KB} defined by Eq. (2.1). The total Klimontovich density for all species can be defined as

$$f_K(\mathbf{x}, \mathbf{v}, t) = \frac{\sum_\alpha m_\alpha f_{K\alpha}(\mathbf{x}, \mathbf{v}, t)}{\sum_\alpha m_\alpha}, \qquad \alpha = A,\, B. \tag{2.43}$$

According to Eqs. (2.11, 2.12), we can define the mean mass and mean velocity for each species:

$$\varrho_\alpha(\mathbf{x}, t) = m_\alpha \int d\mathbf{v} f_\alpha(\mathbf{x}, \mathbf{v}, t) = \frac{m_\alpha}{\mathcal{L}^3} \sum_i^{N_\alpha} W\left(\frac{\mathbf{x} - \boldsymbol{x}_\alpha^{(i)}}{\mathcal{L}}\right), \tag{2.44}$$

$$\varrho_\alpha \bar{\mathbf{v}}_\alpha(\mathbf{x}, t) = m_\alpha \int d\mathbf{v}\, \mathbf{v} f_\alpha(\mathbf{x}, \mathbf{v}, t) = \frac{m_\alpha}{\mathcal{L}^3} \sum_i^{N_\alpha} W\left(\frac{\mathbf{x} - \boldsymbol{x}_\alpha^{(i)}}{\mathcal{L}}\right) \boldsymbol{v}_\alpha^{(i)}, \tag{2.45}$$

and the total mass density and the mass-average velocity of the fluid mixture can be defined as

$$\varrho(\mathbf{x}, t) = \int d\mathbf{v} \sum_\alpha \left(m_\alpha f_\alpha(\mathbf{x}, \mathbf{v}, t)\right), \tag{2.46}$$

$$\varrho \bar{\mathbf{v}}(\mathbf{x}, t) = \int d\mathbf{v}\, \mathbf{v} \sum_\alpha \left(m_\alpha f_\alpha(\mathbf{x}, \mathbf{v}, t)\right). \tag{2.47}$$

The above equations then show that

$$\varrho = \sum_\alpha \varrho_\alpha, \tag{2.48}$$

$$\varrho\,\bar{\mathbf{v}} = \sum_\alpha \varrho_\alpha\,\bar{\mathbf{v}}_\alpha. \tag{2.49}$$

In this sense, considering a volume element $d^3\mathbf{x}$ around the coordinate $\mathbf{x}$, from Eq. (2.49) it follows that

$$\bar{\mathbf{v}} = \frac{\sum_\alpha \varrho_\alpha\,\bar{\mathbf{v}}_\alpha\,d^3\mathbf{x}}{\sum_\alpha \varrho_\alpha\,d^3\mathbf{x}} = \frac{\sum_\alpha \Delta m_\alpha\,\bar{\mathbf{v}}_\alpha}{\sum_\alpha \Delta m_\alpha}. \tag{2.50}$$

Thus the mass-average velocity $\bar{\mathbf{v}}$ of the fluid mixture is defined as a weighted average of $\bar{\mathbf{v}}_\alpha$ taking Δm_α as the weighting factor.

Again, we have assumed that there are no other interactions between different species except for gravity. Furthermore each component is collisionless. The mass conservation equation (2.13) shows that for each component, along the trajectories of particles (or the integral curve of velocity $\bar{\mathbf{v}}_\alpha$) the mass density is conserved:

$$\frac{\partial \varrho_\alpha}{\partial t} + \nabla\cdot(\varrho_\alpha\bar{\mathbf{v}}_\alpha) = 0. \tag{2.51}$$

Furthermore, the total mean density ϱ has the same continuity equation along the integral curve of $\bar{\mathbf{v}}$. Obviously, the mean mass density for each component is not conserved along the integral curve of $\bar{\mathbf{v}}$. In fact along the trajectories of the fluid mixture the continuity equation for each component should be

$$\frac{\partial \varrho_\alpha}{\partial t} + \nabla\cdot(\varrho_\alpha\bar{\mathbf{v}}) + \nabla\cdot\mathbf{j}_\alpha = 0, \tag{2.52}$$

where

$$\mathbf{j}_\alpha = \varrho_\alpha\,(\bar{\mathbf{v}}_\alpha - \bar{\mathbf{v}})\,, \tag{2.53}$$

describes the change of the mass density of species α along the trajectory of the fluid mixture. This can be seen as the mass diffusion flux of species α [Curtiss and Bird, 1996]. Clearly, the total change of different species should be zero, *i.e.*, $\sum_\alpha \mathbf{j}_\alpha = 0$.

Following each integral curve of $\bar{\mathbf{v}}_\alpha$, the evolution equation of the mean ve-

locity for each component obeys Eq. (2.14):

$$\frac{\partial \bar{\mathbf{v}}_\alpha}{\partial t} + (\bar{\mathbf{v}}_\alpha \cdot \nabla)\, \bar{\mathbf{v}}_\alpha = \boldsymbol{g} + \frac{1}{\varrho_\alpha} (\boldsymbol{\mathcal{F}}_\alpha - \nabla \cdot \boldsymbol{\mathcal{P}}_\alpha)\,, \tag{2.54}$$

with

$$\nabla \cdot \boldsymbol{g} = \Lambda - 4\pi G \varrho, \quad \nabla \times \boldsymbol{g} = 0, \tag{2.55}$$

showing that the gravitational field strength $\boldsymbol{g}$ is determined by the whole system. Eq. (2.54) can be alternatively represented as

$$\frac{\partial}{\partial t} (\varrho_\alpha\, \bar{\mathbf{v}}_\alpha) = -\nabla \cdot (\varrho_\alpha\, \bar{\mathbf{v}}_\alpha \cdot \bar{\mathbf{v}}_\alpha) + \varrho_\alpha\, \boldsymbol{g} + (\boldsymbol{\mathcal{F}}_\alpha - \nabla \cdot \boldsymbol{\mathcal{P}}_\alpha)\,, \tag{2.56}$$

with

$$\nabla (\varrho_\alpha\, \bar{\mathbf{v}}_\alpha \cdot \bar{\mathbf{v}}_\alpha) = \varrho_\alpha\, (\bar{\mathbf{v}}_\alpha \cdot \nabla)\, \bar{\mathbf{v}}_\alpha + \bar{\mathbf{v}}_\alpha\, [\nabla \cdot (\varrho_\alpha \bar{\mathbf{v}}_\alpha)]$$

With the definition Eq. (2.49), the equation of motion for the mixture can be obtained by summing Eq. (2.56) over all species

$$\frac{\partial}{\partial t} (\varrho\, \bar{\mathbf{v}}) = -\sum_\alpha \nabla \left(\frac{1}{\varrho_\alpha} \mathbf{j}_\alpha \cdot \mathbf{j}_\alpha \right) - \nabla \cdot (\varrho\, \bar{\mathbf{v}} \cdot \bar{\mathbf{v}}) + \varrho\, \mathbf{g} + \sum_\alpha (\boldsymbol{\mathcal{F}}_\alpha - \nabla \cdot \boldsymbol{\mathcal{P}}_\alpha)\,. \tag{2.57}$$

The first term of right hand side shows the velocity deviation of species α from the mixture velocity. This term can be cancelled out when $\boldsymbol{\mathcal{P}}$ is considered to account for the velocity dispersion from the mean velocity of mixture. The expression Eq. (2.17) for $\boldsymbol{\mathcal{P}}_\alpha$ can be represented as

$$\begin{aligned}
\mathcal{P}^\alpha_{ij} &= \frac{m_\alpha}{\mathcal{L}^3} \sum_i W \left(\frac{\mathbf{x} - \boldsymbol{x}^{(i)}_\alpha}{\mathcal{L}} \right) \left[v^{(i)}_{\alpha i}\, v^{(i)}_{\alpha j} - \bar{\mathrm{v}}_{\alpha i}\, \bar{\mathrm{v}}_{\alpha j} \right] \\
&= \frac{m_\alpha}{\mathcal{L}^3} \sum_i W \left(\frac{\mathbf{x} - \boldsymbol{x}^{(i)}_\alpha}{\mathcal{L}} \right) \left[v^{(i)}_{\alpha i}\, v^{(i)}_{\alpha j} - \frac{\mathrm{j}_{\alpha i}}{\varrho_\alpha} \frac{\mathrm{j}_{\alpha j}}{\varrho_\alpha} - \frac{\mathrm{j}_{\alpha i}\, \bar{\mathrm{v}}_j + \mathrm{j}_{\alpha j}\, \bar{\mathrm{v}}_i}{\varrho_\alpha} - \bar{\mathrm{v}}_i\, \bar{\mathrm{v}}_j \right] \\
&= \frac{m_\alpha}{\mathcal{L}^3} \sum_i W \left(\frac{\mathbf{x} - \boldsymbol{x}^{(i)}_\alpha}{\mathcal{L}} \right) \left[v^{(i)}_{\alpha i}\, v^{(i)}_{\alpha j} - \bar{\mathrm{v}}_i\, \bar{\mathrm{v}}_j \right] - \frac{1}{\varrho_\alpha} \mathrm{j}_{\alpha i}\, \mathrm{j}_{\alpha j} - \left(\mathrm{j}_{\alpha i}\, \bar{\mathrm{v}}_j + \mathrm{j}_{\alpha j}\, \bar{\mathrm{v}}_i \right) \\
&= \tilde{\mathcal{P}}^\alpha_{ij} - \frac{1}{\varrho_\alpha} \mathrm{j}_{\alpha i}\, \mathrm{j}_{\alpha j} - \left(\mathrm{j}_{\alpha i}\, \bar{\mathrm{v}}_j + \mathrm{j}_{\alpha j}\, \bar{\mathrm{v}}_i \right)
\end{aligned} \tag{2.58}$$

where we have used the definition of ϱ_α. Thus we can rewrite $\boldsymbol{\mathcal{P}}_\alpha$ as

$$\nabla \cdot \boldsymbol{\mathcal{P}}_\alpha = \nabla \cdot \tilde{\boldsymbol{\mathcal{P}}}_\alpha - \nabla \left(\frac{1}{\varrho_\alpha} \mathbf{j}_\alpha \cdot \mathbf{j}_\alpha \right) - \nabla \left(\mathbf{j}_\alpha \cdot \bar{\mathbf{v}} + \bar{\mathbf{v}} \cdot \mathbf{j}_\alpha \right). \tag{2.59}$$

Recall that for all species, $\sum_\alpha \mathbf{j}_\alpha = 0$, so summing over all species will reduce the above equation to

$$\sum_\alpha \nabla \cdot \boldsymbol{\mathcal{P}}_\alpha = \sum_\alpha \nabla \cdot \tilde{\boldsymbol{\mathcal{P}}}_\alpha - \sum_\alpha \nabla \left(\frac{1}{\varrho_\alpha} \mathbf{j}_\alpha \cdot \mathbf{j}_\alpha \right). \tag{2.60}$$

Inserting this relation into Eq. (2.57), we find

$$\frac{\partial \bar{\mathbf{v}}}{\partial t} + (\bar{\mathbf{v}} \cdot \nabla) \bar{\mathbf{v}} = \boldsymbol{g} + \frac{1}{\varrho} \sum_\alpha \left(\tilde{\boldsymbol{\mathcal{F}}}_\alpha - \nabla \cdot \tilde{\boldsymbol{\mathcal{P}}}_\alpha \right). \tag{2.61}$$

Here we have used the fact that the gravitational field strength is determined by the monopole moment of the mass distribution in the whole system defined by the window function, so $\boldsymbol{g}$ will be same for all species. Thus $\boldsymbol{\mathcal{F}}_\alpha$ indeed describes the deviation from the mean field gravity for component α. This fact makes $\boldsymbol{\mathcal{F}}_\alpha = \tilde{\boldsymbol{\mathcal{F}}}_\alpha$. However, as a consequence of Eq. (2.60) if one chooses each $\boldsymbol{\mathcal{P}}_\alpha$ to be isotropic, then generally speaking, $\tilde{\boldsymbol{\mathcal{P}}}_\alpha$ cannot be isotropic.

Finally we have constructed a system of fluid-like equations to describe the dynamics of a fluid mixture consisting of two different collisionless components. Since such a system has been derived in Newtonian cosmology, we can refer it as the Eulerian system. We have ignored all other interactions and considered only the gravitational interaction. The equations of the system include Eqs. (2.48, 2.49, 2.51, 2.53, 2.54, 2.55, 2.61). Again, such a system is not closed as already mentioned in section 2.1.1.

As been discussed by Buchert and Domínguez [2005] closure can be achieved if the mean density ϱ_α and the mean velocity $\bar{\mathbf{v}}_\alpha$ vary spatially over length scales much larger than any microscopic length scale. A set of closed hydrodynamic equations can be obtained with the assumption of local quasi-equilibrium. The corrections to equilibrium then are proportional to the relatively small spatial gradients of ϱ_α and $\bar{\mathbf{v}}_\alpha$. However, to describe cosmological structure formation, one has to consider other closure conditions since thermal equilibrium is not

well-defined.

To close the system, one will need to adopt some approximations motivated by physical constraints for both components. The problem is greatly simplified by fact that the only interaction between the two components is the gravitational interaction. In view of this one can assume three cases in the context of cosmological structure formation.

In the first case, $\boldsymbol{\mathcal{F}} = 0$ and $\boldsymbol{\mathcal{P}} = 0$ for both components. In the language of the hydrodynamic approximation, such matter models are called dust or pressureless fluids. In the adhesive model, such a choice is characterized by two assumptions: the irrelevance of small-scale inhomogeneities and the absence of multi-streaming [Buchert and Domínguez, 2005]. However, even though for each component the right hand side of Eq. (2.54) will only have $\boldsymbol{g}$ left, an additional term inevitably appears in the right hand side of Eq. (2.57) if $\bar{\mathbf{v}}_\alpha \neq \bar{\mathbf{v}}_\beta$.

In the second case we assume that one of the component is dust. For the other component, we assume that the corrections to mean field gravity are neglected, and the velocity dispersion corresponding to its trajectory is approximated by an isotropic tensor field. In summary, we can assume $\boldsymbol{\mathcal{F}}_\alpha = \boldsymbol{\mathcal{F}}_\beta = 0$, $\boldsymbol{\mathcal{P}}_\alpha = 0$ and $\boldsymbol{\mathcal{P}}_\beta = p_\beta(\varrho_\beta)\,\boldsymbol{\delta}$, where $\boldsymbol{\delta}$ is the Kronecker delta tensor with components $\delta_{ij} = 0$ for $i \neq j$ and $\delta_{ij} = 1$ for $i = j$. In addition, we assume $p(\varrho) > 0$. Evidently, the appearance of "pressure" resists the attracting effects of gravity. So in this case, it can be expected that the dust component will have a faster concentration growth rate than the other component with a kinetic pressure. This simple model is the basic picture in considering the generation of the BAO in the concordance cosmology.

Briefly, in the concordance cosmology the dynamics of the different components, namely dark matter and the baryon-photon plasma are described by the hydrodynamic approximation. The former is treated as pressureless fluid and undergoes almost no interactions with the plasma. On the other hand, the baryon-photon plasma is treated as a fluid with pressure. The gravitational attraction and the resisting effects of pressure lead to the imprint of the BAO. A succinct description of the generation of the BAO has been given by Eisenstein et al. [2007]. Roughly speaking, considering a point-like overdensity in an adiabatic model, the overdensity will be manifest in all components. The perturbation for the baryon-photon plasma is not only an overdensity but also an overpressure.

This overpressure will equilibrate with the surroundings by driving an expanding sound wave out into the plasma. During this phase the amplitude of the density contrast in the plasma undergoes harmonic motion, or oscillation. The dark matter has decoupled from the plasma at that epoch and thus one will be left with a density contrast at small radius. As the expanding universe cools down recombination occurs and photons start to decouple from the baryons. The oscillations in the baryons are frozen in at this decoupling epoch. The sound speed then plummets. As a consequence, for the concordance cosmology a cold dark matter overdensity will be left at the centre surrounded by a baryon overdensity in a spherical shell $\simeq 150$ Mpc in comoving radius. At $z \ll 10^3$ cold dark matter overdensities and baryon overdensities both attract each other, seeding the usual gravitational instability. Finally the dark matter and baryon perturbations come together.

Here, however, our second case is constructed to describe the later time nonlinear cosmological structure formation with two components. The two components are both dust intrinsically. One component will have corrections from the gravitational multi-streaming effects but the other one has no such corrections. If the mixture of two components behaves as a single dust fluids at a time earlier than the considered time then the formalism above is not needed.

In the third case for both species we assume $\boldsymbol{\mathcal{F}}_\alpha = \boldsymbol{\mathcal{F}}_\beta = 0$, and $\boldsymbol{\mathcal{P}}_\alpha = p_\alpha(\varrho_\alpha)\,\boldsymbol{\delta}$, $\boldsymbol{\mathcal{P}}_\beta = p_\beta(\varrho_\beta)\,\boldsymbol{\delta}$. With these assumptions, the gravitational multi-stream effects arise for both species as corrections to the dust models. Shell crossing occurs but with finite density fields. For this case in the reference frame of the mixture, the velocity dispersion will not be an isotropic one due to the presence of the additional term $\sum_\alpha \nabla(\varrho_\alpha^{-1}\,\mathbf{j}_\alpha \cdot \mathbf{j}_\alpha)$. Furthermore, this term can be replaced by

$$\sum_\alpha \nabla\left(\varrho_\alpha^{-1}\,\mathbf{j}_\alpha \cdot \mathbf{j}_\alpha\right) = \nabla\left[\frac{\varrho}{\varrho_\alpha\,(\varrho-\varrho_\alpha)}\,\mathbf{j}_\alpha \cdot \mathbf{j}_\alpha\right]. \tag{2.62}$$

In this third case with this relation, the dynamical equations for one of the two species can be replaced by the dynamical equations of the mixture Eq. (2.57). If $\mathbf{j}_\alpha$ is previously specified, then the whole system can be described by the dynamics of the fluid mixture.

Generally speaking, $\mathbf{j}_\alpha$ should be related to the physical realization α. In the

classical kinetic theory of diffusion for a mixture with multiple components, such fields are determined by the Maxwell-Stefan relations [Taylor and Krishna, 1993; Krishna and Wesselingh, 1997; Leonardi and Angeli, 2010]

$$-\frac{c_\alpha}{c_t RT}\nabla_T \mu_\alpha = \sum_{\beta=1}^{n} \frac{c_\beta \mathbf{j}_\alpha - c_\alpha \mathbf{j}_\beta}{c_t^2 \mathfrak{D}_{\alpha\beta}}, \quad \alpha = 1, 2, \cdots, n. \quad \alpha \neq \beta, \tag{2.63}$$

where α, $\beta \cdots$ denote different species, $c_\alpha = \varrho_\alpha / \mathcal{M}_\alpha$ is the molar density of species α with molar mass $\mathcal{M}_\alpha$, $c_t = \sum_\alpha c_\alpha$ is the mixture molar density, μ_α is the molar chemical potential of species α, R is the molar gas constant and T is the temperature of the system. Here we use $\mathfrak{D}_{\alpha\beta}$ as the Maxwell-Stefan diffusion coefficients, which are related to the physical properties of the materials. In the context of cosmological structure formation, such a relation is not suitable since, again, the thermal equilibrium is not well-defined. Also we do not know the physical properties of dark matter.

Obviously, a trivial case is to set $\mathbf{j}_\alpha = 0$ which could apply to all three cases. With this assumption, the mean velocities of species are equal to the velocity of the fluid mixture. $\tilde{\boldsymbol{\mathcal{P}}}_\alpha$ then corresponds to the velocity dispersion around the mean velocity of the mixture for component α, while $\tilde{\boldsymbol{\mathcal{F}}}_\alpha$ is still the deviation from the mean field gravity. Since both components are dust fluids we can ignore the difference of species, and set $\sum_\alpha \tilde{\boldsymbol{\mathcal{F}}}_\alpha = \bar{\boldsymbol{\mathcal{F}}}$, $\sum_\alpha \tilde{\boldsymbol{\mathcal{P}}}_\alpha = \bar{\boldsymbol{\mathcal{P}}}$. The whole system then is treated as a dust fluid composed of a "single species" with mean mass density ϱ and mean velocity field $\bar{\mathbf{v}}$.

2.2.2.2 Transforming to comoving coordinates

The cosmological problems will be simplified by using comoving coordinates. Such a coordinate system is attached to a homogeneous and isotropic solution, *i.e.*, the Friedmann-Lemaître background. Structure formation is seeded from the tiny inhomogeneities. In this section we will transform the equations derived in the last subsection into comoving coordinates.

One can define the comoving positions $\boldsymbol{q}_\alpha^{(i)}$, peculiar velocities $\boldsymbol{u}_\alpha^{(i)}$ and gravitational peculiar-accelerations $\boldsymbol{w}_\alpha^{(i)}$ for each species as follows:

$$\boldsymbol{q}_\alpha^{(i)} \equiv \frac{1}{a}\boldsymbol{x}_\alpha^{(i)},$$

$$\begin{aligned} \boldsymbol{u}_\alpha^{(i)} &\equiv \boldsymbol{v}_\alpha^{(i)} - H\,\boldsymbol{x}_\alpha^{(i)}, \\ \boldsymbol{w}_\alpha^{(i)} &\equiv \boldsymbol{g}_\alpha^{(i)} - \frac{\ddot{a}}{a}\,\boldsymbol{x}_\alpha^{(i)}, \end{aligned} \tag{2.64}$$

where a is the scale factor of the background. In a Friedmann-Lemaître background with two components, the Hubble parameter and the scale factor satisfy the Friedmann equations:

$$\begin{aligned} H^2 = \left(\frac{\dot{a}}{a}\right)^2 &= \frac{8\pi G\left(\varrho_{\alpha H} + \varrho_{\beta H}\right)}{3} + \frac{\Lambda}{3}, \\ \frac{\ddot{a}}{a} &= -\frac{4\pi G\left(\varrho_{\alpha H} + \varrho_{\beta H}\right)}{3} + \frac{\Lambda}{3}. \end{aligned} \tag{2.65}$$

With the definitions given in Eq. (2.64), the Newtonian equations of motion in Eqs. (2.2, 2.3, 2.4) can be rewritten as

$$\begin{aligned} \dot{\boldsymbol{q}}_\alpha^{(i)} &= \frac{\boldsymbol{u}_\alpha^{(i)}}{a}, \quad \dot{\boldsymbol{u}}_\alpha^{(i)} = \boldsymbol{w}_\alpha^{(i)} - H\,\boldsymbol{u}_\alpha^{(i)}, \\ \nabla_\alpha^{(i)} \cdot \boldsymbol{w}_\alpha^{(i)} &= -4\pi G a\left[m_\alpha\, a^3 \sum_{i\neq j}^{N_\alpha} \boldsymbol{\delta}\left(\boldsymbol{q}_\alpha^{(i)} - \boldsymbol{q}_\alpha^{(j)}\right) - \varrho_H\right], \\ \nabla_\alpha^{(i)} \times \boldsymbol{w}_\alpha^{(i)} &= \boldsymbol{0}, \end{aligned} \tag{2.66}$$

where $\varrho_H = \varrho_{\alpha H} + \varrho_{\beta H}$ is the total homogeneous and isotropic background density.

In last section, we have defined the mean mass density ϱ_α and the mean velocity $\bar{\mathbf{v}}_\alpha$ for each species. The definition of the mean mass density suggests it should be unchanged in the physical and comoving coordinate systems, $\varrho_\alpha\left(\mathbf{x}, \bar{\mathbf{v}}, t\right) = \varrho_{co}\left(\boldsymbol{q}, \boldsymbol{u}, t\right)$, where $\boldsymbol{q}$ is the comoving coordinate of fluid elements in the sense of coarse-graining. Without causing any confusion, we will drop the subscript "*co*" and use ϱ for the mean mass density in comoving coordinates. Thus we can define the mass density and mean peculiar velocity as

$$\varrho_\alpha\left(\boldsymbol{q}, t\right) \equiv \frac{m_\alpha}{(aL)^3} \sum_i W\left(\frac{\boldsymbol{q} - \boldsymbol{q}_\alpha^{(i)}}{L}\right), \tag{2.67}$$

$$\varrho_\alpha\, \boldsymbol{u}_\alpha\left(\boldsymbol{q}, t\right) \equiv \frac{m_\alpha}{(aL)^3} \sum_i W\left(\frac{\boldsymbol{q} - \boldsymbol{q}_\alpha^{(i)}}{L}\right) \boldsymbol{u}_\alpha^{(i)}, \tag{2.68}$$

where $L \equiv \mathcal{L}/a$ is defined as the comoving coarse-graining length. Then from Eq. (2.64), one has the relation

$$\bar{\mathbf{v}}_\alpha = \boldsymbol{u}_\alpha + H\,\boldsymbol{R}_\alpha = \boldsymbol{u}_\alpha + H\,\mathbf{x} + H\,(\boldsymbol{R}_\alpha - \mathbf{x})\,, \tag{2.69}$$

with

$$\varrho_\alpha\,\boldsymbol{R}_\alpha\,(\mathbf{x},t) = \frac{m_\alpha}{\mathcal{L}^3}\sum_i W\left(\frac{\mathbf{x}-\boldsymbol{x}_\alpha^{(i)}}{\mathcal{L}}\right)\boldsymbol{x}_\alpha^{(i)}. \tag{2.70}$$

Correspondingly, the peculiar counterparts of the vector field $\boldsymbol{\mathcal{F}}_\alpha$ and the velocity dispersion field $\boldsymbol{\mathcal{P}}_\alpha$ around the mean velocity $\bar{\mathbf{v}}_\alpha$ can be defined as

$$\boldsymbol{F}_\alpha\,(\boldsymbol{q},t) \equiv \boldsymbol{\mathcal{F}}_\alpha\,(\mathbf{x},t) - \frac{\ddot{a}}{a}\,\varrho_\alpha\,(\boldsymbol{R}_\alpha - \mathbf{x})\,, \tag{2.71}$$

$$\boldsymbol{\Pi}_\alpha\,(\boldsymbol{q},t) \equiv \boldsymbol{\mathcal{P}}_\alpha\,(\mathbf{x},t) + H^2\,\boldsymbol{\mathcal{I}}_\alpha\,(\mathbf{x},t) - H\,\left(\boldsymbol{\mathcal{D}}_\alpha + \boldsymbol{\mathcal{D}}_\alpha^T\right), \tag{2.72}$$

where $\boldsymbol{R}_\alpha, \boldsymbol{\mathcal{I}}_\alpha, \boldsymbol{\mathcal{D}}_\alpha$ and $\boldsymbol{\mathcal{D}}_\alpha^T$ are defined as the quantities relating to the coarse-graining procedure, with $\boldsymbol{\mathcal{D}}_\alpha^T$ meaning the transposed part of $\boldsymbol{\mathcal{D}}_\alpha$. For the ij component, one has

$$\mathcal{D}_{ij}^T = \mathcal{D}_{ji}.$$

In fact, as been suggested by Buchert and Domínguez [2005], $\boldsymbol{R}_\alpha$ is the center-of-mass position for species α in the subsystem defined by the smoothing window, $\boldsymbol{\mathcal{I}}_\alpha$ is the inertia tensor of the same subsystem with respect to $\boldsymbol{R}_\alpha$, and $\boldsymbol{\mathcal{D}}_\alpha$ is momentum tensor with respect to $\boldsymbol{R}_\alpha$. Their definitions are derived from relations (2.49, 2.70) and given by

$$\mathcal{I}_{\alpha ij}\,(\mathbf{x},t) \equiv \frac{m_\alpha}{\mathcal{L}^3}\sum_i W\left(\frac{\mathbf{x}-\boldsymbol{x}_\alpha^{(i)}}{\mathcal{L}}\right) x_{\alpha i}^{(i)}\,x_{\alpha j}^{(i)} - \varrho_\alpha\,R_{\alpha i}\,R_{\alpha j}, \tag{2.73}$$

and

$$\mathcal{D}_{\alpha ij}\,(\mathbf{x},t) \equiv \frac{m_\alpha}{\mathcal{L}^3}\sum_i W\left(\frac{\mathbf{x}-\boldsymbol{x}_\alpha^{(i)}}{\mathcal{L}}\right) v_{\alpha i}^{(i)}\,x_{\alpha j}^{(i)} - \varrho_\alpha\,\bar{\mathrm{v}}_{\alpha i}\,R_{\alpha j}, \tag{2.74}$$

while the components of $\boldsymbol{F}_\alpha$ and $\boldsymbol{\Pi}_\alpha$ are

$$F_{\alpha i}\,(\boldsymbol{q},t) = \frac{m_\alpha}{(aL)^3}\sum_\alpha W\left(\frac{\boldsymbol{q}-\boldsymbol{q}_\alpha^{(i)}}{L}\right)\left[w_{\alpha i}^{(i)} - w_i\,(\boldsymbol{q},t)\right], \tag{2.75}$$

$$\Pi_{\alpha ij}\left(\boldsymbol{q},t\right)=\frac{m_\alpha}{(aL)^3}\sum_\alpha W\left(\frac{\boldsymbol{q}-\boldsymbol{q}_\alpha^{(i)}}{L}\right)\left[u_{\alpha i}^{(i)}\,u_{\alpha j}^{(i)}-u_{\alpha i}\,u_{\alpha j}\right]. \tag{2.76}$$

With these definitions, one can show that the partial time derivative of Eq. (2.70) produces the relation:

$$\left.\frac{\partial\left(\varrho_\alpha R_{\alpha i}\right)}{\partial t}\right|_{\mathrm{x}}=-\frac{\partial}{\partial \mathrm{x}^j}\frac{m_\alpha}{\mathcal{L}^3}\sum_i W\left(\frac{\mathbf{x}-\boldsymbol{x}_\alpha^{(i)}}{\mathcal{L}}\right)x_{\alpha i}^{(i)}\,v_{\alpha j}^{(i)}+\varrho_\alpha\,\bar{\mathrm{v}}_{\alpha i}, \tag{2.77}$$

where "$|_{\mathrm{x}}$" means the partial time derivative with constant x, and $\frac{\partial}{\partial \mathrm{x}^j}\equiv\partial_j$ acts on the phase coordinate $\mathbf{x}$. Here we have assumed the Einstein summation convention on the index j.

Furthermore, in the comoving coordinate system $\mathbf{j}_\alpha$ can be represented as

$$\begin{aligned}\mathbf{j}_\alpha\left(\mathbf{x},t\right)&=\varrho_\alpha\left(\boldsymbol{u}_\alpha-\boldsymbol{u}\right)+H\varrho_\alpha\left(\boldsymbol{R}_\alpha-\boldsymbol{R}\right)\\&=\boldsymbol{j}_\alpha\left(\boldsymbol{q},t\right)+H\,\boldsymbol{j}_{R\alpha},\end{aligned} \tag{2.78}$$

where $\boldsymbol{R}$ is the centre-of-mass position of the fluid mixture defined by summing over all species

$$\varrho\,\boldsymbol{R}=\sum_\alpha\varrho_\alpha\boldsymbol{R}_\alpha. \tag{2.79}$$

This definition is consistent with the definition of Eqs. (2.67, 2.68, 2.69) if we define the total mass density and total comoving mean velocity as in Eqs. (2.48, 2.49)

$$\varrho\left(\boldsymbol{q},t\right)=\sum\varrho_\alpha\left(\boldsymbol{q},t\right),\quad \varrho\boldsymbol{u}=\sum\varrho_\alpha\,\boldsymbol{u}_\alpha. \tag{2.80}$$

Consequently, with the definition of comoving coordinates, Eqs. (2.64, 2.66), and relations (2.71, 2.72, 2.77), one can rewrite Eq. (2.56) as

$$\begin{aligned}&\left.\frac{\partial\left(\varrho_\alpha u_{\alpha i}\right)}{\partial t}\right|_{\mathrm{x}}+H\,\varrho_\alpha\,u_{\alpha i}-H\,\partial_j\left[\frac{m_\alpha}{\mathcal{L}^3}\sum_i W\left(\frac{\mathbf{x}-\boldsymbol{x}_\alpha^{(i)}}{\mathcal{L}}\right)v_{\alpha j}^{(i)}\,x_{\alpha i}^{(i)}\right]\\&\quad=-\partial_j\left(\varrho_\alpha\,u_{\alpha i}\,u_{\alpha j}\right)+\varrho_\alpha\,w_i+\left(F_{\alpha i}-\partial_j\Pi_{\alpha ij}\right)\\&\quad\quad-H^2\partial_j\left[\frac{m_\alpha}{\mathcal{L}^3}\sum_i W\left(\frac{\mathbf{x}-\boldsymbol{x}_\alpha^{(i)}}{\mathcal{L}}\right)x_{\alpha i}^{(i)}\,x_{\alpha j}^{(i)}\right].\end{aligned} \tag{2.81}$$

The first term on the left side can be derived from the definition of the comov-

ing mean velocity Eqs. (2.67, 2.68). The result will connect the partial time derivatives at fixed $\mathbf{x}$ and $\boldsymbol{q}$ by the relation

$$\left.\frac{\partial\left(\varrho_\alpha u_{\alpha i}\right)}{\partial t}\right|_q + 3H\,\varrho_\alpha\,u_{\alpha i} = \left.\frac{\partial\left(\varrho_\alpha\,u_{\alpha i}\right)}{\partial t}\right|_{\mathrm{x}} - H\,\partial_j\left[\frac{m_\alpha}{\mathcal{L}^3}\sum_i W\left(\frac{\mathbf{x}-\boldsymbol{x}_\alpha^{(i)}}{\mathcal{L}}\right)v_{\alpha j}^{(i)}\,x_{\alpha i}^{(i)}\right] + H^2\,\partial_j\left[\frac{m_\alpha}{\mathcal{L}^3}\sum_i W\left(\frac{\mathbf{x}-\boldsymbol{x}_\alpha^{(i)}}{\mathcal{L}}\right)x_{\alpha i}^{(i)}\,x_{\alpha j}^{(i)}\right]. \tag{2.82}$$

Inserting this equation into Eq. (2.81) one finally obtains the relation

$$\left.\frac{\partial\left(\varrho_\alpha\,\boldsymbol{u}_\alpha\right)}{\partial t}\right|_q + \frac{1}{a}\nabla_{\boldsymbol{q}}\left(\varrho_\alpha\boldsymbol{u}_\alpha\cdot\boldsymbol{u}_\alpha\right) + 4H\,\varrho_\alpha\,\boldsymbol{u}_\alpha = \varrho_\alpha\,\boldsymbol{w} + \left(\boldsymbol{F}_\alpha - \frac{1}{a}\nabla_{\boldsymbol{q}}\cdot\boldsymbol{\Pi}_\alpha\right). \tag{2.83}$$

The direct derivation of Eqs. (2.67, 2.68) also shows the evolution of the mass density $\varrho_\alpha\left(\boldsymbol{q},t\right)$ and the comoving mean velocity. The mass conservation equation is

$$\frac{\partial\varrho_\alpha}{\partial t} + 3H\varrho_\alpha + \frac{1}{a}\nabla_{\boldsymbol{q}}\cdot\left(\varrho_\alpha\,\boldsymbol{u}_\alpha\right) = 0, \tag{2.84}$$

where the time derivative is at fixed $\boldsymbol{q}$. The evolution equation of comoving mean velocity $\boldsymbol{u}_\alpha$ is then given by

$$\frac{\partial}{\partial t}\left(\varrho_\alpha\boldsymbol{u}_\alpha\right) + \frac{1}{a}\nabla_{\boldsymbol{q}}\left(\varrho_\alpha\boldsymbol{u}_\alpha\cdot\boldsymbol{u}_\alpha\right) + 4H\varrho_\alpha\boldsymbol{u}_\alpha = \varrho_\alpha\,\boldsymbol{w} + \left(\boldsymbol{F}_\alpha - \frac{1}{a}\nabla_{\boldsymbol{q}}\cdot\boldsymbol{\Pi}_\alpha\right), \tag{2.85}$$

where the mean peculiar-gravity field strength $\boldsymbol{w}$ satisfies

$$\nabla_{\boldsymbol{q}}\cdot\boldsymbol{w} = -\sum_\alpha 4\pi G a\left(\varrho_\alpha - \varrho_{\alpha H}\right), \quad \nabla_{\boldsymbol{q}}\times\boldsymbol{w} = 0. \tag{2.86}$$

If we drop off the symbol "$|_q$" in Eq. (2.83) then they are same evolution equations for mean velocity of species α, as expected.

Combining Eqs. (2.80, 2.84, 2.85), the evolution equations for the total mass density ϱ and comoving mean velocity of the mixture are

$$\frac{\partial\varrho}{\partial t} + 3H\varrho + \frac{1}{a}\nabla_{\boldsymbol{q}}\cdot\left(\varrho\,\boldsymbol{u}\right) = 0, \tag{2.87}$$

$$\frac{\partial}{\partial t}\left(\varrho \boldsymbol{u}\right)+\frac{1}{a}\nabla_{\boldsymbol{q}}\left(\varrho\,\boldsymbol{u}\cdot\boldsymbol{u}\right)+4H\varrho\boldsymbol{u}=-\sum_{\alpha}\frac{1}{a}\nabla_{\boldsymbol{q}}\left(\frac{\boldsymbol{j}_{\alpha}\cdot\boldsymbol{j}_{\alpha}}{\varrho_{\alpha}}\right)+\varrho\,\boldsymbol{w}+\boldsymbol{\mathcal{S}}_{term}, \tag{2.88}$$

$$\boldsymbol{\mathcal{S}}_{term}=\sum_{\alpha}\left(\boldsymbol{F}_{\alpha}-\frac{1}{a}\nabla_{\boldsymbol{q}}\cdot\boldsymbol{\Pi}_{\alpha}\right). \tag{2.89}$$

Finally with the comoving coordinates, we have constructed a dynamical system through the coarse-graining procedure for a fluid mixture consisting of two different species. As in the Eulerian system, the comoving system is closed by choosing some physical restrictions relating to large-scale structure formation.

We have discussed three different cases in section 2.2.2.1. Unfortunately, the approximations we used in those cases will be modified because of the new hierarchies arising from the transformations Eqs. (2.71, 2.72). A choice of $\boldsymbol{\mathcal{F}}_{\alpha}=0$ and $\boldsymbol{\mathcal{P}}_{\alpha}=p\left(\varrho_{\alpha}\right)\boldsymbol{\delta}$ does not equate to $\boldsymbol{F}_{\alpha}=0$ and $\boldsymbol{\Pi}_{\alpha}=p_{\alpha}\left(\varrho_{\alpha}\right)\boldsymbol{\delta}$. A brief interpretation has been discussed by Buchert and Domínguez [2005]. The equivalence between the comoving system and Eulerian system has to be carefully considered when the approximations are made.

To gain a first insight into the LPT of large-scale structure formation with two components in Newtonian cosmologies, we will focus on the third case. In the comoving coordinates system we suppose that $\boldsymbol{F}_{\alpha}=0$ and $\boldsymbol{\Pi}_{\alpha}=p_{\alpha}\left(\varrho_{\alpha}\right)\boldsymbol{\delta}$. With such a choice we can compare our results with those obtained from the one-component case in the LPT and SPT, respectively.

2.2.2.3 The Euler-Newton-System of two components with pressure in comoving coordinates

As a check, we will now reproduce the SPT in Newtonian cosmologies with two components supported by an isotropic pressure $p(\varrho)$ using the system of equations derived in the subsection above. This very basic investigation has been discussed by many authors within the framework of hydrodynamic approximation. For example, see [Grishchuk and Zel'dovich, 1981; Solov'eva and Nurgaliev, 1985; Solov'eva and Starobinsky, 1985; Mathai et al., 1988; Haubold et al., 1991; Gailis and Frankel, 2006]. Here we consider a non-rotating Eulerian coordinate system in a Newtonian cosmology with two fluid components A and B. Each component should then obey the same basic equations describing the whole system, which

are the continuity equation (2.84) and the Euler equation (2.85):

$$\partial_t \varrho_A + 3H\varrho_A + \frac{1}{a}\nabla_q \cdot (\varrho_A \boldsymbol{u}_A) = 0, \tag{2.90}$$

$$\partial_t \varrho_B + 3H\varrho_B + \frac{1}{a}\nabla_q \cdot (\varrho_B \boldsymbol{u}_B) = 0, \tag{2.91}$$

$$\partial_t \boldsymbol{u}_A + \frac{1}{a}(\boldsymbol{u}_A \cdot \nabla_q)\boldsymbol{u}_A + H\mathbf{u}_A = \boldsymbol{w} - \frac{1}{a}\frac{\nabla_q p_A}{\varrho_A}, \tag{2.92}$$

$$\partial_t \boldsymbol{u}_B + \frac{1}{a}(\boldsymbol{u}_B \cdot \nabla_q)\boldsymbol{u}_B + H\boldsymbol{u}_B = \boldsymbol{w} - \frac{1}{a}\frac{\nabla_q p_B}{\varrho_B}, \tag{2.93}$$

$$\nabla_q \times \boldsymbol{w} = 0, \quad \nabla_q \cdot \boldsymbol{w} = -4\pi G\, a(\varrho - \varrho_H), \tag{2.94}$$

where the term $\nabla p/\varrho$ accounts for the isotropic part of the velocity dispersion tensor with $p = \alpha(\varrho)$. The gravitational field strength Φ is determined by the Poisson equation $\Delta\Phi = 4\pi G\varrho - \Lambda$ where $\Delta = \nabla^2_{\mathbf{x}} = a^{-2}\nabla^2_{\boldsymbol{q}}$ is the Laplace operator in Eulerian space. Its comoving counterpart Ψ can be defined according to Eq. (2.64)

$$\nabla_q \Psi = \nabla_q \Phi + a\,\ddot{a}\,\boldsymbol{q}. \tag{2.95}$$

Now for each component we can define the corresponding density contrast as

$$\delta_\alpha \equiv \frac{\varrho_\alpha - \varrho_{\alpha H}}{\varrho_{\alpha H}}. \tag{2.96}$$

Since the total mass density has been defined to be Eq. (2.80), we can define the total density contrast as

$$\delta(\boldsymbol{q}, t) \equiv \frac{\varrho - \varrho_H}{\varrho_H} = \frac{\varrho_{HA}\delta_A + \varrho_{HB}\delta_B}{\varrho_{HA} + \varrho_{BH}} = f_A\delta_A + f_B\delta_B, \tag{2.97}$$

where $f_{A(B)}$ is the density fraction of component A (B) and should be a constant. This definition has been used by most previous relevant works, and is physically meaningful. Inserting these definitions into Eqs. (2.90, 2.91, 2.92, 2.93, 2.94), we obtain the density fluctuation evolution equations, where focusing on the density parts

$$\partial_t \delta_A + \frac{1}{a}\nabla_q \cdot \boldsymbol{u}_A + \frac{1}{a}\nabla_q(\delta_A \boldsymbol{u}_A) = 0, \tag{2.98}$$

$$\partial_t \delta_B + \frac{1}{a}\nabla_q \cdot \boldsymbol{u}_B + \frac{1}{a}\nabla_q(\delta_B \boldsymbol{u}_B) = 0, \tag{2.99}$$

$$\partial_t \boldsymbol{u}_A + \frac{1}{a}\left(\boldsymbol{u}_A \cdot \nabla_q\right)\boldsymbol{u}_A + H\boldsymbol{u}_A = \frac{1}{a}\nabla_q \delta\Psi - \frac{1}{a}\frac{p_{AH}\nabla_q \delta p_A}{\varrho_{AH}\left(1+\delta\varrho_A\right)}, \tag{2.100}$$

$$\partial_t \boldsymbol{u}_B + \frac{1}{a}\left(\boldsymbol{u}_B \cdot \nabla_q\right)\boldsymbol{u}_B + H\boldsymbol{u}_B = \frac{1}{a}\nabla_q \delta\Psi - \frac{1}{a}\frac{p_{BH}\nabla_q \delta p_B}{\varrho_{BH}\left(1+\delta\varrho_B\right)}, \tag{2.101}$$

$$\Delta_q \delta\Psi = -4\pi G\, a^2 \varrho_H\, \delta. \tag{2.102}$$

In general we should also consider the fluctuations of the velocities of the different components. If we keep only the first order fluctuations, then we will have

$$\partial_t^2 \delta_\alpha + 2H\partial_t \delta_\alpha - a^{-2}\, {c_s}_\alpha{}^2\, \nabla_{\boldsymbol{q}}^2 \delta_\alpha = 4\pi G \sum \varrho_{\alpha H}\delta_\alpha, \tag{2.103}$$

where ${c_s}_\alpha{}^2 = dp_\alpha/d\varrho_\alpha$ is defined as the adiabatic sound speed of the component α. Such equations can be easily analyzed using Fourier transforms [Peebles, 1993; Coles and Lucchin, 2002; Weinberg, 2008]. Then by the definition Eq. (2.97), we obtain the linear evolution equation for total density contrast

$$\partial_t^2 \delta + 2H\partial_t \delta - a^{-2}\nabla_q^2\left(c_{sA}^2\, \delta_A + c_{sB}^2\, \delta_B\right) = 4\pi G \varrho_H \delta. \tag{2.104}$$

Clearly it is impossible to solve this equation until we make some specific approximation about the relation of δ_A and δ_B.

2.2.2.4 The Lagrange-Newton system for two components with pressure in comoving coordinates

We now construct a Lagrange-Newton system for such a fluid mixture. In the last section we have constructed a comoving Eulerian system for a fluid mixture in Newtonian cosmology. If we use an anisotropic velocity dispersion to describe the effect of relative motion between the two species, then we can focus on the dynamics of the fluid mixture without knowing the details of the relative motion. In this case the evolution equations are given by

$$\frac{\partial \varrho}{\partial t} + 3H\varrho + \frac{1}{a}\nabla_{\boldsymbol{q}} \cdot \left(\varrho\, \boldsymbol{u}\right) = 0, \tag{2.105}$$

$$\frac{\partial}{\partial t}\left(\varrho \boldsymbol{u}\right) + \frac{1}{a}\nabla_{\boldsymbol{q}}\left(\varrho\, \boldsymbol{u}\cdot\boldsymbol{u}\right) + 4H\varrho\, \boldsymbol{u} = \varrho\, \boldsymbol{w} - \frac{1}{a}\nabla_q \cdot \tilde{\boldsymbol{\Pi}}, \tag{2.106}$$

with

$$\partial_t \tilde{\Pi}_{ij} + \frac{1}{a} u_k \frac{\partial \tilde{\Pi}_{ij}}{\partial q_k} + 5H\,\tilde{\Pi}_{ij} + \frac{1}{a}\tilde{\Pi}_{ij}\,\frac{\partial u_k}{\partial q_k} = -\frac{1}{a}\left(\tilde{\Pi}_{ik}\frac{\partial u_j}{\partial q_k} + \tilde{\Pi}_{jk}\frac{\partial u_i}{\partial q_k}\right). \quad (2.107)$$

For details, see Appendix A.

To perform the Lagrangian perturbative approach, we now transform the above equations into the Lagrangian comoving coordinates. Following Eq. (2.33) we define the Lagrangian comoving coordinates $\boldsymbol{X}$ along trajectories of the fluid mixture elements as:[4]

$$\boldsymbol{q} = \boldsymbol{X} + \boldsymbol{P}(\boldsymbol{X}, t), \quad \boldsymbol{u} = a\,\dot{\boldsymbol{P}}, \quad \boldsymbol{P}(\boldsymbol{X}, t_{\mathbf{i}}) = 0, \quad (2.108)$$

where we redefine $\boldsymbol{P}$ as the comoving deformation fields. A dot here denotes the Lagrangian time-derivative for an arbitrary tensor, vector or scalar A:

$$\dot{A} = \frac{dA}{dt} = \left.\frac{\partial A}{\partial t}\right|_{\boldsymbol{X}} = \left.\frac{\partial A}{\partial t}\right|_{\boldsymbol{q}} + \frac{1}{a}(\boldsymbol{u}\cdot\nabla_{\boldsymbol{q}})\,A. \quad (2.109)$$

We can derive the evolution equation for the peculiar-gravitational field $\boldsymbol{w}$. A method for calculating this was first introduced by Buchert [1989] and further developed by Buchert and Domínguez [2005]. The result is

$$\dot{\boldsymbol{w}} + 2H\boldsymbol{w} - 4\pi G\varrho_H\boldsymbol{u} = \frac{1}{a}\left[(\boldsymbol{u}\cdot\nabla_{\boldsymbol{q}})\,\boldsymbol{w} - \boldsymbol{u}\,(\nabla_{\boldsymbol{q}}\cdot\boldsymbol{w}) + \nabla_{\boldsymbol{q}}\times\boldsymbol{T}\right] = \boldsymbol{\mathcal{W}}, \quad (2.110)$$

where $\boldsymbol{T}$ is the vector potential of $\varrho\boldsymbol{u}$ and satisfies the conditions

$$\nabla_{\boldsymbol{q}}\cdot\boldsymbol{T} = 0, \quad \Delta_{\boldsymbol{q}}\boldsymbol{T} = 4\pi G a\nabla_{\boldsymbol{q}}\times(\varrho\boldsymbol{u}). \quad (2.111)$$

Here $\Delta_{\boldsymbol{q}} := \nabla^2_{\boldsymbol{q}}$ is the Laplacian operator with respect to $\boldsymbol{q}$. Inserting Eq. (2.108) and formally integrating Eq. (2.110) yields the expression for $\boldsymbol{w}$:

$$\boldsymbol{w}(\boldsymbol{X}, t) = \frac{{a_{\mathbf{i}}}^2}{a^2}\boldsymbol{w}_{\mathbf{i}} + 4\pi G a\varrho_H\boldsymbol{P}(\boldsymbol{X}, t) + \frac{1}{a^2}\int_{t_{\mathbf{i}}}^{t} d\tau\, a^2(\tau)\,\boldsymbol{\mathcal{W}}(\boldsymbol{X}, \tau), \quad (2.112)$$

where $\boldsymbol{w}_{\mathbf{i}}$ describes the initial peculiar-gravitational field.

[4] Note the hydrodynamic approximation has been adopted here.

The combination of Eq. (2.106), Eq. (2.108) and Eq. (2.112) finally produces the second order time derivative equation of the deformation field $\boldsymbol{P}$:

$$\ddot{\boldsymbol{P}} + 2H\dot{\boldsymbol{P}} - 4\pi G\varrho_H \boldsymbol{P} = \frac{{a_{\mathbf{i}}}^2}{a^3}\boldsymbol{w}_{\mathbf{i}} + \frac{1}{a^3}\int_{t_{\mathbf{i}}}^{t} d\tau\, a^2(\tau)\,\boldsymbol{\mathcal{W}}(\boldsymbol{X},\tau) - \frac{1}{\varrho\, a^2}\nabla_{\boldsymbol{q}}\cdot\tilde{\boldsymbol{\Pi}}. \tag{2.113}$$

Thus we come back to the most basic and important equation for the LPT. The physical interpretation of this equation, and the approximations one needs have been introduced in many LPT papers: see [Buchert, 1989; Bildhauer et al., 1992; Ehlers and Buchert, 1996; Buchert and Domínguez, 1998; Buchert and Adler, 1999; Buchert and Domínguez, 2005; Buchert, 2006] and references therein.

As we see, Eq. (2.113) has an exact analytic form and we need to know the expression for $\boldsymbol{\mathcal{W}}$ to solve it. A rigorous procedure would require one to consider the dynamical properties of $\boldsymbol{\mathcal{W}}$, which is beyond the scope of the present work. We will simply assume this term to be zero to simplify the calculations, *i.e.*, $\boldsymbol{\mathcal{W}} = 0$. We then have to transform the right hand side of Eq. (2.113) to the Lagrangian framework.

The mass conservation equation relates the density field to the deformation field $\boldsymbol{P}$ via the Jacobian Eq. (2.36)

$$\frac{a^3\,\varrho(\boldsymbol{X},t)}{{a_{\mathbf{i}}}^3\,\varrho(\boldsymbol{X},t_{\mathbf{i}})} = \frac{\det J_{ij}(\boldsymbol{X},t_{\mathbf{i}})}{\det J_{ij}(\boldsymbol{X},t)} = \frac{J_{\mathbf{i}}}{J}, \quad J_{ij}(\boldsymbol{X},t) = \frac{\partial q_i}{\partial X_j} = \delta_{ij} + \frac{\partial P_i}{\partial X_j}, \tag{2.114}$$

since we have defined $\boldsymbol{P}_{\mathbf{i}} = \boldsymbol{P}(\boldsymbol{X},t_{\mathbf{i}}) = 0$ so that $J_{\mathbf{i}} = 1$. In SPT, the density contrast δ is defined by $\delta \equiv (\varrho - \varrho_H)/\varrho_H$. In LPT we can similarly define the density contrast of the fluid mixture as

$$\begin{aligned}\delta(\boldsymbol{X},t) \equiv \frac{\varrho-\varrho_H}{\varrho_H} &= \left(\frac{{a_{\mathbf{i}}}^3\,\varrho_{\mathbf{i}}}{a^3\,\varrho_H} - J\right)/J \\ &= \left(1 - J - \frac{\nabla_{\boldsymbol{q}}\cdot\boldsymbol{w}_{\mathbf{i}}}{4\pi G a_{\mathbf{i}}\,\varrho_{H\mathbf{i}}}\right)/J.\end{aligned} \tag{2.115}$$

If we assume a quasi-homogeneous initial condition for simplicity, *i.e.*, $\varrho_{\mathbf{i}} \approx \varrho_{H\mathbf{i}}$, then $\boldsymbol{w}_{\mathbf{i}} \approx 0$, the above equation becomes $\delta = (1-J)/J$ and Eq. (2.113) reduces to Eq. (47) of [Buchert and Domínguez, 2005].

2.2.2.5 The perturbative expansion for the Lagrange-Newton system

Even though we have derived exact evolution equations for the deformation field $\boldsymbol{P}$ and the velocity dispersion tensor $\tilde{\boldsymbol{\Pi}}$, it is still difficult to solve such a system analytically. We have to consider a perturbative procedure with the expansion Eq. (2.42) (with comoving deformation $\boldsymbol{P}$).

Before applying the perturbative expansion, we write the i-th component of Eq. (2.113) as

$$\ddot{P}_i + 2H\dot{P}_i - 4\pi G\varrho_H P_i = \frac{W_i^c}{a^3} - \frac{1}{\varrho\, a^2}\left(J^{-1}\right)_{jk}\frac{\partial\tilde{\Pi}_{ki}}{\partial X_j}, \tag{2.116}$$

where $\boldsymbol{W}^c = {a_{\mathbf{i}}}^2\,\boldsymbol{w}_{\mathbf{i}}$ and $\left(J^{-1}\right)_{ij}$ is the inverse to the matrix J_{ij}. Then we transform Eq. (2.107) with respect to the Lagrangian coordinates, with the result

$$\left.\frac{\partial\tilde{\Pi}_{ij}}{\partial t}\right|_X + 5H\tilde{\Pi}_{ij} = -\frac{1}{a}\left(\frac{\partial u_j}{\partial q_k}\tilde{\Pi}_{ki} + \frac{\partial u_i}{\partial q_k}\tilde{\Pi}_{kj} + \frac{\partial u_k}{\partial q_k}\tilde{\Pi}_{ij}\right) = \frac{1}{a}\,\Xi_{ij}. \tag{2.117}$$

Now we can take a third time derivative of Eq. (2.116). For the last term, we have

$$\begin{aligned}
&\frac{d}{dt}\left[\frac{1}{\varrho\, a^2}\left(J^{-1}\right)_{jk}\frac{\partial\tilde{\Pi}_{ki}}{\partial X_j}\right] \\
&= a\left(J^{-1}\right)_{jk}\frac{\partial\tilde{\Pi}_{ki}}{\partial X_j}\frac{d}{dt}\left(\frac{1}{\varrho a^3}\right) + \frac{1}{\varrho a^2}\frac{\partial\tilde{\Pi}_{ki}}{\partial X_j}\frac{d}{dt}\left(J^{-1}\right)_{jk} + H\frac{1}{\varrho\, a^2}\left(J^{-1}\right)_{jk}\frac{\partial\tilde{\Pi}_{ki}}{\partial X_j} \\
&\quad + \frac{1}{\varrho\, a^2}\left(J^{-1}\right)_{jk}\frac{d}{dt}\left(\frac{\partial\tilde{\Pi}_{ki}}{\partial X_j}\right) \\
&= -\left(\frac{1}{\varrho a^3}\frac{d\left(\varrho a^3\right)}{dt} + \frac{1}{J_{jk}}\frac{dJ_{jk}}{dt}\right)\left[\frac{1}{\varrho\, a^2}\left(J^{-1}\right)_{jk}\frac{\partial\tilde{\Pi}_{ki}}{\partial X_j}\right] + H\frac{1}{\varrho\, a^2}\left(J^{-1}\right)_{jk}\frac{\partial\tilde{\Pi}_{ki}}{\partial X_j} \\
&\quad + \frac{1}{\varrho\, a^2}\left(J^{-1}\right)_{jk}\frac{\partial}{\partial X_j}\left(\frac{1}{a}\Xi_{ki} - 5H\tilde{\Pi}_{ki}\right) \\
&= H\frac{1}{\varrho\, a^2}\left(J^{-1}\right)_{jk}\frac{\partial\tilde{\Pi}_{ki}}{\partial X_j} + \frac{1}{\varrho\, a^2}\left(J^{-1}\right)_{jk}\frac{\partial}{\partial X_j}\left(\frac{1}{a}\Xi_{ki} - 5H\tilde{\Pi}_{ki}\right) \\
&= \frac{1}{\varrho\, a^3}\left(J^{-1}\right)_{jk}\frac{\partial\,\Xi_{ki}}{\partial X_j} - 4H\frac{1}{\varrho\, a^2}\left(J^{-1}\right)_{jk}\frac{\partial\tilde{\Pi}_{ki}}{\partial X_j}.
\end{aligned} \tag{2.118}$$

Note that in the second of the equalities on the right hand side the mass conservation law has been applied. Thus we obtain the third order time derivative equation for P_i:

$$\dddot{P}_i + 6H\ddot{P}_i + \left(8H^2 - 12\pi G\varrho_H\right)\dot{P}_i - 4\pi GH\varrho_H P_i = H\frac{W_i^c}{a^3} - \frac{1}{\varrho a^3}\left(J^{-1}\right)_{jk}\frac{\partial \Xi_{ki}}{\partial X_j}. \tag{2.119}$$

This is a basic equation which describes the evolution of the deformation field of a fluid mixture that is composed of two different species. The relative motion between the two species of the fluid mixture is hidden in the term $\tilde{\mathbf{\Pi}}$, from which $\mathbf{\Xi}$ is defined according to (2.117).

We now apply a perturbative expansion to Eq. (2.119). Using the definition of $\tilde{\mathbf{\Pi}}$ and the relation Eq. (2.108), if we take $\boldsymbol{P}^{(1)} \sim \mathcal{O}(\varepsilon)$ as first order, then the first order terms are $\boldsymbol{P}^{(1)}$, $\boldsymbol{u}^{(1)} \sim \mathcal{O}(\varepsilon)$, the terms $\boldsymbol{P}^{(2)}$, $\boldsymbol{u}^{(2)}$, $\Pi^{(2)}_{\alpha ij}$, $\Pi^{(2)}_{ij} \sim \mathcal{O}(\varepsilon^2)$ are second order, and $\Xi_{ij} \sim \mathcal{O}(\varepsilon^3)$ is third order. We stress that the corrections from the velocity dispersion are at least second order. Thus the first order term follows the standard evolution equation for an overdensity in a dust Newtonian cosmology [Bernardeau et al., 2002]. Hereafter we will consider only terms up to second order in $\boldsymbol{P}$ and will omit the superscript "$^{(2)}$", since the differential operator which acts on the first and second order terms will be shown to have the same analytic form in both cases.

On the other hand, we use the scale factor a as the time variable for convenience. Eq. (2.119) then becomes

$$a^3H^3P_i''' + \frac{3}{2}a^2H\left(3H^2+\Lambda\right)P_i'' + \frac{3}{2}aH\left(H^2+2\Lambda\right)P_i' - 4\pi GH\varrho_H P_i = \frac{H}{a^3}W_i^c, \tag{2.120}$$

where we have used the symbol "$' \equiv d/da$". Note here we have ignored the third and higher orders. Furthermore, the background mass density also satisfies the mass conservation law, so that $a^3\varrho_H = {a_\mathbf{i}}^3\varrho_{H\mathbf{i}}$. The initial value W_i^c can be written as

$$W_i^c = 4\pi G a^3\varrho_H\frac{W_i^c}{4\pi G{a_\mathbf{i}}^3\varrho_{H\mathbf{i}}}. \tag{2.121}$$

We can now define a new variable $\tilde{P}_i$ such that

$$\tilde{P}_i = P_i + \frac{W_i^c}{4\pi G{a_\mathbf{i}}^3\varrho_{H\mathbf{i}}}. \tag{2.122}$$

Inserting this new variable into Eq. (2.120) and noting that the initial terms on the right hand side are time independent, one finally arrives at a third-order ordinary differential equation

$$a^3H^3\tilde{P}_i''' + \frac{3}{2}a^2H\left(3H^2+\Lambda\right)\tilde{P}_i'' + \frac{3}{2}aH\left(H^2+2\Lambda\right)\tilde{P}_i' - 4\pi G H \varrho_H \tilde{P}_i = 0. \quad (2.123)$$

Here, $\tilde{\boldsymbol{P}}$ includes terms up to second order. The general solution of this equation can be easily derived from the theory of ordinary differential equations. For a homogeneous linear equation of the third order with the form

$$f_3(x)y'''_{xxx} + f_2(x)y''_{xx} + f_1(x)y'_x + f_0(x)y = 0, \quad (2.124)$$

the general solution is given by

$$\begin{aligned} y &= C_1y_1 + C_2y_2 + C_3\left(y_2\int y_1\,\psi\,dx - y_1\int y_2\,\psi\,dx\right), \\ \psi &= \exp\left(-\int\frac{f_2}{f_3}\,dx\right)\left(y_1\,y_2' - y_1'\,y_2\right)^{-2}, \end{aligned} \quad (2.125)$$

where C_1, C_2, C_3 are constants and y_1, y_2 are two nontrivial independent particular solutions of the homogeneous equation.

2.2.2.6 The solutions in an Einstein-de Sitter universe

We now investigate the solutions of Eq. (2.123) in an Einstein-de Sitter universe which is dominated by dark matter. In this toy model, $\Lambda = 0$ and the solution is straight-forwardly given by

$$\begin{aligned} \tilde{P}_i &= -\left[\frac{C_{1i}^{(1)}+C_{1i}^{(2)}}{a^{3/2}} + a\left(C_{2i}^{(1)}+C_{2i}^{(2)}\right) + \frac{C_{3i}^{(2)}}{a}\right], \\ \frac{W_i^c}{4\pi G {a_{\mathbf{i}}}^3\varrho_{H\mathbf{i}}} &= -\left[\frac{C_{1i}^{(1)}+C_{1i}^{(2)}}{{a_{\mathbf{i}}}^{3/2}} + a_{\mathbf{i}}\left(C_{2i}^{(1)}+C_{2i}^{(2)}\right) + \frac{C_{3i}^{(2)}}{a_{\mathbf{i}}}\right], \end{aligned} \quad (2.126)$$

with C_{1i}, C_{2i}, C_{3i} being three functions of the Lagrangian coordinates $\boldsymbol{X}$ defined by the initial conditions. The first order solutions are given by the $C^{(1)}$ terms.

Recalling that we expand up to second order, the Jacobian becomes

$$J = 1 + \frac{\partial P_i^{(1)}}{\partial X_i} + \frac{\partial P_i^{(2)}}{\partial X_i} + \frac{1}{2}\varepsilon_{ijk}\,\varepsilon^{imn}\,\frac{\partial P_j^{(1)}}{\partial X_m}\,\frac{\partial P_k^{(1)}}{\partial X_n} + \mathcal{O}\left(\varepsilon^3\right). \tag{2.127}$$

The mass density will then be represented up to first order as

$$\varrho^{(1)}\left(\boldsymbol{X}, a\right) = \varrho_H\left(\delta_{\mathbf{i}}{}^{(1)} - \frac{\partial P_i^{(1)}}{\partial X_i}\right) = \varrho_H\left(\frac{\tilde{C}_1^{(1)}}{a^{3/2}} + a\,\tilde{C}_2^{(1)}\right) \tag{2.128}$$

where

$$\delta_{\mathbf{i}}{}^{(1)} = \frac{\tilde{C}_1^{(1)}}{a_{\mathbf{i}}{}^{3/2}} + a_{\mathbf{i}}\tilde{C}_2^{(1)}, \quad \tilde{C}_n = \frac{\partial C_{ni}}{\partial X_i}, \quad n = 1, 2, 3. \tag{2.129}$$

This first order mass density indeed has the normal form of the solution for the overdensity in a dust Newtonian cosmology. The second order mass density then should be expressed as

$$\begin{aligned}&\varrho^{(2)}\left(\boldsymbol{X}, a\right)\\ &= \varrho_H\left[\frac{\partial P_i^{(1)}}{\partial X_i}\,\frac{\partial P_k^{(1)}}{\partial X_k} + \delta_{\mathbf{i}}{}^{(2)} - \frac{\partial P_i^{(2)}}{\partial X_i} - \frac{1}{2}\varepsilon_{ijk}\,\varepsilon^{imn}\,\frac{\partial P_j^{(1)}}{\partial X_m}\,\frac{\partial P_k^{(1)}}{\partial X_n} - \frac{\partial P_i^{(1)}}{\partial X_i}\,\delta_{\mathbf{i}}{}^{(1)}\right].\end{aligned} \tag{2.130}$$

We claim that each order here refers to the corresponding term of the expansion according to the deformation field $\boldsymbol{P}$.

Eq. (2.126) is evidently a Zel'dovich-type solution. Since an Einstein-de Sitter universe has a scale factor which evolves as $a \sim t^{2/3}$, this solution includes the standard dust solution given by the growing term C_2 and the decaying term C_1. The new decaying mode C_3 is second order, and is introduced by the effect of anisotropic velocity dispersion. If the velocity dispersion of the fluid mixture is zero then we can expect that this new decaying mode will be removed. Here the anisotropic velocity dispersion around the peculiar velocity of the mixture arose from the relative motions of two species which form the mixture continuum of the universe. For the special case in which no relative motions appear, the velocity dispersion becomes isotropic as we have assumed that each species has an isotropic velocity dispersion about its own peculiar velocity. Eq. (2.116) then reduces to the well-known evolution equation for the deformation field of a dust fluid supported by isotropic pressure [Buchert and Adler, 1999].

Since Eq. (2.120) includes terms up to second order in the deformation field the details of the relative motion of the different species, being of higher order, do not appear. Consequently, the solution (2.128) is unaffected by the relative motion once the initial conditions are specified. However, the effects of relative motions will be significant at higher orders. It is also clear that in the second order regime, the velocity dispersion $\tilde{\mathbf{\Pi}}$ decays quickly as $\tilde{\mathbf{\Pi}} \sim a^{-5}$. But at higher orders, the spatial derivative of $\tilde{\mathbf{\Pi}}$ will suppress the attenuation.

It is worth noting that the new decaying mode decays more slowly than the standard decaying mode. This is expected as a consequence of the appearance of the anisotropic velocity dispersion, which results in an effective non-perfect fluid [Maartens et al., 1999; Amendola and Finelli, 2005]. Clearly, for velocity dispersion tensors with vanishing anisotropic parts, Eq. (2.116) can be solved using the specified approximations, with only two solutions.

2.2.2.7 Searching for the evolution of single species in an Einstein-de Sitter universe

Although we have stressed that the relative motion between the two species is hidden in $\tilde{\mathbf{\Pi}}$, the possibility of determining the evolution of a single species still exists. Furthermore, the linear part of Eq. (2.117) does not determine the spatial part of $\tilde{\mathbf{\Pi}}$, which should be defined by the same initial conditions applied to each species.

The procedure is straightforward. First, we have obtained Eq. (2.126) to describe the evolution of the fluid mixture up to second order. Next the expression for the peculiar-gravitational strength field $\boldsymbol{w}$ can be easily derived by inserting this solution into Eq. (2.112). Noting that this $\boldsymbol{w}$ is same for the whole mixture system, and that the evolution of each species follows the dynamical equations Eqs. (2.84, 2.85), after replacing $\boldsymbol{w}$ with $\tilde{\boldsymbol{P}}$ we finally arrive at two evolution equations in two unknown variables. This is true for each species. Hence solving these two equations we will find the evolution of both components.

We follow the procedure to derive the solution for each species. The evolution equations of ϱ_α and $\boldsymbol{u}_\alpha$ are then

$$\partial_t \delta\varrho_\alpha + \frac{1}{a}\nabla_{\boldsymbol{q}} \cdot [(1+\delta\varrho_\alpha)\,\boldsymbol{u}_\alpha] = 0, \tag{2.131}$$

$$\partial_t \boldsymbol{u}_\alpha + \frac{1}{a}\left(\boldsymbol{u}_\alpha \cdot \nabla_{\boldsymbol{q}}\right)\boldsymbol{u}_\alpha + H\boldsymbol{u}_\alpha - 4\pi G a \varrho_H \tilde{\boldsymbol{P}} = -\frac{\nabla_{\boldsymbol{q}} p_\alpha\left(\varrho_\alpha\right)}{a\varrho_\alpha}. \tag{2.132}$$

The second equation shows that $\boldsymbol{u}_\alpha$ should have the same order as $\tilde{\boldsymbol{P}}$. Taking a time derivative of Eq. (2.131) and inserting Eq. (2.132) into the result, one obtains an exact evolution equation for $\delta\varrho_\alpha$:

$$\begin{aligned}\partial_t^2\delta\varrho_\alpha + 2H\partial_t\delta\varrho_\alpha - \frac{1}{a^2}\nabla_{\boldsymbol{q}}\cdot\left[\left[\nabla_{\boldsymbol{q}}\cdot\left(1+\delta\varrho_\alpha\right)\boldsymbol{u}_\alpha\right]\boldsymbol{u}_\alpha\right] + \frac{1}{a}\nabla_{\boldsymbol{q}}\cdot\left[\left(1+\delta\varrho_\alpha\right)\boldsymbol{w}\right] \\ - \frac{\nabla_{\boldsymbol{q}}\cdot\left(\nabla_{\boldsymbol{q}}\, p_\alpha\right)}{a^2\,\varrho_{\alpha H}} - \frac{1}{a^2}\nabla_{\boldsymbol{q}}\left[\left(1+\delta\varrho_\alpha\right)\left(\boldsymbol{u}_\alpha\cdot\nabla_{\boldsymbol{q}}\right)\boldsymbol{u}_\alpha\right] = 0.\end{aligned} \tag{2.133}$$

Note that the partial derivative here is with respect to the Eulerian comoving coordinates $\boldsymbol{q}$, and should be transformed to the full time derivative by Eq. (2.109).

To proceed, one has to approximate the "equation of state" of each species. Different choices have been discussed for the gravitational instability of an expanding two-component Newtonian universe (see the references cited in section 2.2.2.3). An exact EOS for a dust continuum with isotropic velocity dispersion has been given by Buchert and Domínguez [1998], *viz.*, $p\left(\boldsymbol{X},t\right) = \kappa\left(\boldsymbol{X}\right)\varrho\left(\boldsymbol{X},t\right)^{5/3}$ with $\kappa \sim \mathcal{O}\left(\varepsilon^2\right)$. In our case, with the assumptions we have made for each species we can expect this EOS to be true for both components, *i.e.*, $p_\alpha = \kappa_\alpha\,\varrho_\alpha^{5/3}$ and κ_α is a function of $\boldsymbol{X}$. Thus up to second order we have $p_\alpha^{(2)} = \kappa_\alpha \varrho_{\alpha H}^{5/3}$.

Eq. (2.133) can now be solved order by order. At first order, the equation becomes

$$\ddot{\delta\varrho}_\alpha^{(1)} + 2H\dot{\delta\varrho}_\alpha^{(1)} + 4\pi G\varrho_H\frac{\partial\tilde{P}_i^{(1)}}{\partial X_i} = 0, \tag{2.134}$$

or with respect to a,

$$\frac{d^2\delta\varrho_\alpha^{(1)}}{da^2} + \frac{3}{2a}\frac{d\delta\varrho_\alpha^{(1)}}{da} + \frac{3}{2a^2}\frac{\partial\tilde{P}_i^{(1)}}{\partial X_i} = 0. \tag{2.135}$$

Furthermore, the evolution equation at second order for $\delta\varrho_\alpha^{(2)}$ is

$$\ddot{\delta\varrho}_\alpha^{(2)} - \left(\dot{\delta\varrho}_\alpha^{(1)}\right)^2 + 2H\dot{\delta\varrho}_\alpha^{(2)} - \frac{\varrho_{\alpha H}^{2/3}}{a^2}\Delta_{\boldsymbol{X}}\kappa_\alpha - \frac{2\left(\boldsymbol{u}^{(1)} - \boldsymbol{u}_\alpha^{(1)}\right)}{a}\cdot\nabla_{\boldsymbol{X}}\dot{\delta\varrho}_\alpha^{(1)}$$

$$+ 4\pi G\varrho_H \left(\frac{\partial \tilde{P}_i^{(2)}}{\partial X_i} + \frac{\partial \tilde{P}_i^{(1)}}{\partial X_i}\delta\varrho_\alpha^{(1)} - \frac{\partial \tilde{P}_i^{(1)}}{\partial X_k}\frac{\partial P_k^{(1)}}{\partial X_i} \right) - \frac{1}{a^2}\frac{\partial u_{\alpha i}}{\partial X_j}\frac{\partial u_{\alpha j}}{\partial X_i} = 0, \tag{2.136}$$

or with respect to a

$$\frac{d^2\delta\varrho_\alpha^{(2)}}{da^2} + \frac{3}{2a}\frac{d\delta\varrho_\alpha^{(2)}}{da} - \left(\frac{d\delta\varrho_\alpha^{(1)}}{da}\right)^2 - \frac{\varrho_{\alpha H}^{2/3}}{a^4H^2}\Delta_{\boldsymbol{X}}\kappa_\alpha - \frac{2\left(\boldsymbol{u}^{(1)} - \boldsymbol{u}_\alpha^{(1)}\right)}{a^2H}\cdot\nabla_{\boldsymbol{X}}\frac{d\delta\varrho_\alpha^{(1)}}{da}$$
$$+ \frac{3}{2a^2}\left(\frac{\partial \tilde{P}_i^{(2)}}{\partial X_i} + \frac{\partial \tilde{P}_i^{(1)}}{\partial X_i}\delta\varrho_\alpha^{(1)} - \frac{\partial \tilde{P}_i^{(1)}}{\partial X_k}\frac{\partial P_k^{(1)}}{\partial X_i} \right) - \frac{1}{a^4H^2}\frac{\partial u_{\alpha i}}{\partial X_j}\frac{\partial u_{\alpha j}}{\partial X_i} = 0. \tag{2.137}$$

Since we have obtained the solution to first and second order in $\tilde{\boldsymbol{P}}$, the procedure to solve Eqs. (2.135, 2.137) is straightforward. Direct calculation shows that the first order term $\delta\varrho_\alpha^{(1)}$ is given by the solution

$$\delta\varrho_\alpha^{(1)} = \frac{\tilde{C}_1^{(1)}}{a^{3/2}} + a\,\tilde{C}_2^{(1)} - \frac{C_{\alpha 1}^{(1)}}{a^{1/2}} + C_{\alpha 2}^{(1)}, \tag{2.138}$$

with $C_{\alpha 1}^{(1)}$ and $C_{\alpha 2}^{(1)}$ given by the initial conditions. This is the well-known first order perturbative solution for a Newtonian cosmology composed of two dust components, where the two components have different mass fractions. Consequently, the first order solution of $\delta\varrho_\beta$ can be derived by considering the relation Eq. (2.80), and the result is

$$\delta\varrho_\beta^{(1)} = \frac{\tilde{C}_1^{(1)}}{a^{3/2}} + a\tilde{C}_2^{(1)} + \zeta\left(\frac{C_{\alpha 1}^{(1)}}{a^{1/2}} - C_{\alpha 2}^{(1)}\right), \tag{2.139}$$

where $\zeta = \varrho_{\alpha H}/\varrho_{\beta H}$ is the mass density ratio of two species in the background spacetime.

Inserting $\delta\varrho_\alpha^{(1)}$, $\boldsymbol{u}^{(1)}$ and $\boldsymbol{u}_\alpha^{(1)}$ into Eq. (2.137), one obtains the second order solution $\delta\varrho_\alpha^{(2)}$. The calculation is tedious but straight-forward. One also should realize that all spatial functions can be related to each other on account of the same initial conditions. In other words, once we have determined the initial distributions and initial peculiar velocities of both species α and β, then we also know the distribution and peculiar velocity of the fluid mixture. A lengthy but

straight-forward calculation combining Eqs. (2.126, 2.130) will lead directly to the second order solution $\delta\varrho_\beta^{(2)}$, which we will not present here.

It is worth stressing that since the velocity dispersion has been treated as second order, its influence on large scale structure ($> L$) will be small. The fluid mixture behaves as a dust fluid at first order. Both species will attract each other quickly through their mutual gravity, and then mix to become a "pure" dust continuum. For higher orders, the effect of the anisotropic velocity dispersion may become significant once one accounts for the term $\boldsymbol{\Xi}$. Such work goes beyond the scope of this thesis and will not be discussed here.

2.2.3 Constructing the Lagrange-Newton system from the viewpoint of each species

In last few subsections we have constructed a Lagrangian-Newtonian system from the viewpoint of the fluid mixture. Here we will construct such a system from the viewpoint of each species, *i.e.*, following the trajectories of each component. For an arbitrary synchronous hypersurface, in general at any point p there will simultaneously exist two components[5] with energy densities ϱ_α and ϱ_β if only gravitational effects are included. The total mass contained in an infinitesimal volume around point p is then

$$\delta M_p\left(\mathbf{x}_p, t\right) = \delta M_\alpha\left(\mathbf{x}_p, t\right) + \delta M_\beta\left(\mathbf{x}_p, t\right) = \left[\varrho_\alpha\left(\mathbf{x}_p, t\right) + \varrho_\beta\left(\mathbf{x}_p, t\right)\right] d^3\mathbf{x}. \quad (2.140)$$

It must be kept in mind that this total mass is not conserved along α's flow line.

We now can define a comoving Lagrangian coordinate system for either of the two components. One just needs to specify on which fluid element this Lagrangian coordinate system is attached. For example, we may assume this Lagrangian coordinate system is defined by fluid A. Then at a time $t_m > t_{\mathbf{i}}$ the Eulerian position $\boldsymbol{q}$ will correspond to two different fluid elements for A and B,

[5] We neglect degenerate cases such as $\varrho_\alpha\left(\mathbf{x}_p, t\right) \neq 0$ but $\varrho_\beta\left(\mathbf{x}_p, t\right) = 0$.

respectively. We will have[6].

$$\boldsymbol{q}\left(\cdot\,,t_m\right)=\boldsymbol{X}+\boldsymbol{P}_A(\boldsymbol{X},t_m)=\boldsymbol{Y}+\boldsymbol{P}_B(\boldsymbol{Y},t_m), \tag{2.141}$$

where $\boldsymbol{Y}$ marks the fluid element B originating from a different initial position to A. Varying t_m will also lead $\boldsymbol{Y}$ to vary, so $\boldsymbol{Y}$ will be a function of $\boldsymbol{X}$ and t_m. One important point is that $\boldsymbol{Y}$ is also the Lagrangian coordinate system for the observer comoving with fluid B. In other words, if we define a comoving Lagrangian coordinate system attached to fluid B, then Eq. (2.141) is still true. To avoid any confusion, we can write the following relation

$$\boldsymbol{X}+\boldsymbol{P}_A\left(\boldsymbol{X}\,,t\right)=\boldsymbol{Y}\left(\boldsymbol{X}\,,t\right)+\boldsymbol{P}_B\left[\boldsymbol{Y}\left(\boldsymbol{X}\,,t\right)\,,t\right]. \tag{2.142}$$

This relation also holds if one defines the Lagrangian coordinate system according to fluid B, just in that case one is interested in the dependence $\boldsymbol{X}\left(\boldsymbol{Y}\,,t\right)$. Hereafter we will assume that the Lagrangian coordinate system is defined according to fluid A. With this in mind, Eq. (2.142) states several key points:

$$\boldsymbol{X}=\boldsymbol{Y}\left(\boldsymbol{X}\,,t_{\mathbf{i}}\right);\qquad \boldsymbol{X}\neq\boldsymbol{Y}\left(\boldsymbol{X}\,,t\right),\quad t>t_{\mathbf{i}}; \tag{2.143}$$

$$\boldsymbol{P}_A\left(\boldsymbol{X}\,,t\right)\neq\boldsymbol{P}_B\left[\boldsymbol{Y}\left(\boldsymbol{X}\,,t\right)\,,t\right],\quad t>t_{\mathbf{i}}; \tag{2.144}$$

$$\boldsymbol{P}_A\left(\boldsymbol{X}\,,t_{\mathbf{i}}\right)=\boldsymbol{P}_B\left[\boldsymbol{Y}\left(\boldsymbol{X}\,,t_{\mathbf{i}}\right)\,,t_{\mathbf{i}}\right]=0; \tag{2.145}$$

$$0=\boldsymbol{P}_B\left[\boldsymbol{Y}\left(\boldsymbol{X}\,,t\right)\,,t_{\mathbf{i}}\right],\quad t>t_{\mathbf{i}}. \tag{2.146}$$

Effectively, $\boldsymbol{Y}(\boldsymbol{X}\,,t)$ is a map from an element comoving with A back along the flow lines of B that instantaneously intersect with those of A at t to the initial Eulerian position at $t_{\mathbf{i}}$ of each successive element of B, as shown in Fig. 2.1. We must assume that there is no crossing of the flow lines of B.

For the Lagrangian picture with one fluid component, mass is conserved along the fluid flow according to Eq. (2.38). So for the two-component case, if we follow the above discussion then for fluid A one always has

$$\varrho_A\left(\mathbf{X}\,,t_{\mathbf{i}}\right)=\varrho_A\left(\mathbf{X}\,,t\right)J_A. \tag{2.147}$$

[6] Here we use A and B standing for two fluid elements, where element A belongs to species α and element B belongs to species β.

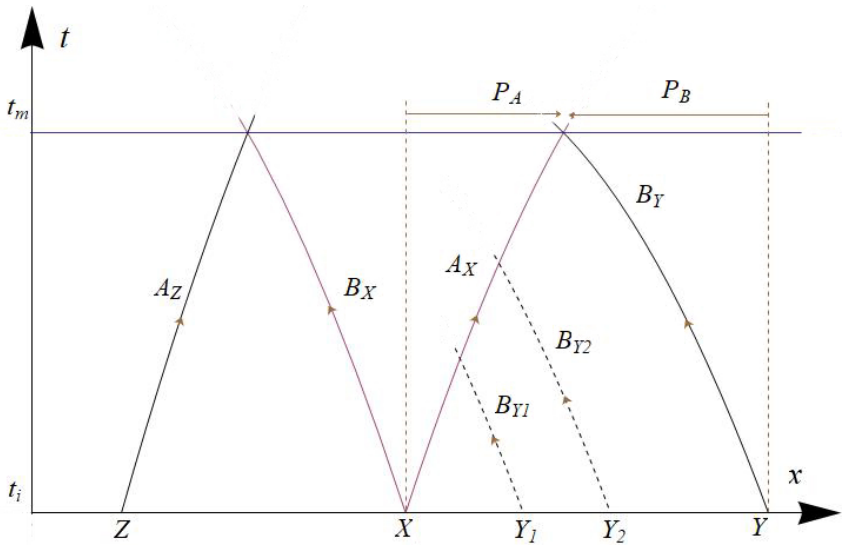

Figure 2.1: Here we use a schematic diagram to show that the relation between $\boldsymbol{X}$ and $\boldsymbol{Y}$. At initial time $t_{\mathbf{i}}$ the Lagrangian coordinates are same as the Eulerian coordinates. For a component A originating from an initial position $\boldsymbol{X}$, following its trajectory at each point there will be an element of component B originating from another initial position, whose trajectory will cross the same point. But for different time, the crossing point will be different, and the initial position of element B will be different. The same situation happens to an element of component B originating from an initial position $\boldsymbol{X}$. Note that this diagram is plotted in Eulerian coordinate space. Note the difference between the trajectories of A_X and B_X has been exaggerated to make the diagram clearer.

But for fluid B the situation will become much more complicated. As noted above, for any point p at a later time, the total mass contained in an infinitesimal volume around this point p is given by Eq. (2.140) with volume $d^3\boldsymbol{q}$. So we should have

$$d^3\boldsymbol{q} = J_A\, d^3\boldsymbol{X} = F\left(\boldsymbol{Y}, t\right) d^3\boldsymbol{Y}, \tag{2.148}$$

where we use $F\left(\boldsymbol{Y}, t\right)$ to stand for the unknown function of $\boldsymbol{Y}$. This function will make the volume elements for A and B at point p the same. Since J_A denotes the transformation between the Eulerian coordinates $\boldsymbol{q}$ and Lagrangian coordinates $\boldsymbol{X}$, then in principle $F\left(\boldsymbol{Y}, t\right)$ can be explained as a transformation between $\boldsymbol{q}$ and $\boldsymbol{Y}$. Recall for $t = t_{\mathbf{i}}$, $\boldsymbol{X} = \boldsymbol{Y}$ and $J_A\left(\boldsymbol{X}, t_{\mathbf{i}}\right) = F\left(\boldsymbol{Y}, t_{\mathbf{i}}\right) = 1$. Also since $\boldsymbol{Y}$

is a function of $\boldsymbol{X}$ and t, one will have

$$d^3\boldsymbol{q} = J_A\, d^3\boldsymbol{X} = \frac{J_A}{J_{AB}} d^3\boldsymbol{Y}, \tag{2.149}$$

which can be easily derived from the chain rule. J_{AB} denotes the transformation between $\boldsymbol{X}$ and $\boldsymbol{Y}$ and should be calculated using Eqs. (2.34, 2.142)

$$J_{AB} = \mathcal{J}\left(Y_i,\, Y_j,\, Y_k\right) = \frac{1}{6}\varepsilon^{ijk}\varepsilon^{lmn} Y_{i|l}\; Y_{j|m}\; Y_{k|n}\,. \tag{2.150}$$

Bearing in mind that we are discussing a moment at a later time $t > t_{\mathbf{i}}$, the total mass is

$$\delta M\left(\boldsymbol{q}_p\,, t\right) = \varrho\left(\boldsymbol{q}\,, t\right) d^3\boldsymbol{q} = \varrho_A\left(\boldsymbol{X}_p\,, t\right) J_A d^3\boldsymbol{X} + \varrho_B\left(\boldsymbol{Y}_p\,, t\right) \frac{J_A}{J_{AB}} d^3\boldsymbol{Y}, \tag{2.151}$$

and the total mass density is

$$\varrho\left(\boldsymbol{q}_p\,, t\right) = \varrho_A\left(\boldsymbol{X}_p\,, t\right) + \varrho_B\left(\boldsymbol{Y}\left(\boldsymbol{X}_p\,, t\right)\,, t\right). \tag{2.152}$$

Now we have to find a similar relation to Eq. (2.147) for fluid B. As we have noted, $\boldsymbol{Y}$ is the Lagrangian coordinate system for the elements of component B. Thus along the flow line of B the mass of B should be conserved, giving the relation

$$\varrho_B\left(\boldsymbol{Y}_p\,, t_{\mathbf{i}}\right) = J_B\, \varrho_B\left(\boldsymbol{Y}_p\,, t\right), \tag{2.153}$$

where J_B has a similar definition to J_A and $\boldsymbol{Y}_p$ is defined by the moment when the elements of A and B meet at point p at $t > t_{\mathbf{i}}$. So following the trajectory of B and mapping back along the flow lines of A to the initial time, we see that usually $\boldsymbol{X}_p \neq \boldsymbol{Y}_p$. The following issue now arises: at the initial time $t_{\mathbf{i}}$ the two elements A and B, which meet at p at a later time t, have different initial Eulerian position, so one might ask whether it is correct to define J_B by Eq. (2.34). To answer this, consider the total mass equation (2.151), noting that along the trajectory of B the element mass of component B does not change. As a consequence, from the viewpoint of B, one has

$$\frac{dM_B}{dt} = 0 = \frac{d}{dt}\int \varrho_B\left(\boldsymbol{Y}_p\,, t\right) \frac{J_A\left(\boldsymbol{X}\,, t\right)}{J_{AB}\left(\boldsymbol{X}\,, t\right)} d^3\boldsymbol{Y} \tag{2.154}$$

$$= \int \frac{d}{dt} \left\{ \varrho_B \left(\boldsymbol{Y}_p , t \right) \frac{J_A \left(\boldsymbol{X} , t \right)}{J_{AB} \left(\boldsymbol{X} , t \right)} \right\} d^3 \boldsymbol{Y},$$

which means

$$\varrho_B \left(\boldsymbol{Y}_p , t \right) \frac{J_A \left(\boldsymbol{X} , t \right)}{J_{AB} \left(\boldsymbol{X} , t \right)} = \varrho_B \left(\boldsymbol{Y}_p , t_{\mathbf{i}} \right) \frac{1}{J_{AB} \left(\boldsymbol{X} , t_{\mathbf{i}} \right)}. \tag{2.155}$$

So if we define $J_B = \frac{J_A(\boldsymbol{X},t)}{J_{AB}(\boldsymbol{X},t)}$ with $J_{AB}(\boldsymbol{X} , t_{\mathbf{i}}) = 1$ then we will recover Eq. (2.153). We can conclude that for the observer comoving with fluid element A the evolution equation of fluid element B obeys Eq. (2.155) but for the observer comoving with B the mass evolution equation of itself will obey Eq. (2.153).

In summary, for the Lagrangian approach in Newtonian cosmologies composed of two gravitationally coupled components, we have the preliminary Lagrangian system from the view point of two species:

$$\boldsymbol{X} + \boldsymbol{P}_A \left(\boldsymbol{X} , t \right) = \boldsymbol{Y} \left(\boldsymbol{X} , t \right) + \boldsymbol{P}_B \left[\boldsymbol{Y} \left(\boldsymbol{X} , t \right) , t \right], \tag{2.156}$$

$$\varrho_A \left(\boldsymbol{X} , t_{\mathbf{i}} \right) = \varrho_A \left(\boldsymbol{X} , t \right) J_A, \tag{2.157}$$

$$\varrho_B \left(\boldsymbol{Y} , t_{\mathbf{i}} \right) = \varrho_B \left(\boldsymbol{Y} , t \right) \frac{J_A \left(\boldsymbol{X} , t \right)}{J_{AB} \left(\boldsymbol{X} , t \right)}, \tag{2.158}$$

$$\varrho \left(\boldsymbol{X} , t \right) = \varrho_A \left(\boldsymbol{X} , t \right) + \varrho_B \left[\boldsymbol{Y} \left(\boldsymbol{X} , t \right) , t \right], \tag{2.159}$$

J_A is given by Eqs. (2.34, 2.142) and J_{AB} is the transformation between $\boldsymbol{X}$ and $\boldsymbol{Y}$. Note that in Eq. (2.158) we have used $\boldsymbol{Y}$ as variables determined by Eq. (2.156). Here $\varrho_B \left(\boldsymbol{Y} \left(\boldsymbol{X} , t \right) , t_{\mathbf{i}} \right)$ is actually a function of time t and position $\boldsymbol{X}$.

2.2.3.1 Derivations of the evolution equations for each species

In last subsection we have constructed the preliminary Lagrangian system of the single species from the perspectives of two species. In this subsection we will apply the perturbation approach as we have previously done in section 2.2.2.5. Again for simplicity, we only consider $\Lambda = 0$ and a small perturbation $\boldsymbol{P} \sim \mathcal{O}(\varepsilon)$ and keep only the first two orders. Recall that the pressure in this case is not a source for gravitational fields.

According to the relation Eq. (2.40), for each element belonging to different

fluids, one will have an alternative expression in comoving Eulerian coordinates

$$0 = \frac{\ddot{a}}{a}\varepsilon^{hji}q_{i\,,j} + 2H\varepsilon^{hji}\dot{q}_{i\,,j} + \varepsilon^{hji}\ddot{q}_{i\,,j} + \frac{1}{a^2\varrho_A^2}\varepsilon^{hji}p_{A\,,j}\varrho_{A\,,i}. \tag{2.160}$$

Remember that the comma here denotes the spatial derivative with respect to comoving Eulerian coordinates. With the assumption that both fluids have equations of state of a similar form, $p = \kappa\varrho^\gamma = \alpha(\varrho)$, the last term in above equation actually is zero

$$\frac{1}{\varrho^2}\nabla p \times \nabla\varrho = \frac{\alpha'(\varrho)}{\varrho^2}\nabla\varrho \times \nabla\varrho = 0. \tag{2.161}$$

Eq. (2.41) is equivalent to the new expression

$$\Lambda - 4\pi G\varrho_{total} = 3\frac{\ddot{a}}{a} + 2H\dot{q}_{i\,,i} + \ddot{q}_{i\,,i} + \frac{1}{a^2\varrho_A}p_{A\,,ii} - \frac{1}{a^2\varrho_A^2}p_{A\,,i}\varrho_{A\,,i}. \tag{2.162}$$

Note that both equations still hold if we replace component A by component B.

We will discuss the perturbation equations for each components A and B separately:

1. *Component A:*

In this case, up to second order, the derivatives with respect to the Lagrangian comoving coordinates $\boldsymbol{X}$ can be represented as

$$\begin{aligned}
J_A &= 1 + P_{Am|m} + \frac{1}{2}\varepsilon^{ijk}\mathcal{J}\left(X_i\,, P_{Aj}\,, P_{Ak}\right) + \mathcal{O}\left(\varepsilon^3\right), \\
\varepsilon^{hji}\ddot{q}_{i\,,j} &= \frac{1}{J_A}\left[\varepsilon^{kih}\ddot{P}_{Ai|k} - \mathcal{J}\left(\ddot{P}_{Ai}\,, X_i\,, P_{Ah}\right) - \mathcal{J}\left(\ddot{P}_{Ai}\,, P_{Ai}\,, X_h\right)\right], \\
\varepsilon^{hji}\dot{q}_{i\,,j} &= \frac{1}{J_A}\left[\varepsilon^{kih}\dot{P}_{Ai|k} - \mathcal{J}\left(\dot{P}_{Ai}\,, X_i\,, P_{Ah}\right) - \mathcal{J}\left(\dot{P}_{Ai}\,, P_{Ai}\,, X_h\right)\right],
\end{aligned} \tag{2.163}$$

so that up to second order Eq. (2.160) becomes

$$\begin{aligned}
\varepsilon^{hji}\left(\ddot{P}_{Ai|\,j} + 2H\dot{P}_{Ai|\,j}\right) &- \mathcal{J}\left(\ddot{P}_{Ai} + 2H\dot{P}_{Ai}\,, X_i\,, P_{Ah}\right) \\
&- \mathcal{J}\left(\ddot{P}_{Ai} + 2H\dot{P}_{Ai}\,, P_{Ai}\,, X_h\right) = 0.
\end{aligned} \tag{2.164}$$

If we only focus on the first order term then the above equation shows that

$$\nabla_{\boldsymbol{X}} \times \left(\ddot{\mathbf{P}} + 2H\dot{\mathbf{P}}\right) = 0, \tag{2.165}$$

which matches Eq. (24a) in [Buchert and Adler, 1999].

Now let us consider Eq. (2.162). We have assumed the deformation fields are small for both components, and we also expect that the initial density contrasts are also small. With these assumptions we can represent the initial mass density by

$$\begin{aligned} \varrho_A\left(\boldsymbol{X}\,,t_{\mathbf{i}}\right) &= \varrho_{AH}\left(t_{\mathbf{i}}\right)\left(1+\delta\varrho_A\left(\boldsymbol{X}\,,t_{\mathbf{i}}\right)\right); \\ \varrho_B\left(\boldsymbol{Y}\,,t_{\mathbf{i}}\right) &= \varrho_{BH}\left(t_{\mathbf{i}}\right)\left(1+\delta\varrho_B\left(\boldsymbol{Y}\,,t_{\mathbf{i}}\right)\right). \end{aligned} \tag{2.166}$$

One thus can represent Eqs. (2.157, 2.158) to second order by

$$\varrho_A\left(\mathbf{X}\,,t\right) = \varrho_{AH}\left(1+\delta\varrho_{A\mathbf{i}} - P_{Am|m} + \mathcal{S}_{2A}\right), \tag{2.167}$$

$$\varrho_B\left(\mathbf{Y}\,,t\right) = \varrho_{BH}\left(1+\delta\varrho_{B\mathbf{i}} - \frac{\partial P_{Bm}}{\partial Y_m} + \mathcal{S}_{2B}\right), \tag{2.168}$$

where $\mathcal{S}_2$ means the second order terms for each component:

$$\mathcal{S}_{2A} = P_{Am|m}\,P_{Aj|j} - \frac{1}{2}\varepsilon^{ijk}\mathcal{J}\left(X_i\,,P_{Aj}\,,P_{Ak}\right) - \delta\varrho_{A\mathbf{i}}\,P_{Am|m}, \tag{2.169}$$

$$\mathcal{S}_{2B} = \frac{\partial P_{Bm}}{\partial Y_m}\frac{\partial P_{Bj}}{\partial Y_j} - \frac{1}{2}\varepsilon^{ijk}\mathcal{J}_Y\left(Y_i\,,P_{Bj}\,,P_{Bk}\right) - \delta\varrho_{B\mathbf{i}}\frac{\partial P_{Bm}}{\partial Y_m}, \tag{2.170}$$

and we use $\mathcal{J}_Y$ for the definition Eq. (2.34) with respect to $\boldsymbol{Y}$. Here for simplicity we retain the terms $\delta\varrho_{A\mathbf{i}} - P_{Am|m}$, which actually should be expressed as the sum of first and second order terms. Furthermore,

$$\dot{q}_{i\,,i} = \dot{P}_{Ai|i} + \mathcal{M}_1^{A2} + \mathcal{O}\left(\varepsilon^3\right), \tag{2.171}$$

$$\ddot{q}_{i\,,i} = \ddot{P}_{Ai|i} + \mathcal{M}_2^{A2} + \mathcal{O}\left(\varepsilon^3\right), \tag{2.172}$$

where

$$\mathcal{M}_1^{A2} = \frac{1}{2}\varepsilon^{ipq}\left[\mathcal{J}\left(\dot{P}_{Ai}\,,X_p\,,P_{Aq}\right) + \mathcal{J}\left(\dot{P}_{Ai}\,,P_{Ap}\,,X_q\right)\right] - \dot{P}_{Aj|j}\,P_{Ak|k}, \tag{2.173}$$

$$\mathcal{M}_2^{A2} = \frac{1}{2}\varepsilon^{ipq}\left[\mathcal{J}\left(\ddot{P}_{Ai}\,,X_p\,,P_{Aq}\right) + \mathcal{J}\left(\ddot{P}_{Ai}\,,P_{Ap}\,,X_q\right)\right] - \ddot{P}_{Aj|j}\,P_{Ak|k}, \tag{2.174}$$

are second order terms. The other terms can be perturbed to be

$$\bar{P}_A = \delta\varrho_{A\mathbf{i}} - P_{Am|m}, \tag{2.175}$$

$$\frac{p_{A\,,ii}}{a^2\varrho_A} = \frac{\varrho_{AH}^{2/3}}{a^2}\Delta_{\boldsymbol{X}}\kappa_\alpha + \mathcal{O}\left(\varepsilon^3\right), \tag{2.176}$$

$$\frac{p_{A\,,i}\varrho_{A\,,i}}{a^2\varrho_A^2} = \mathcal{O}\left(\varepsilon^3\right). \tag{2.177}$$

Here again we adopt $\kappa\left(\boldsymbol{X}\right) \sim \mathcal{O}\left(\varepsilon^2\right)$. As a consequence, the right hand side of Eq. (2.162) becomes

$$r.h.s. = 3\frac{\ddot{a}}{a} - 2\frac{\dot{a}}{a}\dot{\bar{P}}_A - \ddot{\bar{P}}_A + \frac{\varrho_{AH}^{2/3}}{a^2}\Delta_{\boldsymbol{X}}\kappa_\alpha + 2H\mathcal{M}_1^{A2} + \mathcal{M}_2^{A2}, \tag{2.178}$$

Correspondingly, the left hand side of Eq. (2.162) up to second order will give

$$\begin{aligned} l.h.s = \Lambda - 4\pi G(\varrho_{AH} + \varrho_{BH}) - 4\pi G\left[\varrho_{AH}\bar{P}_A + \varrho_{BH}\left(\delta\varrho_{B\mathbf{i}} - \frac{\partial P_{Bi}(\boldsymbol{Y},t)}{\partial Y_i}\right)\right] \\ - 4\pi G\left(\varrho_{AH}\mathcal{S}_{A2} + \varrho_{BH}\mathcal{S}_{B2}\right). \end{aligned} \tag{2.179}$$

Combining Eqs. (2.65, 2.142, 2.178, 2.179), finally Eq. (2.162) becomes

$$\begin{aligned} \ddot{\bar{P}}_A + 2\frac{\dot{a}}{a}\dot{\bar{P}}_A - \frac{\varrho_{AH}^{2/3}}{a^2}\Delta_{\boldsymbol{X}}\kappa_\alpha - 4\pi G\left[\varrho_{AH}\bar{P}_A + \varrho_{BH}\left(\delta\varrho_{B\mathbf{i}} - \frac{\partial P_{Bi}(\boldsymbol{Y},t)}{\partial Y_i}\right)\right] \\ - 4\pi G\left(\varrho_{AH}\mathcal{S}_{A2} + \varrho_{BH}\mathcal{S}_{B2}\right) - 2H\mathcal{M}_1^{A2} - \mathcal{M}_2^{A2} = 0. \end{aligned} \tag{2.180}$$

For a single component A, keeping only the first order terms one recovers the well-known dust linear perturbation equation (2.29).

2. Component B:

Now consider the element of B which has the same initial position $\boldsymbol{X}$ as the element of A. Taking the same Lagrangian coordinates for both elements mean they will obey similar evolution equations. So we can repeat the derivation for component A. The evolution equations for B will be identical to Eqs. (2.164, 2.180) upon exchanging A and B,

$$\begin{aligned} \varepsilon^{hji}\left(\ddot{P}_{Bi|\,j} + 2H\dot{P}_{Bi|\,j}\right) - \mathcal{J}\left(\ddot{P}_{Bi} + 2H\dot{P}_{Bi}\,, X_i\,, P_{Bh}\right) \\ - \mathcal{J}\left(\ddot{P}_{Bi} + 2H\dot{P}_{Bi}\,, P_{Bi}\,, X_h\right) = 0. \end{aligned} \tag{2.181}$$

$$\ddot{\bar{P}}_B + 2\frac{\dot{a}}{a}\dot{\bar{P}}_B - \frac{\varrho_{AH}^{2/3}}{a^2}\Delta_{\boldsymbol{X}}\kappa_\alpha - 4\pi G\left[\varrho_{BH}\bar{P}_B + \varrho_{AH}\left(\delta\varrho_{A\mathbf{i}} - \frac{\partial P_{Ai}(\boldsymbol{Z},t)}{\partial Z_i}\right)\right] \quad (2.182)$$
$$- 4\pi G\left(\varrho_{BH}\mathcal{S}_{B2} + \varrho_{AH}\mathcal{S}_{A2}\right) - 2H\mathcal{M}_1^{B2} - \mathcal{M}_2^{B2} = 0.$$

where we have used the relation (2.142) but with $\boldsymbol{Z}$ instead of $\boldsymbol{Y}$, as we are focusing on the component B which originates from same initial position as A, see Fig. 2.1.

We have derived the evolution equation of the deformation fields for two different components up to second order. Since we assumed the deformation fields are small, the first order terms dominate. We kept the second order terms in above as the basis for future calculations.

Thus for a Newtonian cosmology with two different components, the evolution equations for the two fluids $A(B)$ originating from same initial position $\boldsymbol{X}$, and meeting another element $B(A)$ at same physical position at a later time, are

$$\begin{aligned}
&\ddot{\bar{P}}_A + 2\frac{\dot{a}}{a}\dot{\bar{P}}_A - 4\pi G\left[\varrho_{AH}\bar{P}_A + \varrho_{BH}\left(\delta\varrho_{B\mathbf{i}}\left(\boldsymbol{Y}\right) - \frac{\partial P_{Bi}(\boldsymbol{Y},t)}{\partial Y_i}\right)\right] = 0,\\
&\ddot{\bar{P}}_B + 2\frac{\dot{a}}{a}\dot{\bar{P}}_B - 4\pi G\left[\varrho_{BH}\bar{P}_B + \varrho_{AH}\left(\delta\varrho_{A\mathbf{i}}\left(\boldsymbol{Z}\right) - \frac{\partial P_{Ai}(\boldsymbol{Z},t)}{\partial Z_i}\right)\right] = 0, \qquad (2.183)\\
&\boldsymbol{X} + \boldsymbol{P}_A(\boldsymbol{X},t) = \boldsymbol{Y} + \boldsymbol{P}_B(\boldsymbol{Y},t),\\
&\boldsymbol{X} + \boldsymbol{P}_B(\boldsymbol{X},t) = \boldsymbol{Z} + \boldsymbol{P}_A(\boldsymbol{Z},t),
\end{aligned}$$

These equations have a similar form to the standard equations Eq. (2.103). Again, we have made several assumptions in deriving these equations. The first and most important assumption is that the two components are solely coupled by gravity, and have different initial velocities. This makes the two components at the same initial position evolve along different trajectories. Also each element from one fluid will meet another element from the second fluid at a later time. The second assumption is we require that any shell crossing occurs only after the two different components meet, *i.e.*, the evolution equations (2.183) are only valid before the shell crossing of the same component. We also assumed the deformation fields are small.

Although we have not solved the above equations up to second order, it can be proved that Eq. (2.180) is equivalent to Eq. (2.137) under specific conditions. If we choose $\boldsymbol{X} = \boldsymbol{Y} = \boldsymbol{Z}$, then unsurprisingly one should choose $\boldsymbol{u}_\alpha = \boldsymbol{u}_\beta$. This

condition means $\boldsymbol{u}^{(1)} = \boldsymbol{u}^{(1)}_{\alpha(\beta)}$ so it is straightforward to prove the equivalent of Eqs. (2.137, 2.180).

2.3 The relativistic Lagrangian perturbation approach

In this chapter we have discussed the Lagrangian perturbation approach to large scale structure formation in Newtonian cosmologies. Naturally one should generalize this approach to general relativistic cosmologies. A key point is that relativistic effects will be important when small scale inhomogeneities are large, and small scale inhomogeneities may impact on the large scale average expansion via backreaction.

Early work on this problem was undertaken by Matarrese et al. [1993], who developed a new general-relativistic algorithm to study the nonlinear evolution of density perturbations of an irrotational collisionless fluid. They neglected the interaction with tensor perturbations and adopted a Lagrangian method. Within this framework the dynamics of each fluid element was followed in its own inertial rest frame. It gave an improvement on the Zel'dovich approximation in three spatial dimensions. The cosmological implications of such relativistic effects were studied using the same method in a follow-up paper [Matarrese et al., 1994b], which elucidated the dynamical role of the magnetic part of the Weyl tensor. Second order Lagrangian solutions were subsequently discussed [Matarrese et al., 1994a], and the synchronous and Poisson gauges compared in detail in the case of the Einstein-de Sitter universe [Matarrese et al., 1998].

Croudace et al. [1994] provided a systematic derivation of the Zel'dovich approximation describing the nonlinear evolution of collisionless dust in general relativistic cosmologies. Beginning by evolving dust particles along their world lines, the authors demonstrated that the Szekeres line element is an exact but unstable solution of the evolution equations describing pancake collapse. By employing Hamilton-Jacobi techniques and a spatial gradient expansion of the Einstein equations, they determined a prescription for evolving a seed metric up to the formation of pancakes.

Kasai [1995] developed an alternative approximation scheme in General Relativity for the same purpose, *i.e.*, to describe nonlinear inhomogeneous universes containing irrotational dust. Using a tetrad-based perturbative approach, Kasai obtained a second-order differential equation for the perturbations of the spatial basis vectors, and presented the first-order solution. Subsequent papers then extended and improved this formalism up to second-order solutions [Russ et al., 1996] and to a spherically symmetric model [Morita et al., 1998].

All references we mention above were limited to the class of irrotational dust matter models. To take into account the vortical effect of dust matter, Asada and Kasai [1999] developed a Lagrangian perturbative approach, where the propagation equation for the vorticity as well as the density was exactly solved. Asada [2000] then extended this approach to the case of perfect fluids in a subsequent paper.

The topic was pursued by just a few authors in the following decade. Ellis and Tsagas [2002] discussed the peculiar motion of nonrelativistic matter in a fully covariant way, and derived an exact nonlinear equation which is claimed to provide a fully covariant formulation of the Zel'dovich approximation. Rampf and Rigopoulos [2013] then showed that the Zel'dovich approximation could be obtained from a general relativistic gradient expansion in a ΛCDM cosmology. In particular, by applying a second-order nonlocal coordinate transformation from comoving coordinates to another coordinate system which takes the metric to a Newtonian form, they defined the displacement fields as the difference between the comoving coordinates and the new ones. The resulting density contrast turned out not to be related to the Newtonian potential via the Poisson equation, but via a modified Helmholtz equation, as a consequence of causality. This approach was generalized to tensor perturbations in a subsequent paper [Rampf and Wiegand, 2014].

A sequence of significant papers were published by Buchert and various coauthors [Buchert and Ostermann, 2012; Buchert et al., 2013; Alles et al., 2015; Al Roumi et al., 2017]. They revisited the Lagrangian approach in a fully rigorous manner within the framework of Einstein's equations. With the help of Cartan's coframe, the dynamical equations are explicitly given. The only variable in these equations is the Lagrangian deformation field, which can be expressed by the Cartan coframes. All other variables, such as the curvature tensor, are also

derived by the coframe method. However, this series of papers has been limited to an irrotational dust continuum so that one can write the Einstein equations within a flow-orthogonal foliation. In next chapter, we will extend the matter model to the case of perfect fluids but keep the condition of irrotationality.

CHAPTER 3

Relativistic Lagrangian perturbation theory for irrotational fluids

We have discussed the Lagrangian perturbation theory in a Newtonian cosmology composed of two different dust species in the last chapter, and briefly reviewed the relativistic LPT. In this chapter we will extend relativistic Lagrangian perturbations for a dust matter model to the case of irrotational perfect fluids, and also to cases that are relevant for the modelling of multistream regimes where the dust approximation breaks down. This will provide a framework not only to deal with a relativistic generalization of Newtonian Lagrangian perturbation theory with pressure at late epochs, but also to the fully relativistic situation of the early Universe.

There are several motivations for such an investigation. A primary motivation is to establish a framework which is better suited to studies of the backreaction of inhomogeneities in cosmology as compared to standard perturbation theory. In particular, standard cosmological perturbation theory conventionally assumes that average cosmic evolution is exactly described by a solution to Einstein's equations with a prescribed energy–momentum tensor on a global hypersurface irrespective of the scale of coarse–graining of the matter fields. No fundamental physical principle demands such an outcome [Wiltshire, 2014].

Neglecting backreaction in the primordial plasma may seem to be a reasonable approximation for the evolution of the background universe to leading order, given that it is extremely close to being spatially homogeneous and isotropic at early times. However, backreaction can nonetheless make a significant difference when considering the growth of perturbations. In particular, even if the difference from the Friedmann equation is of order 10^{-5} as a fraction of energy density at decoupling, this is nonetheless of the same order as the density perturbations. A recent study of Cosmic Microwave Background (CMB) anisotropies in the

timescape model found that systematic uncertainties that arise from neglecting such small differences in initial conditions at last scattering, lead to systematic uncertainties of 8–13%, in particular for cosmological parameters at the present epoch [Nazer and Wiltshire, 2015]. This remark applies to the conservative assumption that the background universe does not already contain backreaction arising from earlier epochs that could be compatible with large–scale homogeneity and isotropy [Buchert and Obadia, 2011].

For these reasons, we desire a new approach to cosmological perturbation theory which is intrinsic to the fluid and not anchored to an embedding space. Relativistic Lagrangian perturbation theory represents a promising avenue, as it is intimately tied to physical particles. But as a first step towards a fully realistic theory, we will firstly consider relativistic Lagrangian perturbation theory for the same system that was considered in Ref. [Buchert, 2001], namely a single component perfect fluid with barotropic equation of state. We will also include an explicit cosmological constant term.

This chapter is organized as follows. In section 3.1 we briefly introduce the $3+1$ formalism with Lagrangian spatial coordinates introduced in Chap. 1, presenting the general framework and foliation structure for a general irrotational matter model. We then restrict our attention to a barotropic perfect fluid and discuss in detail the fluid variables and their equation of state. In this context, in section 3.2 we introduce Cartan's coframe formalism, proceeding with the relativistic Lagrangian perturbation approach. We develop the first–order Lagrangian scheme and derive master equations for the trace and trace–free parts of the perturbation field. In section 3.3 we apply the first–order Lagrangian scheme to particular matter models, allowing us to explicitly derive solutions for the trace part, and we illustrate the results. Particular solutions for the gravitoelectric traceless part are studied in appendix B.

3.1 Spacetime foliation structure and 3+1 Einstein equations

In this chapter we will consider a model universe containing a single irrotational fluid, so that a foliation of spacetime into flow–orthogonal hypersurfaces can be

introduced.

3.1.1 Decomposition of Einstein's equations for flow-orthogonal hypersurfaces

In section 1.3.2 we have introduced the basic dynamical equations in 3+1 formalism. The irrotationality assumption on the fluid amounts to the existence of two scalar functions, N and t, such that the 1−form dual to the normalized 4−velocity vector u^μ of the fluid can be written as:[1]

$$u_\mu = -N\,\partial_\mu t, \qquad N = (-\partial^\mu t\,\partial_\mu t)^{-1/2}\ , \tag{3.1}$$

where we choose the spatial coordinates to be spatial Lagrangian (or comoving) coordinates, denoted X^i, that are assumed to be constant along each flow line. In the set of coordinates $(X^\mu) = (t, X^i)$, the components of the fluid 4−velocity vector and its dual are then respectively:

$$u^\mu = \frac{1}{N}(1,0,0,0)\,, \quad u_\mu = (-N,0,0,0)\,, \tag{3.2}$$

while the line element can be written as

$$\mathrm{d}s^2 = g_{\mu\nu}\,\mathrm{d}X^\mu \mathrm{d}X^\nu = -N^2\mathrm{d}t^2 + g_{ij}\,\mathrm{d}X^i\mathrm{d}X^j\ . \tag{3.3}$$

The spatial metric $h_{ij} = g_{\mu\nu}h^\mu{}_i h^\nu{}_j = g_{ij}$ and the lapse function N together will encode the inhomogeneities. (We will later use the more elementary coframe coefficients instead of the 3−metric coefficients.)

Without loss of generality, the energy–momentum tensor of the fluid is given by

$$T_{\mu\nu} = (\epsilon + p)u_\mu u_\nu + p g_{\mu\nu} + \pi_{\mu\nu} + q_\mu u_\nu + q_\nu u_\mu\ , \tag{3.4}$$

where $\pi_{\mu\nu}$ is an anisotropic pressure, with $\pi_{[\mu\nu]} = 0$, $u^\mu\pi_{\mu\nu} = 0$ and $\pi^\mu{}_\mu = 0$, and q_μ the heat flux, with $q_\mu u^\mu = 0$.

Introducing the expansion tensor (as minus the extrinsic curvature $\mathcal{K}$) of the

[1] Again, here Greek letters $\mu, \nu, \cdots$ are spacetime indices running from 0 to 3, while lower-case Latin letters $i, j, \cdots$ are spatial indices running from 1 to 3. We use units in which $c = 1$, if not otherwise stated.

hypersurfaces,

$$\Theta_{ij} \equiv \nabla_\nu n_\mu h^\mu{}_i h^\nu{}_j = \frac{1}{2N}\partial_t g_{ij} \ , \tag{3.5}$$

Einstein's equations with a cosmological constant may be cast into a set of constraint and evolution equations. The constraint equations are the energy and momentum constraints, Eqs. (1.42):[2]

$$\begin{aligned} \mathcal{R} + \Theta^2 - \Theta^i{}_j \Theta^j{}_i &= 16\pi G\,\epsilon \,+\, 2\,\Lambda \ ; \\ \Theta^i{}_{j\|i} - \Theta_{|j} &= -8\pi G q_j \ . \end{aligned} \tag{3.6}$$

The propagation equations are given by

$$\begin{aligned} \Theta^i{}_j &= \frac{1}{2N} g^{ik}\partial_t g_{kj} \ ; \\ N^{-1}\partial_t \Theta^i{}_j &= -\,\Theta\Theta^i{}_j - \mathcal{R}^i{}_j + \mathcal{A}^i{}_j + 4\pi G\left[(\epsilon - p)\,\delta^i{}_j + 2\pi^i{}_j\right] \,+\, \Lambda\,\delta^i{}_j \ , \end{aligned} \tag{3.7}$$

where $a_\mu \equiv u^\nu \boldsymbol{\nabla}_\nu u_\mu = N^{-1} N_{||\mu}$ is the covariant acceleration of the fluid (with $\boldsymbol{\nabla}$ denoting the 4−covariant derivative), and $\mathcal{A}^i{}_j \equiv a^i{}_{\|j} + a^i a_j = N^{-1} N^{\|i}{}_{\|j}$. Combining the trace of the second equation with the energy constraint yields the Raychaudhuri equation:

$$N^{-1}\partial_t \Theta = -\frac{1}{3}\Theta^2 - 2\sigma^2 - 4\pi G(\epsilon + 3p) + \mathcal{A} \,+\, \Lambda \ , \tag{3.8}$$

where $\mathcal{A} \equiv \mathcal{A}^i{}_i = \boldsymbol{\nabla}_\mu a^\mu = N^{-1} N^{\|i}{}_{\|i}$.

With the spacetime described by the given metric, the energy–momentum conservation laws are expressed as follows:

$$\partial_t \epsilon + N\Theta(\epsilon + p) = -N\left(q^\mu{}_{||\mu} + 2q^\mu a_\mu + \sigma_{\mu\nu}\pi^{\mu\nu}\right) \ ; \tag{3.9}$$

$$\begin{aligned} (\epsilon + p)\,a_\mu + p_{||\mu} = &-\left(\pi_{\mu\nu}{}^{||\nu} + a^\nu \pi_{\mu\nu}\right) \\ &- \left(\frac{4}{3}\Theta\, q_\mu + q^\nu \sigma_{\mu\nu} + u^\nu \boldsymbol{\nabla}_\nu q_\mu - q^\nu a_\nu\, u_\mu\right) \ . \end{aligned} \tag{3.10}$$

In what follows, we will specialize to the case of isotropic pressure, $\pi_{\mu\nu} = 0$, and

[2] The symbol $\|$ denotes the covariant derivative with respect to the 3−metric h_{ij}. When applied to scalars it reduces to a partial derivative, denoted $|$, with respect to the Lagrangian coordinates, X^i.

vanishing heat flux, $q_\mu = 0$. Note that with these assumptions we do still allow for some nonperfect fluids, since p is not necessarily the local thermodynamic equilibrium pressure [Ellis et al., 2012].

Such a restriction is required here since both extra terms in general create vorticity, which cannot be covered by the class of flow–orthogonal foliations considered in this work. Let us illustrate this by considering more closely the irrotationality condition for a fluid with negligible heat flux, $q_\mu = 0$, to see how this condition constrains the equation of state and the anisotropic pressure. The vanishing of the vorticity 2−form implies vanishing of the antisymmetrized projected gradient of the acceleration, $a_{[\nu||\mu]} = 0$, since $a_\mu = (\ln N)_{||\mu}$ from Eq. (3.1), being a consequence of the existence of the fluid–orthogonal foliation. From this, one obtains through Eq. (3.10) the following constraint on the energy–momentum components:

$$\epsilon_{||[\mu}\, p_{||\nu]} + (\epsilon + p)_{||[\mu}\, h^{\rho}{}_{\nu]} \nabla_\sigma \pi^\sigma{}_\rho - (\epsilon + p)\, h^{\rho}{}_{[\mu} h^{\sigma}{}_{\nu]} \nabla_\rho \nabla_\tau \pi^\tau{}_\sigma = 0 \,. \tag{3.11}$$

Since $\nabla_\mu \pi^\mu{}_\nu = 0$ would imply the vanishing of the right hand sides of Eq. (3.9)–Eq. (3.10), an anisotropic pressure that does contribute to the dynamics will satisfy $\nabla_\mu \pi^\mu{}_\nu \neq 0$ and thus will not fulfil the above condition in general, producing a vortical flow. Conversely, a barotropic perfect fluid flow with $\pi_{\mu\nu} = 0$ and an effective equation of state of the form $p = \beta(\epsilon)$, automatically satisfies the above constraint. Moreover, for such a fluid, Eq. (3.10) allows one to write the acceleration as a flow–orthogonal projected gradient, and it will indeed obey the relativistic equivalent of the Kelvin–Helmholtz theorem, so that irrotationality will be preserved along the flow lines [Ehlers, 1993; Ellis et al., 2012]. We shall therefore concentrate on the barotropic perfect fluid case in what follows.

3.1.2 Barotropic perfect fluid spacetimes

With assumption of perfect fluids we have $q_\mu = 0$ and $\pi_{\mu\nu} = 0$, and the energy–momentum tensor Eq. (3.4) then reduces to

$$T_{\mu\nu} = (\epsilon + p) u_\mu u_\nu + p g_{\mu\nu} \,, \tag{3.12}$$

while its conservation equations Eq. (3.9)–(3.10) become, respectively

$$\partial_t \epsilon + N\Theta(\epsilon + p) = 0 \; ; \tag{3.13}$$

$$a_\mu = -\frac{p_{||\mu}}{\epsilon + p} \; . \tag{3.14}$$

As a further restriction we will assume that the fluid flow is *barotropic*, *i.e.,* we assume a local relation of the form $p = \beta(\epsilon)$ to effectively hold throughout the entire fluid,[3] that we will henceforth call *the equation of state* or EoS. As noted earlier, such a relation will ensure that the flow remains irrotational. For such a fluid, setting some reference constant energy and rest mass density values ϵ_1, ϱ_1, we may use the EoS to define a formal rest mass density $\varrho(\epsilon)$ and a related specific enthalpy $h(\epsilon)$ – as an injection energy per fluid element and unit formal rest mass [Israel and Stewart, 1976] – respectively, by

$$\varrho \equiv F(\epsilon) = \varrho_1 \exp \int_{\epsilon_1}^{\epsilon} \frac{\mathrm{d}x}{x + \beta(x)} \; ; \tag{3.15}$$

$$h(\epsilon) \equiv \frac{\epsilon + \beta(\epsilon)}{F(\epsilon)} = \frac{\epsilon + p}{\varrho} \; . \tag{3.16}$$

The energy–momentum conservation equations (3.9) and (3.10) then, respectively, provide a conservation law for ϱ,

$$\partial_t \varrho + N\Theta\varrho = 0 \; , \tag{3.17}$$

and a relation between the specific enthalpy (3.16) and the lapse,

$$\frac{N_{||\mu}}{N} = a_\mu = -\frac{h_{||\mu}}{h} \;\; : \;\; (Nh)_{|i} = 0 \; . \tag{3.18}$$

See section 1.3.3 for more details. By an appropriate choice of the hypersurface–labelling function t, the lapse can thus be rescaled so that [Buchert, 2001; Ellis

[3] Considering the local dynamical solution for these variables, there is always a freedom of integration constants that depend on the Lagrangian coordinates, *i.e.*, on the particular fluid element. We assume here that the same relation holds for all fluid elements. Only this assumption makes the dynamical relation an apparent equation of state that is valid throughout the fluid flow. All related variables then also depend on this assumption, which is a restriction imposed on initial data.

et al., 2012]

$$N = \frac{1}{h} = \frac{F(\epsilon)}{\epsilon + \beta(\epsilon)} \,. \tag{3.19}$$

We assume that the fluid remains at equilibrium locally. If it has a nonvanishing rest mass density, then this density will follow the same evolution law (3.17) as $\varrho = F(\epsilon)$, by rest mass conservation. This formal ϱ and the actual rest mass density will then coincide up to a possible different spatial dependence (*cf.*, footnote 3). These two quantities may be made equal by a suitable choice of initial conditions for the rest mass density or local thermodynamic equilibrium assumptions.[4] This would then ensure the validity of the interpretation of ϱ and h as the physical rest mass density (or particle number density) and specific enthalpy of the fluid, respectively. We shall not, however, make such assumptions in the following section 3.2, to keep its level of generality. This will allow us to consider the case of a zero rest mass fluid (for which $F(\epsilon) \neq 0$ and $h(\epsilon)$ are still well–defined), as well as that of a nonzero rest mass density with less constrained initial conditions. It will also allow us to consider the variable p as an effective pressure term — *e.g.*, modelling velocity dispersion — instead of the local thermodynamic equilibrium pressure. For the general treatment including these cases it will suffice to formally define ϱ and h from equations (3.15)–(3.16) using the single barotropic assumption $p = \beta(\epsilon)$. We follow the notation of Ref. [Buchert and Ostermann, 2012] here.

[4] We take the local state of the fluid to belong to a thermodynamic Gibbs space admitting the equation of state $u(s, v)$, where s is the specific entropy, v is the specific volume and $u = \epsilon v$ is the specific internal energy. If we now assume that p is indeed the local thermodynamic equilibrium pressure of the fluid, it can then be expressed as $p(s, v) = -\partial u/\partial v$. Provided that a specific equation of state does not render the above relations degenerate, then these relations may be inverted to provide $v(\epsilon, p)$. Within a barotropic flow satisfying $p = \beta(\epsilon)$, the actual rest mass density v^{-1} thus only depends on the energy density ϵ, which fully determines its initial conditions. From the conservation equations of both quantities, $\partial_t \epsilon/(\epsilon + \beta(\epsilon)) = -N\Theta = \partial_t(v^{-1})/v^{-1}$, this dependency must be $v^{-1} = F(\epsilon)$, for Θ not identically vanishing, up to a constant prefactor which can be absorbed in the choice of ϱ_1. Hence, in this case, $F(\epsilon)$ is indeed the rest mass density of the fluid with no further restriction of generality. Also note that under the same assumptions, s is also a function of ϵ, preserved along the flow lines as the flow is adiabatic: $\partial_t s = 0 = (\mathrm{d}s/\mathrm{d}\epsilon)\,\partial_t \epsilon$, while $\partial_t \epsilon$ is not identically vanishing. The flow is thus *isentropic*, s being a constant s_1 that depends neither on time nor on the fluid element. The barotropic relation then corresponds to the equation $p(\epsilon, s)$ deduced from the thermodynamic equation of state, and taken at constant s, $\beta(\epsilon) = p(\epsilon, s = s_1)$ (see [Israel and Stewart, 1976, 1979; Ehlers, 1993; Friedrich, 1998; Stephani et al., 2003; Ellis et al., 2012]).

3.2 Lagrangian perturbation scheme

In this section we will introduce the coframe formalism to describe spacetime, which is a set of four deformation 1−form fields dual to a generally noncoordinate basis of vectors at every point of the manifold [Ellis and Elst, 1999b; Ellis, 1967; Zakharov et al., 2006]. A general relativistic version of a coframe–based perturbative approach for an irrotational dust continuum has been proposed in Ref. [Kasai, 1995], developed further in Ref. [Matarrese and Terranova, 1996] and in final form, featuring only the coframes as the single perturbation variable in Ref. [Buchert and Ostermann, 2012].

3.2.1 Coframe formulation

Following [Buchert et al., 2013; Alles et al., 2015; Al Roumi et al., 2017], we construct a set of three spatial coframes $\boldsymbol{\eta}^a$ such that the spatial metric can be rewritten in the form

$$ {}^{(3)}\mathbf{g} = G_{ab}\,\boldsymbol{\eta}^a \otimes \boldsymbol{\eta}^b \quad : \quad g_{ij} = G_{ab}\eta^a{}_i\eta^b{}_j \,. \tag{3.20} $$

Here $G_{ab}(\boldsymbol{X})$ is the Gram matrix that encodes all the initial spatial metric perturbations, $G_{ab}(\boldsymbol{X}) \equiv \delta_a{}^i\delta_b{}^j G_{ij}(\boldsymbol{X})$, with the initial metric coefficients, $G_{ij}(\boldsymbol{X}) \equiv g_{ij}(t_{\mathrm{i}}, \boldsymbol{X})$. On the other hand we can also include the temporal component into the matrix and rewrite it as

$$ \tilde{G}_{\alpha\beta} = \begin{pmatrix} -1 & 0 \\ 0 & G_{ab} \end{pmatrix} \,. \tag{3.21} $$

With this we introduce a full set of four spacetime coframes $\boldsymbol{\eta}^\alpha$ to describe the 4−metric ${}^{(4)}\mathbf{g}$:

$$ {}^{(4)}\mathbf{g} = \tilde{G}_{\alpha\beta}\,\boldsymbol{\eta}^\alpha \otimes \boldsymbol{\eta}^\beta \,, \tag{3.22} $$

by defining the coframe components as

$$ \eta^0{}_\mu = (-N, 0, 0, 0) \,,\ \eta^a{}_\mu = (0, \eta^a{}_i) \text{ for } a \neq 0 \,. \tag{3.23} $$

Notice here the Latin $a, b, c, \cdots$ denote the spatial components.

Similar with its definition in 3-metric case, we now define the transformation

between coordinate and noncoordinate bases as: $\mathcal{J} = \sqrt{-g}/\sqrt{-\tilde{G}} = \sqrt{-g}/\sqrt{G}$ (the signature adopted here being $(-1,1,1,1)$, and using notation $g \equiv \det({}^{(4)}\boldsymbol{g})$, $\tilde{G} \equiv \det(\tilde{G}_{\alpha\beta})$ and $G \equiv \det(G_{ab})$). This corresponds to $\mathcal{J} = -\det(\eta^{\alpha}{}_{\mu})$, or,

$$\frac{1}{4!}\epsilon_{\alpha\beta\gamma\delta}\,\boldsymbol{\eta}^{\alpha}\wedge\boldsymbol{\eta}^{\beta}\wedge\boldsymbol{\eta}^{\gamma}\wedge\boldsymbol{\eta}^{\delta} = -\frac{1}{4!}\mathcal{J}\epsilon_{\mu\nu\rho\sigma}\,\mathrm{d}X^{\mu}\wedge\mathrm{d}X^{\nu}\wedge\mathrm{d}X^{\rho}\wedge\mathrm{d}X^{\sigma}\ . \tag{3.24}$$

From Eq. (3.23), in terms of the spatial components of the coframes, $\mathcal{J}$ becomes

$$\mathcal{J} = \frac{1}{3!}N\epsilon_{abc}\epsilon^{ijk}\eta^{a}{}_{i}\eta^{b}{}_{j}\eta^{c}{}_{k} = N\det(\eta^{a}{}_{i})\ , \tag{3.25}$$

while correspondingly, the dual vector basis can be described by the four frames $\boldsymbol{e}_{\alpha} = e_{\alpha}{}^{\mu}\,\partial/\partial X^{\mu}$:

$$\begin{gathered} e_{\alpha}{}^{\mu}\,\eta^{\alpha}{}_{\nu} = \delta^{\mu}{}_{\nu}\ \ ;\ \ e_{\alpha}{}^{\mu}\,\eta^{\beta}{}_{\mu} = \delta_{\alpha}{}^{\beta}\ ; \\ e_{\alpha}{}^{\mu} = -\frac{1}{6\mathcal{J}}\,\epsilon_{\alpha\beta\gamma\delta}\,\epsilon^{\mu\nu\varrho\sigma}\eta^{\beta}{}_{\nu}\eta^{\gamma}{}_{\varrho}\eta^{\delta}{}_{\sigma}\ ; \\ e_{a}{}^{i} = \frac{1}{2\mathcal{J}}N\epsilon_{abc}\epsilon^{ijk}\eta^{b}{}_{j}\eta^{c}{}_{k}\ ; \\ e_{0}{}^{\mu} = \frac{1}{N}(-1,0,0,0)\ ,\ e_{a}{}^{\mu} = (0,e_{a}{}^{i})\ . \end{gathered} \tag{3.26}$$

With this choice, the evolution equations for $\mathcal{J}$ and the expansion tensor coefficients $\Theta^{i}{}_{j}$ read:

$$\begin{aligned} \partial_t\mathcal{J} &= \frac{\partial_t N}{N}\mathcal{J} + \mathcal{J}N\Theta\ ; \\ \Theta^{i}{}_{j} &= \frac{1}{2\mathcal{J}}\epsilon_{abc}\epsilon^{ikl}\partial_t\eta^{a}{}_{j}\eta^{b}{}_{k}\eta^{c}{}_{l}\ ; \\ \frac{\partial_t\Theta^{i}{}_{j}}{N} &= -\Theta\Theta^{i}{}_{j} + \frac{1}{2\mathcal{J}}\epsilon_{abc}\epsilon^{ikl}\partial_t\Big(\frac{1}{N}\partial_t\eta^{a}{}_{j}\Big)\eta^{b}{}_{k}\eta^{c}{}_{l} + \frac{1}{N\mathcal{J}}\epsilon_{abc}\epsilon^{ikl}\partial_t\eta^{a}{}_{j}\partial_t\eta^{b}{}_{k}\eta^{c}{}_{l}\ . \end{aligned} \tag{3.27}$$

From the constraint and evolution equations (3.6)–(3.8), together with the definition of $\mathcal{J}$ and Eqs. (3.27), the Lagrange–Einstein system of an irrotational perfect fluid model is cast into the following form:

$$G_{ab}\,\partial_t\eta^{a}{}_{[i}\eta^{b}{}_{j]} = 0\ ; \tag{3.28}$$

$$\frac{1}{2\mathcal{J}}\epsilon_{abc}\epsilon^{ikl}\,\partial_t\left(\frac{1}{N}\partial_t\eta^{a}{}_{j}\eta^{b}{}_{k}\eta^{c}{}_{l}\right) = \mathcal{A}^{i}{}_{j} - \mathcal{R}^{i}{}_{j} + [4\pi G(\epsilon - p) + \Lambda]\,\delta^{i}{}_{j}\ ; \tag{3.29}$$

$$\epsilon_{abc}\epsilon^{ijk}\partial_t\eta^{a}{}_{i}\partial_t\eta^{b}{}_{j}\eta^{c}{}_{k} = (16\pi G\epsilon\ +\ 2\,\Lambda - \mathcal{R})N\mathcal{J}\ ; \tag{3.30}$$

$$\left(\frac{1}{\mathcal{J}}\epsilon_{abc}\epsilon^{ikl}\partial_t\eta^a{}_j\eta^b{}_k\eta^c{}_l\right)_{\|i} = \left(\frac{1}{\mathcal{J}}\epsilon_{abc}\epsilon^{ikl}\partial_t\eta^a{}_i\eta^b{}_k\eta^c{}_l\right)_{|j} ; \tag{3.31}$$

$$p = \beta(\epsilon) \, . \tag{3.32}$$

The equations (3.28)–(3.31) are not closed unless an EoS, here (3.32), is specified. Recall that the lapse appearing above can be replaced by its expression in terms of ϵ, $N = (\epsilon + \beta(\epsilon))^{-1} F(\epsilon)$. The expansion tensor evolution equation (3.29) may be split into a trace part, which we then combine with the energy constraint (3.30) to obtain the Raychaudhuri equation, and a trace–free part, yielding respectively:

$$\frac{1}{2\mathcal{J}}\epsilon_{abc}\epsilon^{ikl}\partial_t\left(\frac{1}{N}\partial_t\eta^a{}_i\right)\eta^b{}_k\eta^c{}_l = \mathcal{A} - 4\pi G(\epsilon + 3p) \, + \, \Lambda \, ; \tag{3.33}$$

$$\frac{1}{2\mathcal{J}}\left[\epsilon_{abc}\epsilon^{ikl}\partial_t\left(\frac{1}{N}\partial_t\eta^a{}_j\eta^b{}_k\eta^c{}_l\right) - \frac{1}{3}\epsilon_{abc}\epsilon^{mkl}\partial_t\left(\frac{1}{N}\partial_t\eta^a{}_m\eta^b{}_k\eta^c{}_l\right)\delta^i{}_j\right] = \xi^i{}_j - \tau^i{}_j \, , \tag{3.34}$$

where $\tau^i{}_j = \mathcal{R}^i{}_j - \frac{1}{3}\mathcal{R}\delta^i{}_j$ are the coefficients of the trace–free part of the spatial Ricci tensor, and $\xi^i{}_j = \mathcal{A}^i{}_j - \frac{1}{3}\mathcal{A}\,\delta^i{}_j$.

The Lagrange–Einstein system, Eqs. (3.28)–(3.32), is closed and provides the components $\eta^a{}_i$ of coframes, from which one can calculate the evolution of the perturbations. The system comprises 14 equations, where 9 equations describe the evolution for the coefficient functions of 3 spatial Cartan coframe fields, and the remaining 5 equations originate from the 4 constraints and the EoS defining the properties of the fluid.

3.2.2 Perturbation ansatz

3.2.2.1 Spacetime background

We will choose a spatially flat, homogeneous and isotropic model universe as the background spacetime, with the same perfect fluid EoS, and including a possible constant curvature term into the first–order perturbations, (*cf.,* e.g., [Alles et al., 2015]). Accordingly, the spatial metric coefficients of the background will be $a^2(t)\delta_{ij}$, $a(t)$ being the background scale factor. We prescribe a homogeneous lapse $N_H(t)$ for this homogeneous and isotropic background, by setting its relation to the background energy density ϵ_H, formal rest mass density $\varrho_H \equiv F(\epsilon_H)$

and pressure $p_H = \beta(\epsilon_H)$ as being the same relations as those for the inhomogeneous quantities,

$$N_H = \frac{\varrho_H}{\epsilon_H + p_H} = \frac{F(\epsilon_H)}{\epsilon_H + \beta(\epsilon_H)} \,. \tag{3.35}$$

We may then write the background line element as

$$\mathrm{d}s_H^2 = -N_H^2(t)\mathrm{d}t^2 + a^2(t)\,\delta_{ij}\mathrm{d}X^i\mathrm{d}X^j \,. \tag{3.36}$$

Note that the evolution of the background lapse function $N_H(t)$ will be given by its definition (3.35) and the EoS, making it time–dependent for $p_H \neq 0$.[5] One should keep in mind that our choice of time coordinate t will consequently not coincide in general with the usual 'cosmic time' coordinate for the background, and will evolve at a different rate.The usual cosmic time $\tilde{t}$ would rather be defined by $\mathrm{d}\tilde{t} = N_H(t)\mathrm{d}t$, so that the background line element (3.36) would take the usual Friedmannian form for homogeneous and isotropic model universes:[6]

$$\mathrm{d}s_H^2 = -\mathrm{d}\tilde{t}^2 + a^2\big[\tilde{t}\big]\,\delta_{ij}\,\mathrm{d}X^i\mathrm{d}X^j \,. \tag{3.37}$$

With this time variable, the standard Friedmann equations (1.2, 1.3) would indeed be recovered:

$$\begin{aligned}
3\,\frac{\partial_{\tilde{t}}^2 a}{a} &= -\,4\pi G(\epsilon_H + 3p_H) \,+\, \Lambda \,; \\
3\left(\frac{\partial_{\tilde{t}} a}{a}\right)^2 &= 8\pi G\epsilon_H \,+\, \Lambda \,; \\
\partial_{\tilde{t}}\epsilon_H + 3\,\frac{\partial_{\tilde{t}} a}{a}(\epsilon_H + p_H) &= 0 \,.
\end{aligned} \tag{3.38}$$

However, for consistency with the lapsed foliation used for the full inhomogeneous spacetime, we will include the homogeneous lapse N_H into the background and use the coordinate t. In terms of this variable, the acceleration and Friedmann

[5] In general, the background lapse function and background pressure would be inhomogeneous and the scale factor would become space–dependent, as seen from the perturbed hypersurface.

[6] The notation $a\big[\tilde{t}\big]$ signifies that the scale factor still takes the same values, $a[\tilde{t}] := a(t)$, but has a different functional dependence on the alternative time coordinate.

equations are respectively:

$$\frac{3}{N_H^2}\frac{\partial_t^2 a}{a} = -4\pi G(\epsilon_H + 3p_H) \,+\, \Lambda + 3\frac{\partial_t a}{a}\frac{\partial_t N_H}{N_H^3} \;;$$
$$\frac{3}{N_H^2}\left(\frac{\partial_t a}{a}\right)^2 = 8\pi G\epsilon_H \,+\, \Lambda \;, \tag{3.39}$$

while the energy–momentum conservation equation is formally unchanged:

$$\partial_t \epsilon_H + 3\,\frac{\partial_t a}{a}(\epsilon_H + p_H) = 0 \;. \tag{3.40}$$

3.2.2.2 Coframes decomposition

It is important to express the full set of equations in terms of a single perturbation variable, the coframes, so that the Lagrangian perturbation approach is well–defined. Although this is not made explicit in the Lagrange–Einstein system (3.28)–(3.32), it is indeed implicitly the case as the Ricci tensor and covariant derivatives are functionals of the metric, hence of the coframes, and ϵ, p, N and $\mathcal{A}^i{}_j$ can be expressed in terms of the coframes and initial energy density data. The latter relations are obtained *via* the conservation equation (3.17) for $\varrho = F(\epsilon)$ and the evolution equation for $J \equiv \mathcal{J}/N = \det(\eta^a{}_i)$ from the first equation in Eq. (3.27):

$$N\Theta = -\frac{\partial_t F(\epsilon)}{F(\epsilon)} = \frac{\partial_t J}{J} \;\;;\;\; \epsilon = F^{-1}\left(\frac{F(\epsilon_{\mathbf{i}})}{J}\right) \;, \tag{3.41}$$

with $J_{\mathbf{i}} = 1$ here as a result of the choice of initial conditions for the coframes. The barotropic EoS and choice of N then allows us to determine p, N and $\mathcal{A}^i{}_j = N^{-1}\,N^{||i}{}_{||j}$, and to express these fields as functions of $J = \det(\eta^a{}_i)$.

We then follow the previous works and decompose the coframes into a FLRW coframe set and deviations thereof,

$$\boldsymbol{\eta}^a = \eta^a{}_i \mathrm{d}X^i = a(t)\,(\delta^a{}_i + P^a{}_i)\,\mathrm{d}X^i \;. \tag{3.42}$$

At this nonperturbative level, the metric coefficients are then related to the

deformation field by

$$g_{ij} = a^2(t)\left(G_{ij} + 2P_{(ij)} + G_{ab}P^a_{\ i}P^b_{\ j}\right) \ , \tag{3.43}$$

where we have defined

$$P^i_{\ j} = \delta_a^{\ i}P^a_{\ j} \ ; \ P \equiv P^k_{\ k} = \delta_a^{\ k}P^a_{\ k} \ ; \ P_{ij} \equiv G_{ai}P^a_{\ j} \ . \tag{3.44}$$

Recall that the Gram matrix coefficients G_{ab} have been defined to encode the initial metric inhomogeneities, so that the coefficients $P^a_{\ i}$ can be set to zero initially. Also recall that this coframe split is made with respect to a FLRW background with a nontrivial lapse included, and that the functional dependence of a, or of the deformation field, on the time coordinate t will be affected accordingly.

We then expand the deformation fields $P^a_{\ i}$ into a perturbative sum, so that the coframes are given by:

$$\boldsymbol{\eta}^a = a(t)\left(\delta^a_{\ i} + \sum_{m=1}^{\infty} P^{a\ (m)}_{\ i}\right)\mathrm{d}X^i, \tag{3.45}$$

where the mth–order deformation field coefficients $P^{a\ (m)}_{\ i}$ are of order ε^m for some book–keeping parameter $\varepsilon \ll 1$. In this work we will only focus on first–order deformations. The higher orders should be investigated in the future.

3.2.2.3 Initial conditions

To apply the relativistic LPT to the realistic problem we have to set the initial conditions. In this chapter we will follow the steps of Refs. [Alles et al., 2015; Al Roumi et al., 2017] to prescribe the initial data. The deformation field and its time–derivatives are given at some initial time $t_{\mathbf{i}}$ by:

$$P^a_{\ i}(t_{\mathbf{i}}) = 0 \ ; \quad (\partial_t P^a_{\ i})(t_{\mathbf{i}}) = U^a_{\ i} \ ; \quad \left(\partial_t^2 P^a_{\ i}\right)(t_{\mathbf{i}}) = W^a_{\ i} - 2H_{\mathbf{i}}U^a_{\ i} \ , \tag{3.46}$$

where $H \equiv \partial_t a/a$ is the Hubble function. Hereafter, we will normalize the scale factor as $a_{\mathbf{i}} = 1$, where $A_{\mathbf{i}}$ denotes the quantity A evaluated at initial time $t_{\mathbf{i}}$. The six 1−form fields $\boldsymbol{U}^a = U^a_{\ i}\mathrm{d}X^i$ and $\boldsymbol{W}^a = W^a_{\ i}\mathrm{d}X^i$ are 1−form generalizations of the initial Newtonian peculiar–velocity and peculiar–acceleration gradient fields,

respectively.

The Lagrange–Einstein system with its split into trace and traceless parts according to Eqs. (3.28)–(3.34) then translates into constraints on the initial data:

$$U_{[ij]} = 0 \quad ; \quad W_{[ij]} = 0 \; ; \tag{3.47}$$

$$W - U\left(\frac{\partial_t N}{N}\right)_{\mathbf{i}} = 3H_{\mathbf{i}}\left[\left(\frac{\partial_t N}{N}\right)_{\mathbf{i}} - \left(\frac{\partial_t N_H}{N_H}\right)_{\mathbf{i}}\right] + \Lambda\left({N_{\mathbf{i}}}^2 - N_{H\mathbf{i}}^2\right) + {N_{\mathbf{i}}}^2\,\mathcal{A}_{\mathbf{i}} - 4\pi G\left[(\epsilon_{\mathbf{i}} + 3p_{\mathbf{i}}){N_{\mathbf{i}}}^2 - (\epsilon_{H\mathbf{i}} + 3\,p_{H\mathbf{i}})N_{H\mathbf{i}}^2\right] \; ; \tag{3.48}$$

$${}^{\mathrm{tl}}W^a{}_j\,\delta_a{}^i + \left(H_{\mathbf{i}} - \left(\frac{\partial_t N}{N}\right)_{\mathbf{i}}\right){}^{\mathrm{tl}}U^a{}_j\,\delta_a{}^i + U\,{}^{\mathrm{tl}}U^a{}_j\,\delta_a{}^i - \left(U^a{}_k\,\delta_a{}^i U^b{}_j\,\delta_b{}^k - \frac{1}{3}U^a{}_l\,\delta_a{}^k U^b{}_k\,\delta_b{}^l\delta^i{}_j\right) = N_{\mathbf{i}}^2\left(\xi^i{}_j(t_{\mathbf{i}}) - \tau^i{}_j(t_{\mathbf{i}})\right) \; ; \tag{3.49}$$

$$U^2 - U^a{}_i\,\delta_a{}^j U^b{}_j\,\delta_b{}^i + 4H_{\mathbf{i}}U = 16\pi G\left(\epsilon_{\mathbf{i}}{N_{\mathbf{i}}}^2 - \epsilon_{H\mathbf{i}}N_{H\mathbf{i}}^2\right) + 2\Lambda\left({N_{\mathbf{i}}}^2 - N_{H\mathbf{i}}^2\right) - \mathcal{R}_{\mathbf{i}}{N_{\mathbf{i}}}^2 \; ; \tag{3.50}$$

$$\left({N_{\mathbf{i}}}^{-1}U^a{}_j\,\delta_a{}^i\right)_{\|i} = \left({N_{\mathbf{i}}}^{-1}U\right)_{|j} + 2H_{\mathbf{i}}\left({N_{\mathbf{i}}}^{-1}\right)_{|j} \; ; \tag{3.51}$$

$$p_{\mathbf{i}} = \beta(\epsilon_{\mathbf{i}}) \quad ; \quad p_{H\mathbf{i}} = \beta(\epsilon_{H\mathbf{i}}) \; . \tag{3.52}$$

The abbreviations $U \equiv U^a{}_k\,\delta_a{}^k$, $W \equiv W^a{}_k\,\delta_a{}^k$, and ${}^{\mathrm{tl}}W^a{}_i \equiv W^a{}_i - (1/3)W\delta^a{}_i$, ${}^{\mathrm{tl}}U^a{}_i \equiv U^a{}_i - (1/3)U\delta^a{}_i$, are used for the trace and traceless parts, respectively.

3.2.3 First–order Lagrange–Einstein system

We now expand the above Lagrange–Einstein system and its initial conditions to first order[7] in the only dynamical variable in this Lagrangian perturbation approach, namely the deformation field $P^a{}_i$. In what follows we omit the index $^{(1)}$ for the first–order deformation field and the associated initial conditions U_{ij}, W_{ij}, but keep the index for the other variables, as functionals of $P^a{}_i$. We first need to express these functionals explicitly at first order.

[7] Note that initial data can be assumed, without loss of generality, to be first order.

3.2.3.1 Dependent variables at first order

Beginning with the first–order Ricci tensor and scalar curvature, we expand the initial metric coefficients to first order as $G_{ij}(\boldsymbol{X}) = \delta_{ij} + G^{(1)}_{ij}(\boldsymbol{X})$ since they reduce to δ_{ij} at the unperturbed zero–order level. Introducing the first–order quantities $G^{(1)ij} \equiv \delta^i{}_k \delta^j{}_l G^{(1)}_{kl}$, $P^{ij} \equiv \delta^i{}_k \delta^j{}_l P_{kl}$ for the inverse metric, we can then substitute the metric and its inverse, truncated to first order,

$$g_{ij} = a^2 \left(\delta_{ij} + G^{(1)}_{ij} + 2P_{(ij)} \right) \; ; \tag{3.53}$$

$$g^{ij} = a^{-2} \left(\delta^{ij} - G^{(1)ij} - 2P^{(ij)} \right) \; , \tag{3.54}$$

into the definitions of the spatial Christoffel symbols and of the spatial Ricci tensor. We thereby obtain:

$$\Gamma^{k}_{ij}{}^{(1)} = \frac{1}{2}\delta^{kl} \left(G^{(1)}_{il|j} + G^{(1)}_{lj|i} - G^{(1)}_{ij|l} \right) + \delta^{kl} \left(P_{(il)|j} + P_{(lj)|i} - P_{(ij)|l} \right) ; \tag{3.55}$$

$$\mathcal{R}^{(1)}_{ij} = \mathscr{R}_{ij} + P^{k}_{\ [j|k]|i} + P_{[j\ |k]|i}^{\ k} + P_{(ik)|j}^{\ \ \ |k} - P_{(ij)}^{\ \ \ |k}{}_{|k} ; \tag{3.56}$$

$$\mathcal{R}^{(1)} = a^{-2}\mathscr{R} + 2a^{-2} \left(P^{ki}_{\ \ \ |i|k} - P^{|k}_{\ \ \ |k} \right) , \tag{3.57}$$

where $\mathscr{R}_{ij} \equiv G^{(1)|k}_{i[k|j]} + G^{k(1)}_{\ \ [j|k]|i}$, and $\mathscr{R} \equiv \delta^{ij}\mathscr{R}_{ij} = 2\, G^{l}_{\ [k|l]}{}^{|k(1)}$ are the initial conditions for the curvature tensor coefficients and their trace, respectively.

An important difference from the dust case is that here the spatial Ricci scalar will in general not be constrained to evolve as $\mathscr{R}(\boldsymbol{X})\, a(t)^{-2}$ at first order, due to the contributions from the lapse in the momentum constraints. Indeed, as we will see below, these contributions give rise to a nonzero evolution for the (initially vanishing) second term $(P^{ki}_{\ \ \ |i|k} - P^{|k}_{\ \ \ |k})$, or equivalently a nonconserved scalar curvature, $\partial_t \mathcal{R}^{(1)} + 2H\mathcal{R}^{(1)} = a^{-2}\partial_t(a^2\mathcal{R}^{(1)}) \neq 0$, in contrast to the dust case.

Using the barotropic EoS and the corresponding solution (3.41) to the energy conservation equation (3.13), we can also expand ϵ, p, N and $\mathcal{A}^i{}_j$ in terms of the first–order deformation field. We write $\epsilon_{\mathbf{i}} \equiv \epsilon_{H\mathbf{i}}(1+\delta\epsilon_{\mathbf{i}})$ at first order, and expand $J^{-1} = a^{-3}\det(\delta^a{}_i + P^a{}_i)$ at the same order as $a^{-3}(1-P)$. The solution (3.41) for ϵ as a function of J can then be expanded to first order in the perturbation

as

$$\begin{aligned}\epsilon &= F^{-1}\left(\frac{F(\epsilon_{H\mathbf{i}}) + F'(\epsilon_{H\mathbf{i}})\,\epsilon_{H\mathbf{i}}\,\delta\epsilon_{\mathbf{i}} - F(\epsilon_{H\mathbf{i}})\,P}{a^3}\right) \\ &= F^{-1}\left(\frac{F(\epsilon_{H\mathbf{i}})}{a^3}\right) + \left[\frac{1}{a^3}\epsilon_{H\mathbf{i}}\,F'(\epsilon_{H\mathbf{i}})\delta\epsilon_{\mathbf{i}} - P\frac{F(\epsilon_{H\mathbf{i}})}{a^3}\right]\left(F^{-1}\right)'\left(\frac{F(\epsilon_{H\mathbf{i}})}{a^3}\right) . \quad (3.58)\end{aligned}$$

The background energy–momentum conservation equation (3.41) still holds for background quantities, giving

$$F(\epsilon_H) = \frac{F(\epsilon_{H\mathbf{i}})}{a^3} . \quad (3.59)$$

This can be substituted into Eq. (3.58) to give

$$\epsilon = \epsilon_H\left[1 + \frac{F(\epsilon_H)}{\epsilon_H\,F'(\epsilon_H)}\left(\frac{\epsilon_{H\mathbf{i}}\,F'(\epsilon_{H\mathbf{i}})}{F(\epsilon_{H\mathbf{i}})}\,\delta\epsilon_{\mathbf{i}} - P\right)\right] . \quad (3.60)$$

The further use of the definition of F, Eq. (3.15), allows us to simplify the above to

$$\epsilon = \epsilon_H\left[1 - \left(1 + \frac{p_H}{\epsilon_H}\right)\bar{P}\right] , \quad (3.61)$$

which we have written for convenience in terms of a shifted deformation trace,

$$\bar{P} = P\ -\ \alpha_{H\mathbf{i}}\,\delta\epsilon_{\mathbf{i}} , \quad (3.62)$$

where $\alpha_{H\mathbf{i}} = (\epsilon_{H\mathbf{i}} + \beta(\epsilon_{H\mathbf{i}}))^{-1}\,\epsilon_{H\mathbf{i}}$ is a constant, and $\delta\epsilon_{\mathbf{i}}$ is the initial energy perturbation distribution in space.

The pressure can in turn be expanded to first order as $p = \beta(\epsilon)$, yielding

$$p = p_H - \beta'(\epsilon_H)\left(\epsilon_H + p_H\right)\bar{P} . \quad (3.63)$$

Note that the factor $\beta'(\epsilon_H)$ corresponds to the (generally time–dependent) dimensionless ratio of the background speed of sound to speed of light squared, $\beta'(\epsilon_H) = c_S^2(t)/c^2$, if p_H is the thermodynamic equilibrium pressure for the background fluid. We then expand the lapse $N = (\epsilon + p)^{-1}F(\epsilon)$ as

$$N = N_H\left[1 + \beta'(\epsilon_H)\,\bar{P}\right] \quad (3.64)$$

at first order in the deformation field. At this order, one will then have (with $\partial_t P = \partial_t \bar{P}$):

$$\frac{\partial_t N}{N} = \frac{\partial_t N_H}{N_H} + \beta'(\epsilon_H)\,\partial_t \bar{P} - 3H\left(\epsilon_H + \beta(\epsilon_H)\right)\beta''(\epsilon_H)\,\bar{P}\ , \tag{3.65}$$

with

$$\frac{\partial_t N_H}{N_H} = 3H\beta'(\epsilon_H)\ . \tag{3.66}$$

Furthermore, we can calculate the first–order expression for $\mathcal{A}^i{}_j = N^{-1}N^{||i}{}_{||j}$, resulting in

$$\mathcal{A}^{i\ (1)}_{\ j} = a^{-2}\beta'(\epsilon_H)\,\delta^{ik}\bar{P}_{|j|k}\ . \tag{3.67}$$

3.2.3.2 First–order system

The Lagrange–Einstein system (3.28)–(3.31) can then be rewritten at first order in the deformation field as follows:

$$\partial_t P_{[ij]} = 0\ ; \tag{3.68}$$

$$\begin{aligned}\partial_t^2 P^i{}_j + 3H\left[1-\beta'(\epsilon_H)\right]\partial_t P^i{}_j + H\left[1-\beta'(\epsilon_H)-\mathcal{V}(t)\right]\partial_t P\,\delta^i{}_j \\ = N_H^2\mathcal{A}^{i\ (1)}_{\ j} - N_H^2\left(\mathcal{R}^{i\ (1)}_{\ j} - \frac{\mathcal{V}(t)}{4}\mathcal{R}^{(1)}\,\delta^i{}_j\right)\ ;\end{aligned} \tag{3.69}$$

$$\partial_t\left(P^i{}_{j|i} - P_{|j}\right) = -2H\beta'(\epsilon_H)\,\bar{P}_{|j}\ , \tag{3.70}$$

$$H\,\partial_t\bar{P} + 4\pi G\left[\epsilon_H + p_H - (2\epsilon_H + \tilde{\Lambda})\,\beta'(\epsilon_H)\right]N_H^2\bar{P} = -\frac{1}{4}N_H^2\mathcal{R}^{(1)}\ , \tag{3.71}$$

where $\mathcal{A}^{i\ (1)}_{\ j}$, $\mathcal{R}^{i\ (1)}_{\ j} = a^{-2}\delta^{ik}\mathcal{R}^{(1)}_{kj}$ and $\mathcal{R}^{(1)}$ are expressed as functions of $P^a_{\ i}$ according to the formulas given above, $\tilde{\Lambda} \equiv \Lambda/(4\pi G)$, and we used the abbreviation

$$\begin{aligned}\mathcal{V}(t) = &\left[\epsilon_H + p_H - \left(2\epsilon_H + \tilde{\Lambda}\right)\beta'(\epsilon_H)\right]^{-1} \\ &\times\ \left\{\epsilon_H + p_H - \left(3\epsilon_H - p_H + 2\tilde{\Lambda}\right)\beta'(\epsilon_H) + \left(2\epsilon_H + \tilde{\Lambda}\right)\left(\epsilon_H + p_H\right)\beta''(\epsilon_H)\right\}\ .\end{aligned} \tag{3.72}$$

Eq. (3.69) has been obtained from the first–order expansion of the extrinsic curvature evolution equation (3.29) by combining it with the first–order energy constraint (3.71). The EoS (3.32) has already been used to expand ϵ, p and N in terms of the first–order deformation field.

3.2.4 First–order master equations

Following the approach of Ref. [Al Roumi et al., 2017] the above system can be re-expressed by decomposing the deformation fields into trace, trace-free symmetric and antisymmetric parts:

$$P^i_{\ j} = \frac{1}{3} P \delta^i_{\ j} + \Pi^i_{\ j} + \mathfrak{P}^i_{\ j} \,, \tag{3.73}$$

where $\Pi_{ij} = P_{(ij)} - \frac{1}{3} P \delta_{ij}$ and $\mathfrak{P}_{ij} = P_{[ij]}$. We will now derive the governing equations for these parts, named *master equations*. For the trace part we use the new variable (3.62).

Accordingly, (3.68)–(3.69) become:

$$\partial_t \mathfrak{P}_{ij} = 0 \ : \quad \mathfrak{P}_{ij} = \mathfrak{P}_{ij}(t_{\mathbf{i}}) = 0 \,; \tag{3.74}$$

$$\partial_t^2 \bar{P} + 3H \left[2 - 2\beta'(\epsilon_H) - \mathcal{V}(t) \right] \partial_t \bar{P} = N_H^2 \mathcal{A}^{(1)} - N_H^2 \left(1 - \frac{3}{4} \mathcal{V}(t) \right) \mathcal{R}^{(1)} \,; \tag{3.75}$$

$$\partial_t^2 \Pi^i_{\ j} + 3H[1 - \beta'(\epsilon_H)] \partial_t \Pi^i_{\ j} = N_H^2 \left(\xi^{i\ (1)}_{\ j} - \tau^{i\ (1)}_{\ j} \right) \,; \tag{3.76}$$

$$\partial_t \left(\Pi^i_{\ j|i} - \frac{2}{3} \bar{P}_{|j} \right) = -2H\beta' \left(\epsilon_H \right) \bar{P}_{|j} \,, \tag{3.77}$$

where we have also used $\partial_t P = \partial_t \bar{P}$.

Once again the first–order quantities $\mathcal{A}^{(1)}$, $\xi^{i\ (1)}_{\ j}$, $\mathcal{R}^{(1)}$ and $\tau^{i\ (1)}_{\ j}$ are used as shorthand notations but are meant to be expressed in terms of the deformation field. These expressions are obtained from the results above, Eqs. (3.56), (3.57), (3.67), as follows:[8]

$$a^2 \mathcal{A}^{(1)} = \beta'(\epsilon_H) \, \Delta_0 \bar{P} \,; \tag{3.78}$$

$$a^2 \xi^{i\ (1)}_{\ j} = \beta'(\epsilon_H) \left(\bar{P}^{|i}_{\ \ |j} - \frac{\delta^i_{\ j}}{3} \Delta_0 \bar{P} \right); \tag{3.79}$$

[8] The expression given for $\tau^{i\ (1)}_{\ j}$ makes use of the momentum constraints (3.77), which imply, through their spatial derivative, $\partial_t \Pi_{k[i|j]}^{\ \ \ \ \ \ |k} = 0$, and thus $\Pi_{k[i|j]}^{\ \ \ \ \ \ |k} = \Pi_{k[i|j]}^{\ \ \ \ \ \ |k}(t_{\mathbf{i}}) = 0$. Also note that since P and $\bar{P}$ differ by an initial spatial function, we can express (3.78)–(3.81) in terms of either variable. Here we have adopted the most compact possibility, noting that the initial value of $\bar{P}$ is nonzero, whereas (3.80) and (3.81) involve the initial curvature which is independent of the initial perturbation field.

$$a^2\mathcal{R}^{(1)} = \mathscr{R} + 2\left(\Pi^{ki}{}_{|k|i} - \frac{2}{3}P^{|k}{}_{|k}\right) \; ; \tag{3.80}$$

$$a^2\tau^{i\ (1)}_{\ j} = \mathscr{T}^i_{\ j} + 2\,\Pi^i{}_{k|j}^{\ \ |k} - \Pi^i{}_{j}^{\ |k}{}_{|k} - \frac{1}{3}\left(2\,\Pi^k{}_{l|k}^{\ \ |l}\,\delta^i{}_j + P^{|i}{}_{|j} - \frac{1}{3}\Delta_0 P\,\delta^i{}_j\right) \; , \tag{3.81}$$

with $\mathscr{T}^i_{\ j} \equiv \mathscr{R}^i{}_j - \frac{1}{3}\mathscr{R}\delta^i{}_j = \tau^{i\ (1)}_{\ j}(t_{\mathbf{i}})$, and with Δ_0 the coordinate Laplacian operator in the Lagrangian coordinates $\{X^i\}$, $\Delta_0 \equiv \delta^{ij}\partial_i\partial_j$.

3.2.4.1 Master equation for the trace

Contracting the momentum constraints (3.77) with a spatial derivative $_{|j}$ yields the first–order evolution equation for the nontrivial part of the scalar curvature:

$$\begin{aligned}\partial_t\left(P^{ki}{}_{|k|i} - P^{|k}{}_{|k}\right) &= \partial_t\left(\Pi^{ki}{}_{|k|i} - \frac{2}{3}\bar{P}^{|k}{}_{|k}\right) \\ &= -2H\beta'(\epsilon_H)\,\Delta_0\bar{P} \; .\end{aligned} \tag{3.82}$$

From the respective expressions (3.57), (3.78) for $\mathcal{R}^{(1)}$ and $\mathcal{A}^{(1)}$, this amounts to the following evolution for $\mathcal{R}^{(1)}$:

$$\partial_t\mathcal{R}^{(1)} + 2H\mathcal{R}^{(1)} = -4Ha^{-2}\beta'(\epsilon_H)\Delta_0\bar{P} = -4H\mathcal{A}^{(1)} \; , \tag{3.83}$$

which unlike the case of dust does remain coupled to the dynamics of the inhomogeneous perturbation.

Combining this evolution equation with the linearized energy constraint (3.71) and its time–derivative one then obtains the *master equation for the evolution of the trace* (3.62) of the first–order deformation field:[9]

$$\partial_t^2\bar{P} + 2H(1 - 3\beta'(\epsilon_H))\,\partial_t\bar{P} - \mathcal{W}(t)N_H^2\bar{P} = a^{-2}N_H^2\,\beta'\,(\epsilon_H)\,\Delta_0\bar{P}, \tag{3.84}$$

[9] This equation can also be derived by combining the energy constraint (3.71) with the trace (3.75) of the evolution equation to eliminate $\mathcal{R}^{(1)}$, or equivalently by directly expanding the Raychaudhuri equation (3.33) to first–order. In both cases, the master equation for the trace would then be recovered after replacing the first–order acceleration divergence $\mathcal{A}^{(1)}$ by its explicit expansion (3.78).

where $p_H = \beta(\epsilon_H)$ and $N_H = F(\epsilon_H)/(\epsilon_H + p_H)$ still, and

$$\begin{aligned}\mathcal{W}(t) &= 4\pi G\big[\epsilon_H + p_H - (2\epsilon_H + \tilde{\Lambda})\beta'(\epsilon_H)\big]\big[4 - 3\mathcal{V}(t)\big] \\ &= 4\pi G\left[\epsilon_H + p_H + \big(\epsilon_H - 3p_H + 2\tilde{\Lambda}\big)\beta'(\epsilon_H)\right] \\ &\quad - 12\pi G\left(2\epsilon_H + \tilde{\Lambda}\right)\big(\epsilon_H + p_H\big)\beta''(\epsilon_H)\,. \end{aligned} \tag{3.85}$$

To avoid potential confusion, since the time coordinate t used in this paper has a different rate as compared to the conventional cosmic time, it will sometimes be convenient for further applications to use the (time–coordinate–independent) background scale factor a as the time variable instead. With this change of parametrization, the energy constraint (3.71) and the master equation for the trace (3.84) may be rewritten as follows:

$$a\frac{\partial \bar{P}}{\partial a} + \alpha_0 \bar{P} = -\frac{N_H^2}{4\,H^2}\mathcal{R}^{(1)}\,; \tag{3.86}$$

$$\frac{\partial^2 \bar{P}}{\partial a^2} + \frac{\alpha_1}{a}\frac{\partial \bar{P}}{\partial a} - \frac{\alpha_2}{a^2}\bar{P} = \frac{\alpha_3}{a^4}\Delta_0 \bar{P}, \tag{3.87}$$

respectively, with time–dependent coefficients,

$$\begin{aligned}\alpha_0 &= 4\pi G\frac{N_H^2}{H^2}\left[\epsilon_H + p_H - \left(2\epsilon_H + \tilde{\Lambda}\right)\,\beta'\left(\epsilon_H\right)\right]\,; \\ \alpha_1 &= \alpha_0 + 4\pi G\frac{N_H^2}{H^2}\left[\tilde{\Lambda} - 2p_H\right]\,; \\ \alpha_2 &= N_H^2\mathcal{W}(t)/H^2 \quad ; \quad \alpha_3 := N_H^2\beta'\left(\epsilon_H\right)/H^2\,, \end{aligned} \tag{3.88}$$

where we remind that from the background Friedmann equation we have $H^2/N_H^2 = 4\pi G\left(2\epsilon_H + \tilde{\Lambda}\right)/3$.

From Eq. (3.87) we can introduce a time–dependent background Jeans wavenumber $k_J(\epsilon_H)$ by[10]

$$k_J(\epsilon_H) \equiv \frac{1}{c}\sqrt{\frac{\alpha_2}{\alpha_3}} = \frac{1}{c}\sqrt{\frac{\mathcal{W}(t)}{\beta'(\epsilon_H)}}\,, \tag{3.89}$$

provided that the term in the square root is positive. Pressure should be positive for sound waves to resist gravitational collapse, and the existence of the Jeans

[10] We include the factor c explicitly so that the dimensional content of this relation is clear. The right hand side of (3.85) must be divided by c^2 if units $c \neq 1$ are restored.

length is intimately related to the energy conditions satisfied by the matter field.

A remark is in order here. In general, one would expect the evolution of the inhomogeneous deformation to be affected by the local, inhomogeneous speed of sound and density, so that a nonperturbative Lagrangian realization would rather feature a local Jeans wavenumber $k_J(\epsilon)$ [Buchert, 2006]. The dynamics in presence of an important density contrast will thus not be fully captured by the above first–order equation, where ϵ has been expanded in $P^a_{\ i}$ and, accordingly, only zero–order background factors such as $k_J(\epsilon_H)$ survive in front of the first–order $\bar{P}$.

As in the dust case, the advantages of the Lagrangian approach are only fully realized *via* extrapolation, e.g., by computing the energy density as a full nonlinear functional from the first–order deformation. As in the dust case and in contrast to standard Eulerian linear perturbation schemes, applying this procedure to compute the energy density out of the solution to first–order equations such as (3.84), will already capture part of the nonlinear features. This is due to the nonlinear extrapolation and to the use of Lagrangian spatial coordinates which follow the fluid propagation in an exact manner. Further nonlinear effects of inhomogeneous pressure will, however, still be missed due to the absence of local Jeans length contributions in the equation used for $\bar{P}$, compared to what should appear in the nonperturbative evolution equation.

We shall not go beyond this procedure in the present work. Let us nonetheless suggest here a possible direction for improvement. It would require properly defining the local Jeans length in the relativistic context as a functional of the deformation. This quantity would then be substituted for the background Jeans length in the trace master equation. The corresponding nonlinear master equation could then be solved in an iterative manner, by computing at each step the local Jeans length *via* functional extrapolation out of the previous estimate for the deformation field. Note that each step would also involve a search for the traceless part of the deformation, as all of its components would be required for the extrapolation.

The evolution equation (3.84) may be rewritten in an alternative form *via* a time–dependent rescaling of the variable $\bar{P} \mapsto \bar{P}/N_H(t)$. Using the variation

rate (3.66) of the background lapse one finds the more transparent form:

$$\partial_t^2\left(\frac{\bar{P}}{N_H}\right)+2H\partial_t\left(\frac{\bar{P}}{N_H}\right)-4\pi G(\epsilon_H+p_H)N_H^2\left(\frac{\bar{P}}{N_H}\right)=a^{-2}N_H^2\,\beta'(\epsilon_H)\,\Delta_0\left(\frac{\bar{P}}{N_H}\right)\,. \tag{3.90}$$

• **Dust limit:** Both t–variable forms of the trace master equation, Eqs. (3.84) and (3.90), reduce to the dust deformation trace evolution equation of previous series papers in the limit where $p_H=\beta(\epsilon_H)=0$, see also the first-order $\mathbf{P}$ of Eq. (2.41). Indeed, in this case we find $\mathcal{W}(t)=4\pi G\epsilon_H=4\pi G\varrho_H=4\pi G\varrho_{H\mathbf{i}}a^{-3}$ and $N_H(t)=(\epsilon_H+p_H)^{-1}\varrho_H=1$, and consequently the trace master equation becomes:

$$\partial_t^2 P+2H\partial_t P-4\pi G\varrho_{H\mathbf{i}}a^{-3}P=-4\pi G\varrho_{H\mathbf{i}}a^{-3}\delta\epsilon_{\mathbf{i}}\,. \tag{3.91}$$

With $N_H=1$ the time variable used is indeed the standard FLRW time coordinate $\tilde{t}=t$, so that the above time–derivatives coincide with those used in previous papers like Ref. [Al Roumi et al., 2017] (denoted there by overdots). Finally, as evaluating Eq. (3.91) at the initial time gives $W=-4\pi G\varrho_{H\mathbf{i}}\delta\epsilon_{\mathbf{i}}$, its right hand side can always be rewritten as Wa^{-3}, and the dust–case master equation for the trace (Eq. (41) of [Al Roumi et al., 2017]) is thus recovered.

• **Newtonian limit:** The Newtonian limit is obtained by the joint application of the *Minkowski Restriction* (MR) for the deformation field, as introduced for dust in [Buchert and Ostermann, 2012], and of the $c\to\infty$ limit together with the assumption of a nonrelativistic pressure.

The latter two assumptions imply that the pressure is no longer a source of the gravitational field, as the energy density is then $\epsilon\simeq\varrho c^2\gg p$ (where the constant c has been temporarily restored), so that all source terms reduce to the contribution of ϱ. Note that ϱ can indeed be considered as equal to the actual rest mass density in this limit. A further consequence of this is that the lapse becomes trivial, $N=\varrho c^2/(\epsilon+p)\simeq 1$, consistent with its spatial variation rate, $N^{-1}N_{|i}=-(\epsilon+p)^{-1}\,p_{|i}\simeq-(\varrho c^2)^{-1}\,p_{|i}\to 0$ when $c\to\infty$, for any pressure spatial gradient. It is also the case for the (already homogeneous, but generally time–dependent) background lapse that $N_H\simeq 1$. Consequently, the fluid–orthogonal hypersurface time label t now coincides with the fluid's proper time τ (since

$1 \simeq N = \partial_t \tau$) as well as with the standard background cosmic (proper) time $\tilde{t}$. All these notions thus consistently define a time reference that can be used as the Newtonian absolute time. We will denote the corresponding Lagrangian time–derivative operator by an overdot.

With $N = 1$ the line element (3.3) reduces to the one used in [Buchert and Ostermann, 2012] for irrotational dust, and one can thus directly use the corresponding definition of the MR in this context.[11] This restriction amounts to assuming that the initial metric is Euclidean and that the spatial coframes are exact in the three–dimensional hypersurfaces, *i.e.*, that there exist spatial coordinates $x^a = f^a(X^i, t)$ such that $G_{ab} = \delta_{ab}$ and

$$\eta^a{}_i = a(t)\,(\delta^a{}_i + P^a{}_i) = f^a{}_{|i} \ . \tag{3.92}$$

In any $t = const$ hypersurface, the spatial line element then reads $\mathrm{d}s^2 = \delta_{ab}\,\mathrm{d}x^a \mathrm{d}x^b$. The coordinates x^a thus define Cartesian–type Eulerian coordinates in which the metric coefficients are manifestly Euclidean at each time, and they can be used to define a Newtonian spatial reference frame. Through its second equality, Eq. (3.92) also implies that the deformation 1–forms P^a are also exact and accordingly define a deformation vector $\mathbf{P}$, with components P^a,

$$\mathbf{x} = a(t)\big[\mathbf{X} + \mathbf{P}\,(\mathbf{X}, t)\,\big] \quad , \quad P^a{}_i =: P^a{}_{|i} \ . \tag{3.93}$$

With these two assumptions the master equation (3.90) on the trace $P = \delta_a{}^i P^a{}_i$ becomes an equation on the Lagrangian divergence $\boldsymbol{\nabla}_0 \cdot \mathbf{P} = \delta_a{}^i P^a{}_{|i}$ of $\mathbf{P}$:

$$\boldsymbol{\nabla}_0 \cdot \ddot{\mathbf{P}} + 2H\,\boldsymbol{\nabla}_0 \cdot \dot{\mathbf{P}} - 4\pi G \varrho_H \big(\boldsymbol{\nabla}_0 \cdot \mathbf{P} - \delta\varrho_{\mathbf{i}}\big) = a^{-2}\,\frac{\mathrm{d}p_H}{\mathrm{d}\varrho_H}\,\Delta_0\big(\boldsymbol{\nabla}_0 \cdot \mathbf{P} - \delta\varrho_{\mathbf{i}}\big) \ , \tag{3.94}$$

[11] Note that the Minkowski Restriction introduced for the dust case is in principle independent of a possible $c \to \infty$ limit and can still otherwise be applied in a Minkowskian regime, as the name suggests. In the present case, when c is still finite, this procedure would need to be extended to the presence of pressure and consequently of an inhomogeneous lapse. We believe, however, that such an extension to this case would require a modification of the perturbation framework used so far in this paper, through the use of a spacetime foliation better adapted to this purpose, and we will consequently not attempt to provide such a generalization here.

with $\varrho_H = a^{-3}\varrho_{H\mathbf{i}}$ still, and $\varrho_\mathbf{i} = \varrho_{H\mathbf{i}}(1+\delta\varrho_\mathbf{i})$. Note that, although the pressure itself no longer contributes as a source of gravitation, its spatial gradient still produces an acceleration (as obviously expected in a Newtonian framework), which is why it still affects the dynamics of $\boldsymbol{\nabla}_0 \cdot \mathbf{P}$ above through the sound speed squared factor $\mathrm{d}p_H/\mathrm{d}\varrho_H$ in front of its Laplacian.

The above equation (3.94) matches[12] the corresponding equation for the deformation vector obtained in the Newtonian Lagrangian framework, Eq. (24b) in [Buchert and Adler, 1999] or Eq. (45) in [Buchert and Domínguez, 2005] written for the longitudinal part of the deformation vector. By definition, this part obeys the same evolution equation as the Lagrangian divergence of the vector, as can be seen in the unnumbered equations involving that divergence before Eq. (24a) in [Buchert and Adler, 1999] . Note that in this reference, the Laplacian term features a local sound speed squared (related to the local Jeans length) $\mathrm{d}p/\mathrm{d}\varrho$, but it is already noted there that it should actually be replaced by the background value for consistency with the first–order expansion, and it is indeed replaced by the corresponding background expression in [Buchert and Domínguez, 2005].

3.2.4.2 Master equation for the traceless part

The first–order evolution of the traceless symmetric part $\Pi^i{}_j$ is given by Eq. (3.76), with $\xi^{i\ (1)}_{\ j}$ and $\tau^{i\ (1)}_{\ j}$ substituted into (3.79) and (3.81), respectively. Eliminating the initial traceless curvature $\mathscr{T}^i_{\ j}$ by evaluation of the evolution equation, at the time corresponding to the initial condition (3.113), then first yields the following evolution equation for the traceless symmetric part:

$$\partial_t^2\Pi^i{}_j + 3H\big[1-\beta'(\epsilon_H)\big]\partial_t\Pi^i{}_j + \frac{N_H^2}{a^2}\left(2\,\Pi^i{}_{k|j}{}^{|k} - \Pi^i{}_{j|k}{}^{|k} - \frac{2}{3}\,\Pi^k{}_{l|k}{}^{|l}\,\delta^i{}_j\right)$$
$$= \frac{N_H^2}{3a^2}\Big(\big[1+3\beta'(\epsilon_H)\big]\,\mathcal{D}^i{}_j\bar{P} - \big[1+3\beta'(\epsilon_{H\mathbf{i}})\big]\,\mathcal{D}^i{}_j\bar{P}_\mathbf{i}\Big)$$

[12] Eq. (3.94) features additional contributions from the initial density perturbations $\delta\varrho_\mathbf{i}$ as compared to the original Newtonian result obtained in [Buchert and Adler, 1999]. These perturbations were indeed neglected there, by assuming $\varrho_\mathbf{i} = \varrho_{H\mathbf{i}}$, as is also assumed in Zel'dovich's original work for the dust case [Zel'dovich, 1970a]. However, as is demonstrated in Appendix A of [Buchert and Adler, 1999], such an assumption can be made without loss of generality in the Newtonian context within the first–order perturbation scheme in the deformation vector, through a suitable change of Lagrangian coordinates, making both approaches equivalent.

$$+\frac{N_H^2}{a^2 N_{H_\mathbf{i}}^2}\left({}^{\mathrm{tl}}W^i{}_j + H_\mathbf{i}\left[1-3\beta'(\epsilon_{H\mathbf{i}})\right]{}^{\mathrm{tl}}U^i{}_j\right) . \tag{3.95}$$

Here $\bar{P}_\mathbf{i} = -\alpha_{H\mathbf{i}}\,\delta\epsilon_\mathbf{i}$ due to the vanishing of the initial spatial perturbation field, and we have introduced the coordinate traceless spatial Hessian operator $\mathcal{D}^i{}_j \equiv \delta^{ik}\partial_k\partial_j - (1/3)\delta^i{}_j\Delta_0$. This equation still explicitly features the trace, but it can be fully expressed in terms of $\Pi^i{}_j$ by making use of the momentum constraints (3.77). The latter can indeed be rewritten as

$$\frac{1}{N_H}\,\partial_t\Pi^i{}_{j|i} = \frac{2}{3}\,\partial_t\left(\frac{\bar{P}_{|j}}{N_H}\right) . \tag{3.96}$$

A time–integration and spatial differentiation of this equation allows one to express $\mathcal{D}^i{}_j\bar{P}$ as

$$\frac{\mathcal{D}^i{}_j\bar{P}}{N_H} = \frac{\mathcal{D}^i{}_j\bar{P}_\mathbf{i}}{N_{H\mathbf{i}}} + \frac{1}{2}\int_{t_\mathbf{i}}^{t}\frac{\partial_t\left(3\,\Pi^k{}_{j|k}{}^{|i} - \Pi^k{}_{l|k}{}^{|l}\,\delta^i{}_j\right)}{N_H}\,\mathrm{d}t' . \tag{3.97}$$

The pair of equations (3.95), (3.97) together comprise the *master equation for the traceless part.* When $p_H = 0$, one simply has $N_H(t) = 1$ and $\beta'(\epsilon_H) = 0$ so that this master equation indeed reduces to the corresponding one in the dust case, Eq. (43) in [Al Roumi et al., 2017].

3.2.4.3 Master equations for free and scattered gravitational waves

Following the approach developed in [Alles et al., 2015; Al Roumi et al., 2017], we can gain more insight into the evolution of $\Pi^i{}_j$ by splitting the full master equation for the traceless variable into gravitoelectric and gravitomagnetic parts. To this end, we first define a corresponding split of the initial conditions for the traceless variables:

$${}^{\mathrm{tl}}U^i{}_j = {}^{\mathrm{tl},E}U^i{}_j + {}^{\mathrm{tl},H}U^i{}_j \;;\; {}^{\mathrm{tl}}W^i{}_j = {}^{\mathrm{tl},E}W^i{}_j + {}^{\mathrm{tl},H}W^i{}_j \;; \tag{3.98}$$

$${}^{\mathrm{tl},H}U^i{}_{j|i} = 0 \;;\; {}^{\mathrm{tl},H}W^i{}_{j|i} = 0 \;; \tag{3.99}$$

$$2\,\Delta_0{}^{\mathrm{tl},E}U^i{}_j + {}^{\mathrm{tl},E}U^k{}_{l|k}{}^{|l}\,\delta^i{}_j - 3\,{}^{\mathrm{tl},E}U^i{}_{k|j}{}^{|k} = 0 \;; \tag{3.100}$$

$$2\,\Delta_0{}^{\mathrm{tl},E}W^i{}_j + {}^{\mathrm{tl},E}W^k{}_{l|k}{}^{|l}\,\delta^i{}_j - 3\,{}^{\mathrm{tl},E}W^i{}_{k|j}{}^{|k} = 0 . \tag{3.101}$$

The last two equations hold because of the following geometric identity (taking its first two time–derivatives and evaluating them at the initial time):

$$\left(2\,\Delta_0\Pi^i{}_j + \Pi^k{}_{l|k}{}^{|l}\,\delta^i{}_j - 3\,\Pi^i{}_{k|j}{}^{|k}\right)_{|i} = 0\,. \tag{3.102}$$

This in turn is due to the following consequence of the momentum constraints (see footnote 8): $\Pi^k{}_{[i|j]|k} = 0$.

We can then define the gravitoelectric and gravitomagnetic traceless parts, respectively, ${}^{E}\Pi^i{}_j$ and ${}^{H}\Pi^i{}_j$, as initially vanishing and having initial first time–derivatives ${}^{\mathrm{tl},E}U^i{}_j$ and ${}^{\mathrm{tl},H}U^i{}_j$. They obey the following evolution equations:

$$\begin{aligned}
&\partial_t^2\,{}^{H}\Pi^i{}_j + 3H\left[1-\beta'(\epsilon_H)\right]\partial_t\,{}^{H}\Pi^i{}_j - \frac{N_H^2}{a^2}\Delta_0\,{}^{H}\Pi^i{}_j \\
&\quad = \frac{N_H^2}{a^2 N_{H_{\mathbf{i}}}^2}\left({}^{\mathrm{tl,H}}W^i{}_j + H_{\mathbf{i}}\left[1-3\beta'(\epsilon_{H\mathbf{i}})\right]{}^{\mathrm{tl,H}}U^i{}_j\right)\,; \qquad (3.103)\\
&\partial_t^2\,{}^{E}\Pi^i{}_j + 3H\left[1-\beta'(\epsilon_H)\right]\partial_t\,{}^{E}\Pi^i{}_j + \frac{N_H^2}{3a^2}\Delta_0\,{}^{E}\Pi^i{}_j \\
&\quad = \frac{N_H^2}{3a^2}\Big(\left[1+3\beta'(\epsilon_H)\right]\mathcal{D}^i{}_j\bar{P} - \left[1+3\beta'(\epsilon_{H\mathbf{i}})\right]\mathcal{D}^i{}_j\bar{P}_{\mathbf{i}}\Big) \\
&\qquad + \frac{N_H^2}{a^2 N_{H_{\mathbf{i}}}^2}\left({}^{\mathrm{tl,E}}W^i{}_j + H_{\mathbf{i}}\left[1-3\beta'(\epsilon_{H\mathbf{i}})\right]{}^{\mathrm{tl,E}}U^i{}_j\right)\,. \qquad (3.104)
\end{aligned}$$

Eq. (3.103) is the *master equation for free gravitational waves*, while Eq. (3.104), after elimination of the coupling to the trace, is the *master equation for the gravitational wave part that is scattered at the perfect fluid source.* We will discuss the coupling to the trace of this latter equation in more detail below.

The above evolution equations ensure that we indeed get a decomposition of the traceless deformation field obeying (3.95) at all times:

$$\Pi^i{}_j = {}^{E}\Pi^i{}_j + {}^{H}\Pi^i{}_j\,. \tag{3.105}$$

They will also propagate the initial constraints (3.98)–(3.101) that define the split of ${}^{\mathrm{tl}}U^i{}_j$ and ${}^{\mathrm{tl}}W^i{}_j$. This will ensure the preservation at all times of the divergence–free nature of free gravitational waves as well as the geometric identity on their

scattered part, similar to the dust case:

$$ {}^{H}\Pi^{i}{}_{j|i} = 0 \,, \tag{3.106} $$

$$ 2\,\Delta_0 {}^{E}\Pi^{i}{}_{j} + {}^{E}\Pi^{k}{}_{l|k}{}^{|l}\,\delta^{i}_{j} - 3\,{}^{E}\Pi^{i}{}_{k|j}{}^{|k} = 0 \,. \tag{3.107} $$

The (also propagating) momentum constraints (3.96) split as follows:

$$ {}^{H}\Pi^{i}{}_{j|i} = 0 \quad ; \quad \frac{1}{N_H}\,\partial_t {}^{E}\Pi^{i}{}_{j|i} = \frac{2}{3}\,\partial_t\!\left(\frac{\bar{P}_{|j}}{N_H}\right) \quad . \tag{3.108} $$

Observe that ${}^{H}\Pi^{i}{}_{j}$ decouples from the trace in both the momentum constraints and the evolution equation, while ${}^{E}\Pi^{i}{}_{j}$ remains coupled to the trace in both cases. Alternatively, using a time integral of the momentum constraints,

$$ {}^{E}\Pi^{i}{}_{j|i} = \frac{2}{3}\int_{t_{\mathrm{i}}}^{t} N_H\,\partial_t\!\left(\frac{\bar{P}_{|j}}{N_H}\right)\mathrm{d}t' \,, \tag{3.109} $$

the geometric constraint (3.107) on ${}^{E}\Pi^{i}{}_{j}$ can be expressed as follows:

$$ \Delta_0 {}^{E}\Pi^{i}{}_{j} = \mathcal{D}^{i}{}_{j}\left(\int_{t_{\mathrm{i}}}^{t} N_H\,\partial_t\!\left(\frac{\bar{P}}{N_H}\right)\mathrm{d}t'\right) \,. \tag{3.110} $$

This is to be compared to the dust–case relation, Eq. (51) in [Al Roumi et al., 2017], to which it reduces when $p_H = 0$ and accordingly $N_H(t) = 1$: $\Delta_0 {}^{E}\Pi^{i}{}_{j} = \mathcal{D}^{i}{}_{j}(\bar{P} - \bar{P}_{\mathrm{i}}) = \mathcal{D}^{i}{}_{j}P$. Hence, in the presence of pressure, in contrast to the dust case, the gravitoelectric traceless part and the trace, although still tightly coupled, will in general have different time behaviours.

With the antisymmetric part vanishing at all times, the evolution equations for the trace and for the gravitoelectromagnetic split of the traceless symmetric part, coupled through the momentum constraints, characterize the behaviour of the first–order Lagrangian deformation field for this general barotropic single fluid. These evolution equations have yet to be complemented by the set of initial constraints (3.47)–(3.52), to which we turn now.

3.2.5 First–order initial conditions

The constraints on the initial conditions for the deformation field, the density and the spatial curvature are expressed at the first–order level as follows:

$$U_{[ij]} = 0 \quad ; \quad W_{[ij]} = 0 \, ; \tag{3.111}$$

$$W - 6H_{\mathbf{i}}\,\beta'(\epsilon_{H\mathbf{i}})\,U = -N_{H\mathbf{i}}^2\,\alpha_{H\mathbf{i}}\left[\mathcal{W}(t_{\mathbf{i}})\,\delta\epsilon_{\mathbf{i}} + \beta'(\epsilon_{H\mathbf{i}})\,\Delta_0(\delta\epsilon_{\mathbf{i}})\right] \, ; \tag{3.112}$$

$$\begin{aligned} {}^{\mathrm{tl}}W^i_{\ j} + H_{\mathbf{i}}\left[1 - 3\,\beta'(\epsilon_{H\mathbf{i}})\right]{}^{\mathrm{tl}}U^i_{\ j} &= -N_{H\mathbf{i}}^2\,\mathscr{T}^i_{\ j} \\ &\quad - N_{H\mathbf{i}}^2\,\alpha_{H\mathbf{i}}\,\beta'(\epsilon_{H\mathbf{i}})\left[(\delta\epsilon_{\mathbf{i}})^{|i}{}_{|j} - \frac{1}{3}\Delta_0(\delta\epsilon_{\mathbf{i}})\,\delta^i_{\ j}\right] ; \end{aligned} \tag{3.113}$$

$$H_{\mathbf{i}}U = -\frac{1}{4}\mathscr{R}N_{H\mathbf{i}}^2 + 4\pi G\,N_{H\mathbf{i}}^2\,\alpha_{H\mathbf{i}}\,\delta\epsilon_{\mathbf{i}} \times \left[\epsilon_{H\mathbf{i}} + p_{H\mathbf{i}} - (2\epsilon_{H\mathbf{i}} + \tilde{\Lambda})\,\beta'(\epsilon_{H\mathbf{i}})\right] ; \tag{3.114}$$

$$U^i_{\ j|i} - U_{|j} = 2H_{\mathbf{i}}\,\alpha_{H\mathbf{i}}\,\beta'(\epsilon_{H\mathbf{i}})\,(\delta\epsilon_{\mathbf{i}})_{|j} \, ; \tag{3.115}$$

$$p_{\mathbf{i}} = p_{H\mathbf{i}} + \epsilon_{H\mathbf{i}}\,\beta'(\epsilon_{H\mathbf{i}})\,\delta\epsilon_{\mathbf{i}} \quad ; \quad p_{H\mathbf{i}} = \beta(\epsilon_{H\mathbf{i}}) \, . \tag{3.116}$$

This set of initial conditions can also be obtained by evaluating the linearized Lagrange–Einstein system at an initial time. It can be complemented by the requirements (3.98)–(3.101) which define the initial split into gravitoelectric and gravitomagnetic parts of the traceless deformation field. Note that the above set keeps more variables coupled than the corresponding ones in [Al Roumi et al., 2017]. This is to be expected, since in the dust case a vanishing pressure and a constant lapse allowed for the elimination of ϵ and Λ between the first two constraints, leaving only a relation between U, W and $\mathscr{R}$. Here, we also have contributions from p, Λ (due to the lapse factor in the Λ term) and the nonvanishing $\mathcal{A}_{\mathbf{i}}{}^{(1)}$. Accordingly, the dependence on the initial energy density $\epsilon_{\mathbf{i}}$ and its spatial derivatives can no longer be explicitly removed in general. However, as in the dust case, the scalar constraints (3.112) and (3.114), together with the initial EoS (3.116), show that only two independent first–order initial conditions need to be given for the scalar variables U, W, $\mathscr{R}$, $\epsilon_{\mathbf{i}}$, and $p_{\mathbf{i}}$. One could for instance only specify U and W as can be done in the dust case, fully determining the other scalar initial conditions. In contrast to the dust case, however, determining $\epsilon_{\mathbf{i}}$ in this situation would involve solving for the Laplacian differential

equation (3.112).

3.3 Application to specific equations of state

Concrete results can be obtained by looking at special cases of the barotropic EoS. In this section, we will first consider the family of linear relations between the pressure and the energy density. We then proceed to a special nonlinear polytropic EoS that allows one to model the isotropic part of a velocity dispersion field up to late epochs of nonlinear structure formation.

3.3.1 Case of a linear Equation of State: $p = w\epsilon$

In the previous section we have derived the evolution equations for the first–order deformation field, sourced by a general barotropic fluid. In this section we will consider the simplest barotropic EoS as an example, where $p = \beta(\epsilon) = w\epsilon$ with w a constant parameter obeying the dominant energy condition, $-1 \leq w \leq 1$. In addition to the radiation fluid, with $w = 1/3$, other interesting cases include a "stiff fluid" corresponding to a free scalar field source, with $w = 1$, and a "curvature" or "string gas" equation of state, with $w = -1/3$. When $p = w\epsilon$ we can readily apply the procedure suggested in [Alles et al., 2015; Al Roumi et al., 2017] to find the relativistic Lagrangian first–order solutions.

The formal rest mass density $F(\epsilon)$ and the lapse are found to be as follows:

$$N = \frac{F(\epsilon)}{\epsilon + \beta(\epsilon)} = \frac{\varrho_1}{\epsilon_1(1+w)} \left(\frac{\epsilon}{\epsilon_1}\right)^{-w/(1+w)} , \tag{3.117}$$

if $w \neq -1$, where we defined $F(\epsilon) = \varrho_1 \, (\epsilon/\epsilon_1)^{1/(1+w)}$. (The case $w = -1$ for a "vacuum energy equation of state" can be treated separately by the explicit cosmological term.) The solution (3.41) of the energy conservation law then yields the energy density, and the lapse as deduced from (3.117), as the following respective functionals of the coframes, with $J = \det(\eta^a{}_i)$:

$$\epsilon = \epsilon_{\mathbf{i}} \, J^{-(1+w)} \; ; \; N = N_{\mathbf{i}} \, J^w \; . \tag{3.118}$$

Similar equations hold for the background spacetime,

$$\epsilon_H = \epsilon_{H\mathbf{i}}\, a^{-3(1+w)} \; ; \; N_H = N_{H\mathbf{i}}\, a^{3w} \; ; \; \frac{\partial_t N_H}{N_H} = 3wH \; . \tag{3.119}$$

Given the linear barotropic EoS, the pressure and background pressure are immediately deduced from the expression of the corresponding energy densities, and will share their functional dependencies.

3.3.1.1 First–order equations

With the linear EoS $\beta(\epsilon) = w\epsilon$, $\beta'(\epsilon_H)$ reduces to the constant value w, $\beta''(\epsilon_H)$ vanishes at all times, and $\alpha_{H\mathbf{i}} = (1+w)^{-1}$. Consistent with a first–order evaluation of the exact formulas above, the first–order expressions (3.61)–(3.65) for $\bar{P}$, ϵ, p, $F(\epsilon)$, N and their rate of evolution thus simplify to

$$\begin{aligned}
\bar{P} &= P - (1+w)^{-1}\delta\epsilon_{\mathbf{i}} \; ; \\
\epsilon &= \epsilon_H\Big[1-(1+w)\bar{P}\Big] \quad ; \quad p = p_H - w(1+w)\,\epsilon_H\,\bar{P} \; ; \\
F(\epsilon) &= F(\epsilon_H)\big[1-\bar{P}\big] \; ; \\
N &= N_H\big[1+w\bar{P}\big] \quad ; \quad \frac{\partial_t N}{N} = 3wH + w\,\partial_t\bar{P} \; .
\end{aligned} \tag{3.120}$$

Eq. (3.72) then reduces to

$$\mathcal{V}(t) = \frac{\epsilon_H(1-w)^2 - 2w\tilde{\Lambda}}{\epsilon_H(1-w) - w\tilde{\Lambda}} \; , \tag{3.121}$$

and the first–order Lagrange–Einstein system (3.71), (3.74)–(3.77) becomes:[13]

$$\begin{aligned}
&\partial_t\mathfrak{P}_{ij} = 0 \; : \quad \mathfrak{P}_{ij} = \mathfrak{P}_{ij}(t_{\mathbf{i}}) = 0 \; ; \\
&\partial_t^2\bar{P} + 3H\,\frac{\epsilon_H(1-w)^2 + 2w^2\tilde{\Lambda}}{\epsilon_H(1-w) - w\tilde{\Lambda}}\,\partial_t\bar{P}
\end{aligned}$$

[13] It is worth noting in the case when $\Lambda = 0$, $\mathcal{V}(t)$ simplifies further and reduces to the constant $1-w$, so that (3.122) becomes

$$\partial_t^2\bar{P} + 3H(1-w)\partial_t\bar{P} = N_{H\mathbf{i}}^2\, a^{6w}\left[\mathcal{A}^{(1)} - \frac{1+3w}{4}\mathcal{R}^{(1)}\right] \; .$$

$$= N_{H\mathbf{i}}^2\, a^{6w}\left[\mathcal{A}^{(1)} - \frac{\epsilon_H(1-w)(1+3w)+2w\tilde{\Lambda}}{4\epsilon_H(1-w)-4w\tilde{\Lambda}}\mathcal{R}^{(1)}\right]; \tag{3.122}$$

and

$$\partial_t^2\Pi^i{}_j + 3H(1-w)\partial_t\Pi^i{}_j = N_{H\mathbf{i}}^2\, a^{6w}\left(\xi^{i\ (1)}_{\ j} - \tau^{i\ (1)}_{\ j}\right); \tag{3.123}$$

$$H\,\partial_t\bar{P} + 4\pi G\big[\epsilon_H(1-w) - w\tilde{\Lambda}\big]N_{H\mathbf{i}}^2\, a^{6w}\,\bar{P} = -\frac{1}{4}N_{H\mathbf{i}}^2\, a^{6w}\,\mathcal{R}^{(1)}; \tag{3.124}$$

$$\partial_t\left(\Pi^i{}_{j|i} - \frac{2}{3}\bar{P}_{|j}\right) = -2wH\bar{P}\,. \tag{3.125}$$

The acceleration gradient and its trace and traceless parts are expressed in terms of the deformation field at first order according to Eqs. (3.67), (3.78), (3.79), yielding

$$\mathcal{A}^{i\ (1)}_{\ j} = a^{-2}w\,\bar{P}^{|i}_{\ \ |j}\ ; \tag{3.126}$$

$$\mathcal{A}^{(1)} = a^{-2}w\,\Delta_0\bar{P}\ ; \tag{3.127}$$

$$\xi^{i\ (1)}_{\ j} = a^{-2}w\,\mathcal{D}^i{}_j\bar{P}\,, \tag{3.128}$$

while the first–order expressions (3.57), (3.80), (3.81) of the Ricci tensor and its trace/traceless split are formally unchanged.

Since for the chosen EoS, $\mathcal{W}(t)$ yields

$$\mathcal{W}(t) = 4\pi G\left[\epsilon_{H\mathbf{i}}\, a^{-3(1+w)}(1-w)(1+3w) + 2w\tilde{\Lambda}\right], \tag{3.129}$$

the master equation (3.84) for the trace of the perturbation now reads:

$$\begin{aligned}&\partial_t^2\bar{P} + 2H(1-3w)\partial_t\bar{P} - 4\pi G N_{H\mathbf{i}}^2\big[\epsilon_{H\mathbf{i}}(1-w)(1+3w)\,a^{3(w-1)} + 2w\tilde{\Lambda}\,a^{6w}\big]\bar{P}\\ &\quad = wN_{H\mathbf{i}}^2\,a^{6w-2}\Delta_0\bar{P}\,.\end{aligned} \tag{3.130}$$

In turn, the master equation (3.95) for the traceless symmetric part of the deformation field becomes

$$\begin{aligned}&\partial_t^2\Pi^i{}_j + 3H(1-w)\partial_t\Pi^i{}_j\\ &\quad + N_{H\mathbf{i}}^2\,a^{6w-2}\left\{2\Pi^i{}_{k|j}^{\ \ |k} - \Pi^i{}_{j|k}^{\ \ |k} - \frac{2}{3}\Pi^k{}_{l|k}^{\ \ |l}\delta^i{}_j - \frac{1}{3}(1+3w)\mathcal{D}^i{}_j\left(\bar{P}-\bar{P}_{\mathbf{i}}\right)\right\}\end{aligned}$$

$$= a^{6w-2}\left[{}^{\mathrm{tl}}W^{i}_{\ j} + (1-3w)H_{\mathbf{i}}\,{}^{\mathrm{tl}}U^{i}_{\ j}\right] \ , \tag{3.131}$$

with, from the momentum constraints (3.125),

$$a^{-3w}\,\mathcal{D}^{i}_{\ j}\bar{P} = \mathcal{D}^{i}_{\ j}\bar{P}_{\mathbf{i}} + \int_{t_{\mathbf{i}}}^{t} \frac{\partial_t\left(3\,\Pi^{k}_{\ j|k}{}^{|i} - \Pi^{k}_{\ l|k}{}^{|l}\,\delta^{i}_{\ j}\right)}{2\,a^{3w}}\,\mathrm{d}t' \ . \tag{3.132}$$

We can finally rewrite the set of initial conditions (3.111)–(3.116) for the linear EoS:

$$U_{[ij]} = 0 \quad ; \quad W_{[ij]} = 0 \ ; \tag{3.133}$$

$$W - 6wH_{\mathbf{i}}U = -\frac{N^2_{H\mathbf{i}}}{1+w}\Big(w\,\Delta_0(\delta\epsilon_{\mathbf{i}}) + 4\pi G\big[\epsilon_{H\mathbf{i}}(1-w)(1+3w) + 2w\tilde{\Lambda}\big]\delta\epsilon_{\mathbf{i}}\Big) \ ; \tag{3.134}$$

$${}^{\mathrm{tl}}W^{i}_{\ j} + (1-3w)H_{\mathbf{i}}\,{}^{\mathrm{tl}}U^{i}_{\ j} = -N^2_{H\mathbf{i}}\left[\mathscr{T}^{i}_{j} + \frac{w}{1+w}\mathcal{D}^{i}_{\ j}(\delta\epsilon_{\mathbf{i}})\right] ; \tag{3.135}$$

$$H_{\mathbf{i}}\,U = -\frac{1}{4}\mathscr{R}N^2_{H\mathbf{i}} + \frac{4\pi G N^2_{H\mathbf{i}}}{1+w}\left[\epsilon_{H\mathbf{i}}(1-w) - w\tilde{\Lambda}\right]\delta\epsilon_{\mathbf{i}} \ ; \tag{3.136}$$

$$U^{i}_{\ j|i} - U_{|j} = 2\,\frac{w}{1+w}H_{\mathbf{i}}\,(\delta\epsilon_{\mathbf{i}})_{|j} \ ; \tag{3.137}$$

$$p_{\mathbf{i}} = p_{H\mathbf{i}} + w\,\epsilon_{H\mathbf{i}}\,\delta\epsilon_{\mathbf{i}} \quad ; \quad p_{H\mathbf{i}} = w\,\epsilon_{H\mathbf{i}} \ . \tag{3.138}$$

3.3.1.2 Solutions for the trace of the deformation field

We will now further investigate the behaviour of the trace P of the first–order deformation. For simplicity, we will restrict attention to the case of a vanishing cosmological constant, $\Lambda = 0$, as may be reasonably assumed during the radiation–dominated era. In this case Eqs. (3.86)–(3.88) reduce to

$$a\frac{\partial\bar{P}}{\partial a} + \frac{3}{2}(1-w)\bar{P} = \frac{-3}{32\pi G\epsilon_{H\mathbf{i}}}a^{3(1+w)}\mathcal{R}^{(1)} \ ; \tag{3.139}$$

$$\frac{\partial^2\bar{P}}{\partial a^2} + \frac{\alpha_1}{a}\frac{\partial\bar{P}}{\partial a} - \frac{\alpha_2}{a^2}\bar{P} = \alpha_{3\mathbf{i}}\,a^{3w-1}\Delta_0\bar{P} \ , \tag{3.140}$$

with the constant parameters

$$\alpha_1 = \frac{3(1-3w)}{2} \quad ; \quad \alpha_2 = \frac{3(1-w)(3w+1)}{2} \ ; \quad \alpha_{3\mathbf{i}} = \frac{3w}{8\pi G\epsilon_{H\mathbf{i}}} \ . \tag{3.141}$$

If $w > 0$ (implying $\alpha_{3\mathbf{i}} > 0$), as we will assume in the following, then Eq. (3.140) is a second–order hyperbolic partial differential equation (PDE).[14] This equation is formally analogous to the standard Eulerian propagation equations for a linearized density contrast [Tsagas et al., 2008; Ellis et al., 2012; Peter and Uzan, 2009] once those are re–expressed in terms of the variable scale factor a.[15] In the Eulerian case, assuming global flat–space spatial coordinates, one can find the analytical general solution using a Fourier transformation. A discussion of the differences between the Eulerian and Lagrangian approaches has been given in [Al Roumi et al., 2017]. (See also the related discussion in [Villa et al., 2014].) Ref. [Al Roumi et al., 2017] also elucidated a procedure for finding general–relativistic Lagrangian first–order solutions for the deformation field in the dust case. We show here that this procedure can be readily extended to the presence of pressure and apply it to the determination of a Lagrangian solution for the trace part.[16] First, we can use the formal identity of Eq. (3.140), written in Lagrangian coordinates on the nontrivial spacetime manifold, with an equation written in Euclidean space. We can thus work within this flat space with its effective 'Eulerian' Cartesian spatial coordinates x^i and solve equation (3.140) with $\Delta_0 \mapsto \delta^{ij}\,\partial_{x^i}\partial_{x^j}$ for the unknown $\bar{P}(a, \mathbf{x})$. On this space we can then indeed apply an inverse Fourier transformation

$$\bar{P}(a, \mathbf{x}) = \iiint \bar{P}_k(a, \mathbf{k})\, e^{-i\mathbf{k}\cdot\mathbf{x}}\, \mathrm{d}^3\mathbf{k}\ , \tag{3.142}$$

and accordingly get a second–order linear ordinary differential equation:

$$\frac{d^2\bar{P}_k}{da^2} + \frac{\alpha_1}{a}\frac{d\bar{P}_k}{da} - \left(\alpha_2 a^{-2} - \alpha_{3\mathbf{i}}\, k^2 a^{3w-1}\right)\bar{P}_k = 0\ , \tag{3.143}$$

---

[14] It would be an elliptic PDE for $w < 0$ (*i.e.* $\alpha_{3\mathbf{i}} < 0$), while for the parabolic case $w = 0$ (and consequently $\alpha_{3\mathbf{i}} = 0$) it reduces, as expected, to the evolution equation for the dust case, with decoupled time and space variables.

[15] Note that in terms of the conventional cosmic time $\tilde{t}$ introduced in (3.37), Eq. (3.123) reduces to $\partial_{\tilde{t}}^2\bar{P} + (2-3w)a^{-1}\partial_{\tilde{t}}a\partial_{\tilde{t}}\bar{P} - 4\pi G\left[(1-w)(1+3w)\epsilon_H + 2w\tilde{\Lambda}\right]\bar{P} = wa^{-2}\Delta_0\bar{P}$. This is formally equivalent to the linearized Eulerian equation (3.2.17) of Ref. [Tsagas et al., 2008] in that the coefficients agree, but both the dependent and (spatial) independent variables differ.

[16] A complementary picture of an equivalent procedure is shown in Appendix B.2 and applied to the search for a particular solution for the traceless part.

where we have used $\mathbf{k}\cdot\mathbf{x} \equiv \delta_{ij}k^i x^j$ and $k \equiv (\delta_{ij}k^i k^j)^{1/2}$. The background Jeans wavenumber (3.89) then satisfies

$$\begin{aligned} k_J^2 &= \frac{\alpha_2}{\alpha_{3\mathbf{i}}} a^{-3(1+w)} \\ &= 4\pi G \epsilon_{H\mathbf{i}} \frac{(1-w)(3w+1)}{w\, a^{3(1+w)}} \,, \end{aligned} \tag{3.144}$$

where we recall that $0 < w \leq 1$ is assumed. The behaviour of the solution to Eq. (3.140) will then depend on the relative values of k and $a\, k_J(\epsilon_H)$.

One can first proceed by investigating the extreme cases, as is commonly done in the Eulerian analyses. When $k \ll a\, k_J(\epsilon_H)$, Eq. (3.143) may be solved as

$$\bar{P}_k = a^{1+3w} C_{k,1} + a^{\frac{3}{2}(w-1)} C_{k,2} \,, \tag{3.145}$$

where $C_{k,1(2)}$ are two functions of $\mathbf{k}$ encoding the initial conditions. This corresponds, as expected, to the unstable regime since the term with coefficient $C_{k,1}$ is a growing mode.

In the opposite situation when $k \gg a\, k_J(\epsilon_H)$, the solution reads

$$\begin{aligned} &\bar{P}_k = a^{\frac{9w-1}{4}} \left[J_{\hat{\nu}}\left(B\, a^{\frac{1+3w}{2}} k \right) C_{k,1} + Y_{\hat{\nu}}\left(B\, a^{\frac{1+3w}{2}} k \right) C_{k,2} \right] ; \\ &B = \frac{2\sqrt{\alpha_{3\mathbf{i}}}}{1+3w} \quad ; \quad \hat{\nu} = \frac{9w-1}{2+6w} \quad , \end{aligned} \tag{3.146}$$

with different $\mathbf{k}$–dependent coefficients $C_{k,1(2)}$ and where $J_\nu(x)$ and $Y_\nu(x)$ denote the Bessel functions of the first and second kind, respectively. This corresponds to a 'stable' regime of acoustic oscillations, although their amplitude will grow over time (as $a^{(3w-1)/2}$ for large a) for an unusual EoS with $w > 1/3$. The latter remark includes the "stiff fluid" EoS $w = 1$, for which the above solution is exact at all times, since it corresponds to $k_J(\epsilon_H) = 0$.

From the expression (3.144) of $k_J(\epsilon_H)$, the noncomoving Jeans wavenumber $a\, k_J(\epsilon_H)$ decreases over time, so that even an initially unstable solution will eventually enter the stable regime. Such a solution will cross the threshold $k \simeq a\, k_J(\epsilon_H)$ and it may be useful to be able to describe this transition period as well. As in the Newtonian case in the Eulerian approach, with different coefficients (see, *e.g.*, [Gailis and Frankel, 2006]), the Bessel functions actually allow for an

explicit solution of Eq. (3.143) for any mode at all times. The general solution is the same as (3.146) up to a change of the order of the Bessel functions:

$$\bar{P}_k = a^{\frac{9w-1}{4}}\left[J_\nu\left(B\,a^{\frac{1+3w}{2}}k\right)C_{k,1} + Y_\nu\left(B\,a^{\frac{1+3w}{2}}k\right)C_{k,2}\right];$$
$$B = \frac{2\sqrt{\alpha_{3\mathbf{i}}}}{1+3w} \quad ; \quad \nu = \frac{5+3w}{2+6w}\,. \tag{3.147}$$

The integration constants $C_{k,1(2)}$ are derived from the initial conditions on $\bar{P}$ and its time–derivative, $\bar{P}_\mathbf{i}(\mathbf{X})$ and $U(\mathbf{X})$. To this end, one formally replaces these quantities by functions of the 'Eulerian' coordinates x^i on the Euclidean space, with the same functional dependence, $\bar{P}_\mathbf{i}(\mathbf{x})$ and $U(\mathbf{x})$. One is then working on flat–space, and the respective Fourier transforms $\bar{P}_k(a = a_\mathbf{i} = 1, \mathbf{k})$ and $(\partial_t\bar{P}_k)(a = 1, \mathbf{k}) = H_\mathbf{i}(\partial_a\bar{P}_k)(a = 1, \mathbf{k})$ can be computed, from which $C_{k,1(2)}(\mathbf{k})$ are deduced. Knowing these, $\bar{P}(a, \mathbf{k})$ is expressed as the full solution given by Eq. (3.147) and its inverse Fourier transform (3.142) gives $\bar{P}(a, \mathbf{x})$ in Euclidean space.

Finally, one can formally replace the Eulerian spatial coordinates by the Lagrangian ones in $\bar{P}(a, \mathbf{x})$ while preserving the functional form. The resulting Lagrangian function $\bar{P}(a, \mathbf{X})$ then indeed gives a solution to the evolution equation (3.140) in the nonconstant curvature spatial sections, thanks to the algebraic identity of this equation with its Euclidean space counterpart.

It is now a Lagrangian solution, however, and must be interpreted as such: the coordinates X^i are comoving with the inhomogeneous fluid flow. They are interpreted as local coordinates on the perturbed manifold; accordingly the solution $P(a, \mathbf{X})$ describes perturbations as they evolve in the perturbed space. This also implies that there is no diffeomorphism to transform the Lagrangian coordinates back to Eulerian space, even though the evolution equation is formally exactly the same. Note that the Fourier modes $\bar{P}(a, \mathbf{k})$ are only an intermediate resolution step as they only correspond to modes in the ancillary Euclidean space. As the inversion of the solution (3.147) does not allow for an explicit general analytic expression, it requires the specification of the initial conditions and will usually involve numerical integration with the given $C_{k,1(2)}(\mathbf{k})$ to realize this solution procedure.

3.3.2 Case of a polytropic Equation of State: $p = \kappa\varrho^\gamma$

As a second class of models we will now turn to the nonlinear case of polytropic equations of state.

3.3.2.1 Equation of state and resolution procedure

We consider the polytropic EoS, $p = \kappa\varrho^\gamma$, $\varrho = F(\epsilon)$, where κ is the polytropic constant, and $\gamma > 1$ the polytropic exponent. For such flows the pressure and the energy density obey the relation [Ellis et al., 2012; Rezzolla and Zanotti, 2013]

$$\epsilon = \beta^{-1}(p) = \frac{1}{\gamma - 1}\, p + A\, p^{1/\gamma} = \frac{1}{\gamma - 1}\, \kappa\, \varrho^\gamma + A\, \kappa^{1/\gamma} \varrho\ , \tag{3.148}$$

where A is a constant parameter. We will assume in this section that the formal $\varrho = F(\epsilon)$ actually coincides with the rest mass density of the fluid, *e.g., via* suitable initial conditions. For $A = 0$, we again obtain the (non–dust) linear case $p = w\epsilon$ with $w := \gamma - 1 > 0$. In the following, we will instead consider the case $A\,\kappa^{1/\gamma} = 1$ (in particular $A > 0$), corresponding to an EoS of the type of a nonrelativistic adiabatic ideal gas, the energy density being the sum of the rest mass density and an internal energy density equal to $p/(\gamma - 1)$.

As a relevant example, we will focus on the case $\gamma = 5/3$ [17], which has been proven to be an exact solution for a locally isotropic distribution with velocity dispersion, derived from relativistic kinetic theory of collisionless matter [Ehlers, 1993]. (See also [Treciokas and Ellis, 1971] and references therein.) This EoS also coincides with the corresponding exact solution in Newtonian cosmology derived from kinetic theory [Buchert and Domínguez, 1998, 2005]. In this latter papers it is also shown that this particular EoS arises in the inhomogeneous case by closing the hierarchy of kinetic equations through truncation of the third and higher reduced moments. In the inhomogeneous case this law is, however, phenomenological, since there is a nonvanishing anisotropic part; neglecting this part strictly results in shear–free motion confirming the exactness of the law in the homogeneous case.

The conservation law (3.17), combined with $p = \kappa\varrho^\gamma$, gives for the evolution

[17] Notice here the pressure also sources the gravitation, whereas in section 2.2.2.7 we have assumed the effective dynamical pressure arising from velocity dispersion is second-order.

of p:

$$\partial_t p + \gamma N \Theta p = 0 \;\; ; \;\; \gamma = \frac{5}{3} \;\; . \tag{3.149}$$

The same relation holds within the background spacetime, so that $p_H\, a^5 = p_{H\mathbf{i}}\, a_{\mathbf{i}}{}^5$. The assumption of the background sources following the same EoS also gives, for $\gamma = 5/3$:

$$\begin{aligned} \epsilon_H &= \beta^{-1}(p_H) = \frac{3}{2} p_H + A\, p_H^{3/5} \;\; ; \\ \beta'(\epsilon_H) &= \frac{2}{3}\, \frac{5}{5 + 2\, A\, p_H^{-2/5}} \;\; ; \\ \beta''(\epsilon_H) &= \frac{80\, A\, p_H^{-7/5}}{9 \left(5 + 2\, A\, p_H^{-2/5}\right)^3} \;\; . \end{aligned} \tag{3.150}$$

The procedure outlined in the last subsection for solving the trace master equation, Eq. (3.87), in terms of Fourier transformation within a set of coordinates formally equivalent to Eulerian spatial coordinates, is still applicable in this case. We can thus substitute (3.150) and (3.88) in the Eulerian coordinate analogue of (3.87), and solve the corresponding ordinary differential evolution equation for each Fourier mode. This has to be performed by numerical integration as the more complicated time–evolution of the coefficients prevents an explicit analytic solution. Once initial conditions are specified we can then numerically compute the inverse Fourier transform, and formally replace the (Eulerian) spatial coordinates by the Lagrangian coordinates X^i (see section 3.3.1.2) to obtain the solution for $\bar{P}(t, X^i)$.

3.3.2.2 Behavior of the first–order trace for a model overdense region

As an instructive toy model, we will now consider the evolution of an initial Gaussian deformation describing a spherical local overdensity:

$$-\bar{P}_{\mathbf{i}} = \alpha_{H\mathbf{i}} \delta\epsilon_{\mathbf{i}} = c_{\mathbf{i}} \exp\left(-\frac{R^2}{2\sigma^2}\right) \;\; , \tag{3.151}$$

where σ and $c_{\mathbf{i}}$ respectively define the characteristic scale and maximum amplitude of the initial perturbation, and $R \equiv \left(\delta_{ij} X^i X^j\right)^{1/2}$ is a Lagrangian coordinate

'radius'.[18] We will take $c_{\mathbf{i}} > 0$ and $c_{\mathbf{i}} \ll 1$, which can be seen to describe a small initial overdensity, since the initial rest mass density contrast,

$$\delta_{\mathbf{i}} := \frac{\varrho_{\mathbf{i}}}{\varrho_{H\mathbf{i}}} - 1 = \frac{F(\epsilon_{\mathbf{i}})}{F(\epsilon_{H\mathbf{i}})} - 1 = \frac{F(\epsilon_{H\mathbf{i}}[1+\delta\epsilon_{\mathbf{i}}]) - F(\epsilon_{H\mathbf{i}})}{F(\epsilon_{H\mathbf{i}})} \,, \tag{3.152}$$

is well approximated by $\alpha_{H\mathbf{i}}\,\delta\epsilon_{\mathbf{i}} = -\bar{P}_{\mathbf{i}}$ for $c_{\mathbf{i}} \ll 1$. The actual value of the amplitude $c_{\mathbf{i}}$ is irrelevant for the evolution of $\bar{P}$ itself, since it obeys a linear equation. However, it will matter for the nonlinear evaluation of any physical quantity such as ϱ determined by the solution for $\bar{P}$. Indeed, in the Relativistic Zel'dovich Approximation observables have to be extrapolated by evaluating them as exact functionals of the deformation field once the latter is known, even if it arises as a solution to the Lagrange–Einstein equations restricted to a given order in the deformation. To best illustrate the effect of this extrapolation procedure, we choose a rather large overdensity with the arbitrary amplitude $c_{\mathbf{i}} = 10^{-3}$ at an initial time that corresponds to the epoch of last scattering.

As we will see, this will let the unstable perturbations enter the mildly nonlinear regime (where $|\bar{P}| < 1$ but is of order 1) around the present epoch, *i.e.*, around $a = a_0 \simeq 1090$ since we set $a_{\mathbf{i}} = 1$. The other independent initial condition amounts to specifying the first time–derivative $(\partial_t \bar{P})(t_{\mathbf{i}})$. For this we simply consider an initially stationary deformation and set $(\partial_t \bar{P})(t_{\mathbf{i}}) = U = 0$.

The present formalism focuses on the description of a single fluid source, as it allows for a description in terms of a single velocity field and a single EoS. We shall consequently make the simplifying assumption of a universe model filled with a single–component matter fluid and a cosmological constant. The description of model universes with multicomponent fluids is beyond the scope of the present paper, and is left to future work. The background density parameters Ω_m, Ω_Λ for a single matter component and the cosmological constant respectively, satisfy $\Omega_m + \Omega_\Lambda = 1$. We will take the present epoch value $\Omega_\Lambda^0 = 0.692$ in agreement with the best–fit ΛCDM parameters from the Planck collaboration [Ade et al.,

[18] We have chosen the set of Lagrangian coordinates X^i such that the components of the spatial metric at initial time, G_{ij}, are approximately δ_{ij} (at leading order) in these coordinates. They can thus be considered as Cartesian–like coordinates, and R is accordingly a fluid–comoving radial coordinate. It does not, however, coincide with the spatial metric distance between the fluid elements of the respective Lagrangian coordinates (X^i) and $(0,0,0)$. (This is true irrespective of a possible normalization by $a(t)$ to make it a background–comoving distance.)

2016a].

The background is also affected by the polytropic EoS (3.148) of the source fluid. As noted above, our polytrop is exact for the background and is parameterized by the arbitrary constant κ, or equivalently A as we set $A\kappa^{1/\gamma} = 1$. Specifying its value amounts to choosing the initial instability scale as determined by $k_J(\epsilon_{H\mathbf{i}})$. It also controls the ratio between pressure and rest mass density at a given time, and hence the deviation of the background from a dust–fluid ΛCDM model. The value we adopt for our examples below, $A{p_{H\mathbf{i}}}^{-2/5} = 3/2$, requires the background fluid pressure to be relativistic (and radiation–like) at the initial time, $p_{H\mathbf{i}} = \epsilon_{H\mathbf{i}}/3$, with $p_{H\mathbf{i}}/\varrho_{H\mathbf{i}} = 2/3$. However, it subsequently quickly becomes negligible as $p_H/\varrho_H \propto a^{-2}$, keeping the late–time dynamics of the background very close to that of the ΛCDM model.

We choose to make the lengths R, σ dimensionless by setting the initial instability scale $k_J(\epsilon_{H\mathbf{i}})^{-1}$ (as derived from substituting (3.150) into (3.89) at the initial time) to be our length unit. Thus $\sigma < 1$ means that the scale of the initial perturbation is below the Jeans scale $k_J(\epsilon_{H\mathbf{i}})^{-1}$, and above it for $\sigma > 1$. For the value of A adopted in the present example and estimating $\varrho_{H\mathbf{i}}$ from ΛCDM background parameters [Ade et al., 2016a], this length unit is approximately 98 kpc. This would correspond to a large background comoving initial overdensity size of $a_0\, k_J(\epsilon_{H\mathbf{i}})^{-1} \simeq 107$ Mpc.[19] Figs. 3.1-3.3 show the numerical results for $\bar{P}$ with the procedure, initial conditions and parameters given above, for three different values of σ.

The first case, $\sigma = 10$ (Fig. 3.1), corresponds to a super–Jeans length, hence unstable, initial perturbation. Figs. 3.1(a), (b) show the numerical results for the evolution of the perturbation $-\bar{P}$ as a function of the scale factor at several values of R, and over the whole range of radii R for increasing values of a, respectively. As expected, this perturbation is unstable and remains so by growing at all times, the pressure gradient being insufficient to prevent the collapse of the structure.

[19] Note that $k_J(\epsilon_{H\mathbf{i}})^{-1}$ defines an initial instability 'scale' only in terms of Lagrangian coordinates, *e.g.*, in terms of R. This means that the corresponding 'background–comoving' distance, $a(t)k_J(\epsilon_{H\mathbf{i}})^{-1}$ evaluated at present time, does not coincide with the present–day physical size of an object that would initially have been of this scale, as such a size must be evaluated using the actual, deformed, spatial metric. (See previous footnote.) It may be seen as a rough estimate of this size where the deformations $G^{(1)}_{ab}$, P^a_i are fully neglected in the evaluation of the integrated spatial line element.

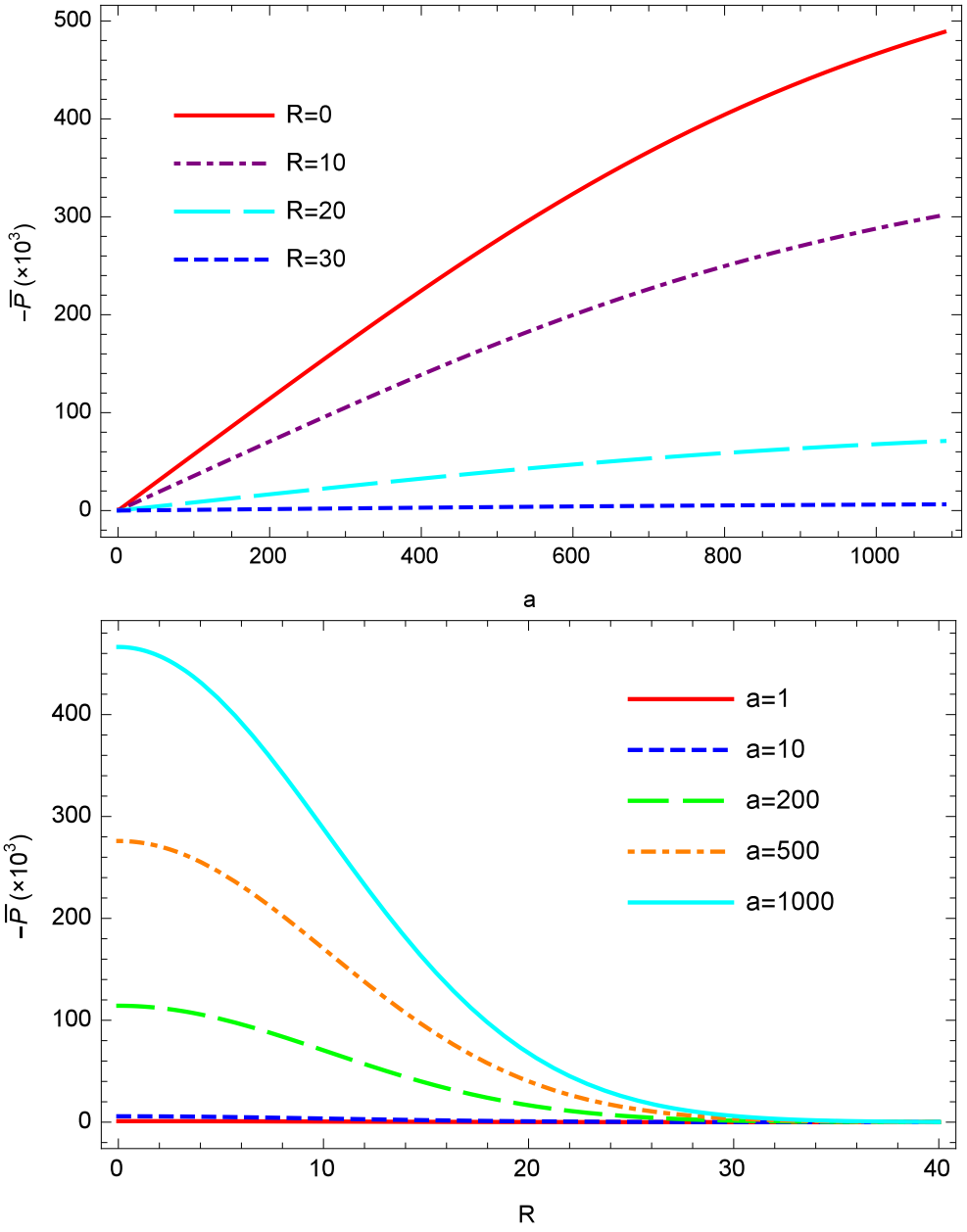

Figure 3.1: Numerical solution for the first–order trace $-\bar{P}$ in Lagrangian space, for an initial spherical Gaussian overdensity with a peak amplitude of 10^{-3} at $R = 0$ and a standard deviation σ such that $k_J(\epsilon_{Hi})\,\sigma = 10$. (a *Top*). Evolution of $-\bar{P}$ as a function of a for fixed values of the Lagrangian radius R. From top to bottom: $R = 0$, 10, 20 and 30. (b *Bottom*). Spatial variation of $-\bar{P}$ with R, for several values of the background scale factor. From bottom to top: $a = 1$, 10, 200, 500 and 1000. The perturbation strongly grows over time, indicating that the structure is collapsing.

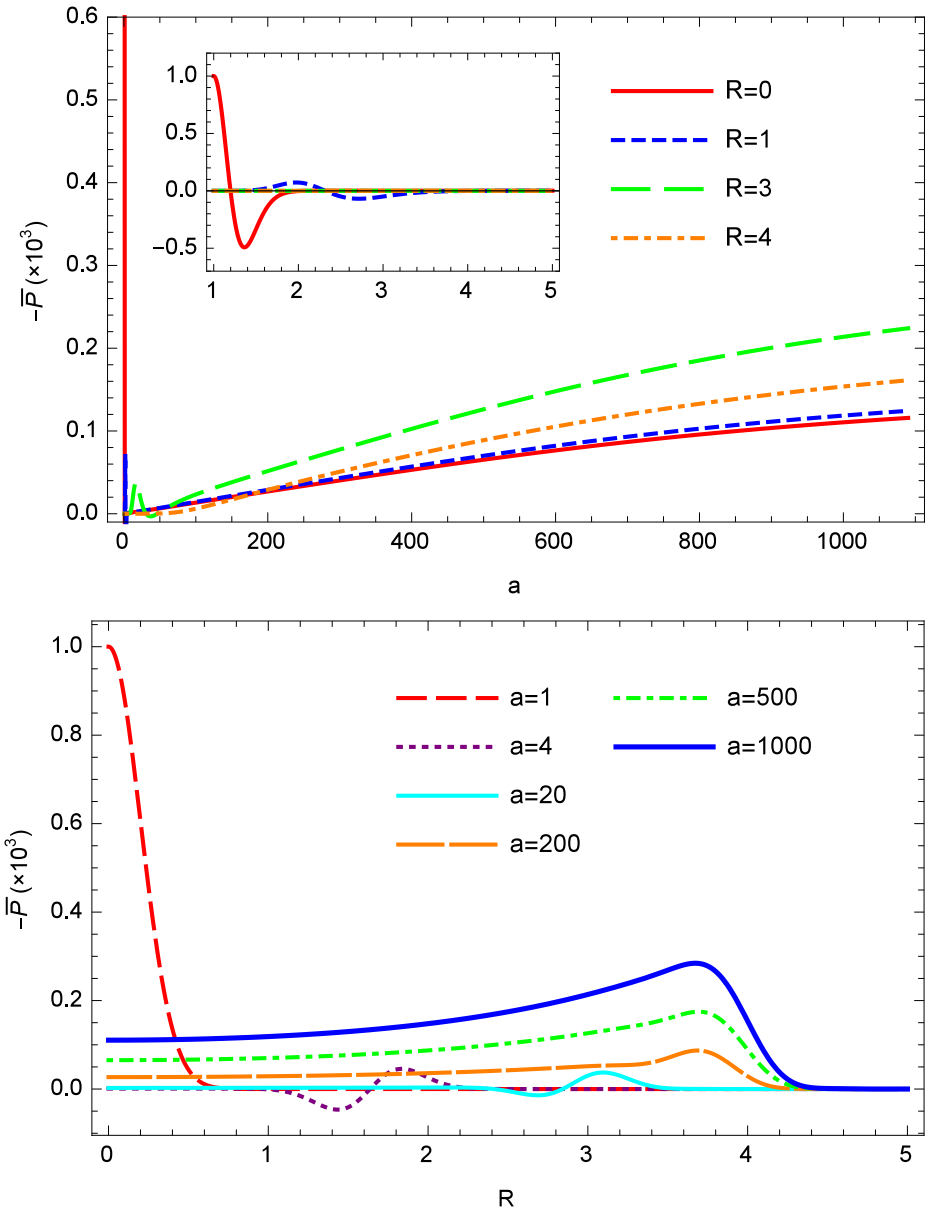

Figure 3.2: Numerical solution for the first–order trace $-\bar{P}$ in Lagrangian space, for an initial spherical Gaussian overdensity with a peak amplitude of 10^{-3} at $R = 0$ and a standard deviation σ such that $k_J(\epsilon_{H\mathbf{i}})\,\sigma = 0.2$. (a *Top*). Evolution of $-\bar{P}$ as a function of a at fixed distance R. From top to bottom at $a = 1000$: $R = 3$, $R = 4$, $R = 1$ and $R = 0$. The inset panel shows a detail of the early evolution (small values of a), where only the $R = 0$ (solid line) and $R = 1$ (dashed line) are visibly nonzero. (b *Bottom*). Spatial variation of $-\bar{P}$ with the Lagrangian radius, for several values of the background scale factor. The structure is first damped and spread out by the Lagrangian pressure gradient, before starting to grow back after the critical wavenumber $a\,k_J(\epsilon_H)$ has increased, as the perturbation enters the unstable regime.

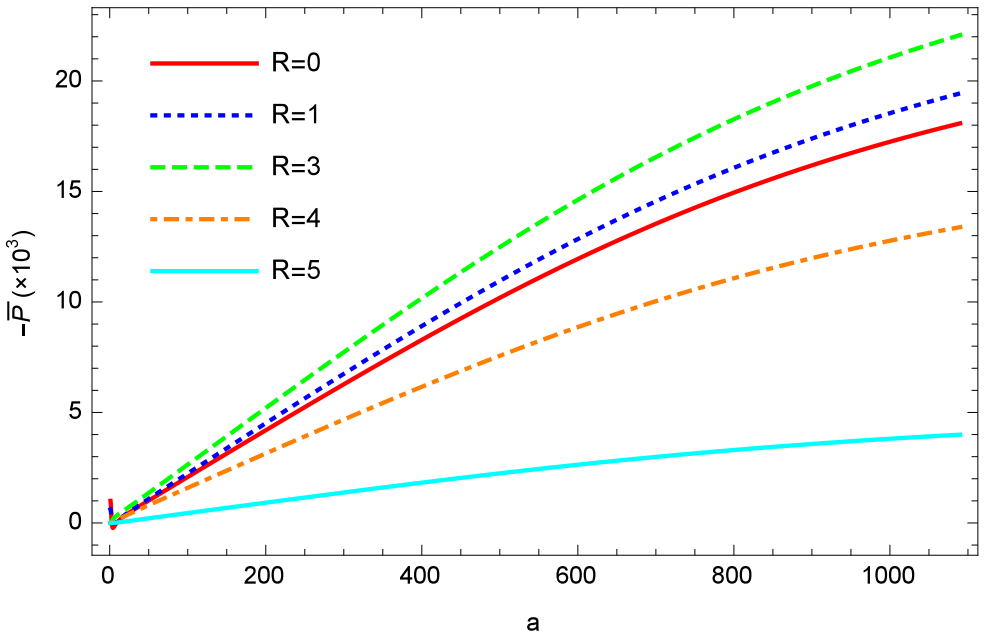

(a)

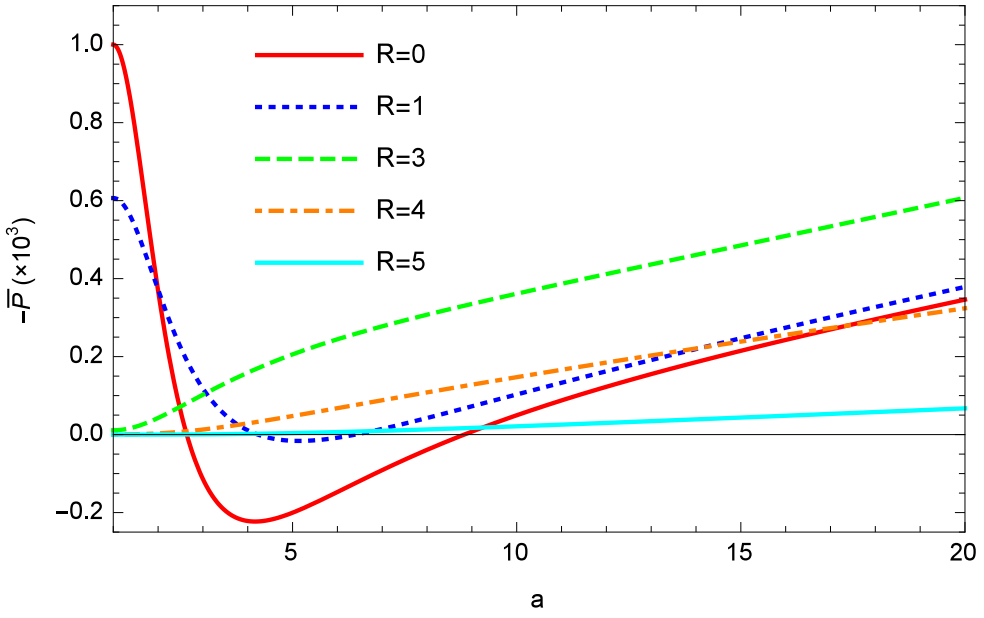

(b)

Figure 3.3: *Continued in the next page.*

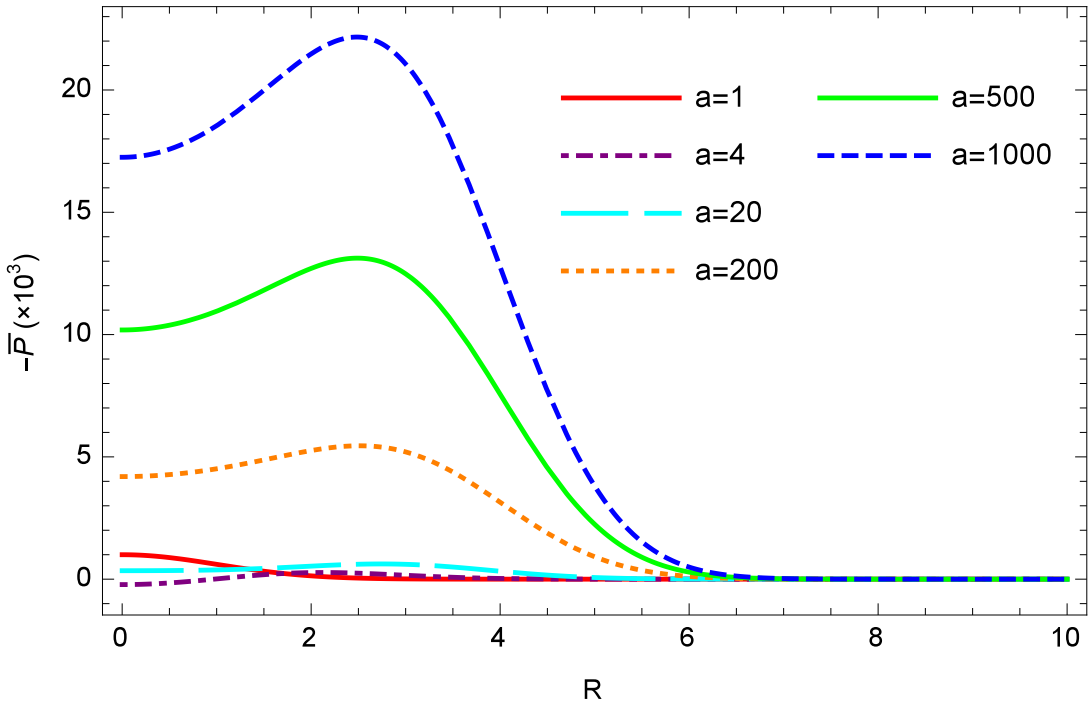

(c)

Figure 3.3: Numerical solution for the first–order trace $-\bar{P}$ in Lagrangian space, for an initial spherical Gaussian overdensity with a peak amplitude of 10^{-3} at $R = 0$ and a standard deviation σ such that $k_J(\epsilon_{Hi})\,\sigma = 1$. (a) and (b). Evolution of $-\bar{P}$ as a function of a at a given distance R, for late and early times, respectively. From top to bottom at $a = 1000$ for (a): $R = 3$, $R = 1$, $R = 0$, $R = 4$, $R = 5$; same order for (b) at $a = 20$. (c). Spatial variation of $-\bar{P}$ with R, for fixed values of the background scale factor. From top to bottom at $R = 0$: $a = 1000$, $a = 500$, $a = 200$, $a = 1$, $a = 20$, $a = 4$. The behaviour is rather similar to the previous case of $k_J(\epsilon_{Hi})\,\sigma = 0.2$; as expected, the unstable regime is, however, reached sooner, and the perturbation then grows similarly to the case of $k_J(\epsilon_{Hi})\,\sigma = 10$, up to much above its initial amplitude.

The evolution is similar to the dust case with the fast onset of a linear growth of the perturbation with a before a late–time slow down due to the presence of Λ.

The second case, $\sigma = 0.2$ (Fig. 3.2), illustrates the opposite situation of an initially sub–Jeans length perturbation. Figs. 3.2(a),(b) show the numerical solution for $-\bar{P}$ in this situation along the same reasoning as for Figs. 3.1(a),(b). At the early stage, the pressure gradient dominates and opposes the gravitational collapse. The perturbation behaves as an acoustic wave and is damped as it propagates away from the initial peak at $R = 0$. However, the instability wavenumber $a\, k_J(\epsilon_H)$ quickly starts increasing over time (cf., Fig. 3.4). That is why around $a = 50$ to 100 the perturbation starts to grow as its typical wavelength ends up below the critical value and it enters the unstable regime. The peak of this growing structure remains at a mostly stationary Lagrangian position, at $R \simeq 3.7$, while its amplitude still remains small and below the initial value $-\bar{P}(a = 1, R = 0) = 10^{-3}$ up to present time ($a \simeq 1090$).

For comparison we also consider the special case where the initial scale lies at the stability threshold, $\sigma = 1$. The evolution of the corresponding solution for $-\bar{P}$ with a at several radii is shown in Figs. 3.3(a),(b), with the latter highlighting the early evolution ($1 \leq a \leq 20$). Fig. 3.3(c) shows the spatial dependence of $-\bar{P}$ with R at some values of the scale factor. The behaviour of the perturbation in this case is indeed intermediate, with an initial acoustic damping and propagation away from $R = 0$ similarly to the $\sigma = 0.2$ case, but more rapidly entering an unstable regime, after $a \simeq 5$. The amplitude of the perturbation then starts growing with a dust–like behaviour up to beyond 20 times its initial value at present time, with a shifted peak as in the $\sigma = 0.2$ case, that stays around $R \simeq 2.5$. The results obtained here for different values of σ are in agreement with the expectation that the larger the initial perturbation scale, the sooner the structure will collapse due to a weaker pressure, and the larger the amplitude of the pressure will grow until the present epoch.

3.3.2.3 Evaluating the nonlinear density contrast

As we recalled above, even the first–order Lagrangian perturbation scheme allows one to probe part of the nonlinear regime in the evaluation of observable quantities. This involves extrapolating these observables as exact, nonlinear functionals

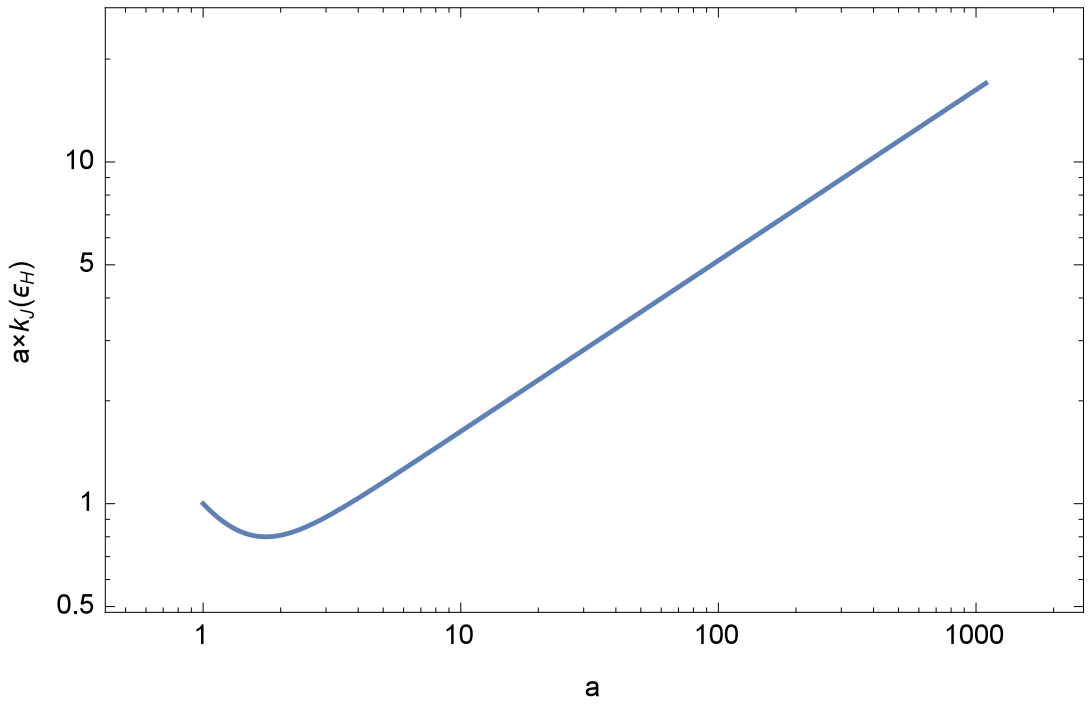

Figure 3.4: Evolution of the instability wavenumber $a\, k_J(\epsilon_H)$ with the scale factor a for the polytropic EoS considered here. As this wavenumber only depends on the background by construction, this result applies to all examples considered in this subsection 3.3.2.

of the deformation field, the latter being evaluated as a solution to its first–order evolution equations and constraints. Adopting this procedure for the rest mass density we evaluate it as the exact integral to the rest mass conservation equation (3.17):

$$\varrho = \frac{\varrho_{\mathbf{i}}}{J} \quad ; \quad J = \det(\eta^a{}_i) = a^3 \det(\delta^a{}_i + P^a{}_i) \,, \tag{3.153}$$

where P^a_i are the components of the deformation field. The density contrast δ is then deduced from the above:

$$\delta \equiv \frac{\varrho - \varrho_H}{\varrho_H} = \frac{\varrho_{\mathbf{i}}}{\varrho_{H\mathbf{i}} a^{-3} J} - 1 \quad ; \quad a^{-3} J = \det(\delta^a{}_i + P^a{}_i) \,, \tag{3.154}$$

and it is evaluated by replacing P^a_i by the first–order solution. Using the polytropic EoS with the values of γ, κ and A adopted here, the lapse may be computed

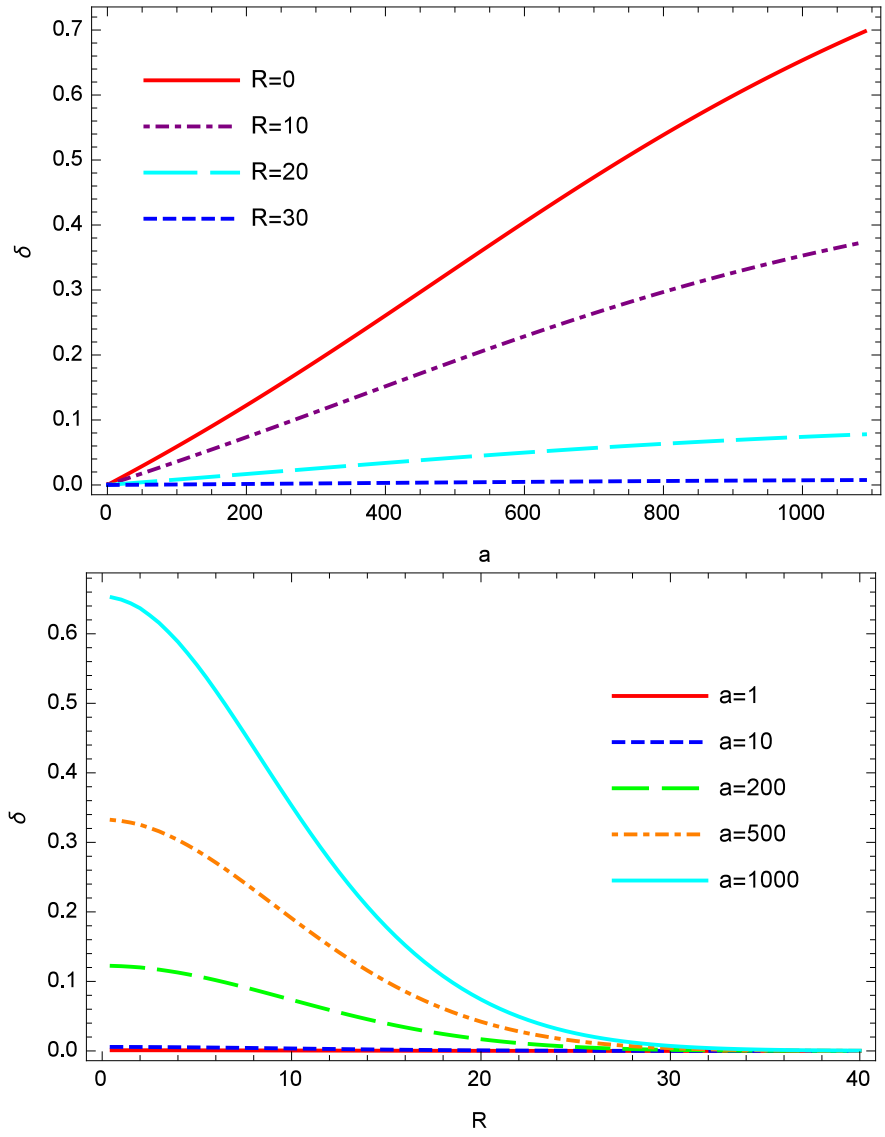

Figure 3.5: Numerical evaluation of the nonlinear density contrast δ as extrapolated from the first–order Lagrangian perturbation, where the initial $-\bar{P}$ is the same spherical Gaussian field as for Fig. 3.1, with peak value of 10^{-3} and $k_J(\epsilon_{Hi})\,\sigma = 10$. (a *Top*). Evolution of δ with the background scale factor at fixed distances R. From top to bottom: $R = 0$, 10, 20 and 30. (b *Bottom*). Spatial variation of δ with the Lagrangian radius, for given values of a. From bottom to top: $a = 1$, 10, 200, 500 and 1000. The overall behaviour of δ is similar to the results of Fig. 3.1 for the first–order $-\bar{P}$ in the same situation, but the extrapolated density contrast grows faster at late times near the $R = 0$ maximal overdensity. Additional nonlinear effects concerning the comparison with a standard perturbation approach, not studied here, could also be made visible by using instead as the x–axis for (b) the actual spatial metric distance to the $R = 0$ fluid element (as an 'Eulerian radius'), altering the spatial dependence. (See the discussion in section 3.3.2.4.)

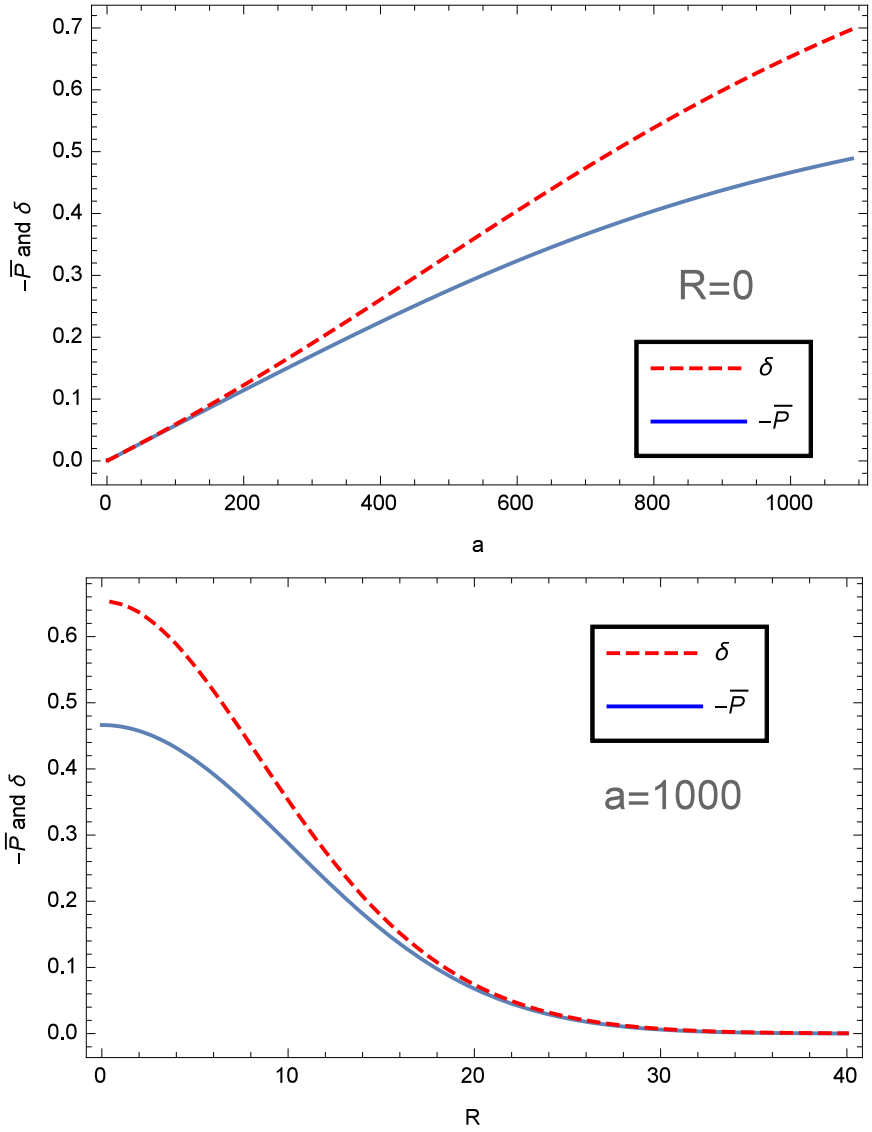

Figure 3.6: Comparison of the extrapolated nonlinear density contrast δ (dashed line) with the first–order solution for the sign–reverted deformation trace $-\bar{P}$ (solid line) within the same setting as Figs. 3.1 and 3.5. (a *Top*). Comparison of the evolution of both quantities as a function of a at the centre of the overdensity ($R = 0$). (b *Bottom*). Comparison of the spatial variation of both quantities with R at a late time ($a = 1000$). In this situation, the perturbation grows large enough to enter the nonlinear regime and to render the time evolution and spatial behaviour of the extrapolated δ clearly deviate from those of $-\bar{P}$.

from

$$N = \frac{\varrho}{\epsilon + p} = \frac{\varrho}{\varrho + \frac{\gamma}{\gamma-1}\kappa\varrho^{\gamma}} = \frac{1}{1 + \frac{5}{3}(1+\delta)^{2/3}\, a^{-2}} \,, \tag{3.155}$$

with δ expressed from the deformation field as above. This formula shows that the lapse is 1 in empty regions ($\delta = -1$) and decreases with increasing density contrast at a given time. The deviation $(1 - N)$ rapidly decreases over time as $\propto a^{-2}$, with late times values of order 10^{-6} (when $a \simeq 1000$), as long as δ remains at most of order unity.

We will now illustrate this process for our polytropic EoS by two examples. Note that this evaluation requires the knowledge of all components of the deformation field, including the traceless part. We specify procedures in Appendix B to obtain a particular (gravitoelectric) solution for the first–order traceless part from the initial conditions for the trace in specific cases. These procedures have been used to determine a consistent solution for the full deformation field in the examples below. We have also made use of the fact that the initial density $\varrho_{\mathbf{i}} = F(\epsilon_{H\mathbf{i}}\,[1+\delta\epsilon_{\mathbf{i}}])$ is well approximated by $F(\epsilon_{H\mathbf{i}})(1+\alpha_{H\mathbf{i}}\,\delta\epsilon_{\mathbf{i}}) = \varrho_{H\mathbf{i}}(1-\bar{P}_{\mathbf{i}})$ for a small, still linear, initial density perturbation (with $\alpha_{H\mathbf{i}} = 3/4$ for the chosen EoS parameters) for the evaluation of δ.

3.3.2.3.1 Localized overdensity:

Let us first retain the 'spherical' initial overdensity example studied thus far in this section, with the initial conditions for the trace given by (3.151), with $c_{\mathbf{i}} = 10^{-3}$, and $U = 0$. The first–order solution for the trace in this situation has been determined above, and is complemented by a gravitoelectric solution for the first–order traceless part through the use of the procedure shown in Appendix B.2 that directly applies to this case. The determinant J is then computed from this solution as in Appendix B.4, giving δ from Eq. (3.154).

Note that when all components of the deformation field are very small, *i.e.*, when it lies fully in the linear regime, then the extrapolated δ remains quantitatively close to $-\bar{P}$, which corresponds to its expansion at first order in the deformation field. This is the case in the initially stable or marginally stable cases $\sigma = 0.2$ and $\sigma = 1$, where the initial acoustic damping of the perturbation keeps its amplitude small up to the present time despite the late–time growth. In both of these cases, the resulting density contrast indeed remains indistinguishable

from the value of $-\bar{P}$ already depicted above (Figs. 3.2–3.3).

We will consequently focus from now on on the case $\sigma = 10$, where the unstable deformation reaches into the mildly nonlinear regime before the present time, as can be seen for the trace (whose amplitude reaches about 0.5 at the present epoch). Figs. 3.5(a),(b) show the result of the nonlinear evaluation of the density contrast in this situation, as a function of a at given radii R, and as a function of the radius at several moments in its evolution, respectively. Although the general behaviour is roughly similar to that of $-\bar{P}$ (*cf.* Fig. 3.1), nonlinear effects are visible in the amplified growth of δ at late times near $R = 0$, with a maximal overdensity reaching about 0.7 at present. This nonlinear deviation of the density contrast functional with respect to its first–order estimate $-\bar{P}$ is made explicit by the direct comparison of the peak ($R = 0$) amplitude evolution of δ and $-\bar{P}$ as a function of the background scale factor in Fig. 3.6(a). The spatial dependence on R of both quantities at late times, compared in Fig. 3.6(b) at $a = 1000$, is also visibly affected by the amplified growth of the density contrast where $\bar{P}$ is no longer small, *i.e.*, around $R = 0$.

3.3.2.3.2 Lagrangian plane–wave:

The second toy model we consider is that of a single Lagrangian plane–wave deformation. The choices of background parameters and the length unit ($k_J(\epsilon_{H\mathbf{i}}) = 1$) are unchanged. The initial perturbation is now chosen to be

$$-\bar{P}_{\mathbf{i}} = c_{\mathbf{i}} \cos(KX) \quad ; \quad U = 0 \,, \tag{3.156}$$

where we will again take $c_{\mathbf{i}} = 10^{-3}$ as an initial amplitude. This situation corresponds to an initially stationary plane wave in the given Lagrangian coordinate set,[20] $-\bar{P}_{\mathbf{i}} = c_{\mathbf{i}} \cos(\delta_{ij} K^i X^j + \phi_0)$ with $\phi_0 = 0$ and a wave–vector $\mathbf{K}$ along the

[20] Similarly to the interpretation of R for the previous example, it is important to keep in mind that the perturbation we are considering here only has a sinusoidal plane–wave dependence in the chosen Lagrangian coordinates X^i. It would have a different functional dependence in terms of actual physical (metric) spatial distance between two points on a given hypersurface $t = const$. One expects for instance, at a given late time t and along a given spatial geodesic line, the distance between the successive perturbation nodes at $KX = -\pi/2$ and $KX = \pi/2$ (surrounding a collapsing overdensity) to be shorter than the distance between the nodes at $KX = \pi/2$ and $KX = 3\pi/2$ (surrounding an expanding underdensity), despite all nodes being equally separated in terms of the Lagrangian coordinate X.

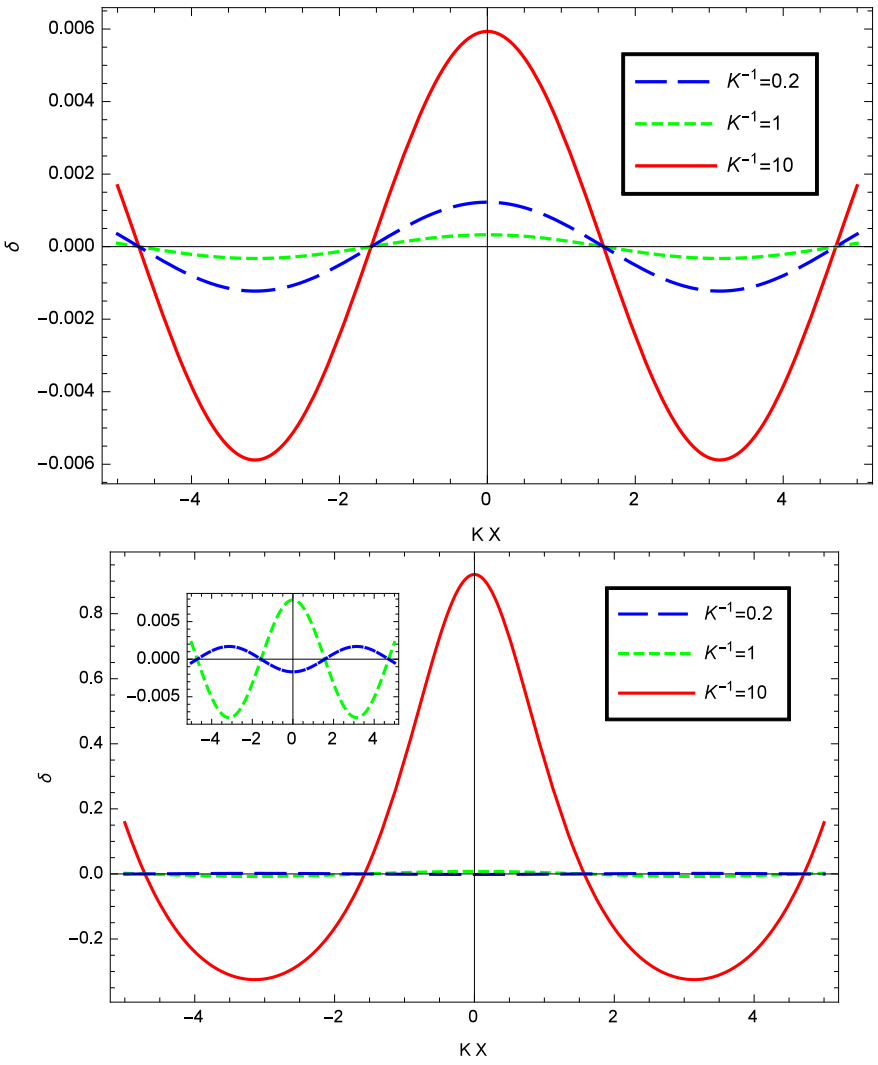

Figure 3.7: Numerical evaluation of the nonlinear density contrast δ as extrapolated from the first–order Lagrangian perturbation. The first–order deformation trace is taken as a plane–wave in Lagrangian coordinates of wave–vector $\mathbf{K}$ (of norm K) along the X coordinate, $-\bar{P} \propto \cos(KX)$, of initial amplitude 10^{-3}. The result is shown at a given time as a function of KX for three possible values of K, which is expressed in units $k_J(\epsilon_{H\mathbf{i}}) = 1$. (a *Top*). At $a = 10$, for $K = 0.1$ ($K^{-1} = 10$), $K = 5$ ($K^{-1} = 0.2$) and $K = 1$ by order of decreasing amplitude. (b *Bottom*). At $a = 1000$, for $K = 0.1$ ($K^{-1} = 10$), $K = 1$ and $K = 5$ ($K^{-1} = 0.2$) by order of decreasing amplitude. The side panel displays the (otherwise barely visible) latter two curves on a different vertical scale. The most unstable overdensity, for $K^{-1} = 10$, displays a non–sinusoidal asymmetric shape at late times as it reaches the mildly nonlinear regime. This shape would be further nonlinearly modified, *via* a different x–axis dependence, if this axis were expressed alternatively in terms of an Eulerian–type, regularly spaced (in terms of spatial metric distances), x coordinate.

first coordinate X, with components $K^i = (K, 0, 0)$. The first–order trace solution then remains in this plane wave mode form in the Lagrangian coordinates at all times, $\bar{P} = \hat{P}_{\mathbf{K}}(t)\cos(KX)$. The amplitude $\hat{P}_{\mathbf{K}}(t)$ evolves according to the ordinary differential equation (B.2) which is solved by numerical integration for a given wavenumber K. A gravitoelectric solution for the traceless part is then determined along the lines of Appendix B.1, where the relevant amplitude $\hat{Q}_{\mathbf{K}}(t)$ is again numerically evaluated, knowing $\hat{P}_{\mathbf{K}}(t)$, through its defining time–integration formula (B.3). From these, one can calculate the density contrast in the same way as in the previous example, with the determinant J evaluated as detailed in Appendix B.4.

Here we again study three cases distinguished by their wavenumber in direct analogy to the previous example, with K^{-1} playing the role of the characteristic length σ. We accordingly choose $K^{-1} = 0.2$, $K^{-1} = 1$ and $K^{-1} = 10$, which at the initial time are stable, marginally stable and unstable, respectively. The corresponding spatial dependence of δ as a function of KX for the three wavenumber choices is shown at an early time ($a = 10$) in Fig. 3.7(a), and at a late time ($a = 1000$) in Fig. 3.7(b). In this situation, in the first two cases the components of the deformation field again remain small at all times, due to initial acoustic oscillations, and the density contrast accordingly follows the sinusoidal shape of $-\bar{P}$ at all times. This is also the case for the unstable mode $K^{-1} = 10$ at $a = 10$ when it is still in the linear regime. At $a = 1000$, however, this mode clearly deviates from this behaviour as its amplitude is no longer linear. In particular, an asymmetry develops between the under– and overdensity magnitudes as the latter is sharply amplified by the nonlinear evolution of δ.

3.3.2.4 Discussion

In both examples above, the Lagrangian scheme and the proposed extrapolation procedure exhibit nonlinear effects on the overdensity for unstable perturbations when they become large enough. The amplitude of large overdensities in these examples is clearly underestimated by evaluating the first–order expression $-\bar{P}$ instead of using the nonlinear extrapolation for δ.

An even higher initial overdensity amplitude could actually lead to a vanishing determinant $a^{-3}J$ at the maximum overdensity at a late enough time,

implying $\varrho \to \infty$ with deformation coefficients still of order 1. This situation corresponds to a shell–crossing, beyond which the first–order Lagrangian scheme in no longer valid. The presence of pressure can delay its occurrence by damping the perturbation.

An improvement of the perturbative scheme to account for further local nonlinear effects in the dynamical evolution, e.g., allowing for a nonlinear coefficient to define the Jeans length is needed, however, to fully circumvent this problem. Indeed, velocity dispersion effects may in principle allow us to model the multistream regime, and the stabilization of structure formation in the form of virialization, avoiding shell–crossings [Buchert, 2000b; Buchert and Domínguez, 2005].

We emphasize that the current Lagrangian perturbation scheme already contains another effect of nonlinear structure evolution, which lies in the exact propagation of the spatial coordinates used along the fluid flow lines. This is analogous to the inclusion of quadratic convection terms within linear Lagrangian time derivatives in the Newtonian framework.[21]

Let us suggest a procedure that would be required to make these effects explicit also in the relativistic context; its concrete application is beyond the scope of this work. Eulerian–like coordinates could first be recovered, at least along a given spatial geodesic direction, by labelling points at equal intervals of spatial metric distances. This would involve solving for the initial metric components G_{ab} such that their Ricci tensor is consistent with the initial conditions (3.113)–(3.114) for given initial deformation field data, and then functionally evaluating and integrating the line element as given by (B.18) from the first–order solution for $P^a_{\ i}$. The resulting length, as a function of a Lagrangian coordinate, could then be used as an estimate of the Eulerian coordinate distance. Finally, this relation would have to be numerically inverted so that a given Lagrangian function obtained through the Relativistic Zel'dovich Approximation, such as $\varrho(X^i)$, could be expressed as a function of the Eulerian coordinate x estimated by this procedure. A different functional dependence on this spatial distance

[21] In addition to the time derivatives being taken at different fixed spatial coordinates, a difference also comes from the spatial derivative operators, such as the Laplacian Δ_0 appearing in the trace master equation (3.84), being expressed in terms of Lagrangian coordinates and thus differing from the corresponding Eulerian operators. (See Buchert and Adler [1999] for the explicit transformation.)

(which may be normalized by $a(t)$ to become a background–comoving distance), as compared to the fluid–comoving coordinates X^i, would thus include nonlinear effects of the fluid–propagation–dependent coordinate transformation. Recall, however, that Eulerian observers do not exist in a relativistic (intrinsic) description and, strictly, a coordinate transformation to Eulerian space can only be conducted after the Minkowski Restriction of the relativistic solution has been executed.

CHAPTER 4

Summary

4.1 Conclusion

In recent decades, Lagrangian Perturbation Theory (LPT) has been proved to be a powerful and practical tool in many different applications. The intrinsic nonlinearity encoded in the transformation between the Lagrangian coordinates and the Eulerian coordinates ensures the possibility of LPT modelling large scale structure formation beyond the linear regime. Even in a perturbative approach, the first-order solution of LPT will recover much more nonlinear information when mapped into the Eulerian space of Newtonian cosmologies. Higher-order perturbations will subsequently add more substructures to the description of structure formation. With these advantages for studies of large scale structure formation, in this thesis we have applied the LPT to two different cases.

In Chapter 2, we first reviewed the adhesive approach. Such an approach has been constructed to overcome the shortcomings of the LPT, namely the breakdown of LPT at the epoch of formation of caustics in the density field. By modelling the velocity dispersion of multi-stream flow as dynamical pressure terms, the caustic structure still forms but with a finite density field. Thus we can follow the structure formation process beyond shell-crossing.

Afterwards, we investigated the dynamics of a fluid mixture in Newtonian cosmologies, which is composed of two different fluid species. Each species is assumed to be a dust fluid. Both species are coupled to each other only by gravity with different 4-velocities and different density fields. We then developed the corresponding adhesive approach for such a system.

We have assumed that the velocity dispersion of each species is small. The corrections to dust matter are then second-order, corresponding to the velocity

dispersion. We discussed the dynamical equations for such a fluid mixture and derived the solutions up to second-order. We found that for such a fluid mixture, in the perturbative approach the zeroth-order is no doubt the background term. The first-order term is the standard dust matter model. If we neglect third order and higher terms, then the second-order will introduce a new decaying mode, which decays more slowly than the standard decaying mode in the SPT. Up to second-order, the dynamical solution of the fluid mixture satisfies the Zel'dovich solution. But once we consider even higher orders, then it is expected that more substructures will be added. With the solution of the fluid mixture, we can also obtain the evolution of each species.

In Chapter 2, we also investigated a second method to study the dynamics of the fluid mixture. In this second method, we studied the evolution of the fluid element of each species, originating from the same initial position. We claimed that under specific conditions, the first method and the second method give the same results.

In Chapter 3 we have generalized the Lagrangian perturbation approach to the nonlinear evolution of inhomogeneous general relativistic universe models containing a single perfect fluid obeying a general barotropic equation of state. By choosing a suitable set of coframes, we obtained the master partial differential equations for the evolution of the trace and traceless parts of the first–order deformation field that reduce to the corresponding equations in the dust case. The trace part also matches the Newtonian limit of the corresponding Lagrangian perturbation problem.

We discussed the procedure proposed in previous papers [Buchert and Ostermann, 2012; Alles et al., 2015; Al Roumi et al., 2017] of how to find the solution for perturbations that propagate in the perturbed space, and applied this procedure to specific toy models, illustrating the mildly nonlinear evolution of the density contrast. We also discussed the limits of a first–order Lagrangian scheme, and we proposed ideas for a nonperturbative generalization, which is needed especially in application to cases where the pressure term is taken to model multistreaming beyond the mildly nonlinear regime.

4.2 Discussion and outlook

Let us now turn to the limitations of what has been studied thus far. In both cases we have only considered toy models as yet. Realistic large-scale structure formation includes complications that go beyond such toy models.

In Chapter 2 only the first two orders of solutions have been derived and displayed. The higher orders which could produce much more substructures have been ignored. Such omissions may be unacceptable depending on the precision with which one wants to study the formation and evolution of large-scale structures. In this case we only applied our method in an Einstein-de Sitter universe. An obvious next step is to generalize this to a ΛCDM universe. Furthermore, it would be interesting to test such an approach with N-body simulations.

The work in Chapter 3 is a first-step investigation of the perturbative scheme to account for the local nonlinear effects in the dynamical evolution in relativistic universes with an irrotational perfect fluid. Building on this work we should further study the dynamical evolution of nonlinear structures in a relativistic universe consisting of two different fluids: *e.g.*, baryons and dark matter. We hope that the tools developed here will assist in future development of an approach to describe the evolution of large-scale structures in our Universe in a better and more precise way.

APPENDIX A

Derivation of comoving velocity dispersion

In an Eulerian coordinate system, Eq. (2.58) indicates that one can absorb the quantity $\mathbf{j}_\alpha$ into the new velocity dispersion field $\tilde{\boldsymbol{\mathcal{P}}}_\alpha$. This new field describes the velocity dispersion around the mean velocity $\boldsymbol{u}$ of the mixture. It can be shown that one can define a similar new field in the comoving coordinate system, namely

$$\Pi_{\alpha ij} = \tilde{\Pi}_{\alpha ij} - \frac{1}{\varrho_\alpha} j_{\alpha i}\, j_{\alpha j} - \left(j_{\alpha i} u_j + j_{\alpha j} u_i\right), \tag{A.1}$$

where

$$\begin{aligned} \tilde{\Pi}_{\alpha ij}\left(\boldsymbol{q}, t\right) &= \frac{m_\alpha}{(aL)^3} \sum_\alpha W\left(\frac{\boldsymbol{q} - \boldsymbol{q}_\alpha^{(i)}}{L}\right)\left[u_{\alpha i}^{(i)} u_{\alpha j}^{(i)} - u_i u_j\right] \\ &= \frac{m_\alpha}{(aL)^3} \sum_\alpha W\left(\frac{\boldsymbol{q} - \boldsymbol{q}_\alpha^{(i)}}{L}\right) u_{\alpha i}^{(i)} u_{\alpha j}^{(i)} - \varrho_\alpha u_i u_j. \end{aligned} \tag{A.2}$$

The partial time derivative of $\tilde{\Pi}_{\alpha ij}$ can be determined by direct calculation, with the result

$$\begin{aligned} \partial_t \tilde{\Pi}_{\alpha ij} + 5H\tilde{\Pi}_{\alpha ij} =& 2W_{\alpha(ij)} + \frac{1}{a}\partial_k j_{\alpha k}\, u_i u_j \\ &- \frac{\varrho_\alpha}{\varrho} \sum_\alpha \left(2F_{\alpha(i} u_{j)} - \frac{2}{a}\partial_k \tilde{\Pi}_{\alpha k(i} u_{j)}\right) - a^{-1}\partial_k L_{\alpha ijk}, \end{aligned} \tag{A.3}$$

where $F_{\alpha i}$ is defined by (2.75) and

$$W_{\alpha ij} \equiv \frac{m_\alpha}{(aL)^3} \sum_i W\left(\frac{\boldsymbol{q} - \boldsymbol{q}_\alpha^{(i)}}{L}\right)\left(w_{\alpha i}^{(i)} u_{\alpha j}^{(i)} - w_i u_j\right), \tag{A.4}$$

$$L_{\alpha ijk} \equiv \frac{m_\alpha}{(aL)^3} \sum_i W\left(\frac{\boldsymbol{q} - \boldsymbol{q}_\alpha^{(i)}}{L}\right)\left(u_{\alpha i}^{(i)}\, u_{\alpha j}^{(i)}\, u_{\alpha k}^{(i)} - u_i u_j u_k\right). \tag{A.5}$$

To close the hierarchy of Eq. (A.3) we have to consider an approximation for the new tensor field $\boldsymbol{L}_\alpha$ defined in Eq. (A.5). The simplest case is to assume $\sum \tilde{\boldsymbol{L}}_\alpha = 0$ where [Buchert and Domínguez, 1998]

$$\tilde{L}_{\alpha ijk} = L_{\alpha ijk} - u_k \tilde{\Pi}_{\alpha ij} - u_j \tilde{\Pi}_{\alpha ik} - u_i \tilde{\Pi}_{\alpha jk} - LL_{\alpha ijk}, \tag{A.6}$$

$$LL_{\alpha ijk} = 3\varrho_\alpha u_i u_j u_k - \varrho_\alpha u_{\alpha i} u_j u_k - \varrho_\alpha u_i u_{\alpha j} u_k - \varrho u_i u_j u_{\alpha k}, \tag{A.7}$$

$$\tilde{L}_{ijk} = L_{ijk} - u_k \tilde{\Pi}_{ij} - u_j \tilde{\Pi}_{ik} - u_i \tilde{\Pi}_{jk}, \tag{A.8}$$

and we have defined $L_{ijk} \equiv \sum L_{\alpha ijk}$ and $\tilde{L}_{ijk} \equiv \sum \tilde{L}_{\alpha ijk}$.

Under the assumption that $\boldsymbol{F}_\alpha = 0$, as in section 2.2.2.2, one finally obtains an evolution equation for $\tilde{\Pi}_{ij} \equiv \tilde{\Pi}_{\alpha ij} + \tilde{\Pi}_{\beta ij}$, *viz.*

$$\partial_t \tilde{\Pi}_{ij} + \frac{1}{a} u_k \partial_k \tilde{\Pi}_{ij} + 5H\tilde{\Pi}_{ij} + \frac{1}{a}\tilde{\Pi}_{ij}\,\partial_k u_k = -\frac{1}{a}\left(\tilde{\Pi}_{ik}\partial_k u_j + \tilde{\Pi}_{jk}\partial_k u_i\right). \tag{A.9}$$

Note that since the small scale inhomogeneities are irrelevant, in a rough approximation, $\sum \boldsymbol{W}_\alpha \approx 0$. However, care must be taken in implementing such an approximation.

The first assumption $\boldsymbol{F}_\alpha = 0$ means the mean field gravity is dominant. This corresponds to a "top-down evolution" of cosmological structure formation where scales below those of collapsing objects are relatively homogeneous. Such models usually refer to the case of hot dark matter, which can have a large velocity dispersion. But this scenario faces difficulties since the angular fluctuations in the temperature of the cosmic microwave background it predicts are too large relative to observations.

The "down-top evolution", on the other hand, describes a hierarchical clustering where the first structures are formed on a much smaller mass scales ($M \sim 10^5 - 10^6 M_\odot$) and then structures on larger scales are formed by the successive effects of gravitational instability [Coles and Lucchin, 2002]. In this case, both the velocity dispersion and the deviations from mean field gravity will be relevant.

The second assumption is that for each species $\boldsymbol{\Pi}_\alpha = p_\alpha(\varrho_\alpha)\,\boldsymbol{\delta}$, *i.e.*, the velocity dispersion is isotropic around the corresponding mean velocity field. Thus the velocity dispersion field $\tilde{\boldsymbol{\Pi}}_\alpha$ around the mean velocity of the mixture will not be isotropic. The effects of relative motion between species are described

by the anisotropic parts of $\tilde{\mathbf{\Pi}}$, and extra terms for the isotropic parts. Such approximations are mathematically simple but not a good description of realistic problems.

The third approximation is that we have used is $\sum \boldsymbol{W}_\alpha = 0$. This actually can be seen as a consequence of the first approximation. The irrelevance of small scale inhomogeneities means roughly $\boldsymbol{w}_\alpha^{(i)} \sim \boldsymbol{w}$, so $\boldsymbol{W}_\alpha \sim \boldsymbol{w}\,\boldsymbol{j}_\alpha$ and finally $\sum \boldsymbol{W}_\alpha \sim 0$.

The fourth approximation, where $\tilde{\boldsymbol{L}} = 0$, is based on the assumption that the velocity dispersion around the mean velocity of mixture is small. In other words, $\boldsymbol{j}_\alpha$ is then relatively small. We are then investigating a mixture composed of two species, with a small relative speed between the species.

All of these approximations limit possible applications of the approach we discussed here to the complicated problem of a realistic cosmology. Nonetheless we will adopt all these approximations as a first step towards a more sophisticated framework.

APPENDIX B

Examples of solutions for the gravitoelectric traceless part

In this work we will not attempt to find the general solution of equations (3.95)–(3.96) for the traceless part. We will, however, discuss a procedure for finding one possible solution, which will be valid within the Lagrangian coordinates map for suitably chosen traceless–part initial conditions. For any barotropic EoS, this yields one example of a full solution for all components of the deformation field $P^a_{\ i}$. It can then be substituted into exact nonlinear formulae to extrapolate functionals of the coframes such as metric distances or the rest mass density, following the reasoning of the Relativistic Zel'dovich Approximation as defined for the dust case in [Buchert and Ostermann, 2012]. To find such an example solution, we will focus on the gravitoelectric part which is directly coupled to the trace, and accordingly we set the gravitomagnetic part to zero.

B.1 Case of a comoving plane wave

Let us first assume that the first–order trace solution can be written as a single plane wave mode in the given set of Lagrangian spatial coordinates X^i:

$$\bar{P}(t, X^i) = \varphi(\mathbf{K}\cdot\mathbf{X})\,\hat{P}_{\mathbf{K}}(t)\,, \tag{B.1}$$

for some constant Lagrangian wave vector $\mathbf{K}$, where $\mathbf{K}\cdot\mathbf{X} := \delta_{ij}K^iX^j$, and $\varphi(\mathbf{K}\cdot\mathbf{X}) = \cos(\mathbf{K}\cdot\mathbf{X}+\phi_0)$, for some constant phase ϕ_0. This form is a solution of the first–order trace master equation, if and only if $\hat{P}_{\mathbf{K}}(t)$ is a solution of the

ordinary differential equation

$$\frac{\mathrm{d}^2}{\mathrm{d}t^2}\hat{P}_{\mathbf{K}} + 2H(1-3\beta'(\epsilon_H))\,\frac{\mathrm{d}}{\mathrm{d}t}\hat{P}_{\mathbf{K}} - \mathcal{W}(t)N_H^2\,\hat{P}_{\mathbf{K}} = -a^{-2}N_H^2\,\beta'\left(\epsilon_H\right)K^2\,\hat{P}_{\mathbf{K}}\ , \tag{B.2}$$

with $K = (\delta_{ij}K^iK^j)^{1/2}$. Then $P = \bar{P} - \bar{P}_{\mathbf{i}} = \varphi(\mathbf{K}\cdot\mathbf{X})\,(\hat{P}_{\mathbf{K}}(t) - \hat{P}_{\mathbf{K}}(t_{\mathbf{i}}))$. Setting

$$\begin{aligned}\hat{Q}_{\mathbf{K}}(t) &= \int_{t_{\mathbf{i}}}^{t} N_H(t')\;\partial_t\left(\frac{\hat{P}_{\mathbf{K}}}{N_H}\right)(t')\;\mathrm{d}t' \\ &= \hat{P}_{\mathbf{K}}(t) - \hat{P}_{\mathbf{K}}(t_{\mathbf{i}}) - 3\int_{t_{\mathbf{i}}}^{t} H(t')\,\beta'(\epsilon_H)(t')\,\hat{P}_{\mathbf{K}}(t')\;\mathrm{d}t'\ ,\end{aligned} \tag{B.3}$$

the time integral of the momentum constraints (3.96) is

$$\Pi^i{}_{j|i} = \frac{2}{3}\hat{Q}_{\mathbf{K}}(t)K_j\,\varphi'(\mathbf{K}\cdot\mathbf{X})\ . \tag{B.4}$$

We now take $\Pi^i{}_j$ to be a purely longitudinal mode and get the following solution to the momentum constraints (with $K_j := \delta_{jl}\,K^l$):

$$\Pi^i{}_j = \left(\frac{K^iK_j}{K^2} - \frac{1}{3}\delta^i{}_j\right)\hat{Q}_{\mathbf{K}}(t)\,\varphi(\mathbf{K}\cdot\mathbf{X}) \tag{B.5}$$

$$= \left(\frac{K^iK_j}{K^2} - \frac{1}{3}\delta^i{}_j\right)\left(\frac{\hat{Q}_{\mathbf{K}}(t)}{\hat{P}_{\mathbf{K}}(t) - \hat{P}_{\mathbf{K}}(t_{\mathbf{i}})}\right)P(t,X^i)\ . \tag{B.6}$$

Substituting this form into the master equation (3.95) shows that it is indeed consistently a solution of both equations for the traceless part. This solution is a pure gravitoelectric one, amounting to setting the gravitomagnetic part to zero by a choice of vanishing gravitomagnetic traceless part of the initial conditions: $\Pi^i{}_j = {}^E\Pi^i{}_j$. Indeed, it is straightforward to show from the above formula that $2\,\Delta_0\Pi^i{}_j + \Pi^k{}_{l|k}{}^{|l}\,\delta^i{}_j - 3\,\Pi^i{}_{k|j}{}^{|k} = 0$, *i.e.*, this $\Pi^i{}_j$ obeys the defining relation (3.107) for the gravitoelectric part and does evolve according to (3.104).

Choosing this solution amounts to specifying the following (gravitoelectric) initial conditions:

$${}^{\mathrm{tl}}U^i{}_j = \left(\frac{K^iK_j}{K^2} - \frac{1}{3}\delta^i{}_j\right)\left(U + 3H_{\mathbf{i}}\,\beta'(\epsilon_{H\mathbf{i}})\,\alpha_{H\mathbf{i}}\,\delta\epsilon_{\mathbf{i}}\right)\ ; \tag{B.7}$$

$$
{}^{\mathrm{tl}}W^{i}_{\ j} = \left(\frac{K^{i}K_{j}}{K^{2}} - \frac{1}{3}\delta^{i}_{\ j}\right)\Big(W + 3H_{\mathbf{i}}\,\beta'(\epsilon_{H\mathbf{i}})\,U \\
+ 3\left[\partial_t(H\beta'(\epsilon_H))(t_{\mathbf{i}}) + 2\,H_{\mathbf{i}}^{2}\,\beta'(\epsilon_{H\mathbf{i}})\right]\alpha_{H\mathbf{i}}\,\delta\epsilon_{\mathbf{i}}\Big)\,. \tag{B.8}
$$

This is compatible with the set of constraints on the initial conditions given in section 3.2.5, in particular the initial momentum constraints (3.115) and Eq. (3.113), provided that the latter is used to specify the traceless part of the initial first–order Ricci tensor $\mathscr{T}^{i}_{\ j}$.

The corresponding full perturbation field $P^{i}_{\ j} = \Pi^{i}_{\ j} + \frac{1}{3}\delta^{i}_{\ j}P$ then reads:

$$
P^{i}_{\ j} = \frac{K^{i}K_{j}}{K^{2}}\left(\frac{\hat{Q}_{\mathbf{K}}(t)}{\hat{P}_{\mathbf{K}}(t) - \hat{P}_{\mathbf{K}}(t_{\mathbf{i}})}\right) + \frac{1}{3}\delta^{i}_{\ j}\left(1 - \frac{\hat{Q}_{\mathbf{K}}(t)}{\hat{P}_{\mathbf{K}}(t) - \hat{P}_{\mathbf{K}}(t_{\mathbf{i}})}\right)P\,. \tag{B.9}
$$

Note that the corresponding deformation 1–forms $P^{a}_{\ i} = \delta^{a}_{\ k}P^{k}_{\ i}$ are not exact due to the different time evolution of the trace and electric traceless parts. This contrasts with the dust case where a purely electric perturbation would lead to integrable coframes [Al Roumi et al., 2017], so that only the non–flat initial metric would prevent an Euclidean spatial metric at all times in that situation. By linearity of the equations, a solution for $\Pi^{i}_{\ j}$ can also be obtained when the trace is a finite sum of such plane waves, or the sum of the two time–evolution modes solutions of the evolution equation (B.2) for a given wave vector $\mathbf{K}$, simply by summing the corresponding solutions as given by (B.5).

B.2 Case of a spatially localized solution

We here assume either that the spatial slices are globally diffeomorphic to the Euclidean space $\mathbb{R}^3$, *i.e.*, that they can be covered by a single chart, or that the deformation field can be assumed to vanish outside a given chart. In either case it suffices to work within the Euclidean space spanned by the spatial coordinates in a given chart.

Let us now consider a spatially localized solution for the trace, *e.g.*, a local overdensity evolving from an initial Gaussian perturbation in terms of the given set of spatial Lagrangian coordinates, as studied in the numerical examples of section 3.3. More specifically, we require that the solution for the trace is always

a square–integrable function of the spatial coordinates in the chart, so that its Fourier transform in these coordinates can be performed and inverted. We can write accordingly:

$$\bar{P}(t, X^i) = \iiint e^{-i\mathbf{K}\cdot\mathbf{X}} \hat{P}(t, \mathbf{K}) \, \mathrm{d}^3\mathbf{K} \, , \tag{B.10}$$

where $\hat{P}(t, \mathbf{K})$ is a solution of the evolution equation (B.2) at fixed $\mathbf{K}$, with the initial conditions set by the forward Fourier transform in the chart coordinates:

$$\hat{P}(t_\mathbf{i}, \mathbf{K}) = -\frac{1}{(2\pi)^3} \alpha_{H\mathbf{i}} \iiint e^{i\mathbf{K}\cdot\mathbf{X}} \delta\epsilon_\mathbf{i}(\mathbf{X}) \, \mathrm{d}^3X \, ; \tag{B.11}$$

$$(\partial_t \hat{P})(t_\mathbf{i}, \mathbf{K}) = \frac{1}{(2\pi)^3} \iiint e^{i\mathbf{K}\cdot\mathbf{X}} U(\mathbf{X}) \, \mathrm{d}^3X \, . \tag{B.12}$$

Note that the above approach represents an alternative and complementary formulation of the method of solution presented in [Al Roumi et al., 2017] which formally replaces the Lagrangian coordinates by 'Eulerian' ones. In the present work it is applied in sections 3.3.1.2 and 3.3.2. The reformulation suggested here allows us to be more explicit about the required assumptions, as well as expressing the coordinate components of tensors such as $\Pi^i{}_j$ in a more convenient form. In both formulations, the use of plane–wave modes and flat–space Fourier transformations is sufficient since the Lagrangian first–order master equations to be solved only involve the metric–independent coordinate spatial derivatives $_{|i}$ and Laplacian $\Delta_0 = {}_{|i|j}\,\delta^{ij}$ as spatial derivative operators.

By linearity of the equations, a solution for the (gravitoelectric) traceless part is obtained by summation of the plane wave solutions for all Fourier modes:

$$\Pi^i{}_j = {}^E\Pi^i{}_j = \iiint e^{-i\mathbf{K}\cdot\mathbf{X}} \frac{K^i K_j}{K^2} \hat{Q}(t, \mathbf{K}) \, \mathrm{d}^3\mathbf{K} - \frac{1}{3} \delta^i{}_j \iiint e^{-i\mathbf{K}\cdot\mathbf{X}} \hat{Q}(t, \mathbf{K}) \, \mathrm{d}^3\mathbf{K} \, , \tag{B.13}$$

with

$$\hat{Q}(t, \mathbf{K}) = \int_{t_\mathbf{i}}^{t} N_H(t') \, \partial_t \left(\frac{\hat{P}(t, \mathbf{K})}{N_H(t)} \right)(t') \, \mathrm{d}t' \, . \tag{B.14}$$

Using this solution again implies a specific choice of initial conditions for the traceless deformation field (in particular taking it to be gravitoelectric) and for

the traceless part of the spatial Ricci tensor.

In the case of spherically symmetric initial conditions in the chart coordinates, *i.e.*, when $\delta\epsilon_{\mathbf{i}}(X^i)$ and $U(X^i)$ only depend on $R := (\delta_{ij}X^iX^j)^{1/2}$, their Fourier transform will also depend only on K. From the evolution equation (B.2), this feature is preserved over time, so that one can write $\hat{P}(t,\mathbf{K})$ as $\hat{P}(t,K)$ and consequently $\hat{Q}(t,\mathbf{K})$ as $\hat{Q}(t,K)$ and $\bar{P}(t,X^i)$ as $\bar{P}(t,R)$. The above solution for $\Pi^i{}_j$ can then be computed as

$$\Pi^i{}_j = \left(\frac{X^iX_j}{R^2} - \frac{1}{3}\,\delta^i{}_j\right) q(t,R)\ , \tag{B.15}$$

with $X_j = \delta_{jk}X^k$ and

$$\begin{aligned} q(t,R) = {}& \frac{4\pi}{R}\int_0^\infty K\sin(RK)\,\hat{Q}(t,K)\,\mathrm{d}K \\ & - \frac{4\pi}{R^3}\int_0^\infty\left(\frac{\sin(RK)}{K} - R\cos(RK)\right)\hat{Q}(t,K)\,\mathrm{d}K\ . \end{aligned} \tag{B.16}$$

B.3 Time integral of the gravitoelectric evolution equation

The above procedure gives a way of obtaining a traceless part consistent with the momentum constraints and evolution equations in particular situations, and when only initial conditions on the trace part (or on the energy density) are explicitly specified. Alternatively, and still focusing on a purely gravitoelectric traceless part, a solution can be derived from the gravitoelectric traceless evolution equation (3.104), if the trace part and the (gravitoelectric) traceless initial conditions are known. This evolution equation can indeed be rewritten as

$$\begin{aligned} & \partial_t\left(\frac{a^3}{N_H}\,\partial_t{}^E\Pi^i{}_j\right) = -\frac{aN_H}{3}\mathcal{D}^i{}_j\left(\int_{t_{\mathbf{i}}}^t N_H\,\partial_t\left(\frac{\bar{P}}{N_H}\right)\mathrm{d}t'\right) \\ & + \frac{aN_H}{3}\Big(\big[1+3\beta'(\epsilon_H)\big]\,\mathcal{D}^i{}_j\bar{P} - \big[1+3\beta'(\epsilon_{H\mathbf{i}})\big]\,\mathcal{D}^i{}_j\bar{P}_{\mathbf{i}}\Big) \\ & + \frac{aN_H}{N_{H_{\mathbf{i}}}^2}\left({}^{\mathrm{tl,E}}W^i{}_j + H_{\mathbf{i}}\big[1-3\beta'(\epsilon_{H\mathbf{i}})\big]\,{}^{\mathrm{tl,E}}U^i{}_j\right)\ , \end{aligned} \tag{B.17}$$

after replacing $\Delta_0 {}^{E}\Pi^{i}{}_{j}$ by its integral expression (3.110) in terms of $\bar{P}$. It can be readily time–integrated twice to give ${}^{E}\Pi^{i}{}_{j}$. This yields the full $\Pi^{i}{}_{j}$ if the initial conditions are chosen such that the gravitomagnetic part vanishes.

In contrast to the previous subsections, this procedure can be applied in general, allowing the gravitoelectric initial conditions for the traceless part to be freely set. However, this requires the initial conditions ${}^{\mathrm{tl}}U^{i}{}_{j} = {}^{\mathrm{tl,E}}U^{i}{}_{j}$ and ${}^{\mathrm{tl}}W^{i}{}_{j} = {}^{\mathrm{tl,E}}W^{i}{}_{j}$ to be explicitly specified. While the trace parts relate to the energy density and spatial scalar curvature, the tracefree parts are related to properties of the gravitational wave components at the initial time. The latter have to be set in such a way as to fulfil the momentum constraints and their time derivative at the initial time, as well as the geometric constraints (3.100)–(3.101) for the gravitoelectric parts.

B.4 On the evaluation of physical quantities

From given solutions for the trace and traceless parts, the full deformation field is straightforwardly obtained as $P^{i}{}_{j} = \Pi^{i}{}_{j} + (1/3)P\,\delta^{i}{}_{j}$, with $P = \bar{P} - \bar{P}_{\mathbf{i}}$. This expression can then be inserted into the Lagrangian functional expressions for various physical quantities in terms of the deformation field. They can then be directly evaluated without any further linearization. This extrapolation is a crucial part of the Relativistic Zel'dovich Approximation as introduced in Buchert and Ostermann [2012], and it generally requires the knowledge of all components of the deformation field. One would for instance directly compute a spatial distance from the line element

$$\mathrm{d}s^2 = a(t)^2 G_{ab}\left(\delta^{a}{}_{i} + P^{a}{}_{i}\right)\left(\delta^{b}{}_{j} + P^{b}{}_{j}\right)\mathrm{d}X^{i}\mathrm{d}X^{j}\,, \tag{B.18}$$

where knowledge of $G_{ab}(X^k)$ is also required. In turn, the rest mass density (with initial conditions set in such a way that it does coincide with $\varrho = F(\epsilon)$) would be computed as

$$\varrho = \frac{\varrho_{\mathbf{i}}}{J} = \frac{\varrho_{H\mathbf{i}}\left(1 + \alpha_{H\mathbf{i}}\,\delta\epsilon_{\mathbf{i}}\right)}{a^3 \det\left(\delta^{a}{}_{i} + P^{a}{}_{i}\right)}\,. \tag{B.19}$$

For the evaluation of the latter, note that in the case of a plane wave (with one or both time–evolution modes), the deformation field components can be written

as,

$$P^i_{\ j} = \lambda_1 \frac{K^i K_j}{K^2} + \lambda_2 \, \delta^i_{\ j} \ , \tag{B.20}$$

and similarly in the case of a localized spherically symmetric perturbation,

$$P^i_{\ j} = \lambda_1 \frac{X^i X_j}{K^2} + \lambda_2 \, \delta^i_{\ j} \ . \tag{B.21}$$

In the plane wave case, the coefficients $\lambda_1(t, X^k)$, $\lambda_2(t, X^k)$ are directly deduced from (B.9) or from a sum of two such solutions, while in the localized spherically symmetric case, $\lambda_1(t, X^k) = q(t, R)$ and $\lambda_2(t, X^k) = \big(P(t, R) - q(t, R)\big)/3$.

The determinant of the spatial coframe coefficients, from which ϱ is evaluated, is then expressed in both cases by

$$J = a^3 (1 + \lambda_2)^2 \, (1 + \lambda_1 + \lambda_2) \ , \tag{B.22}$$

leading to an infinite rest mass density (from shell–crossing) whenever $\lambda_2 \to -1$ or $\lambda_1 + \lambda_2 \to -1$.

Such an extrapolation procedure provides the exact metrical distances, density and other physical properties as produced by the deformation field at a given order. In particular, this provides powerful approximations for the Ricci and Weyl curvatures that are not available in standard perturbation theory. It is, however, clear that the resulting expressions are approximations that must be controlled. We can furthermore combine the exact functional for a given deformation with exact averages of Einstein's equations. An example was given in [Buchert et al., 2013] that also showed that the resulting prescription can even lead to exact results. E.g., the combination of the first–order Lagrangian dust model with exact averages led to an exact formula for the kinematical backreaction within a class of averaged Lemaître–Tolman–Bondi solutions [Buchert et al., 2013].

Bibliography

B. P Abbott, R. Abbott, Ligo Scientific Collaboration, Collaboration Virgo, et al. 2016. Observation of Gravitational Waves from a Binary Black Hole Merger. *Phys. Rev. Lett.*, 116(6):061102.

R. Adam, P. A. R. Ade, N. Aghanim, et al. 2016. Planck 2015 results - I. Overview of products and results. *Astron. Astrophys.*, 594(A1).

J. Adamek, D. Daverio, R. Durrer, et al. 2016. General relativity and cosmic structure formation. *Nature Physics*, 12:346.

J. Adamek, C. Clarkson, D. Daverio, et al. 2017. Safely smoothing spacetime: backreaction in relativistic cosmological simulations. *arXiv:1706.09309*.

P. A. R. Ade, N. Aghanim, C. Armitage-Caplan, et al. 2014. Planck 2013 results. XXVI. Background geometry and topology of the Universe. *Astron. Astrophys.*, 571(A26).

P. A. R. Ade, N. Aghanim, M. Arnaud, et al. 2016a. Planck 2015 results - XIII. Cosmological parameters. *Astron. Astrophys.*, 594(A13).

P. A. R. Ade, N. Aghanim, et al. 2016b. Planck 2015 results - XVIII. Background geometry and topology of the Universe. *Astron. Astrophys.*, 594(A18).

N. Aghanim, M. Arnaud, M. Ashdown, et al. 2016. Planck 2015 results - XI. CMB power spectra, likelihoods, and robustness of parameters. *Astron. Astrophys.*, 594(A11).

F. Al Roumi, T. Buchert, and A. Wiegand. 2017. Lagrangian theory of structure formation in relativistic cosmology. IV. Lagrangian approach to gravitational waves. *Phys. Rev. D*, 96(12):123538.

A. Alles, T. Buchert, F. Al Roumi, et al. 2015. Lagrangian theory of structure formation in relativistic cosmology III: gravitoelectric perturbation and solution schemes at any order. *Phys. Rev. D*, 92(2):023512.

R. A. Alpher. 1948. A Neutron-Capture Theory of the Formation and Relative Abundance of the Elements. *Phys. Rev.*, 74(11):1577–1589.

R. A. Alpher and R. Herman. 1948a. Evolution of the Universe. *Nature*, 162: 774.

R. A. Alpher and R. C. Herman. 1948b. On the Relative Abundance of the Elements. *Phys. Rev.*, 74(12):1737–1742.

R. A. Alpher and R. C. Herman. 1949. Remarks on the Evolution of the Expanding Universe. *Phys. Rev.*, 75(7):1089–1095.

R. A. Alpher and R. C. Herman. 1950. Theory of the Origin and Relative Abundance Distribution of the Elements. *Rev. Mod. Phys.*, 22(2):153–212.

R. A. Alpher, H. Bethe, and G. Gamow. 1948. The Origin of Chemical Elements. *Phys. Rev.*, 73(7):803–804.

L. Amendola and F. Finelli. 2005. Effects of a Decaying Cosmological Fluctuation. *Phys. Rev. Lett.*, 94(22):221303.

L. Amendola and S. Tsujikawa. 2008. Phantom crossing, equation-of-state singularities, and local gravity constraints in f(R) models. *Phys. Lett. B*, 660(3): 125–132.

L. Amendola, R. Gannouji, D. Polarski, et al. 2007a. Conditions for the cosmological viability of $f(R)$ dark energy models. *Phys. Rev. D*, 75(8):083504.

L. Amendola, D. Polarski, and S. Tsujikawa. 2007b. Are $f(R)$ Dark Energy Models Cosmologically Viable? *Phys. Rev. Lett.*, 98(13):131302.

V. I. Arnold, S. F. Shandarin, and Ya B. Zeldovich. 1982. The large scale structure of the universe I. General properties. One-and two-dimensional models. *Geophys. & Astrophy. Fluid Dynamics*, 20(1-2):111–130.

H. Asada. 2000. Lagrangian description of fluid flow with pressure in relativistic cosmology. *Phys. Rev. D*, 62(12):127301.

H. Asada and M. Kasai. 1999. Lagrangian description of the fluid flow with vorticity in the relativistic cosmology. *Phys. Rev. D*, 59(12):123515.

J. M. Bardeen. 1980. Gauge-invariant cosmological perturbations. *Phys. Rev. D*, 22(8):1882.

A. Barnes. 1973. On shear free normal flows of a perfect fluid. *Gen. Relativ. Gravit.*, 4(2):105–129.

J. D. Barrow and R. Maartens. 1998. Anisotropic stresses in inhomogeneous universes. *Phys. Rev. D*, 59(4):043502.

R. Bartnik. 1988. Remarks on cosmological spacetimes and constant mean curvature surfaces. *Commun. Math. Phys.*, 117(4):615–624.

C. L. Bennett, A. J. Banday, K. M. Grski, G. Hinshaw, P. Jackson, P. Keegstra, A. Kogut, G. F. Smoot, D. T. Wilkinson, and E. L. Wright. 1996. Four-Year COBE DMR Cosmic Microwave Background Observations: Maps and Basic Results. *Astrophys. J. Lett.*, 464(1):L1–L4.

F. Bernardeau, S. Colombi, E. Gaztañaga, et al. 2002. Large-scale structure of the Universe and cosmological perturbation theory. *Phys. Rep.*, 367:1–248.

F. Bernardeau, M. Crocce, and R. Scoccimarro. 2008. Multipoint propagators in cosmological gravitational instability. *Phys. Rev. D*, 78(10):103521.

F. Bernardeau, M. Crocce, and R. Scoccimarro. 2012. Constructing regularized cosmic propagators. *Phys. Rev. D*, 85(12):123519.

L. Bianchi. 1898. On the Three-Dimensional Spaces Which Admit a Continuous Group of Motions. *Gen. Relativ. Gravit.*, 33(12):2171–2253.

S. Bildhauer, T. Buchert, and M. Kasai. 1992. Solutions in Newtonian cosmology - The pancake theory with cosmological constant. *Astron. Astrophys.*, 263:23–29.

M. Birkinshaw, S. F. Gull, and H. Hardebeck. 1984. The SunyaevZeldovich effect towards three clusters of galaxies. *Nature*, 309:34.

J. A. Bittencourt. 2004. *Fundamentals of plasma physics*. Springer, New York.

D. Blas, M. Garny, and T. Konstandin. 2013. On the nonlinear scale of cosmological perturbation theory. *J. Cos. & Astropart. Phys.*, 2013(09):024.

K. Bolejko and M. N. Célérier. 2010. Szekeres Swiss-cheese model and supernova observations. *Phys. Rev. D*, 82(10):103510.

J. R. Bond, L. A. Kofman, and D. Pogosyan. 1996. How filaments of galaxies are woven into the cosmic web. *Nature*, 380:603.

H. Bondi. 1947. Spherically Symmetrical Models in General Relativity. *Mon. Not. R. Astron. Soc.*, 107(5-6):410–425.

N. Bose and A. S. Majumdar. 2013. Effect of cosmic backreaction on the future evolution of an accelerating universe. *Gen. Relativ. Gravit.*, 45(10):1971–1987.

F. Bouchet. 1996. Introductory overview of Eluerian & Lagrangian perturbation theories. *arXiv: astro-ph/9603013*.

F. R. Bouchet, R. Juszkiewicz, S. Colombi, and R. Pellat. 1992. Weakly nonlinear gravitational instability for arbitrary Omega. *Astrophys. J.*, 394(1):L5–L8.

F. R. Bouchet, S. Colombi, E. Hivon, and R. Juszkiewicz. 1995. Perturbative Lagrangian approach to gravitational instability. *Astron. Astrophys.*, 296:575.

V. R. Bouillot, J. M. Alimi, P. S. Corasaniti, et al. 2015. Probing dark energy models with extreme pairwise velocities of galaxy clusters from the DEUS-FUR simulations. *Mon. Not. R. Astron. Soc.*, 450(1):145–159.

T. Buchert. 1989. A class of solutions in Newtonian cosmology and the pancake theory. *Astron. Astrophys.*, 223(1-2):9–24.

T. Buchert. 1992. Lagrangian theory of gravitational instability of Friedman-Lemaître cosmologies and the 'Zel'dovich approximation. *Mon. Not. R. Astron. Soc.*, 254(4):729–737.

T. Buchert. 1993. Lagrangian perturbation theory: a key-model for large-scale structure. *Astron. Astrophys.*, 267(2):L51–L54.

T. Buchert. 1994. Lagrangian theory of gravitational instability of Friedman-Lemaître cosmologies-a generic third-order model for nonlinear clustering. *Mon. Not. R. Astron. Soc.*, 267(4):811–820.

T. Buchert. 1996a. Lagrangian Perturbation Approach to the Formation of Lagre-scale Structure. In *"International School of Physics Enrico Fermi", Course CXXXII: Dark Matter in the Universe*, pages 543–564, Amsterdam The Netherlands, 1996a. IOP Press.

T. Buchert. 1996b. Averaging Hypotheses in Newtonian Cosmology. *arXiv: astro-ph/9512107*.

T. Buchert. 2000a. On Average Properties of Inhomogeneous Fluids in General Relativity: Dust Cosmologies. *Gen. Relativ. Gravit.*, 32(1):105.

T. Buchert. 2000b. Stabilization of Large Scale Structure by Adhesive Gravitational Clustering. In *From Stars to the Universe*, Ann. Shanghai Obs., Acad. Sin., No. 21, pages 85–92.

T. Buchert. 2001. On Average Properties of Inhomogeneous Fluids in General Relativity: Perfect Fluid Cosmologies. *Gen. Relativ. Gravit.*, 33(8):1381.

T. Buchert. 2006. The non-perturbative regime of cosmic structure formation. *Astron. Astrophys.*, 454(2):415–422.

T. Buchert. 2008. Dark Energy from structure: a status report. *Gen. Relativ. Gravit.*, 40(2):467–527.

T. Buchert. 2011. Toward physical cosmology: focus on inhomogeneous geometry

and its non-perturbative effects. *Class. Quantum Grav.*, 28:164007.

T. Buchert and S. Adler. 1999. Lagrangian theory of structure formation in pressure-supported cosmological fluids. *Astron. Astrophys.*, 343:317–324.

T. Buchert and A. Domínguez. 1998. Modeling multi-stream flow in collisionless matter: approximations for large-scale structure beyond shell-crossing. *Astron. Astrophys.*, 335:395–402.

T. Buchert and A. Domínguez. 2005. Adhesive gravitational clustering. *Astron. Astrophys.*, 438(2):443–460.

T. Buchert and J. Ehlers. 1993. Lagrangian theory of gravitational instability of Friedman-Lemaître cosmologies-second-order approach: an improved model for nonlinear clustering. *Mon. Not. R. Astron. Soc.*, 264(2):375–387.

T. Buchert and J. Ehlers. 1997. Averaging inhomogeneous Newtonian cosmologies. *Astron. Astrophys.*, 320:1–7.

T. Buchert and G. Götz. 1987. A class of solutions for self-gravitating dust in Newtonian gravity. *J. Math. Phys.*, 28:2714.

T. Buchert and N. Obadia. 2011. Effective inhomogeneous inflation: curvature inhomogeneities of the Einstein vacuum. *Class. Quantum Grav.*, 28(16): 162002.

T. Buchert and M. Ostermann. 2012. Lagrangian theory of structure formation in relativistic cosmology I: Lagrangian framework and definition of a nonperturbative approximation. *Phys. Rev. D*, 86(2):023520.

T. Buchert, A. Domínguez, and J. Pérez-Mercader. 1999. Extending the scope of models for large-scale structure formation in the universe. *Astron. Astrophys.*, 349:343–353.

T. Buchert, C. Nayet, and A. Wiegand. 2013. Lagrangian theory of structure formation in relativistic cosmology II: average properties of a generic evolution model. *Phys. Rev. D*, 87(12):123503.

T. Buchert, M. Carfora, G. F. R. Ellis, et al. 2015. Is there proof that backreaction of inhomogeneities is irrelevant in cosmology? *Class. Quantum Grav.*, 32(21):215021.

T. Buchert, A. A. Coley, H. Kleinert, et al. 2016. Observational challenges for the standard FLRW model. *Int. J. Mod. Phys. D*, 25(03):1630007.

T. Buchert, P. Mourier, and X. Roy. 2018. Cosmological backreaction and its

dependence on spacetime foliation. *arXiv: 1805.10455*.

R. R. Caldwell and M. Kamionkowski. 2009. The Physics of Cosmic Acceleration. *Annual Review of Nuclear and Particle Science*, 59(1):397–429.

R. R. Caldwell and Eric V. Linder. 2005. Limits of Quintessence. *Phys. Rev. Lett.*, 95(14):141301.

R. R. Caldwell, R. Dave, and P. J. Steinhardt. 1998. Cosmological Imprint of an Energy Component with General Equation of State. *Phys. Rev. Lett.*, 80 (8):1582–1585.

H. Campbell, C. B. D'Andrea, R. C. Nichol, et al. 2013. Cosmology with Photometrically Classified Type Ia Supernovae from the SDSS-II Supernova Survey. *Astrophys. J.*, 763(2):88.

S. M. Carroll. 2001. The Cosmological Constant. *Living Rev. Relativity*, 4(1):1.

S. M. Carroll, W. H. Press, and E. L. Turner. 1992. The Cosmological Constant. *Ann. Rev. Astron. Astrophys.*, 30(1):499–542.

P. Catelan. 1995. Lagrangian dynamics in non-flat universes and nonlinear gravitational evolution. *Mon. Not. R. Astron. Soc.*, 276(1):115–124.

M. N. Célérier. 2000. Do we really see a cosmological constant in the supernovae data? *Astron. Astrophys.*, 353:63–71.

M. N. Célérier. 2012. Some clarifications about Lematre-Tolman models of the Universe used to deal with the dark energy problem. *Astron. Astrophys.*, 543 (A71).

M. N. Célérier, K. Bolejko, and A. Krasiński. 2010. A (giant) void is not mandatory to explain away dark energy with a Lematre-Tolman model. *Astron. Astrophys.*, 518(A21).

S. Chandrasekhar and L. R. Henrich. 1942. An Attempt to Interpret the Relative Abundances of the Elements and Their Isotopes. *Astrophys. J.*, 95:288–298.

C. Clarkson and O. Umeh. 2011. Is backreaction really small within concordance cosmology? *Class. Quantum Grav.*, 28(16):164010.

C. Clarkson, G. Ellis, J. Larena, and O. Umeh. 2011. Does the growth of structure affect our dynamical models of the Universe? The averaging, backreaction, and fitting problems in cosmology. *Rep. Prog. Phys.*, 74(11):112901.

T. Clifton, P. G. Ferreira, A. Padilla, and C. Skordis. 2012. Modified gravity

and cosmology. *Phys. Rep.*, 513(1):1–189.

P. Coles and F. Lucchin. 2002. *Cosmology The Origin and Evolution of Cosmic Structure*. Second edition edition.

M. Colless, G. Dalton, S. J. Maddox, et al. 2001. The 2dF Galaxy Redshift Survey: spectra and redshifts. *Mon. Not. R. Astron. Soc.*, 328(4):1039–1063.

E. K. Conklin. 1969. Velocity of the Earth with Respect to the Cosmic Background Radiation. *Nature*, 222:971.

A. Conley, J. Guy, M. Sullivan, et al. 2011. Supernova Constraints and Systematic Uncertainties from the First Three Years of the Supernova Legacy Survey. *Astrophys. J. Supp. Seri.*, 192(1):1.

E. J. Copeland, M. Sami, and S. Tsujikawa. 2006. DYNAMICS OF DARK ENERGY. *Int. J. Mod. Phys. D*, 15(11):1753–1935.

B. E. Corey and D. T. Wilkinson. 1976. A Measurement of the Cosmic Microwave Background Anisotropy at 19 GHz. *Bulletin of the American Astronomical Society*, 8:351.

M. Crocce and R. Scoccimarro. 2006a. Renormalized cosmological perturbation theory. *Phys. Rev. D*, 73(6):063519.

M. Crocce and R. Scoccimarro. 2006b. Memory of initial conditions in gravitational clustering. *Phys. Rev. D*, 73(6):063520.

K. M. Croudace, J. Parry, D. S. Salopek, and J. M. Stewart. 1994. Applying the Zeldovich approximation to general relativity. *Astrophys. J.*, 423(1):22–32.

C. F. Curtiss and R. Byron Bird. 1996. Multicomponent diffusion in polymeric liquids. *Proc. Natl. Acad. Sci.*, 93(15):7440–7445.

L. H. Dam, A. Heinesen, and D. L. Wiltshire. 2017. Apparent cosmic acceleration from Type Ia supernovae. *Mon. Not. R. Astron. Soc.*, 472(1):835–851.

M. Davis, G. Efstathiou, C. S. Frenk, and S. D. M. White. 1985. The evolution of large-scale structure in a universe dominated by cold dark matter. *Astrophys. J.*, 292:371–394.

P. de Bernardis, P. A. R. Ade, J. J. Bock, et al. 2000. A flat Universe from high-resolution maps of the cosmic microwave background radiation. *Nature*, 404:955.

W. de Sitter. 1917. On Einstein's Theory of Gravitation and its Astronomical

Consequences. *Mon. Not. R. Astron. Soc.*, 78(1):3–28.

W. de Sitter. 1930a. On the distances and radial velocities of extra-galactic Nebulae, and the explanation of the latter by the relativity theory of inertia. *Proc. Nati. Acad. Sci. of USA*, 16(7):474–488.

W. de Sitter. 1930b. On the magnitudes, diameters and distances of the extragalactic nebulae and their apparent radial velocities. *Bulletin of the Astronomical Institutes of the Netherlands*, 5(184):157–171.

W. de Sitter. 1930c. The expanding universe. Discussion of Lemaître's solution of the equations of the inertial field. *Bulletin of the Astronomical Institutes of the Netherlands*, 5:211–218.

W. de Sitter. 1930d. Further Remarks on the Astronomical Consequences of the Theory of the Expanding Universe. *Bulletin of the Astronomical Institutes of the Netherlands*, 5:274–276.

S. Dengiz. 2011. 3+1 Orthogonal and Conformal Decomposition of the Einstein Equation and the ADM Formalism for General Relativity. *arXiv: 1103.1220*.

N. Deruelle, M. Sasaki, and Y. Sendouda. 2008. "Detuned" $f(R)$ gravity and dark energy. *Phys. Rev. D*, 77(12):124024.

R. H. Dicke, P. J. E. Peebles, P. G. Roll, and D. T. Wilkinson. 1965. Cosmic Black-Body Radiation. *Astrophys. J.*, 142:414–419.

H. Dingle. 1933. On E. A. Milne's theory of world structure and the expansion of the universe. *Zeitschrift für Astrophysik*, 7:167–179.

A. Domínguez. 2000. Hydrodynamic approach to the evolution of cosmological structures. *Phys. Rev. D*, 62(10):103501.

A. Domínguez. 2002. Study of corrections to the dust model via perturbation theory. *Mon. Not. R. Astron. Soc.*, 334(2):435–443.

J. A. G. Duley, M. A. Nazer, and D. L. Wiltshire. 2013. Timescape cosmology with radiation fluid. *Class. Quantum Grav.*, 30(17):175006.

A. S. Eddington. 1930. On the Instability of Einstein's Spherical World. *Mon. Not. R. Astron. Soc.*, 90(7):668–678.

G. Efstathiou, W. J. Sutherland, and S. J. Maddox. 1990. The cosmological constant and cold dark matter. *Nature*, 348:705.

J. Ehlers. 1971. *General Relativity and Kinetic Theory*. New York: Academic

Press, Italian.

J. Ehlers. 1993. Contributions to the relativistic mechanics of continuous media. *Gen. Relativ. Gravit.*, 25(12):1225.

J. Ehlers and T. Buchert. 1996. Newtonian Cosmology in Lagrangian Formulation: Foundations and Perturbation Theory. *Gen. Relativ. Gravit.*, 29(6): 733–764.

A. Einstein. 1917. Cosmological Considerations in the General Theory of Relativity. *Sitzungsber.Preuss.Akad.Wiss.Berlin (Math.Phys.)*, 1917:142–152.

A. Einstein. 1918. *Critical Comment on a Solution of the Gravitational Field Equations Given by Mr. de Sitter, The Collected Papers of Albert Einstein,* The Berlin Years: Writings, 1918-1921, volume 7. Princeton University Press.

A. Einstein and W. de Sitter. 1932. On the Relation between the Expansion and the Mean Density of the Universe. *Proc. Nati. Acad. Sci.*, 18(3):213.

A. Einstein and E. G. Straus. 1945. The Influence of the Expansion of Space on the Gravitation Fields Surrounding the Individual Stars. *Rev. Mod. Phys.*, 17 (2-3):120–124.

D. J. Eisenstein, H. J. Seo, and M. White. 2007. On the Robustness of the Acoustic Scale in the Low-Redshift Clustering of Matter. *Astrophys. J.*, 664 (2):660.

G. F. R. Ellis. 1967. Dynamics of Pressure-Free Matter in General Relativity. *J. Math. Phys.*, 8(5):1171.

G. F. R. Ellis. 1984. *Relativistic Cosmology: Its Nature, Aims and Problems*, pages 215–288. Springer Netherlands, Dordrecht.

G. F. R. Ellis. 2006. The Bianchi models: Then and now. *Gen. Relativ. Gravit.*, 38(6):1003–1015.

G. F. R. Ellis. 2011. Inhomogeneity effects in cosmology. *Class. Quantum Grav.*, 28(16):164001.

G. F. R. Ellis and M. Bruni. 1989. Covariant and gauge-invariant approach to cosmological density fluctuations. *Phys. Rev. D*, 40(6):1804.

G. F. R. Ellis and Henk van Elst. 1999a. Cosmological models (Cargese lectures 1998). *arXiv: gr-qc/9812046*.

G. F. R. Ellis and Henk van Elst. 1999b. Cosmological models. In Marc lachièze

Rey, editor, *Theoretical and Observational Cosmology*, NATO Science Series C: Mathematical and Physical Sciences. Springer Netherlands.

G. F. R. Ellis and W. Stoeger. 1987. The 'fitting problem' in cosmology. *Class. Quantum Grav.*, 4(6):1697.

G. F. R. Ellis and C. G. Tsagas. 2002. Relativistic approach to nonlinear peculiar velocities and the Zeldovich approximation. *Phys. Rev. D*, 66(12):124015.

G. F. R. Ellis, R. Maartens, and M. A. H. MacCallum. 2012. *Relativistic Cosmology*. Cambridge Universe Press.

K. Enqvist. 2008. Lemaitre-Tolman-Bondi model and accelerating expansion. *Gen. Relativ. Gravit.*, 40(2):451–466.

S. Ettori. 2003. Are we missing baryons in galaxy clusters? *Mon. Not. R. Astron. Soc.*, 344(2):L13–L16.

S. Ettori and A. C. Fabian. 1999. ROSAT PSPC observations of 36 high-luminosity clusters of galaxies: constraints on the gas fraction. *Mon. Not. R. Astron. Soc.*, 305(4):834–848.

D. J. Fixsen, E. S. Cheng, D. A. Cottingham, et al. 1994. Cosmic microwave background dipole spectrum measured by the COBE FIRAS instrument. *Astrophys. J.*, 420(2):445–449.

D. J. Fixsen, E. S. Cheng, J. M. Gales, et al. 1996. The Cosmic Microwave Background Spectrum from the Full COBE FIRAS Data Set. *Astrophys. J.*, 473(2):576.

É. Flanagan. 2005. Can superhorizon perturbations drive the acceleration of the Universe? *Phys. Rev. D*, 71(10):103521.

A. Friedmann. 1922. On the Curvature of Space, *Republished:* Gen. Relativ. Gravit., 1999, 31(12):1991-2000. *Zeitschrift für Physik*, 10:377–386.

A. Friedmann. 1924. On the Possibility of a World with Constant Negative Curvature of Space, *Republished:* Gen. Relativ. Gravit., 1999, 31(12):2001-2008. *Zeitschrift für Physik*, 21:326–332.

H. Friedrich. 1998. Evolution equations for gravitating ideal fluid bodies in general relativity. *Phys. Rev. D*, 57(4):2317–2322.

J. A. Frieman, M. S. Turner, and D. Huterer. 2008. Dark Energy and the Accelerating Universe. *Ann. Rev. Astron. Astrophys.*, 46(1):385–432.

T. Futamase. 1988. Approximation Scheme for Constructing a Clumpy Universe in General Relativity. *Phys. Rev. Lett.*, 61(19):2175–2178.

T. Futamase. 1989. An approximation scheme for constructing inhomogeneous universes in general relativity. *Mon. Not. R. Astron. Soc.*, 237(1):187–200.

R. M. Gailis and N. E. Frankel. 2006. Two-component cosmological fluids with gravitational instabilities. *J. Math. Phys.*, 47(062505).

G. Gamow. 1942. Concerning the origin of chemical elements. *J. Wash. Acad. Sci.*, 32(12):353–355.

G. Gamow. 1946. Expanding Universe and the Origin of Elements. *Phys. Rev.*, 70(7-8):572–573.

G. Gamow. 1948a. The Origin of Elements and the Separation of Galaxies. *Phys. Rev.*, 74(4):505–506.

G. Gamow. 1948b. The Evolution of the Universe. *Nature*, 162:680.

A. Goobar and B. Leibundgut. 2011. Supernova Cosmology: Legacy and Future. *Annual Review of Nuclear and Particle Science*, 61(1):251–279.

J. R. Gott III, M. Jurić, D. Schlegel, et al. 2005. A Map of the Universe. *Astrophys. J.*, 624(2):463.

É. Gourgoulhon. 2007. 3+1 Formalism and Bases of Numerical Relativity. *arXiv: gr-qc/0703035*.

S. R. Green and R. M. Wald. 2011. New framework for analyzing the effects of small scale inhomogeneities in cosmology. *Phys. Rev. D*, 83(8):084020.

S. R. Green and R. M. Wald. 2013. Examples of backreaction of small-scale inhomogeneities in cosmology. *Phys. Rev. D*, 87(12):124037.

S. R. Green and R. M. Wald. 2015. Comments on Backreaction. *arXiv: 1506.06452*.

J. N. Grieb, A. G. Sánchez, S. Salazar-Albornoz, et al. 2017. The clustering of galaxies in the completed SDSS-III Baryon Oscillation Spectroscopic Survey: cosmological implications of the Fourier space wedges of the final sample. *Mon. Not. R. Astron. Soc.*, 467(2):2085–2112.

L. P. Grishchuk and Ya. B. Zel'dovich. 1981. Gravitational instability in a multicompoent fluid. *Sov. Astron.*, 25(3):267–271.

S. N. Gurbatov, A. I. Saichev, and S. F. Shandarin. 1989. The large-scale structure of the Universe in the frame of the model equation of nonlinear diffusion. *Mon. Not. R. Astron. Soc.*, 236(2):385–402.

A. H. Guth and S. Y. Pi. 1982. Fluctuations in the New Inflationary Universe. *Phys. Rev. Lett.*, 49(15):1110–1113.

H. J. Haubold, A. M. Mathai, and J. P. Mücket. 1991. On gravitational instability in a multi-component cosmological medium. *Astron. Nachr.*, 312(1):1–6.

S. W. Hawking. 1982. The development of irregularities in a single bubble inflationary universe. *Phys. Lett. B*, 115(4):295–297.

P. S. Henry. 1971. Isotropy of the 3 K Background. *Nature*, 231:516.

G. Hinshaw, M. R. Nolta, C. L. Bennett, et al. 2007. Three-Year Wilkinson Microwave Anisotropy Probe (WMAP) Observations: Temperature Analysis. *Astrophys. J. Supp. Seri.*, 170(2):288.

F. Hoyle and M. S. Vogeley. 2002. Voids in the Point Source Catalogue Survey and the Updated Zwicky Catalog. *Astrophys. J.*, 566(2):641.

F. Hoyle and M. S. Vogeley. 2004. Voids in the Two-Degree Field Galaxy Redshift Survey. *Astrophys. J.*, 607(2):751.

W. Hu and I. Sawicki. 2007. Models of $f(R)$ cosmic acceleration that evade solar system tests. *Phys. Rev. D*, 76(6):064004.

E. Hubble. 1929. A relation between distance and radial velocity among extra-galactic nebulae. *Proc. Nati. Acad. Sci.*, 15(3):168.

H. Iguchi, T. Nakamura, and K. Nakao. 2002. Is Dark Energy the Only Solution to the Apparent Acceleration of the Present Universe? *Progress of Theoretical Physics*, 108(5):809–818.

J. Isenberg and A. D. Rendall. 1998. Cosmological spacetimes not covered by a constant mean curvature slicing. *Class. Quantum Grav.*, 15(11):3679.

A. Ishibashi and R. M. Wald. 2006. Can the acceleration of our universe be explained by the effects of inhomogeneities? *Class. Quantum Grav.*, 23(1): 235.

W. Israel and J. M. Stewart. 1976. Transient Relativistic Thermodynamics and Kinetic Theory. *Ann. Phys. (NY)*, 100(310).

W. Israel and J. M. Stewart. 1979. Transient relativistic thermodynamics and

kinetic theory. *Annals of Physics*, 118(2):341–372.

J. B. Jiménez, Á. de la Cruz-Dombriz, P. K. S. Dunsby, et al. 2014. Backreaction mechanism in multifluid and extended cosmologies. *JCAP*, 2014(05):031.

A. Joyce, B. Jain, J. Khoury, et al. 2015. Beyond the cosmological standard model. *Phys. Rep.*, 568:1–98.

R. Kantowski. 1998. Some Relativistic Cosmological Models. *Gen. Relativ. Gravit.*, 30(11):1665–1700.

R. Kantowski and R. K. Sachs. 1966. Some Spatially Homogeneous Anisotropic Relativistic Cosmological Models. *J. Math. Phys.*, 7(3):443–446.

M. Kasai. 1993. Inhomogeneous cosmological models which are homogeneous and isotropic on average. *Phys. Rev. D*, 47(8):3214–3221.

M. Kasai. 1995. Tetrad-based perturbative approach to inhomogeneous universes: A general relativistic version of the Zel'dovich approximation. *Phys. Rev. D*, 52(10):5605–5611.

T. Kenji. 2000. Distances and Lensing in Cosmological Void Models. *Astrophys. J.*, 529(1):38.

W. O. Kermack and W. H. McCrea. 1933. On Milne's Theory of World Structure. *Mon. Not. R. Astron. Soc.*, 93(7):519–529.

H. Kodama and M. Sasaki. 1984. Cosmological Perturbation Theory. *Prog. Theor. Phys. Supp.*, 78:1–166.

E. W. Kolb. 2011. Backreaction of inhomogeneities can mimic dark energy. *Class. Quantum Grav.*, 28(16):164009.

E. W. Kolb, S. Matarrese, and A. Riotto. 2006. On cosmic acceleration without dark energy. *New J. Phys.*, 8(12):322.

J. M. Kovac, E. M. Leitch, C. Pryke, et al. 2002. Detection of polarization in the cosmic microwave background using DASI. *Nature*, 420:772.

C. T. Kowal. 1968. Absolute Magnitudes of Supernovae. *Astron. J.*, 73(10): 1021–1024.

A. Krasiński. 1997. *Inhomogeneous Cosmological Models*. Cambridge University Press.

L. M. Krauss and M. S. Turner. 1995. The cosmological constant is back. *Gen.*

Relativ. Gravit., 27(11):1137–1144.

R. Krishna and J. A. Wesselingh. 1997. The Maxwell-Stefan approach to mass transfer. *Chemical Engineering Science*, 52(6):861–911.

M. Kuhlen, M. Vogelsberger, and R. Angulo. 2012. Numerical Simulations of the Dark Universe: State of the Art and the Next Decade. *arXiv: 1209.5745*.

K. Lanczos. 1922. Ein vereinfachendes Koordinatensystem für die Einsteinschen Gravitationsgleichungen. *Phys. Zeits.*, 23:537–539.

J. Larena. 2009. Spatially averaged cosmology in an arbitrary coordinate system. *Phys. Rev. D*, 79(8):084006.

D. Larson, J. Dunkley, G. Hinshaw, et al. 2011. Seven-year Wilkinson Microwave Anisotropy Probe (WMAP) Observations: Power Spectra and WMAP-derived Parameters. *The Astrophysical Journal Supplement Series*, 192(2):16.

M. Lavinto, S. Räsänen, and S. J. Szybka. 2013. Average expansion rate and light propagation in a cosmological Tardis spacetime. *JCAP*, 2013(12):051.

B. M. Leith, S. C. Cindy Ng, and D. L. Wiltshire. 2008. Gravitational Energy as Dark Energy: Concordance of Cosmological Tests. *Astrophys. J. Lett.*, 672 (2):L91.

G. Lemaître. 1925. Note on de Sitter's Universe. *Publications du Laboratoire d'Astronomie et de Geodesie de l'Universite de Louvain*, 2:37–41.

G. Lemaître. 1927. *In French:* Un univers homogène de masse constante et de rayon croissant, rendant compte de la vitesse radiale des nébuleuses extra-galactiques, *Translation:*A Homogeneous Universe of Constant Mass and Increasing Radius accounting for the Radial Velocity of Extra-galactic Nebul *Republished in* Mon. Not. R. Astron. Soc. 91(5):483-490,1931. *Annales de la Société Scientifique de Bruxelles*, 47A:49–59.

G. Lemaître. 1931. The Beginning of the World from the Point of View of Quantum Theory. *Nature*, 127:706.

G. Lemaître. 1933. Republication of: The Expanding Universe. *Gen. Relativ. Gravit.*, 29(5):641–680.

G. Lemaître and A. S. Eddington. 1931. The Expanding Universe. *Mon. Not. R. Astron. Soc.*, 91(5):490–501.

E. Leonardi and C. Angeli. 2010. On the MaxwellStefan Approach to Diffusion: A General Resolution in the Transient Regime for One-Dimensional Systems.

J. Phys. Chem. B, 114(1):151–164.

M. Li, X. D. Li, S. Wang, and Y. Wang. 2011a. Dark Energy. *Commun. Theor. Phys.*, 56(3):525.

X. D. Li, S. Li, S. Wang, et al. 2011b. Probing cosmic acceleration by using the SNLS3 SNIa dataset. *JCAP*, 2011(07):011.

E. Lifshitz. 1946. On the gravitational stability of the expanding universe, *Republication:* Gen. Relativ. Gravit., 49(2):18. *J. Phys. (USSR)*, 10:116–129.

E. V. Linder. 2008. The dynamics of quintessence, the quintessence of dynamics. *Gen. Relativ. Gravit.*, 40(2):329–356.

E. V. Linder. 2009. Exponential gravity. *Phys. Rev. D*, 80(12):123528.

K. Lundmark. 1924. The Determination of the Curvature of Space-Time in de Sitter's World. *Mon. Not. R. Astron. Soc.*, 84(9):747–770.

R. Maartens, J. Triginer, and D. R. Matravers. 1999. Stress effects in structure formation. *Phys. Rev. D*, 60(10):103503.

S. Matarrese and D. Terranova. 1996. Post-Newtonian cosmological dynamics in Lagrangian coordiantes. *Mon. Not. R. Astron. Soc.*, 283(2):400–418.

S. Matarrese, O. Pantano, and D. Saez. 1993. General-relativistic approach to the nonlinear evolution of collisionless matter. *Phys. Rev. D*, 47(4):1311 .

S. Matarrese, O. Pantano, and D. Saez. 1994a. A relativistic approach to gravitational instability in the expanding Universe: second-order lagrangian solutions. *Mon. Not. R. Astron. Soc.*, 271(3):513–522.

S. Matarrese, O. Pantano, and D. Saez. 1994b. General Relativistic Dynamics of Irrotational Dust: Cosmological Implications. *Phys. Rev. Lett.*, 72(3):320–323.

S. Matarrese, S. Mollerach, and M. Bruni. 1998. Relativistic second-order perturbations of the Einstein–de Sitter universe. *Phys. Rev. D*, 58(4):043504.

A. M. Mathai, H. J. Haubold, J. P. Mücket, S. Gottlöber, and V. Müller. 1988. Gravitational instability in a multicomponent cosmological medium. *J. Math. Phys.*, 29(2069).

J. C. Mather, E. S. Cheng, Jr. Eplee, R. E., et al. 1990. A preliminary measurement of the cosmic microwave background spectrum by the Cosmic Background Explorer (COBE) satellite. *Astrophys. J.*, 354:L37–L40.

W. H. McCrea and G. C. McVittie. 1931. The Expanding Universe. *Mon. Not. R. Astron. Soc.*, 92(1):7–12.

G. C. McVittie. 1932. Condensations in an Expanding Universe. *Mon. Not. R. Astron. Soc.*, 92(6):500–518.

G. C. McVittie. 1933. The Mass-Particle in an Expanding Universe. *Mon. Not. R. Astron. Soc.*, 93(5):325–339.

E. A. Milne. 1932. World Structure and the Expansion of the Universe. *Nature*, 130:9.

C. W. Misner. 1968. The Isotropy of the Universe. *Astrophys. J.*, 151:431–457.

M. Morita and T. Tatekawa. 2001. Extending Lagrangian perturbation theory to a fluid with velocity dispersion. *Mon. Not. R. Astron. Soc.*, 328(3):815–828.

M. Morita, K. Nakamura, and M. Kasai. 1998. Relativistic Zel'dovich approximation in a spherically symmetric model. *Phys. Rev. D*, 57(10):6094.

A. Moss, J. P. Zibin, and D. Scott. 2011. Precision cosmology defeats void models for acceleration. *Phys. Rev. D*, 83(10):103515.

F. Moutarde, J.-M. Alimi, F. R. Bouchet, et al. 1991. Precollapse sacle invariance in gravitational instability. *Astrophys. J.*, 382:377–381.

M. A. Nazer and D. L. Wiltshire. 2015. Cosmic microwave background anisotropies in the timescape cosmology. *Phys. Rev. D*, 91(6):063519.

H. Nussbaumer. 2014. Einsteins conversion from his static to an expanding universe. *The European Physical Journal H*, 39(1):37–62.

A. Nwankwo, M. Ishak, and J. Thompson. 2011. Luminosity distance and redshift in the Szekeres inhomogeneous cosmological models. *JCAP*, 2011(05): 028.

C. O'Raifeartaigh and B. McCann. 2014. Einsteins cosmic model of 1931 revisited: an analysis and translation of a forgotten model of the universe. *The European Physical Journal H*, 39(1):63–85.

C. O'Raifeartaigh, M. O'Keeffe, W. Nahm, et al. 2017. Einsteins 1917 static model of the universe: a centennial review. *Eur. Phys. J. H*, 42(3):431–474.

J. J. Ostrowski and B. F. Roukema. 2017. On the Green and Wald formalism. In M. Bianchi, R. T. Jantzen, and R. Ruffini, editors, *Proceedings of the Fourteenth Marcel Grossmann Meeting*, pages 2290–2295, Singapore, 2017. World

Scientific.

T. Padmanabhan. 2003. Cosmological constant - the weight of the vacuum. *Phys. Rep.*, 380(5):235–320.

D. C. Pan, M. S. Vogeley, F. Hoyle, et al. 2012. Cosmic voids in Sloan Digital Sky Survey Data Release 7. *Mon. Not. R. Astron. Soc.*, 421(2):926–934.

G. Pantazis, S. Nesseris, and L. Perivolaropoulos. 2016. Comparison of thawing and freezing dark energy parametrizations. *Phys. Rev. D*, 93(10):103503.

R. B. Partridge and D. T. Wilkinson. 1967. Isotropy and Homogeneity of the Universe from Measurements of the Cosmic Microwave Background. *Phys. Rev. Lett.*, 18(14):557–559.

P. J. E. Peebles. 1993. *Principle of Physical Cosmology.* Princeton University Press, Princeton, New Jersey.

P. J. E. Peebles and A. Nusser. 2010. Nearby galaxies as pointers to a better theory of cosmic evolution. *Nature*, 465:565.

P. J. E. Peebles and B. Ratra. 1988. Cosmology with a time-variable cosmological 'constant'. *Astrophys. J.*, 325:L17–L20.

P. J. E. Peebles and B. Ratra. 2003. The cosmological constant and dark energy. *Rev. Mod. Phys.*, 75(2):559–606.

A. A. Penzias and R. W. Wilson. 1965. A Measurement of Excess Antenna Temperature at 4080 Mc/s. *Astrophys. J.*, 142:419–421.

W. J. Percival, R. C. Nichol, D. J. Eisenstein, et al. 2007. The Shape of the Sloan Digital Sky Survey Data Release 5 Galaxy Power Spectrum. *Astrophys. J.*, 657(2):645.

S. Perlmutter, G. Aldering, G. Goldhaber, et al. 1999. Measurements of Ω and Λ from 42 High-Redshift Supernovae. *Astrophys. J.*, 517(2):565.

P. Peter and J. P. Uzan. 2009. *Primordial Cosmology.* Oxford University Press.

M. M. Phillips. 1993. The absolute magnitudes of Type IA supernovae. *Astrophys. J. Lett.*, 413:L105–L108.

H. Ping, F. Long-Long, and F. Li-Zhi. 2005. Distributions of the Baryon Fraction on Large Scales in the Universe. *Astrophys. J.*, 623(2):601.

E. Poisson and C. M. Will. 2014. *Gravity: Newtonian, Post-Newtonian, Rela-*

tivistic. Cambridge University Press, Cambridge; New York.

A. Pradhan and B. Saha. 2015. Accelerating dark energy models of the universe in anisotropic Bianchi type space-times and recent observations. *Physics of Particles and Nuclei*, 46(3):310–346.

C. Rampf and G. Rigopoulos. 2013. Zel'dovich approximation and general relativity. *Mon. Not. R. Astron. Soc. Lett.*, 430(1):L54–L58.

C. Rampf and A. Wiegand. 2014. Relativistic Lagrangian displacement field and tensor perturbations. *Phys. Rev. D*, 90(12):123503.

S. Räsänen. 2004. Dark energy from back-reaction. *JCAP*, 2004(02):003.

S. Räsänen. 2010. Light propagation in statistically homogeneous and isotropic universes with general matter content. *JCAP*, 2010(03):018.

S. Räsänen. 2011. Backreaction: directions of progress. *Class. Quantum Grav.*, 28(16):164008.

M. J. Rees and D. W. Sciama. 1968. Large-scale Density Inhomogeneities in the Universe. *Nature*, 217:511.

A. D. Rendall. 1996. Constant mean curvature foliations in cosmological space-times. *Helvetica Physica Acta*, 69(4):490–500.

A. Rest, D. Scolnic, R. J. Foley, et al. 2014. Cosmological Constraints from Measurements of Type Ia Supernovae Discovered during the First 1.5 yr of the Pan-STARRS1 Survey. *Astrophys. J.*, 795(1):44.

L. Rezzolla and O. Zanotti. 2013. *Relativistic hydrodynamics*. Oxford University Press, New York.

A. G. Riess, A. V. Filippenko, P. Challis, et al. 1998. Observational Evidence from Supernovae for an Accelerating Universe and a Cosmological Constant. *Astron. J.*, 116(3):1009.

A. G. Riess, P. E. Nugent, R. L. Gilliland, et al. 2001. The Farthest Known Supernova: Support for an Accelerating Universe and a Glimpse of the Epoch of Deceleration. *Astrophys. J.*, 560(1):49.

A. G. Riess, L. G. Strolger, J. Tonry, et al. 2004. Type Ia Supernova Discoveries at z $>$ 1 from the Hubble Space Telescope: Evidence for Past Deceleration and Constraints on Dark Energy Evolution. *Astrophys. J.*, 607(2):665.

A. G. Riess, L. G. Strolger, S. Casertano, et al. 2007. New Hubble Space

Telescope Discoveries of Type Ia Supernovae at z $\geq$ 1: Narrowing Constraints on the Early Behavior of Dark Energy. *Astrophys. J.*, 659(1):98.

H. P. Robertson. 1928. LXXXVI. On relativistic cosmology. *The London, Edinburgh, and Dublin Philosophical Magazine and Journal of Science*, 5(31): 835–848.

H. P. Robertson. 1929. On the foundations of relativistic cosmology. *Proc. Nati. Acad. Sci. of USA*, 15(11):822–829.

H. P. Robertson. 1933a. Relativistic Cosmology. *Rev. Mod. Phys.*, 5(1):62–90.

H. P. Robertson. 1933b. On E. A. Milne's Theory of World Structure. *Zeitschrift für Astrophysik*, 7:153–166.

H. P. Robertson. 1935. Kinematics and World-Structure. *Astrophys. J.*, 82.

H. P. Robertson. 1936a. Kinematics and World-Structure II. *Astrophys. J.*, 83.

H. P. Robertson. 1936b. Kinematics and World-Structure III. *Astrophys. J.*, 83.

X. Roy. 2014. On the 1+3 Formalism in General Relativity. *arXiv: 1405.6319v1*.

S. E. Rugh and H. Zinkernagel. 2002. The quantum vacuum and the cosmological constant problem. *Studies in History and Philosophy of Science Part B: Studies in History and Philosophy of Modern Physics*, 33(4):663–705.

H. Russ, M. Morita, M. Kasai, and G. Börner. 1996. Zel'dovich-type approximation for an inhomogeneous universe in general relativity: Second-order solutions. *Phys. Rev. D*, 53(12):6881.

E. Russell, C. B. Kln, and O. K. Pashaev. 2014. Bianchi I model: an alternative way to model the present-day Universe. *Mon. Not. R. Astron. Soc.*, 442(3): 2331–2341.

D. Saadeh, S. M. Feeney, A. Pontzen, et al. 2016. How Isotropic is the Universe? *Phys. Rev. Lett.*, 117(13):131302.

R. K. Sachs and A. M. Wolfe. 1967. Perturbations of a Cosmological Model and Angular Variations of the Microwave Background. *Astrophys. J.*, 147:73–90.

A. G. Sánchez, R. Scoccimarro, M. Crocce, et al. 2017. The clustering of galaxies in the completed SDSS-III Baryon Oscillation Spectroscopic Survey: Cosmological implications of the configuration-space clustering wedges. *Mon. Not. R. Astron. Soc.*, 464(2):1640–1658.

D. J. Sand, T. Treu, G. P. Smith, et al. 2004. The Dark Matter Distribution in the Central Regions of Galaxy Clusters: Implications for Cold Dark Matter. *Astrophys. J.*, 604(1):88.

A. R. Sandage. 1970. Cosmology: A search for two numbers. *Physics Today*, 23 (2):34–41.

D. M. Scolnic, D. O. Jones, A. Rest, et al. 2018. The Complete Light-curve Sample of Spectroscopically Confirmed SNe Ia from PanSTARRS1 and Cosmological Constraints from the Combined Pantheon Sample. *Astrophys. J.*, 859(2):101.

N. R. Sen. 1934. On the Stability of Cosmological Models. *Gen. Relativ. Gravit.*, 29(11):1477–1488.

N. G. Sergei, I. S. Aleksandr, and F. S. Sergey. 2012. Large-scale structure of the Universe. The Zeldovich approximation and the adhesion model. *Physics-Uspekhi*, 55(3):223.

S. F. Shandarin. 1980. Evolution of perturbations in Friedmann models of the Universe. *Astrophysics*, 16(4):439–445.

S. F. Shandarin and Ya. B. Zeldovich. 1989. The large-scale structure of the universe: Turbulence, intermittency, structures in a self-gravitating medium. *Rev. Mod. Phys.*, 61(2):185–220.

S. F. Shandarin, A. G. Doroshkevich, and Ya. B. Zel'dovich. 1983. The large-scale structure of the universe. *Soviet Physics Uspekhi*, 26(1):46.

T. Shinji. 2013. Quintessence: a review. *Class. Quantum Grav.*, 30(21):214003.

M. F. Shirokov and I. Z. Fisher. 1963. Isotropic Space with Discrete Gravitational-Field Sources. On the Theory of a Nonhomogeneous Isotropic Universe. *Gen. Relativ. Gravit.*, 30(9):1411–1427.

A. Silvestri and M. Trodden. 2009. Approaches to understanding cosmic acceleration. *Rep. Prog. Phys.*, 72(9):096901.

P. R. Smale. 2011. Gamma-ray burst distances and the timescape cosmology. *Mon. Not. R. Astron. Soc.*, 418(4):2779–2784.

P. R. Smale and D. L. Wiltshire. 2011. Supernova tests of the timescape cosmology. *Mon. Not. R. Astron. Soc.*, 413(1):367–385.

G. F. Smoot, M. V. Gorenstein, and R. A. Muller. 1977. Detection of Anisotropy in the Cosmic Blackbody Radiation. *Phys. Rev. Lett.*, 39(14):898–901.

G. F. Smoot, C. L. Bennett, A. Kogut, et al. 1992. Structure in the COBE differential microwave radiometer first-year maps. *Astrophys. J.*, 396(1):L1–L5.

L. V. Solov'eva and I. S. Nurgaliev. 1985. Gravitational instability in a mutlicomponent expanding medium. *Sov. Astron.*, 29(3):267–272.

L. V. Solov'eva and A. A. Starobinsky. 1985. Gravitational instability of a two-component medium in an expanding universe. *Sov. Astron.*, 29(4):367–371.

D. N. Spergel, L. Verde, H. V. Peiris, et al. 2003. First-Year Wilkinson Microwave Anisotropy Probe (WMAP) Observations: Determination of Cosmological Parameters. *Astrophys. J. Supp. Seri.*, 148(1):175.

D. N. Spergel, R. Bean, O. Doré, et al. 2007. Three-Year Wilkinson Microwave Anisotropy Probe (WMAP) Observations: Implications for Cosmology. *Astrophys. J. Supp. Seri.*, 170(2):377.

V. Springel, S. D. M. White, A. Jenkins, et al. 2005. Simulations of the formation, evolution and clustering of galaxies and quasars. *Nature*, 435:629.

V. Springel, C. S. Frenk, and S. D. M. White. 2006. The large-scale structure of the Universe. *Nature*, 440(7088):1137–1144.

H. Stephani. 1987. Some perfect fluid solutions of Einstein's field equations without symmetries. *Class. Quantum Grav.*, 4(1):125.

H. Stephani, D. Kramer, M. MacCallum, et al. 2003. *Exact solutions of Einstein's field equations*. Cambridge monographs on mathematical physics. Cambridge University Press, Cambridge.

J. M. Stewart and D. W. Sciama. 1967. Peculiar Velocity of the Sun and its Relation to the Cosmic Microwave Background. *Nature*, 216:748.

G. Stromberg. 1925. Analysis of radial velocities of globular clusters and non-galactic nebulae. *Astrophys. J.*, 61:353–362.

M. Sullivan, J. Guy, A. Conley, et al. 2011. SNLS3: Constraints on Dark Energy Combining the Supernova Legacy Survey Three-year Data with Other Probes. *Astrophys. J.*, 737(2):102.

R. A. Sunyaev and Ya. B. Zeldovich. 1970. Small-scale fluctuations of relic radiation. *Astrophys. Space Sci.*, 7(1):3–19.

R. A. Sunyaev and Ya. B. Zel'dovich. 1980. Microwave Background Radiation as a Probe of the Contemporary Structure and History of the Universe. *Ann.*

Rev. Astron. Astrophys., 18(1):537–560.

Y. Suto and M. Sasaki. 1991. Quasinonlinear theory of cosmological self-gravitating systems. *Phys. Rev. Lett.*, 66(3):264–267.

N. Suzuki, D. Rubin, C. Lidman, et al. 2012. The Hubble Space Telescope Cluster Supernova Survey. V. Improving the Dark-energy Constraints above z $>$ 1 and Building an Early-type-hosted Supernova Sample. *Astrophys. J.*, 746 (1):85.

S. Suzuki. 1928. On the Thermal Equilibrium of Dissocintion of Atom-Naclei. *Proceedings of the Physico-Mathematical Society of Japan. 3rd Series*, 10(7): 166–169.

D. A. Szafron. 1977. Inhomogeneous cosmologies: New exact solutions and their evolution. *J. Math. Phys.*, 18(8):1673–1677.

P. Szekeres. 1975. A class of inhomogeneous cosmological models. *Commun. Math. Phys.*, 41(1):55–64.

A. Taruya, F. Bernardeau, T. Nishimichi, et al. 2012. Direct and fast calculation of regularized cosmological power spectrum at two-loop order. *Phys. Rev. D*, 86(10):103528.

T. Tatekawa. 2005a. Third-order perturbative solutions in the Lagrangian perturbation theory with pressure. *Phys. Rev. D*, 71:044024.

T. Tatekawa. 2005b. Third-order perturbative solutions in the Lagrangian perturbation theory with pressure II: Effect of the transverse modes. *Phys. Rev. D*, 72(2):024005.

T. Tatekawa. 2013. Fourth-order perturbative equations in Lagrangian perturbation theory for a cosmological dust fluid. *Prog. Theor. Exp. Phys.*, 2013 (1).

T. Tatekawa, M. Suda, K. Maeda, et al. 2002. Perturbation theory in Lagrangian hydrodynamics for a cosmological fluid with velocity dispersion. *Phys. Rev. D*, 66(6):064014.

R. Taylor and R. Krishna. 1993. *Multicomponent mass transfer*. Wiley Series in Chemical Engineering. John Wiley & Sons, INC., New York.

A. V. Tikhonov and I. D. Karachentsev. 2006. Minivoids in the Local Volume. *Astrophys. J.*, 653(2):969.

R. C. Tolman. 1922. Thermodynamic treatment of the possible formation of

Helium from Hydrogen. *J. Amer. Chem. Soc.*, 44(9):1902–1908.

R. C. Tolman. 1929. On the possible line elements for the Universe. *Proc. Nati. Acad. Sci. of USA*, 15(4):297–304.

R. C. Tolman. 1930. On the estimation of distances in a curved universe with a non-static line element. *Proc. Nati. Acad. Sci.*, 16(7):511.

R. C. Tolman. 1934a. *Relativity, Thermodynamics and Cosmology*. Clarendon Press, Oxford.

R. C. Tolman. 1934b. Effect of Inhomogeneity on Cosmological Models. *Proc. Nati. Acad. Sci. of USA*, 20(3):169–176.

K. Tomita. 2001. A local void and the accelerating Universe. *Mon. Not. R. Astron. Soc.*, 326(1):287–292.

R. Treciokas and G. F. R. Ellis. 1971. Isotropic solutions of the Einstein-Boltzmann equations. *Commun. Math. Phys.*, 23(1):1–22.

C. G. Tsagas, A. Challinor, and R. Maartens. 2008. Relativistic cosmology and large-scale structure. *Phys. Rep.*, 465:61–147.

M. S. Turner, G. Steigman, and L. M. Krauss. 1984. Flatness of the Universe: Reconciling Theoretical Prejudices with Observational Data. *Phys. Rev. Lett.*, 52(23):2090–2093.

H. C. Urey and C. A. Bradley. 1931. On the Relative Abundances of Isotopes. *Phys. Rev.*, 38(4):718–724.

R. A. Vanderveld, É. É. Flanagan, and I. Wasserman. 2007. Systematic corrections to the measured cosmological constant as a result of local inhomogeneity. *Phys. Rev. D*, 76(8):083504.

E. Villa, S. Matarrese, and D. Maino. 2014. Cosmological dynamics: from the Eulerian to the Lagrangian frame. Part I. Newtonian approximation. *JCAP*, 06(041).

R. M. Wald. 1984. *General Relativity*. The Univerty of Chicago Press, Chicago 60637.

A. G. Walker. 1934. The principle of least action in Milne's kinematical relativty. *Proceedings of the Royal Society of London. Series A - Mathematical and Physical Sciences*, 147(862):478.

A. G. Walker. 1937. On Milne's Theory of World-Structure. *Proc. Lond. Math.*

Soc., s2-42(1):90–127.

A. G. Walker and E. A. Milne. 1935. On the Formal Comparison of Milne's Kinematical System with the Systems of General Relativity. *Mon. Not. R. Astron. Soc.*, 95(3):263–269.

D. H. Weinberg, M. J. Mortonson, D. J. Eisenstein, et al. 2013. Observational probes of cosmic acceleration. *Phys. Rep.*, 530(2):87–255.

S. Weinberg. 1989. The cosmological constant problem. *Rev. Mod. Phys.*, 61(1): 1–23.

S. Weinberg. 2008. *Cosmology*. Oxford University Press.

C. Wetterich. 1988. Cosmology and the fate of dilatation symmetry. *Nuclear Physics B*, 302(4):668–696.

A. Wiegand and T. Buchert. 2010. Multiscale cosmology and structure-emerging dark energy: A plausibility analysis. *Phys. Rev. D*, 82(2):023523.

D. L. Wiltshire. 2007a. Exact Solution to the Averaging Problem in Cosmology. *Phys. Rev. Lett.*, 99(25):251101.

D. L. Wiltshire. 2007b. Cosmic clocks, cosmic variance and cosmic averages. *New J. Phys.*, 9(10):377.

D. L. Wiltshire. 2008. Gravitational energy and cosmic acceleration. *Int. J. Mod. Phys. D*, 17(03n04):641–649.

D. L. Wiltshire. 2009. Average observational quantities in the timescape cosmology. *Phys. Rev. D*, 80(12):123512.

D. L. Wiltshire. 2011. What is dust?Physical foundations of the averaging problem in cosmology. *Class. Quantum Grav.*, 28(16):164006.

D. L. Wiltshire. 2014. Cosmic structure, averaging and dark energy. In M. Novello and S. E. Perez Bergliaffa, editors, *Cosmology and Gravitation: Proc. XVth Brazilian School*, pages 203–244. Cambridge Scientific Publishers.

W. M. Wood-Vasey, G. Miknaitis, C. W. Stubbs, et al. 2007. Observational Constraints on the Nature of Dark Energy: First Cosmological Results from the ESSENCE Supernova Survey. *Astrophys. J.*, 666(2):694.

A. Yoshisato and M. Morikawa. 2006. Why is the Zel'dovich approximation so accurate? *Astrophys. J.*, 637(2):555–560.

A. F. Zakharov, V. A. Zinchuk, and V. N. Pervushin. 2006. Tetrad Formalism and Reference Frames in General Relativity. *Phys. Part. Nuclei*, 37(1):104.

R. M. Zalaletdinov. 1992. Averaging out the Einstein equations. *Gen. Relativ. Gravit.*, 24(10):1015–1031.

R. M. Zalaletdinov. 1993. Towards a theory of macroscopic gravity. *Gen. Relativ. Gravit.*, 25(7):673–695.

Ya B. Zel'dovich. 1963. The initial stages of the evolution of the universe. *Soviet Atomic Energy*, 14(1):83–91.

Ya. B. Zel'dovich. 1970a. Gravitational Instability: An Approximate Theory for Large Density Perturbations. *Astron. Astrophys.*, 5:84–89.

Ya B. Zel'dovich. 1970b. Fragmentation of a homogeneous medium under the action of gravitation. *Astrophysics*, 6(2):164–174.

Ya. B. Zeldovich. 1978. The theory of the large scale structure of the universe. In D. Dordrecht, editor, *The large scale structure of the universe*, pages 409–421. Reidel Publishing Co.

J. P. Zibin. 2011. Can decaying modes save void models for acceleration? *Phys. Rev. D*, 84(12):123508.

J. P. Zibin, A. Moss, and D. Scott. 2008. Can We Avoid Dark Energy? *Phys. Rev. Lett.*, 101(25):251303.

I. Zlatev, L. Wang, and P. J. Steinhardt. 1999. Quintessence, Cosmic Coincidence, and the Cosmological Constant. *Phys. Rev. Lett.*, 82(5):896–899.

N. V. Zotov and W. R. Stoeger. 1992. Averaging Einstein's equations. *Class. Quantum Grav.*, 9(4):1023.